

# PyCAMA report generated by trop12-proc

trop12-proc

2024-09-30 (02:30)

## 1 Short Introduction

### 1.1 The list of parameters

You may want to keep the list given in table 1 at hand when viewing the results.

## 2 Definitions

The averages shown here are *unweighted* averages:

$$\bar{x} = \frac{1}{N} \sum_{i=1}^N x_i \quad (1)$$

with  $N$  the number of observations in the dataset.

The spread of the measurements is indicated with the variance  $V(x)$ , or rather the standard deviation  $\sigma(x) = \sqrt{V(x)}$ .

$$V(x) = \frac{1}{N-1} \sum_{i=1}^N (x_i - \bar{x})^2 \quad (2)$$

We also report the more robust statistics median, minimum, maximum, various percentiles and inter quartile range.

The median  $m$  is the value of parameter  $x$  for which half of the observations of  $x$  is smaller than  $m$ :

$$P(x \leq m) = P(x \geq m) = \int_{-\infty}^m f(x) dx = \frac{1}{2} \quad (3)$$

with  $f(x)$  the probability density function.

The median is a special case of a percentile. Instead of  $1/2$  in equation 3, other threshold values can be used. We report results for 1 %, 5 %, 10 %, 15.9 %, 25 %, 75 %, 84.1 %, 90 %, 95 % and 99 %. The inter quartile range is the difference between the 75 % and 25 % percentiles. Similarly the minimum and maximum values correspond to the 0 % and 100 % percentiles respectively.

For normally distributed parameters the mean and median are the same, while the  $\mu \pm \sigma$  values and the 15.9 % and 84.1 % percentiles coincide.

To get a measure for the relation of one variable  $x_{(k)}$  with another  $x_{(l)}$ , we calculate the covariance matrix  $C_{kl}$ .

$$C_{kl} = C(x_{(k)}, x_{(l)}) = \frac{1}{N-1} \sum_{i=1}^N (x_{(k),i} - \bar{x}_{(k)})(x_{(l),i} - \bar{x}_{(l)}) \quad (4)$$

Rather than a dimensionally dependent covariance, it is often easier to interpret a correlation matrix  $R_{kl}$ , a matrix of Pearson's  $r$  coefficients:

$$R_{kl} = R(x_{(k)}, x_{(l)}) = \frac{C_{kl}}{\sqrt{C_{kk}C_{ll}}} = \frac{C_{kl}}{\sqrt{V(x_k)V(x_l)}} \quad (5)$$

The diagonal elements of the covariance matrix are the variances of the elements,  $V(x_{(k)}) = C_{kk}$  and obviously  $R_{kk} = 1$ .

Variable	mean $\pm \sigma$	Count	Mode	IQR	Median	Minimum	Maximum
qa value [1]	0.963 $\pm$ 0.116	24681585	0.995	0.0	1.000	0.350	1.000
cloud pressure crb [hPa]	754 $\pm$ 195	24681585	905	291	810	130	$1.058 \times 10^3$
cloud pressure crb precision [hPa]	28.0 $\pm$ 58.0	24681585	0.750	17.9	3.01	$8.911 \times 10^{-3}$	868
cloud fraction crb [1]	0.407 $\pm$ 0.355	24681585	0.996	0.646	0.303	0.0	1.000
cloud fraction crb precision [1]	$(4.832 \pm 16.325) \times 10^{-4}$	24681585	$2.500 \times 10^{-4}$	$3.224 \times 10^{-4}$	$2.729 \times 10^{-4}$	$1.071 \times 10^{-8}$	0.506
scene albedo [1]	$0.399 \pm 0.300$	24681585	$1.500 \times 10^{-2}$	0.496	0.350	$2.691 \times 10^{-3}$	5.34
scene albedo precision [1]	$(3.281 \pm 4.375) \times 10^{-4}$	24681585	$2.500 \times 10^{-4}$	$1.655 \times 10^{-4}$	$1.876 \times 10^{-4}$	$4.111 \times 10^{-5}$	$2.163 \times 10^{-2}$
apparent scene pressure [hPa]	787 $\pm$ 171	24681585	944	245	842	130	$1.038 \times 10^3$
apparent scene pressure precision [hPa]	17.4 $\pm$ 39.0	24681585	0.500	7.46	1.89	$5.728 \times 10^{-2}$	244
chi square [1]	$(0.487 \pm 1.388) \times 10^4$	24681585	0.450	$5.739 \times 10^3$	$1.428 \times 10^3$	0.255	$3.082 \times 10^6$
number of iterations [1]	2.75 $\pm$ 1.07	24681585	2.31	1.000	2.00	1.000	14.0
fluorescence [ $\text{mol s}^{-1} \text{m}^{-2} \text{nm}^{-1} \text{sr}^{-1}$ ]	$(9.715 \pm 60.114) \times 10^{-10}$	24681585	$2.500 \times 10^{-10}$	$4.856 \times 10^{-9}$	$9.467 \times 10^{-10}$	$-1.860 \times 10^{-6}$	$2.213 \times 10^{-6}$
fluorescence precision [ $\text{mol s}^{-1} \text{m}^{-2} \text{nm}^{-1} \text{sr}^{-1}$ ]	$(1.700 \pm 0.668) \times 10^{-9}$	24681585	$9.500 \times 10^{-10}$	$9.377 \times 10^{-10}$	$1.602 \times 10^{-9}$	$3.964 \times 10^{-10}$	$5.768 \times 10^{-9}$
chi square fluorescence [1]	$(0.628 \pm 1.224) \times 10^5$	24681585	750	$5.132 \times 10^4$	$1.857 \times 10^4$	110	$9.163 \times 10^6$
degrees of freedom fluorescence [1]	6.00 $\pm$ 0.00	24681585	5.95	0.0	6.00	6.00	6.00
number of spectral points in retrieval [1]	59.0 $\pm$ 0.1	24681585	58.5	0.0	59.0	54.0	59.0
wavelength calibration offset [nm]	$(-4.259 \pm 11.182) \times 10^{-3}$	24681585	$4.000 \times 10^{-4}$	$1.241 \times 10^{-2}$	$-2.721 \times 10^{-3}$	-0.156	0.122

Table 2: Percentile ranges

Variable	1 %	5 %	10 %	15.9 %	25 %	75 %	84.1 %	90 %	95 %	99 %
qa value [1]	0.500	0.500	0.900	1.000	1.000	1.000	1.000	1.000	1.000	1.000
cloud pressure crb [hPa]	244	372	462	533	621	912	942	963	982	$1.009 \times 10^3$
cloud pressure crb precision [hPa]	0.180	0.364	0.509	0.654	0.910	18.8	47.0	98.2	193	249
cloud fraction crb [1]	0.0	$1.001 \times 10^{-2}$	$2.149 \times 10^{-2}$	$3.852 \times 10^{-2}$	$7.410 \times 10^{-2}$	0.721	0.910	1.000	1.000	1.000
cloud fraction crb precision [1]	$9.106 \times 10^{-5}$	$1.000 \times 10^{-4}$	$1.000 \times 10^{-4}$	$1.183 \times 10^{-4}$	$1.666 \times 10^{-4}$	$4.890 \times 10^{-4}$	$6.815 \times 10^{-4}$	$8.549 \times 10^{-4}$	$1.157 \times 10^{-3}$	$3.185 \times 10^{-3}$
scene albedo [1]	$1.233 \times 10^{-2}$	$2.181 \times 10^{-2}$	$3.659 \times 10^{-2}$	$6.220 \times 10^{-2}$	0.129	0.625	0.743	0.832	0.919	1.10
scene albedo precision [1]	$5.913 \times 10^{-5}$	$8.229 \times 10^{-5}$	$9.968 \times 10^{-5}$	$1.120 \times 10^{-4}$	$1.317 \times 10^{-4}$	$2.971 \times 10^{-4}$	$4.325 \times 10^{-4}$	$6.739 \times 10^{-4}$	$1.217 \times 10^{-3}$	$2.333 \times 10^{-3}$
apparent scene pressure [hPa]	321	444	526	593	678	923	948	964	979	999
apparent scene pressure precision [hPa]	0.185	0.372	0.513	0.649	0.855	8.32	25.6	58.2	119	185
chi square [1]	0.408	0.972	3.42	15.9	117	$5.856 \times 10^3$	$9.325 \times 10^3$	$1.309 \times 10^4$	$1.923 \times 10^4$	$3.958 \times 10^4$
number of iterations [1]	2.00	2.00	2.00	2.00	2.00	3.00	4.00	4.00	4.00	6.00
fluorescence [ $\text{mol s}^{-1} \text{m}^{-2} \text{nm}^{-1} \text{sr}^{-1}$ ]	$-1.506 \times 10^{-8}$	$-7.414 \times 10^{-9}$	$-4.442 \times 10^{-9}$	$-2.734 \times 10^{-9}$	$-1.310 \times 10^{-9}$	$3.546 \times 10^{-9}$	$5.054 \times 10^{-9}$	$6.569 \times 10^{-9}$	$8.937 \times 10^{-9}$	$1.516 \times 10^{-8}$
fluorescence precision [ $\text{mol s}^{-1} \text{m}^{-2} \text{nm}^{-1} \text{sr}^{-1}$ ]	$7.514 \times 10^{-10}$	$8.403 \times 10^{-10}$	$9.162 \times 10^{-10}$	$1.006 \times 10^{-9}$	$1.170 \times 10^{-9}$	$2.108 \times 10^{-9}$	$2.330 \times 10^{-9}$	$2.635 \times 10^{-9}$	$2.940 \times 10^{-9}$	$3.597 \times 10^{-9}$
chi square fluorescence [1]	344	834	$1.665 \times 10^3$	$2.867 \times 10^3$	$5.469 \times 10^3$	$5.679 \times 10^4$	$1.001 \times 10^5$	$1.694 \times 10^5$	$3.067 \times 10^5$	$6.253 \times 10^5$
degrees of freedom fluorescence [1]	6.00	6.00	6.00	6.00	6.00	6.00	6.00	6.00	6.00	6.00
number of spectral points in retrieval [1]	59.0	59.0	59.0	59.0	59.0	59.0	59.0	59.0	59.0	59.0
wavelength calibration offset [nm]	$-3.800 \times 10^{-2}$	$-2.375 \times 10^{-2}$	$-1.802 \times 10^{-2}$	$-1.405 \times 10^{-2}$	$-9.909 \times 10^{-3}$	$2.501 \times 10^{-3}$	$4.598 \times 10^{-3}$	$6.459 \times 10^{-3}$	$1.026 \times 10^{-2}$	$2.297 \times 10^{-2}$

Table 3: Parameterlist and basic statistics for the analysis for observations in the northern hemisphere

Variable	mean $\pm \sigma$	Count	IQR	Median	Minimum	Maximum	25 % percentile	75 % percentile
qa value [1]	$0.979 \pm 0.074$	13358972	0.0	1.000	0.350	1.000	1.000	1.000
cloud pressure crb [hPa]	$739 \pm 206$	13358972	316	788	130	$1.058 \times 10^3$	597	913
cloud pressure crb precision [hPa]	$25.8 \pm 55.1$	13358972	16.1	3.50	$8.911 \times 10^{-3}$	868	0.957	17.1
cloud fraction crb [1]	$0.381 \pm 0.342$	13358972	0.588	0.262	0.0	1.000	$7.514 \times 10^{-2}$	0.663
cloud fraction crb precision [1]	$(4.310 \pm 8.561) \times 10^{-4}$	13358972	$2.948 \times 10^{-4}$	$2.824 \times 10^{-4}$	$8.405 \times 10^{-7}$	0.326	$1.778 \times 10^{-4}$	$4.726 \times 10^{-4}$
scene albedo [1]	$0.390 \pm 0.281$	13358972	0.446	0.351	$2.691 \times 10^{-3}$	4.27	0.147	0.593
scene albedo precision [1]	$(3.172 \pm 4.523) \times 10^{-4}$	13358972	$1.604 \times 10^{-4}$	$1.795 \times 10^{-4}$	$4.112 \times 10^{-5}$	$2.163 \times 10^{-2}$	$1.240 \times 10^{-4}$	$2.844 \times 10^{-4}$
apparent scene pressure [hPa]	$780 \pm 181$	13358972	262	835	130	$1.035 \times 10^3$	667	929
apparent scene pressure precision [hPa]	$15.7 \pm 37.6$	13358972	6.04	1.91	$5.728 \times 10^{-2}$	241	0.861	6.90
chi square [1]	$(0.495 \pm 1.244) \times 10^4$	13358972	$5.476 \times 10^3$	$1.391 \times 10^3$	0.255	$3.082 \times 10^6$	166	$5.643 \times 10^3$
number of iterations [1]	$2.79 \pm 0.97$	13358972	1.000	3.00	1.000	14.0	2.00	3.00
fluorescence [ $\text{mol s}^{-1} \text{m}^{-2} \text{nm}^{-1} \text{sr}^{-1}$ ]	$(5.718 \pm 68.284) \times 10^{-10}$	13358972	$4.884 \times 10^{-9}$	$6.409 \times 10^{-10}$	$-1.860 \times 10^{-6}$	$2.213 \times 10^{-6}$	$-1.758 \times 10^{-9}$	$3.126 \times 10^{-9}$
fluorescence precision [ $\text{mol s}^{-1} \text{m}^{-2} \text{nm}^{-1} \text{sr}^{-1}$ ]	$(1.744 \pm 0.696) \times 10^{-9}$	13358972	$9.849 \times 10^{-10}$	$1.629 \times 10^{-9}$	$3.964 \times 10^{-10}$	$5.768 \times 10^{-9}$	$1.198 \times 10^{-9}$	$2.183 \times 10^{-9}$
chi square fluorescence [1]	$(0.851 \pm 1.455) \times 10^5$	13358972	$7.198 \times 10^4$	$2.925 \times 10^4$	110	$9.163 \times 10^6$	$1.081 \times 10^4$	$8.279 \times 10^4$
degrees of freedom fluorescence [1]	$6.00 \pm 0.00$	13358972	0.0	6.00	6.00	6.00	6.00	6.00
number of spectral points in retrieval [1]	$59.0 \pm 0.1$	13358972	0.0	59.0	54.0	59.0	59.0	59.0
wavelength calibration offset [nm]	$(-6.181 \pm 11.189) \times 10^{-3}$	13358972	$1.272 \times 10^{-2}$	$-4.762 \times 10^{-3}$	-0.145	$8.573 \times 10^{-2}$	$-1.206 \times 10^{-2}$	$6.686 \times 10^{-4}$

Table 4: Parameterlist and basic statistics for the analysis for observations in the southern hemisphere

Variable	mean $\pm \sigma$	Count	IQR	Median	Minimum	Maximum	25 % percentile	75 % percentile
qa value [1]	$0.945 \pm 0.150$	11322613	0.0	1.000	0.350	1.000	1.000	1.000
cloud pressure crb [hPa]	$771 \pm 180$	11322613	262	830	130	$1.041 \times 10^3$	649	911
cloud pressure crb precision [hPa]	$30.7 \pm 61.2$	11322613	20.9	2.49	$1.013 \times 10^{-2}$	530	0.873	21.8
cloud fraction crb [1]	$0.437 \pm 0.368$	11322613	0.712	0.361	0.0	1.000	$7.247 \times 10^{-2}$	0.784
cloud fraction crb precision [1]	$(5.447 \pm 22.221) \times 10^{-4}$	11322613	$3.646 \times 10^{-4}$	$2.593 \times 10^{-4}$	$1.071 \times 10^{-8}$	0.506	$1.526 \times 10^{-4}$	$5.171 \times 10^{-4}$
scene albedo [1]	$0.409 \pm 0.322$	11322613	0.560	0.349	$6.483 \times 10^{-3}$	5.34	0.106	0.666
scene albedo precision [1]	$(3.409 \pm 4.189) \times 10^{-4}$	11322613	$1.724 \times 10^{-4}$	$1.965 \times 10^{-4}$	$4.111 \times 10^{-5}$	$7.590 \times 10^{-3}$	$1.421 \times 10^{-4}$	$3.145 \times 10^{-4}$
apparent scene pressure [hPa]	$796 \pm 157$	11322613	224	848	130	$1.038 \times 10^3$	693	917
apparent scene pressure precision [hPa]	$19.4 \pm 40.4$	11322613	10.5	1.86	$6.239 \times 10^{-2}$	244	0.849	11.4
chi square [1]	$(0.479 \pm 1.541) \times 10^4$	11322613	$6.006 \times 10^3$	$1.483 \times 10^3$	0.263	$2.231 \times 10^6$	65.9	$6.072 \times 10^3$
number of iterations [1]	$2.71 \pm 1.17$	11322613	1.000	2.00	1.000	14.0	2.00	3.00
fluorescence [ $\text{mol s}^{-1} \text{m}^{-2} \text{nm}^{-1} \text{sr}^{-1}$ ]	$(1.443 \pm 4.832) \times 10^{-9}$	11322613	$4.810 \times 10^{-9}$	$1.331 \times 10^{-9}$	$-7.211 \times 10^{-7}$	$8.592 \times 10^{-7}$	$-8.394 \times 10^{-10}$	$3.970 \times 10^{-9}$
fluorescence precision [ $\text{mol s}^{-1} \text{m}^{-2} \text{nm}^{-1} \text{sr}^{-1}$ ]	$(1.649 \pm 0.630) \times 10^{-9}$	11322613	$8.721 \times 10^{-10}$	$1.577 \times 10^{-9}$	$4.880 \times 10^{-10}$	$5.371 \times 10^{-9}$	$1.134 \times 10^{-9}$	$2.006 \times 10^{-9}$
chi square fluorescence [1]	$(0.365 \pm 0.801) \times 10^5$	11322613	$2.933 \times 10^4$	$9.434 \times 10^3$	122	$1.805 \times 10^6$	$2.734 \times 10^3$	$3.207 \times 10^4$
degrees of freedom fluorescence [1]	$6.00 \pm 0.00$	11322613	0.0	6.00	6.00	6.00	6.00	6.00
number of spectral points in retrieval [1]	$59.0 \pm 0.1$	11322613	0.0	59.0	57.0	59.0	59.0	59.0
wavelength calibration offset [nm]	$(-1.993 \pm 10.742) \times 10^{-3}$	11322613	$1.094 \times 10^{-2}$	$-3.879 \times 10^{-4}$	-0.156	0.122	$-6.932 \times 10^{-3}$	$4.004 \times 10^{-3}$

**Table 5:** Parameterlist and basic statistics for the analysis for observations over water

Variable	mean $\pm \sigma$	Count	IQR	Median	Minimum	Maximum	25 % percentile	75 % percentile
qa value [1]	$0.975 \pm 0.083$	17394636	0.0	1.000	0.350	1.000	1.000	1.000
cloud pressure crb [hPa]	$771 \pm 194$	17394636	281	840	130	$1.041 \times 10^3$	642	923
cloud pressure crb precision [hPa]	$32.0 \pm 62.7$	17394636	22.1	3.11	$1.013 \times 10^{-2}$	362	0.976	23.1
cloud fraction crb [1]	$0.397 \pm 0.339$	17394636	0.603	0.313	0.0	1.000	$7.712 \times 10^{-2}$	0.680
cloud fraction crb precision [1]	$(4.886 \pm 12.607) \times 10^{-4}$	17394636	$4.170 \times 10^{-4}$	$2.925 \times 10^{-4}$	$1.071 \times 10^{-8}$	0.506	$1.680 \times 10^{-4}$	$5.850 \times 10^{-4}$
scene albedo [1]	$0.352 \pm 0.295$	17394636	0.516	0.289	$3.052 \times 10^{-3}$	5.34	$7.327 \times 10^{-2}$	0.589
scene albedo precision [1]	$(3.801 \pm 5.003) \times 10^{-4}$	17394636	$2.053 \times 10^{-4}$	$2.056 \times 10^{-4}$	$4.125 \times 10^{-5}$	$2.163 \times 10^{-2}$	$1.405 \times 10^{-4}$	$3.458 \times 10^{-4}$
apparent scene pressure [hPa]	$788 \pm 175$	17394636	243	848	130	$1.035 \times 10^3$	681	924
apparent scene pressure precision [hPa]	$23.6 \pm 44.7$	17394636	18.9	2.52	$5.975 \times 10^{-2}$	244	0.938	19.9
chi square [1]	$(0.410 \pm 1.340) \times 10^4$	17394636	$4.511 \times 10^3$	808	0.255	$2.231 \times 10^6$	26.0	$4.537 \times 10^3$
number of iterations [1]	$2.52 \pm 1.02$	17394636	1.000	2.00	1.000	14.0	2.00	3.00
fluorescence [ $\text{mol s}^{-1} \text{m}^{-2} \text{nm}^{-1} \text{sr}^{-1}$ ]	$(7.561 \pm 52.897) \times 10^{-10}$	17394636	$4.453 \times 10^{-9}$	$6.474 \times 10^{-10}$	$-1.860 \times 10^{-6}$	$1.617 \times 10^{-6}$	$-1.342 \times 10^{-9}$	$3.111 \times 10^{-9}$
fluorescence precision [ $\text{mol s}^{-1} \text{m}^{-2} \text{nm}^{-1} \text{sr}^{-1}$ ]	$(1.615 \pm 0.669) \times 10^{-9}$	17394636	$9.291 \times 10^{-10}$	$1.488 \times 10^{-9}$	$3.964 \times 10^{-10}$	$5.624 \times 10^{-9}$	$1.076 \times 10^{-9}$	$2.005 \times 10^{-9}$
chi square fluorescence [1]	$(0.467 \pm 0.971) \times 10^5$	17394636	$3.830 \times 10^4$	$1.440 \times 10^4$	110	$2.233 \times 10^6$	$4.616 \times 10^3$	$4.292 \times 10^4$
degrees of freedom fluorescence [1]	$6.00 \pm 0.00$	17394636	0.0	6.00	6.00	6.00	6.00	6.00
number of spectral points in retrieval [1]	$59.0 \pm 0.1$	17394636	0.0	59.0	55.0	59.0	59.0	59.0
wavelength calibration offset [nm]	$(-4.181 \pm 11.709) \times 10^{-3}$	17394636	$1.245 \times 10^{-2}$	$-2.541 \times 10^{-3}$	-0.156	0.122	$-9.906 \times 10^{-3}$	$2.542 \times 10^{-3}$

Variable	mean $\pm \sigma$	Count	IQR	Median	Minimum	Maximum	25 % percentile	75 % percentile
qa value [1]	$0.915 \pm 0.191$	5265353	0.0	1.000	0.350	1.000	1.000	1.000
cloud pressure crb [hPa]	$707 \pm 191$	5265353	282	731	130	$1.035 \times 10^3$	579	861
cloud pressure crb precision [hPa]	$18.6 \pm 43.4$	5265353	12.6	2.82	$1.141 \times 10^{-2}$	828	0.760	13.3
cloud fraction crb [1]	$0.435 \pm 0.404$	5265353	0.937	0.249	0.0	1.000	$6.317 \times 10^{-2}$	1.000
cloud fraction crb precision [1]	$(5.088 \pm 26.539) \times 10^{-4}$	5265353	$1.797 \times 10^{-4}$	$2.458 \times 10^{-4}$	$2.197 \times 10^{-7}$	0.427	$1.328 \times 10^{-4}$	$3.125 \times 10^{-4}$
scene albedo [1]	$0.533 \pm 0.288$	5265353	0.496	0.455	$1.884 \times 10^{-2}$	4.27	0.288	0.783
scene albedo precision [1]	$(1.982 \pm 1.539) \times 10^{-4}$	5265353	$9.097 \times 10^{-5}$	$1.511 \times 10^{-4}$	$4.111 \times 10^{-5}$	$6.299 \times 10^{-3}$	$1.179 \times 10^{-4}$	$2.089 \times 10^{-4}$
apparent scene pressure [hPa]	$780 \pm 162$	5265353	258	819	130	$1.028 \times 10^3$	661	919
apparent scene pressure precision [hPa]	$1.78 \pm 1.67$	5265353	1.64	1.21	$5.728 \times 10^{-2}$	134	0.720	2.36
chi square [1]	$(0.728 \pm 1.533) \times 10^4$	5265353	$8.395 \times 10^3$	$3.773 \times 10^3$	0.872	$3.082 \times 10^6$	$1.093 \times 10^3$	$9.488 \times 10^3$
number of iterations [1]	$3.37 \pm 1.00$	5265353	1.000	3.00	1.000	14.0	3.00	4.00
fluorescence [ $\text{mol s}^{-1} \text{m}^{-2} \text{nm}^{-1} \text{sr}^{-1}$ ]	$(1.390 \pm 7.545) \times 10^{-9}$	5265353	$6.100 \times 10^{-9}$	$1.924 \times 10^{-9}$	$-1.715 \times 10^{-6}$	$2.213 \times 10^{-6}$	$-1.531 \times 10^{-9}$	$4.569 \times 10^{-9}$
fluorescence precision [ $\text{mol s}^{-1} \text{m}^{-2} \text{nm}^{-1} \text{sr}^{-1}$ ]	$(1.942 \pm 0.623) \times 10^{-9}$	5265353	$7.754 \times 10^{-10}$	$1.854 \times 10^{-9}$	$4.855 \times 10^{-10}$	$5.768 \times 10^{-9}$	$1.508 \times 10^{-9}$	$2.283 \times 10^{-9}$
chi square fluorescence [1]	$(0.111 \pm 0.172) \times 10^6$	5265353	$1.200 \times 10^5$	$3.507 \times 10^4$	132	$9.163 \times 10^6$	$9.066 \times 10^3$	$1.290 \times 10^5$
degrees of freedom fluorescence [1]	$6.00 \pm 0.00$	5265353	0.0	6.00	6.00	6.00	6.00	6.00
number of spectral points in retrieval [1]	$59.0 \pm 0.1$	5265353	0.0	59.0	54.0	59.0	59.0	59.0
wavelength calibration offset [nm]	$(-4.316 \pm 9.599) \times 10^{-3}$	5265353	$1.290 \times 10^{-2}$	$-2.896 \times 10^{-3}$	$-8.372 \times 10^{-2}$	$5.813 \times 10^{-2}$	$-1.003 \times 10^{-2}$	$2.871 \times 10^{-3}$

Spectral offset ( $\lambda_{\text{true}} - \lambda_{\text{nominal}}$ )

	Number of points in the spectrum												
	$\chi^2$ of fluorescence retrieval												
	Number of iterations												
	$\chi^2$	Fluorescence											
Solar zenith angle	$2.082 \times 10^{-2}$	$-1.221 \times 10^{-2}$	$-6.985 \times 10^{-2}$	0.120	0.115	$-8.416 \times 10^{-2}$	$1.645 \times 10^{-2}$	$2.405 \times 10^{-2}$	$6.135 \times 10^{-2}$	$2.819 \times 10^{-3}$	$1.742 \times 10^{-2}$	$-9.129 \times 10^{-2}$	
Viewing zenith angle	1.000	$-4.430 \times 10^{-3}$	$-0.227$	0.482	0.526	-0.222	$3.318 \times 10^{-2}$	0.341	0.252	-0.367	$3.316 \times 10^{-3}$	0.336	
Latitude	$-1.221 \times 10^{-2}$	$-4.430 \times 10^{-3}$	1.000	$-5.122 \times 10^{-2}$	-0.107	$-7.210 \times 10^{-2}$	$1.983 \times 10^{-3}$	$-4.131 \times 10^{-2}$	$-3.762 \times 10^{-3}$	$-6.289 \times 10^{-2}$	0.104	$8.040 \times 10^{-4}$	-0.157
Cloud pressure	$-6.985 \times 10^{-2}$	-0.227	$-5.122 \times 10^{-2}$	1.000	-0.313	-0.388	0.870	-0.103	-0.520	-0.242	0.168	$-6.446 \times 10^{-3}$	-0.245
Cloud fraction	0.120	0.482	-0.107	-0.313	1.000	0.922	-0.490	0.316	0.284	0.327	$-3.889 \times 10^{-3}$	$1.484 \times 10^{-3}$	0.259
Scene albedo	0.115	0.526	$-7.210 \times 10^{-2}$	-0.388	0.922	1.000	-0.449	0.367	0.486	0.328	$7.697 \times 10^{-2}$	$2.599 \times 10^{-3}$	0.229
	$-8.416 \times 10^{-2}$	-0.222	$1.983 \times 10^{-3}$	0.870	-0.490	-0.449	1.000	$-8.695 \times 10^{-2}$	-0.310	-0.271	0.243	$-5.237 \times 10^{-3}$	-0.324
	$1.645 \times 10^{-2}$	$3.318 \times 10^{-2}$	$-4.131 \times 10^{-2}$	-0.103	0.316	0.367	$-8.695 \times 10^{-2}$	1.000	0.283	0.107	0.325	$-5.904 \times 10^{-4}$	$-8.419 \times 10^{-3}$
	$2.405 \times 10^{-2}$	0.341	$-3.762 \times 10^{-3}$	-0.520	0.284	0.486	-0.310	0.283	1.000	0.206	$-5.105 \times 10^{-3}$	$2.872 \times 10^{-3}$	0.121
	$6.135 \times 10^{-2}$	0.252	$-6.289 \times 10^{-2}$	-0.242	0.327	0.328	-0.271	0.107	0.206	1.000	-0.262	$4.288 \times 10^{-4}$	0.302
	$2.819 \times 10^{-3}$	-0.367	0.104	0.168	$-3.889 \times 10^{-3}$	$7.697 \times 10^{-2}$	0.243	0.325	$-5.105 \times 10^{-3}$	-0.262	1.000	$-3.025 \times 10^{-3}$	-0.397
	$1.742 \times 10^{-2}$	$3.316 \times 10^{-3}$	$8.040 \times 10^{-4}$	$-6.446 \times 10^{-3}$	$1.484 \times 10^{-3}$	$2.599 \times 10^{-3}$	$-5.237 \times 10^{-3}$	$-5.904 \times 10^{-4}$	$2.872 \times 10^{-3}$	$4.288 \times 10^{-4}$	$-3.025 \times 10^{-3}$	1.000	$-8.642 \times 10^{-3}$
	$-9.129 \times 10^{-2}$	0.336	-0.157	-0.245	0.259	0.229	-0.324	$-8.419 \times 10^{-3}$	0.121	0.302	-0.397	$-8.642 \times 10^{-3}$	1.000

Table 7: Correlation matrix

Spectral offset ( $\lambda_{\text{true}} - \lambda_{\text{nominal}}$ )

	Number of points in the spectrum											
	$\chi^2$ of fluorescence retrieval											
Viewing zenith angle												
Solar zenith angle												
Latitude												
Cloud pressure												
Cloud fraction												
Scene albedo												
Apparent scene pressure												
$\chi^2$												

Table 8: Covariance matrix

383	8.17	-11.4	-266	0.831	0.677	-281	$4.466 \times 10^3$	0.503	$7.214 \times 10^{-9}$	$6.751 \times 10^3$	$3.249 \times 10^{-2}$	$-1.997 \times 10^{-2}$
8.17	402	-4.24	-885	3.44	3.17	-760	$9.235 \times 10^3$	7.32	$3.041 \times 10^{-8}$	$-9.019 \times 10^5$	$6.341 \times 10^{-3}$	$7.529 \times 10^{-2}$
-11.4	-4.24	$2.279 \times 10^3$	-476	-1.81	-1.03	16.2	$-2.738 \times 10^4$	-0.192	$-1.805 \times 10^{-8}$	$6.070 \times 10^5$	$3.660 \times 10^{-3}$	$-8.358 \times 10^{-2}$
-266	-885	-476	$3.795 \times 10^4$	-21.6	-21.6	-22.7	$2.898 \times 10^4$	-2.773 $\times 10^5$	-108	$-2.831 \times 10^{-7}$	$4.006 \times 10^6$	-0.120
0.831	3.44	-1.81	-21.6	0.126	$9.843 \times 10^{-2}$	-29.7	$1.556 \times 10^3$	0.108	$6.976 \times 10^{-10}$	-169	$5.030 \times 10^{-5}$	$1.030 \times 10^{-3}$
0.677	3.17	-1.03	-22.7	$9.843 \times 10^{-2}$	$9.024 \times 10^{-2}$	-23.1	$1.531 \times 10^3$	0.156	$5.928 \times 10^{-10}$	$2.830 \times 10^3$	$7.446 \times 10^{-5}$	$7.708 \times 10^{-4}$
-281	-760	16.2	$2.898 \times 10^4$	-29.7	-23.1	$2.922 \times 10^4$	$-2.063 \times 10^5$	-56.7	$-2.783 \times 10^{-7}$	$5.094 \times 10^6$	$-8.537 \times 10^{-2}$	-0.618
$4.466 \times 10^3$	$9.235 \times 10^3$	$-2.738 \times 10^4$	$-2.773 \times 10^5$	$1.556 \times 10^3$	$1.531 \times 10^3$	$-2.063 \times 10^5$	$1.927 \times 10^8$	$4.199 \times 10^3$	$8.950 \times 10^{-6}$	$5.529 \times 10^8$	-0.782	-1.31
0.503	7.32	-0.192	-108	0.108	0.156	-56.7	$4.199 \times 10^3$	1.14	$1.322 \times 10^{-9}$	-668	$2.930 \times 10^{-4}$	$1.453 \times 10^{-3}$
$7.214 \times 10^{-9}$	$3.041 \times 10^{-8}$	$-1.805 \times 10^{-8}$	$-2.831 \times 10^{-7}$	$6.976 \times 10^{-10}$	$5.928 \times 10^{-10}$	$-2.783 \times 10^{-7}$	$8.950 \times 10^{-6}$	$1.322 \times 10^{-9}$	$3.614 \times 10^{-17}$	$-1.929 \times 10^{-4}$	$2.458 \times 10^{-13}$	$2.031 \times 10^{-11}$
$6.751 \times 10^3$	$-9.019 \times 10^5$	$6.070 \times 10^5$	$4.006 \times 10^6$	-169	$2.830 \times 10^3$	$5.094 \times 10^6$	$5.529 \times 10^8$	-668	$-1.929 \times 10^{-4}$	$1.498 \times 10^{10}$	-35.3	-544
$3.249 \times 10^{-2}$	$6.341 \times 10^{-3}$	$3.660 \times 10^{-3}$	-0.120	$5.030 \times 10^{-5}$	$7.446 \times 10^{-5}$	$-8.537 \times 10^{-2}$	-0.782	$2.930 \times 10^{-4}$	$2.458 \times 10^{-13}$	-35.3	$9.094 \times 10^{-3}$	$-9.216 \times 10^{-6}$
$-1.997 \times 10^{-2}$	$7.529 \times 10^{-2}$	$-8.358 \times 10^{-2}$	-0.534	$1.030 \times 10^{-3}$	$7.708 \times 10^{-4}$	-0.618	-1.31	$1.453 \times 10^{-3}$	$2.031 \times 10^{-11}$	-544	$-9.216 \times 10^{-6}$	$1.250 \times 10^{-4}$

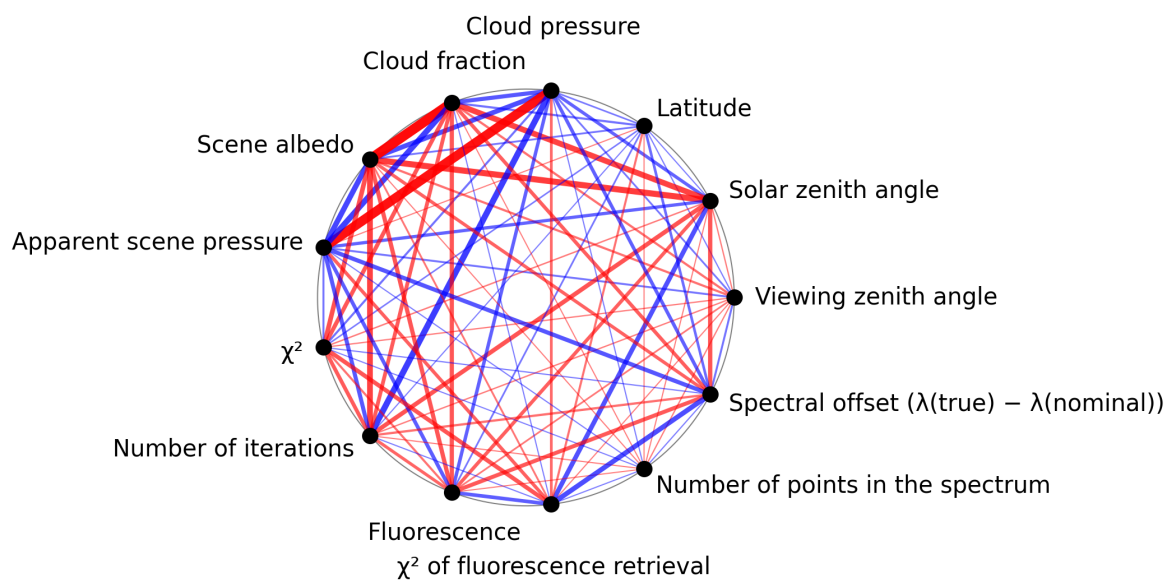


Figure 1: Map of correlation graph for 2024-09-14 to 2024-09-16.

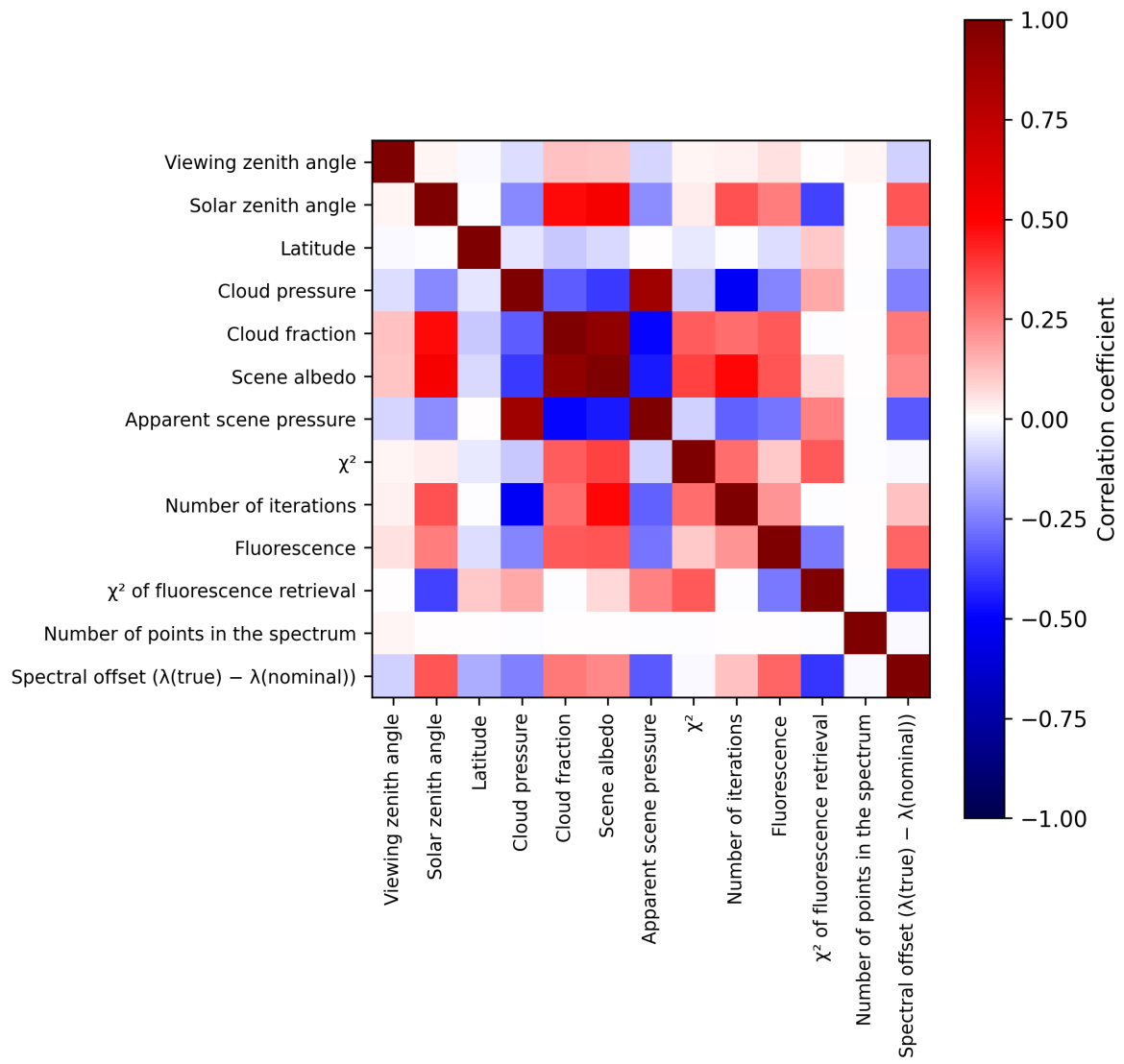


Figure 2: Map of correlation matrix for 2024-09-14 to 2024-09-16.

### 3 Granule outlines

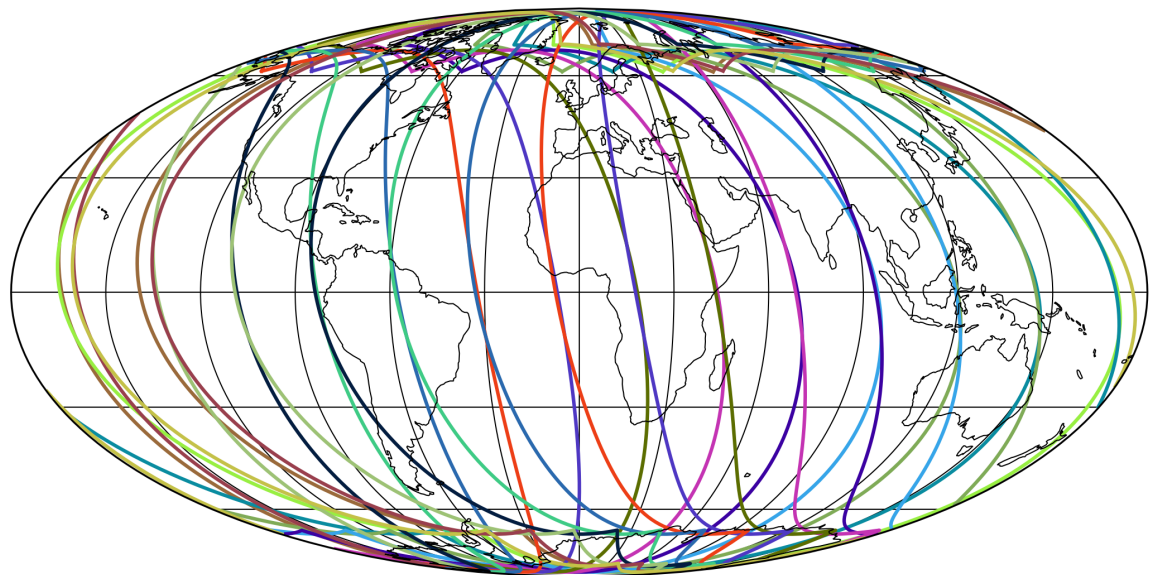


Figure 3: Outline of the granules.

## 4 Input data monitoring

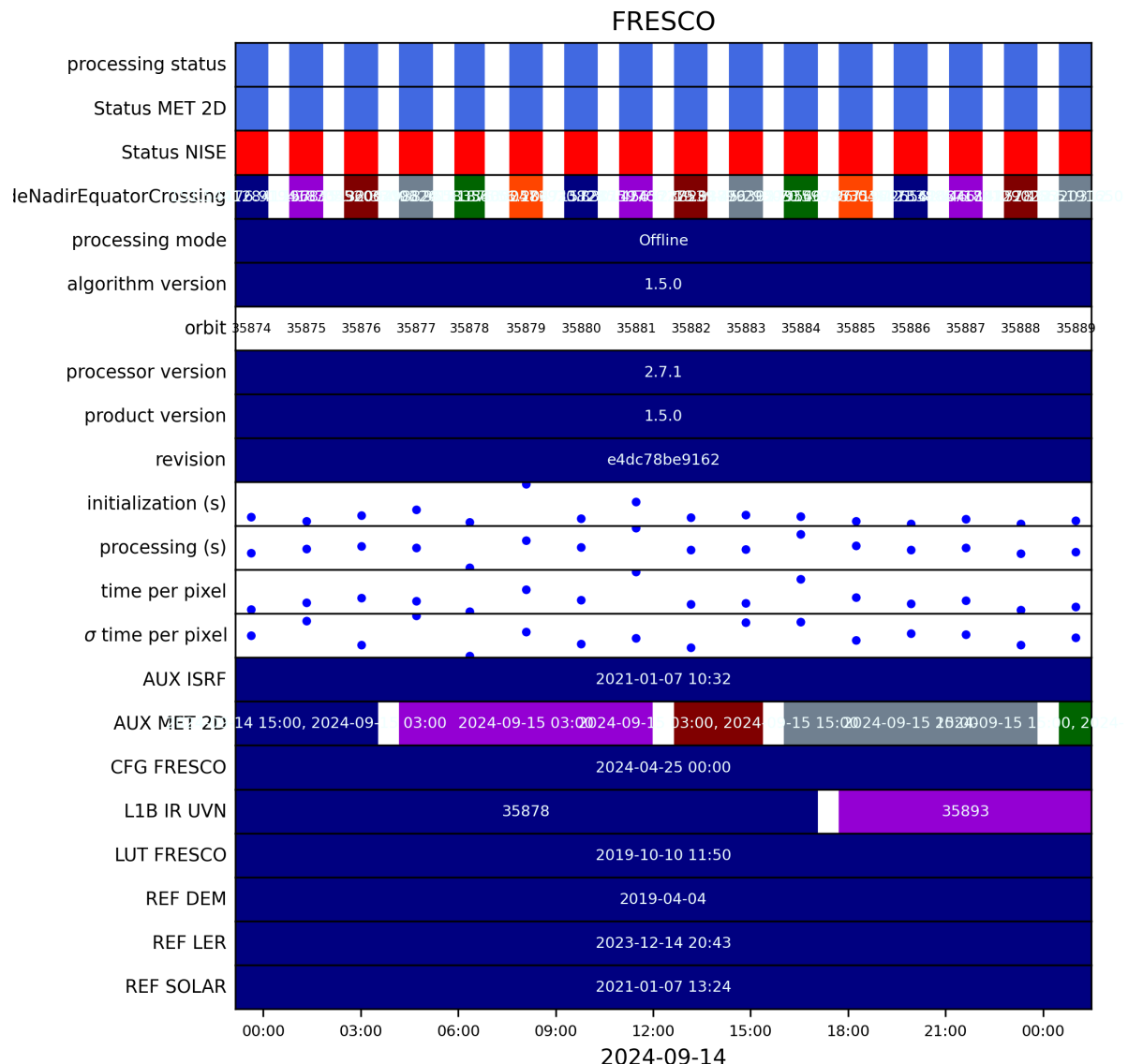


Figure 4: Input data per granule

## 5 Warnings and errors

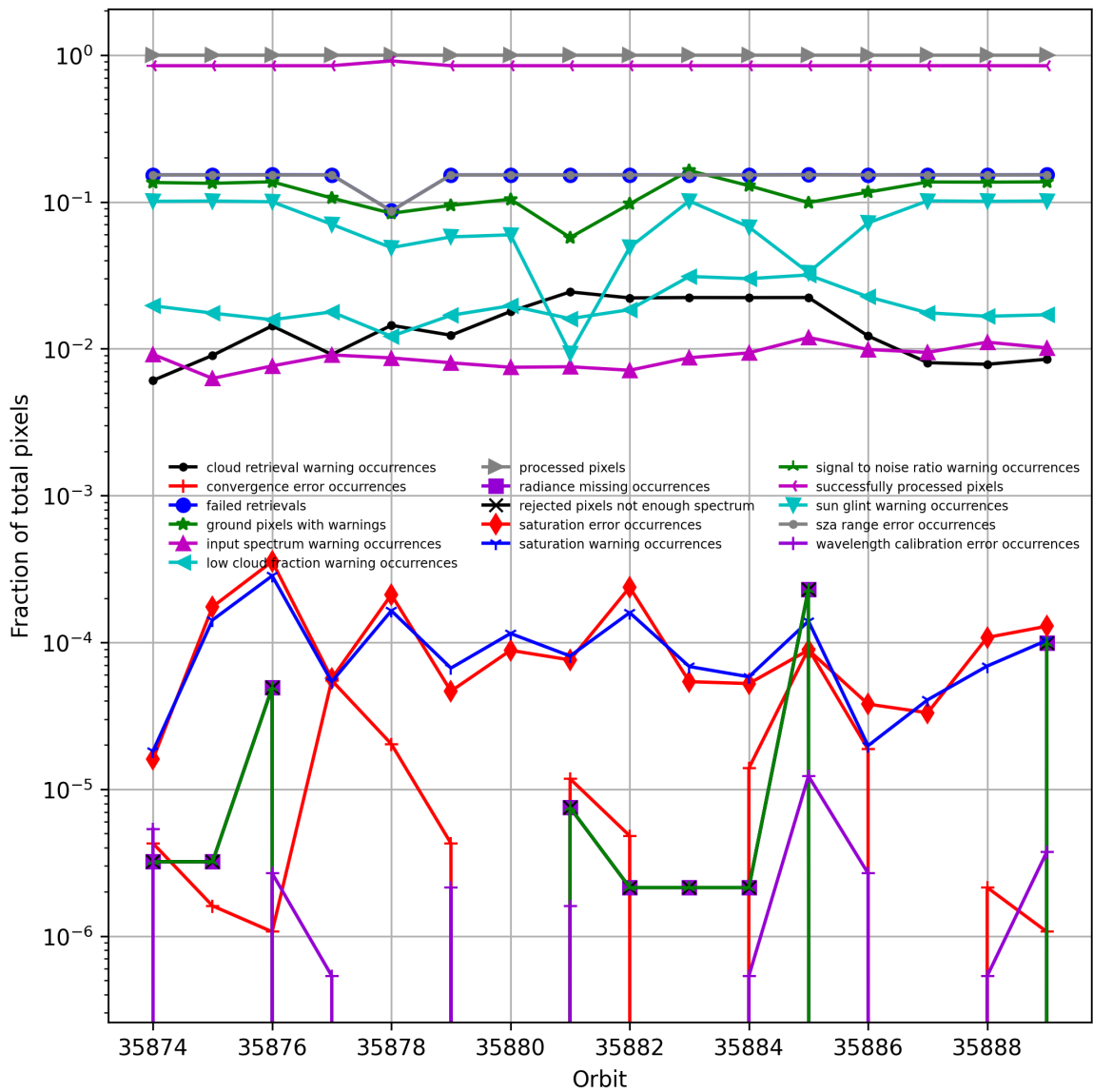


Figure 5: Fraction of pixels with specific warnings and errors during processing

## 6 World maps

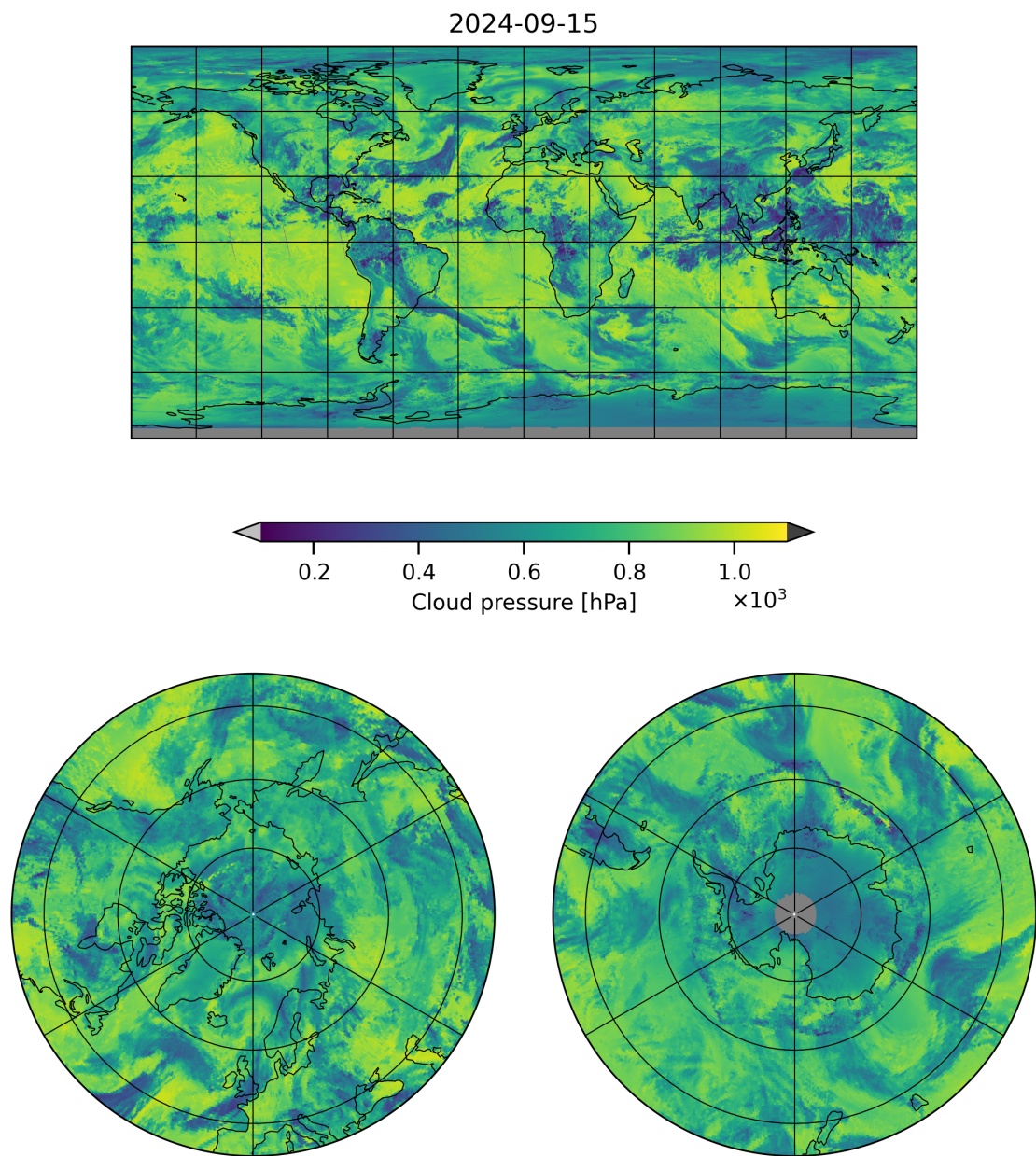


Figure 6: Map of “Cloud pressure” for 2024-09-14 to 2024-09-16

2024-09-15

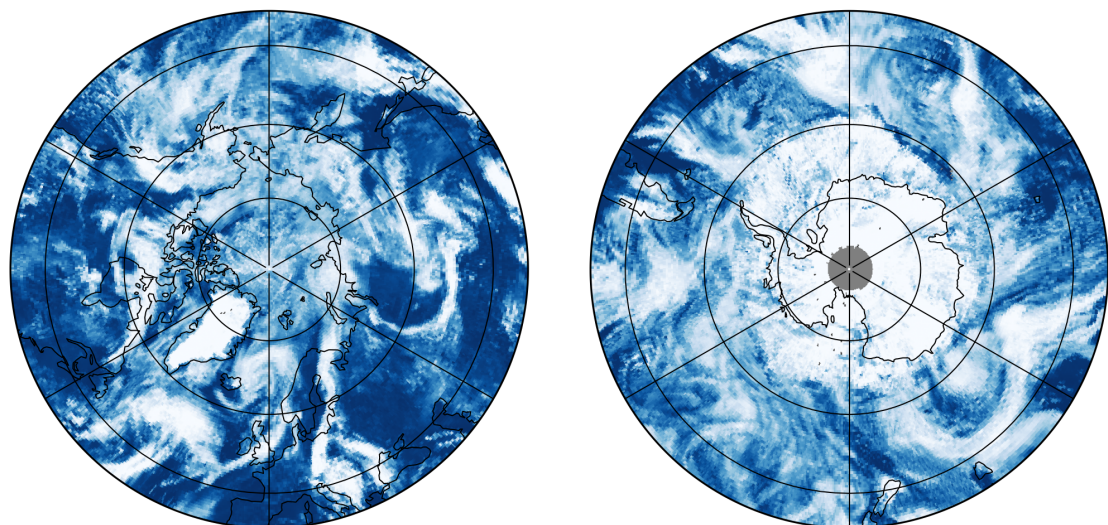
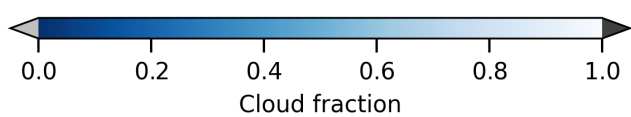
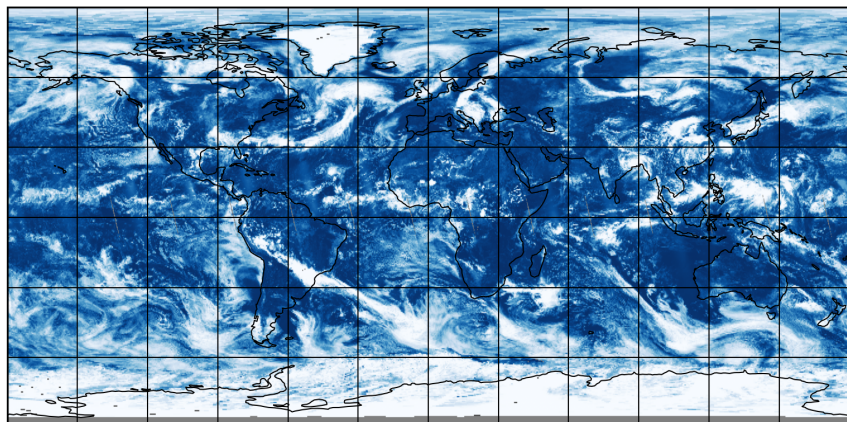


Figure 7: Map of “Cloud fraction” for 2024-09-14 to 2024-09-16

2024-09-15

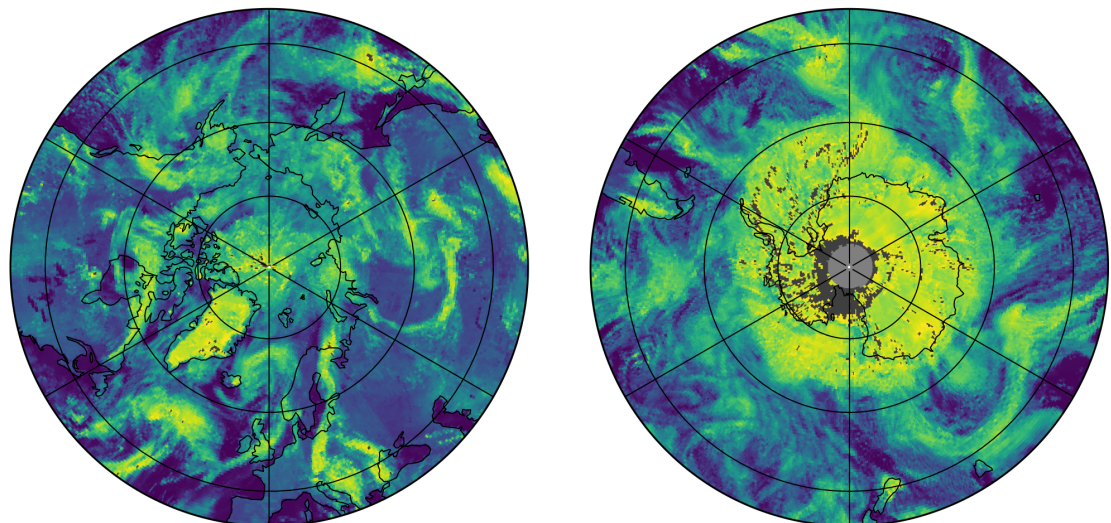
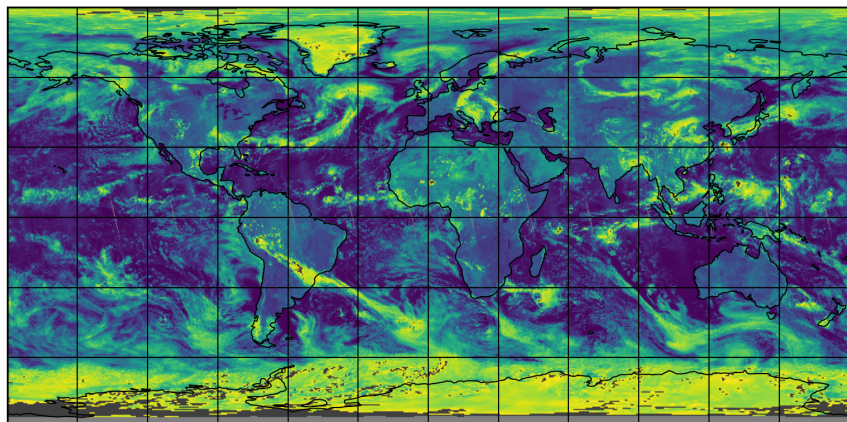


Figure 8: Map of “Scene albedo” for 2024-09-14 to 2024-09-16

2024-09-15

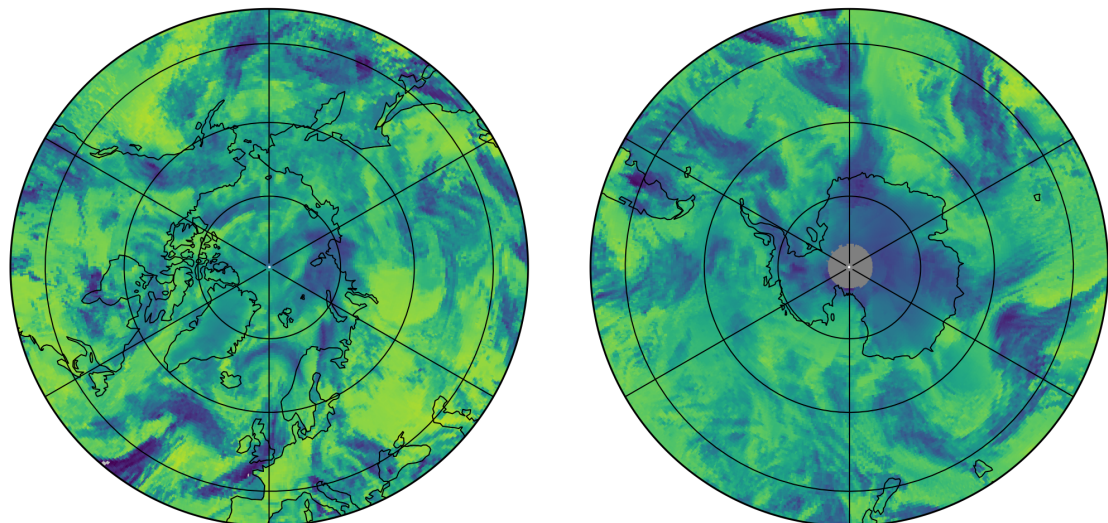
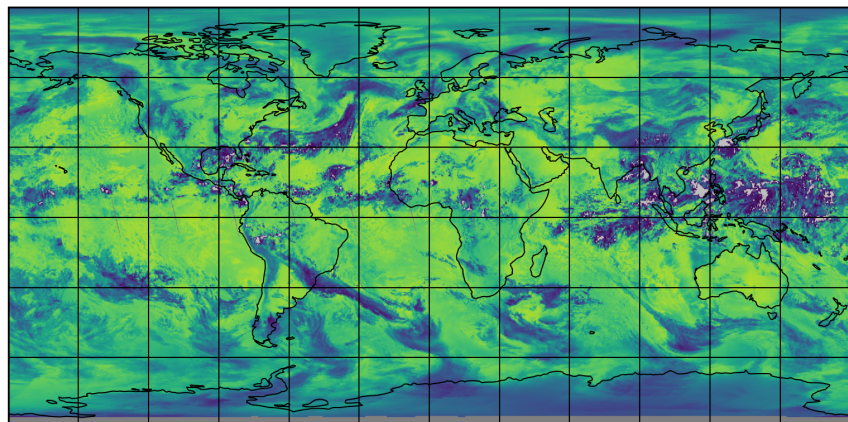


Figure 9: Map of “Apparent scene pressure” for 2024-09-14 to 2024-09-16

2024-09-15

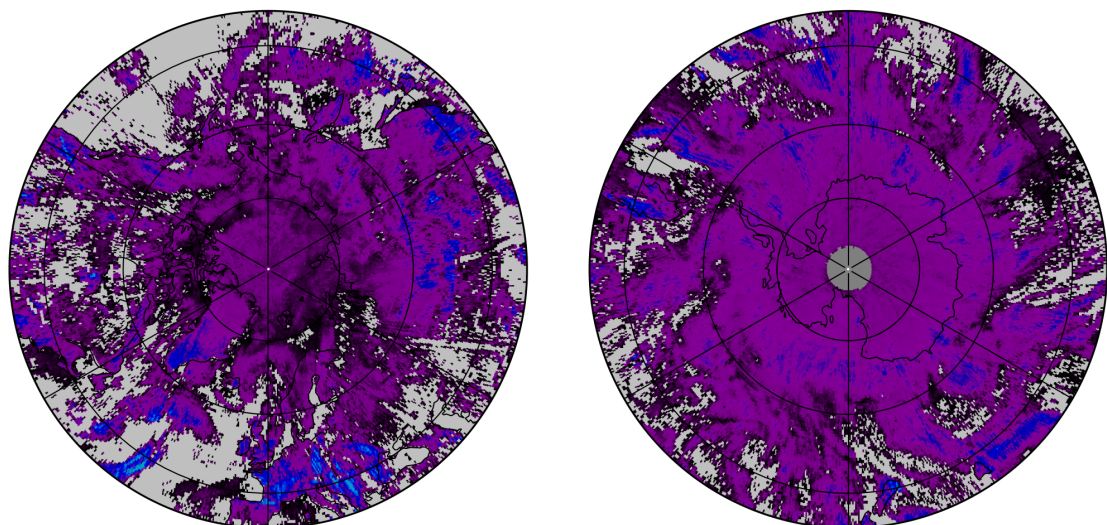
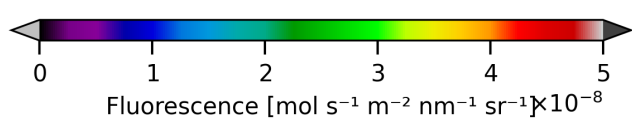
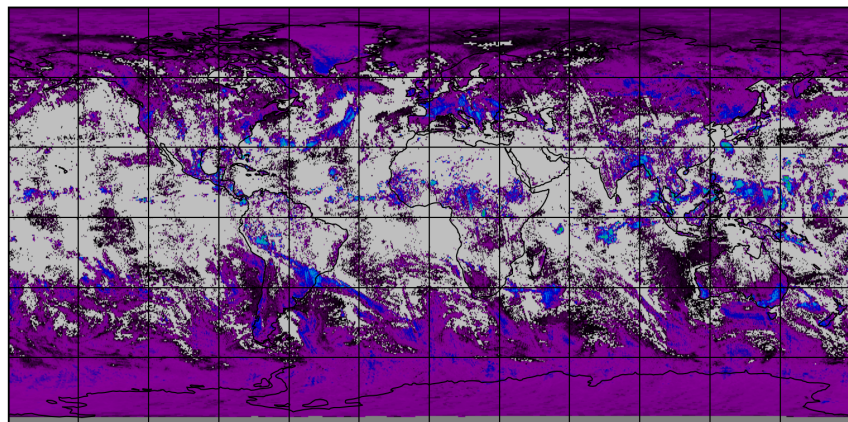


Figure 10: Map of “Fluorescence” for 2024-09-14 to 2024-09-16

2024-09-15

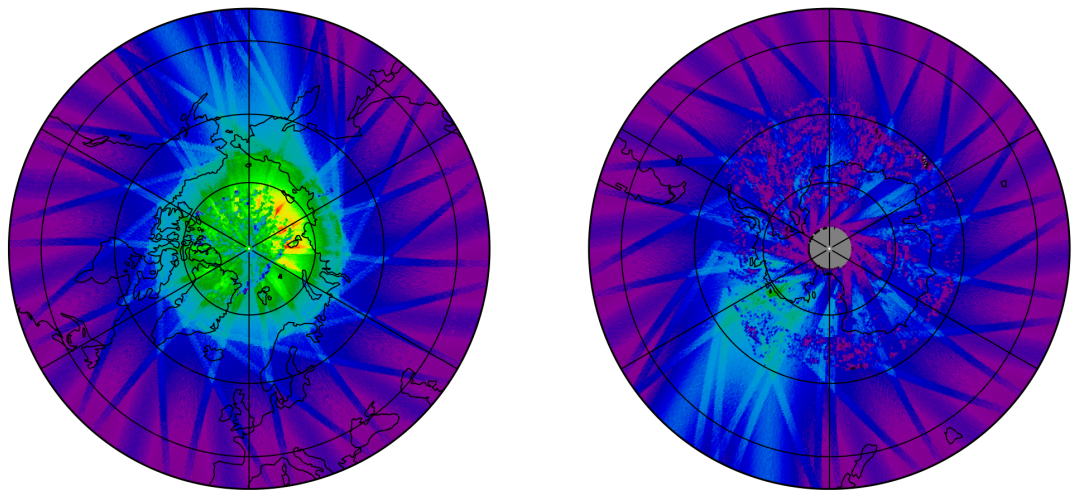
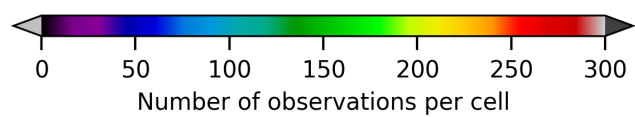
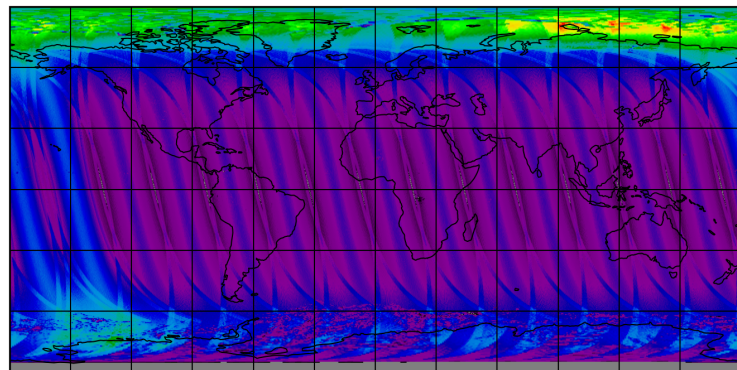


Figure 11: Map of the number of observations for 2024-09-14 to 2024-09-16

## 7 Zonal average

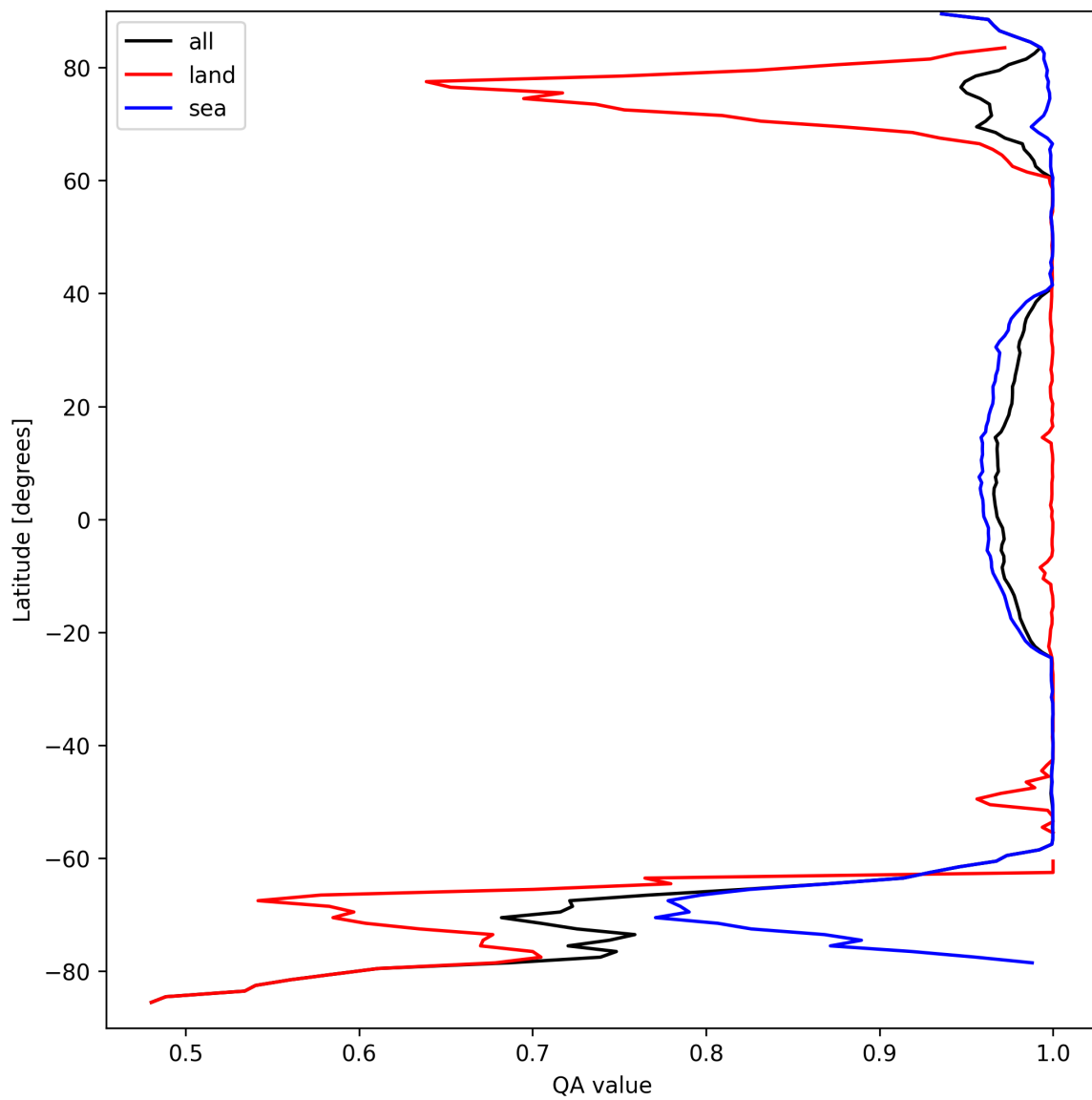


Figure 12: Zonal average of “QA value” for 2024-09-14 to 2024-09-16.

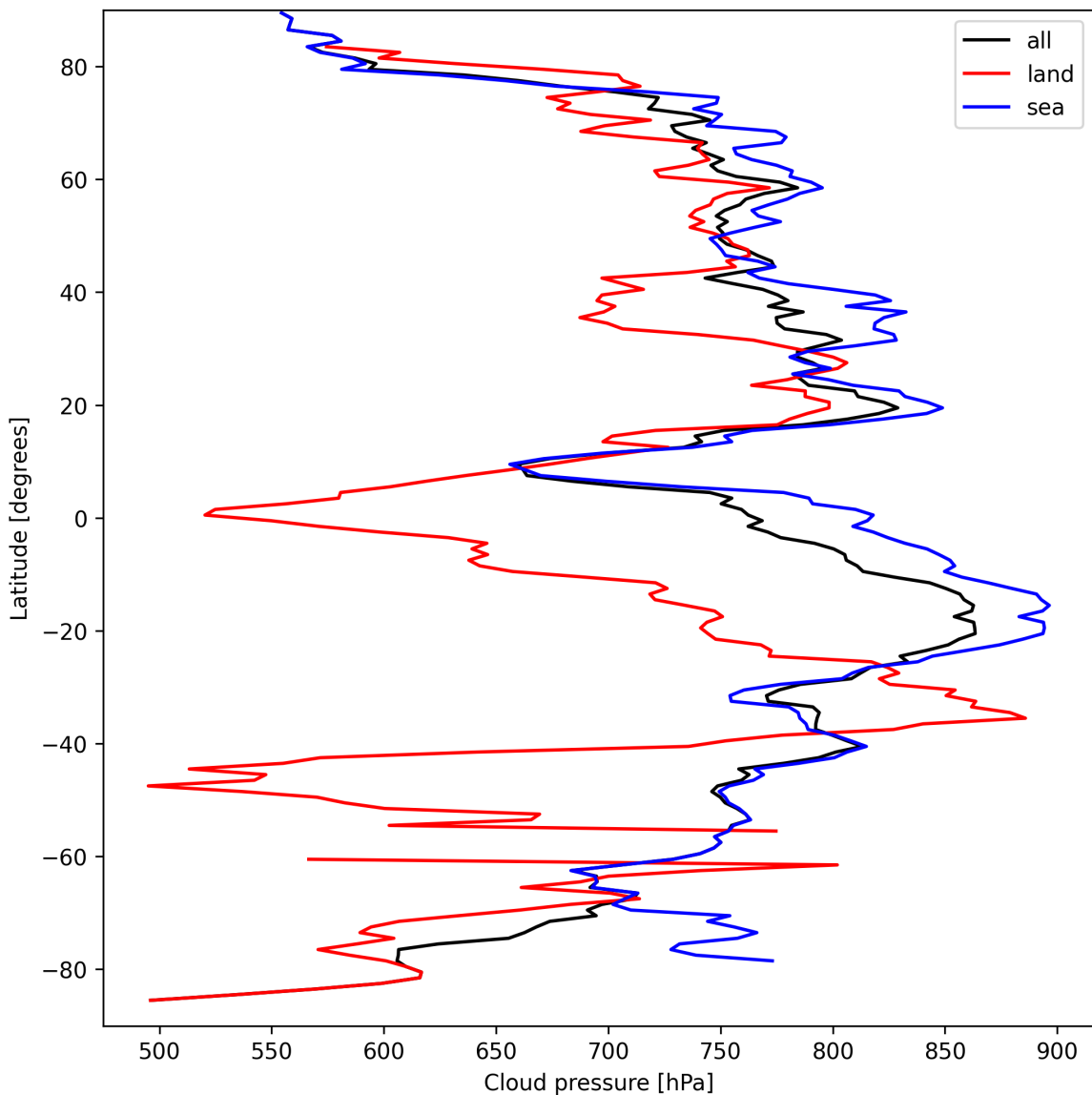


Figure 13: Zonal average of “Cloud pressure” for 2024-09-14 to 2024-09-16.

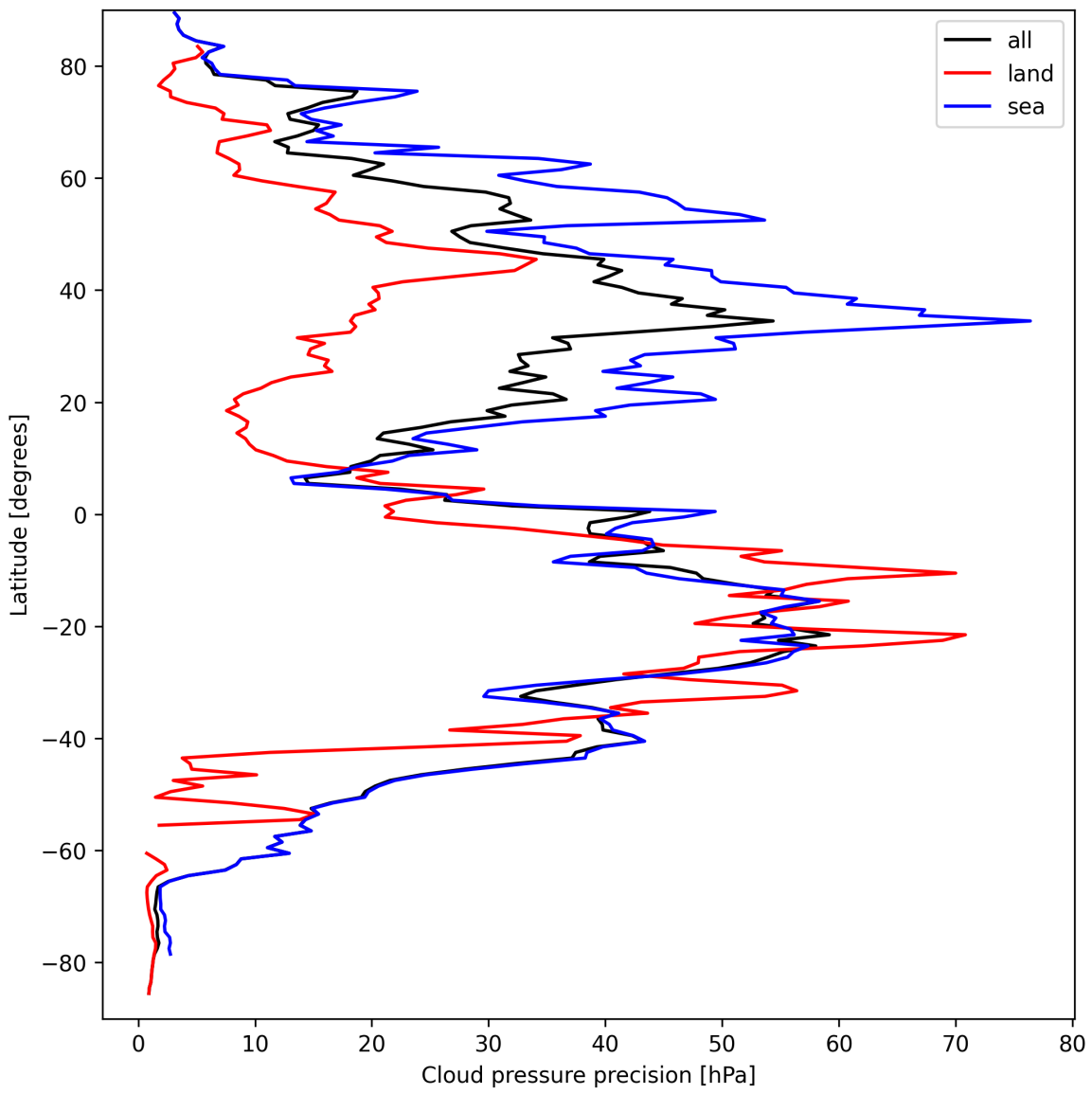


Figure 14: Zonal average of “Cloud pressure precision” for 2024-09-14 to 2024-09-16.

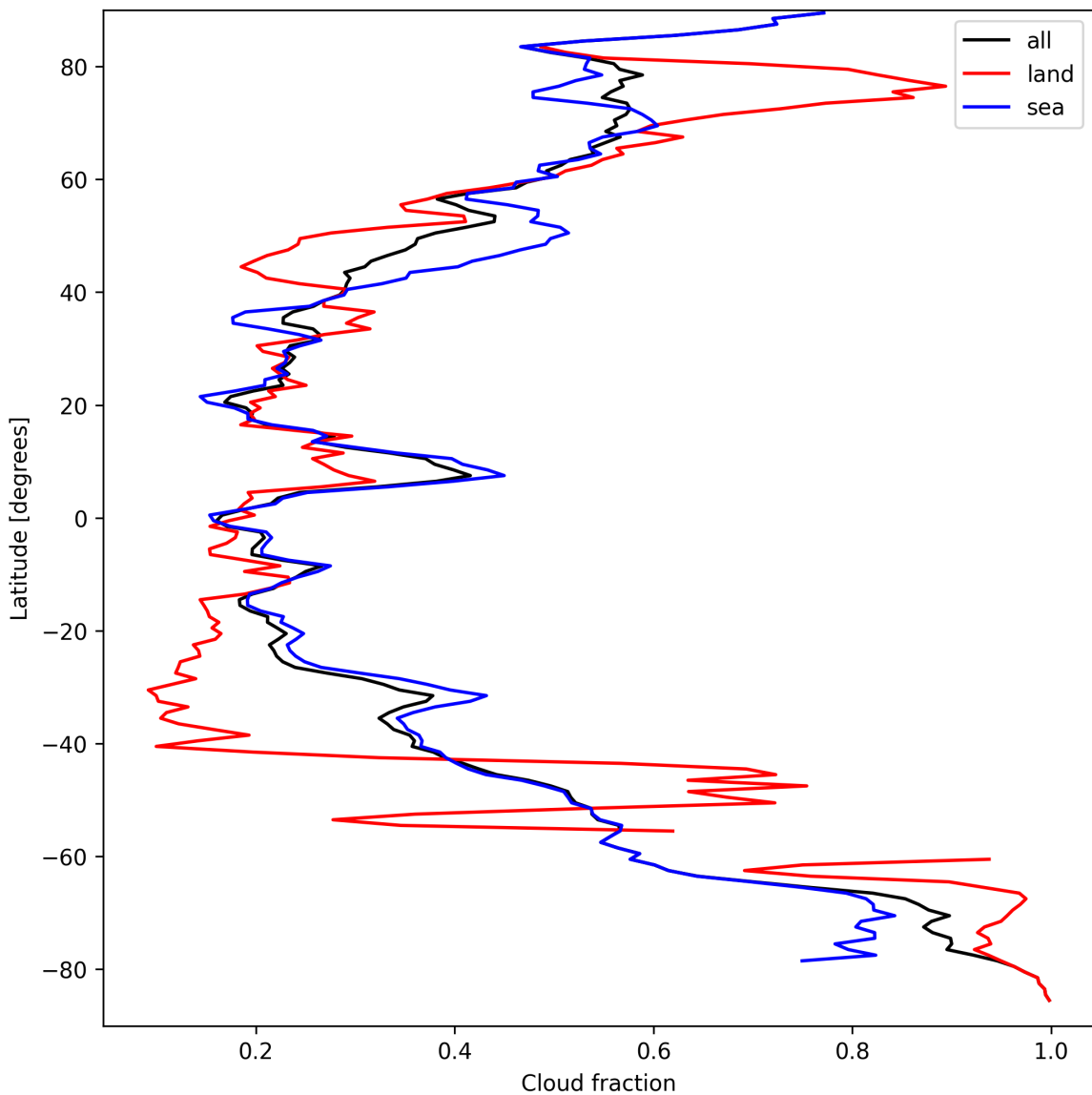


Figure 15: Zonal average of “Cloud fraction” for 2024-09-14 to 2024-09-16.

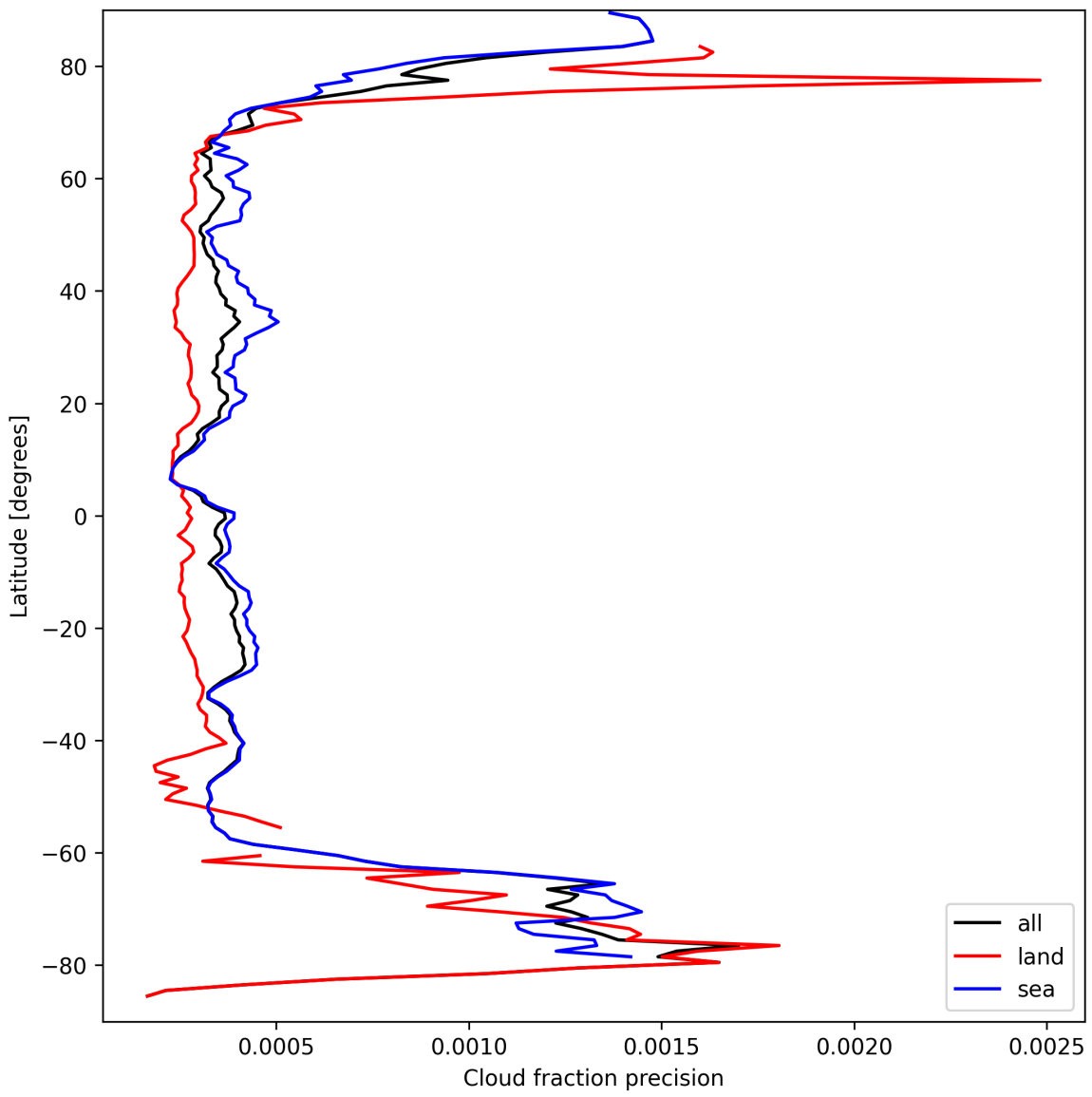


Figure 16: Zonal average of “Cloud fraction precision” for 2024-09-14 to 2024-09-16.

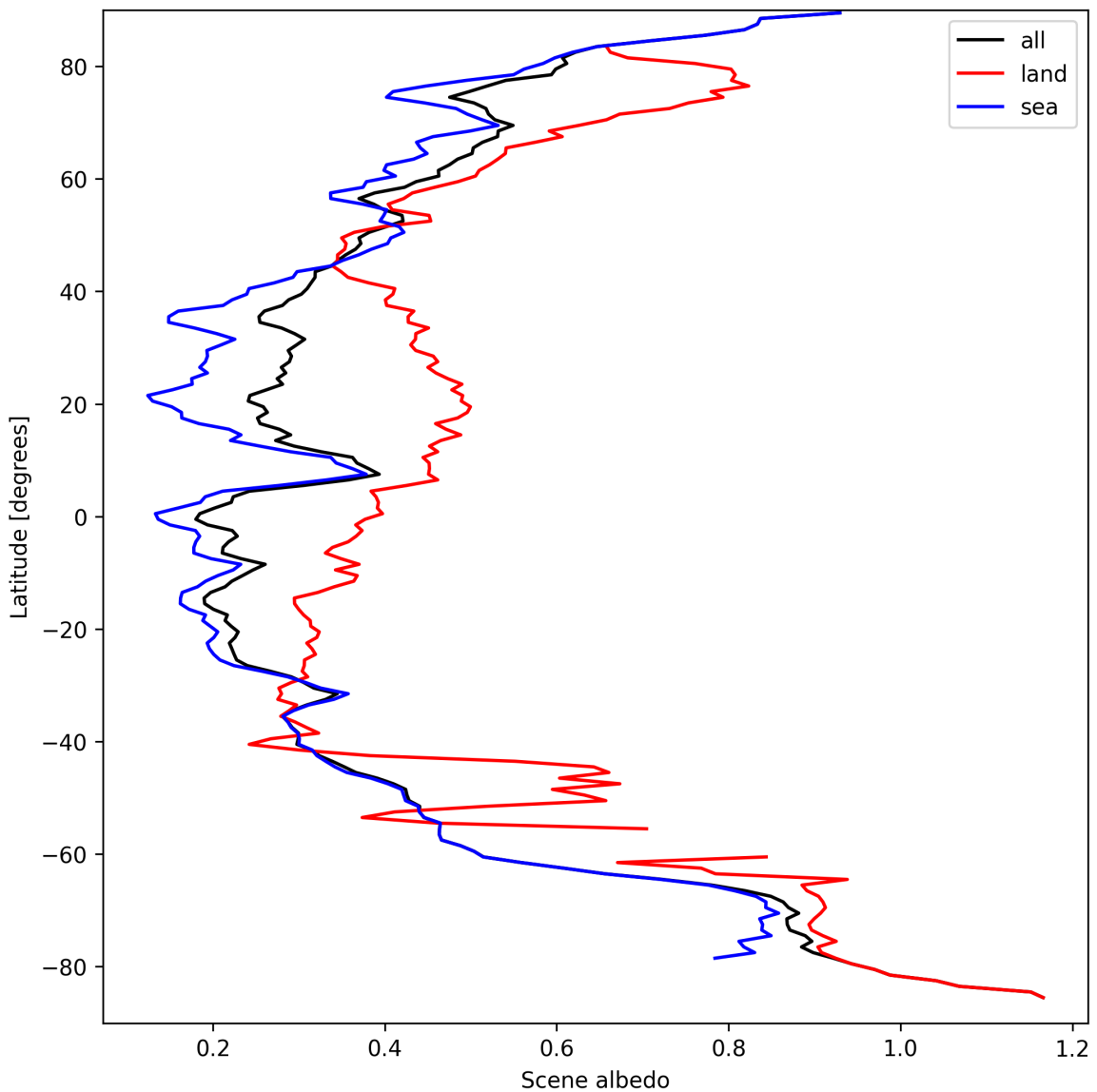


Figure 17: Zonal average of “Scene albedo” for 2024-09-14 to 2024-09-16.

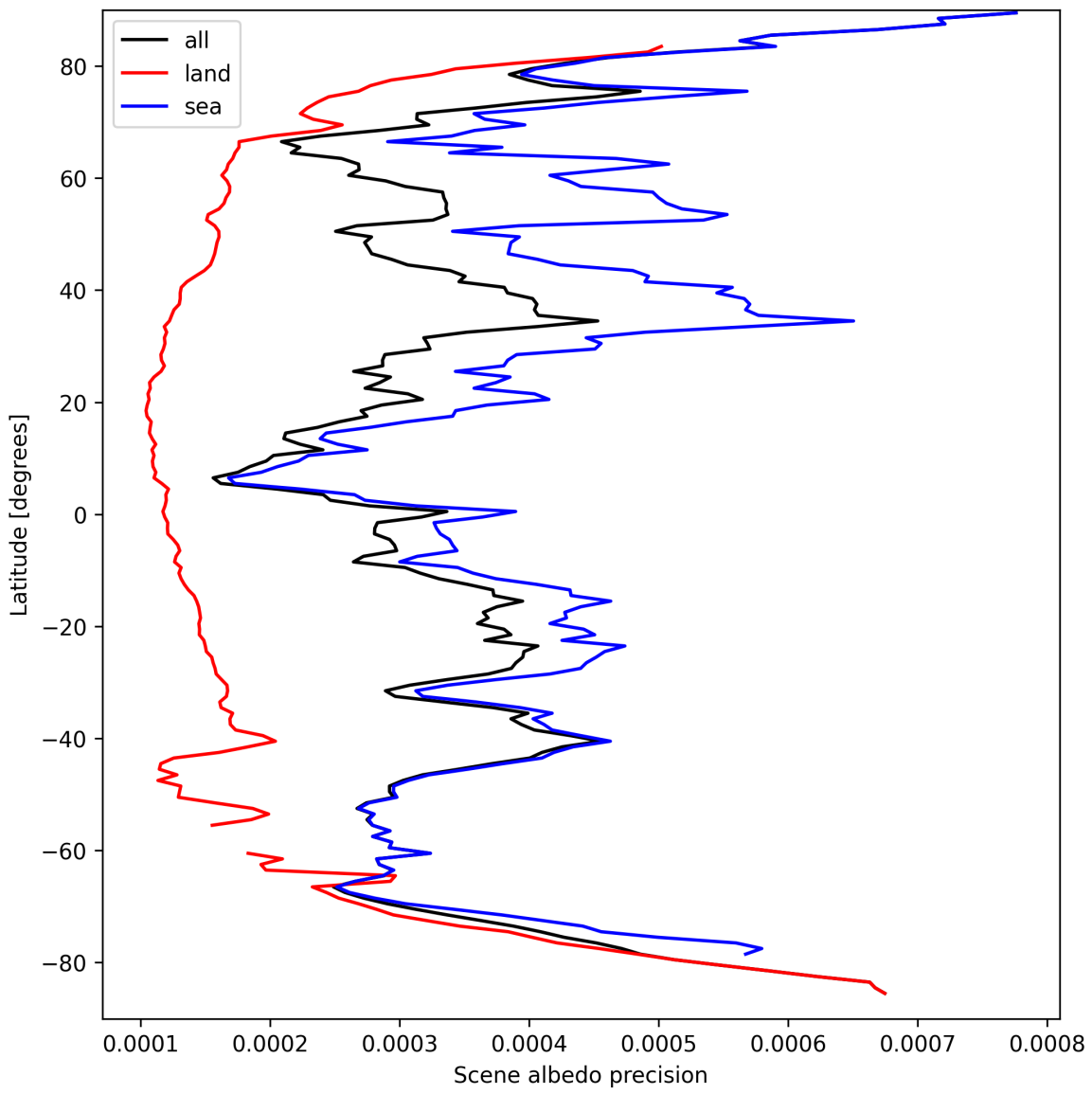


Figure 18: Zonal average of “Scene albedo precision” for 2024-09-14 to 2024-09-16.

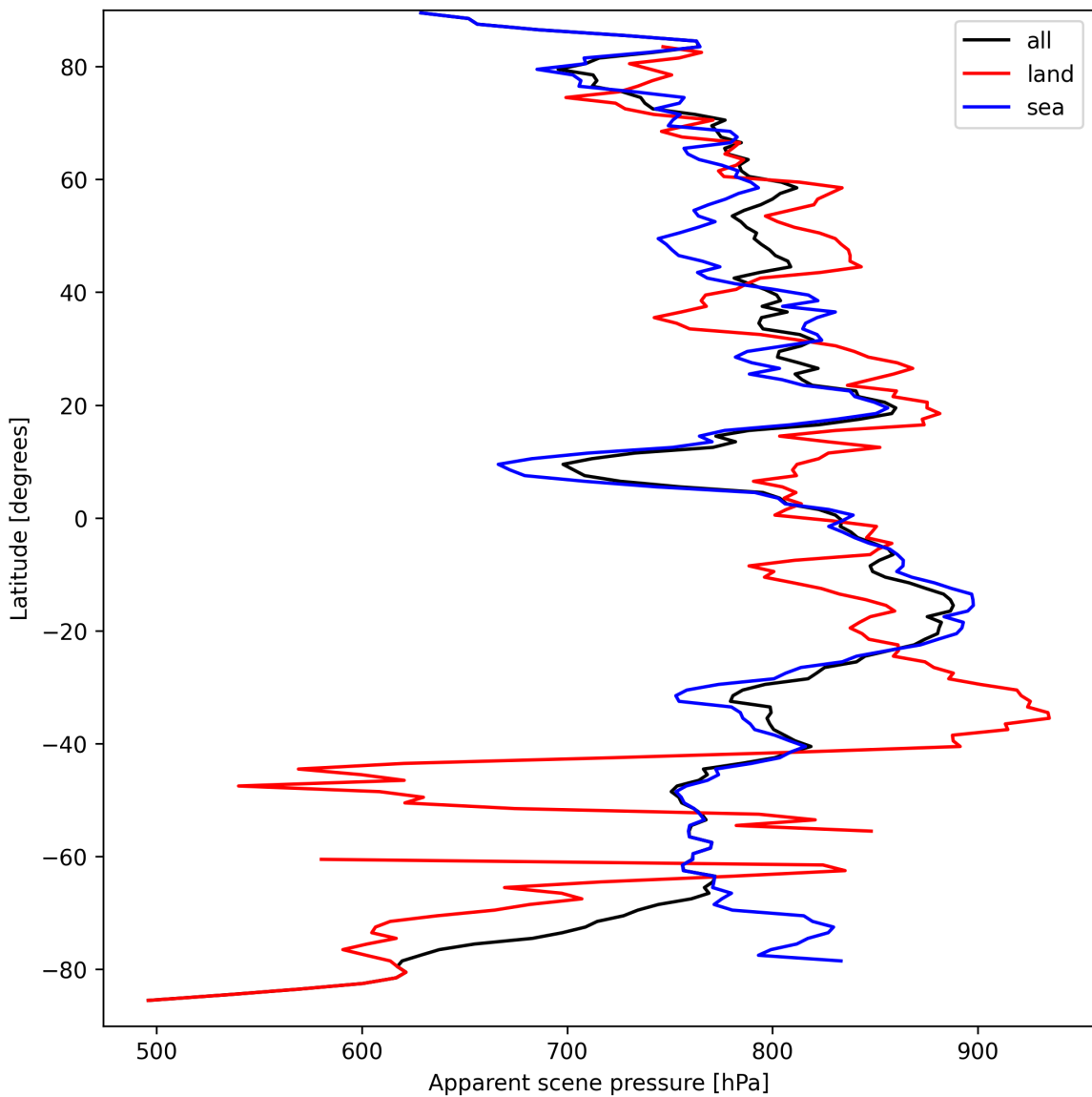


Figure 19: Zonal average of “Apparent scene pressure” for 2024-09-14 to 2024-09-16.

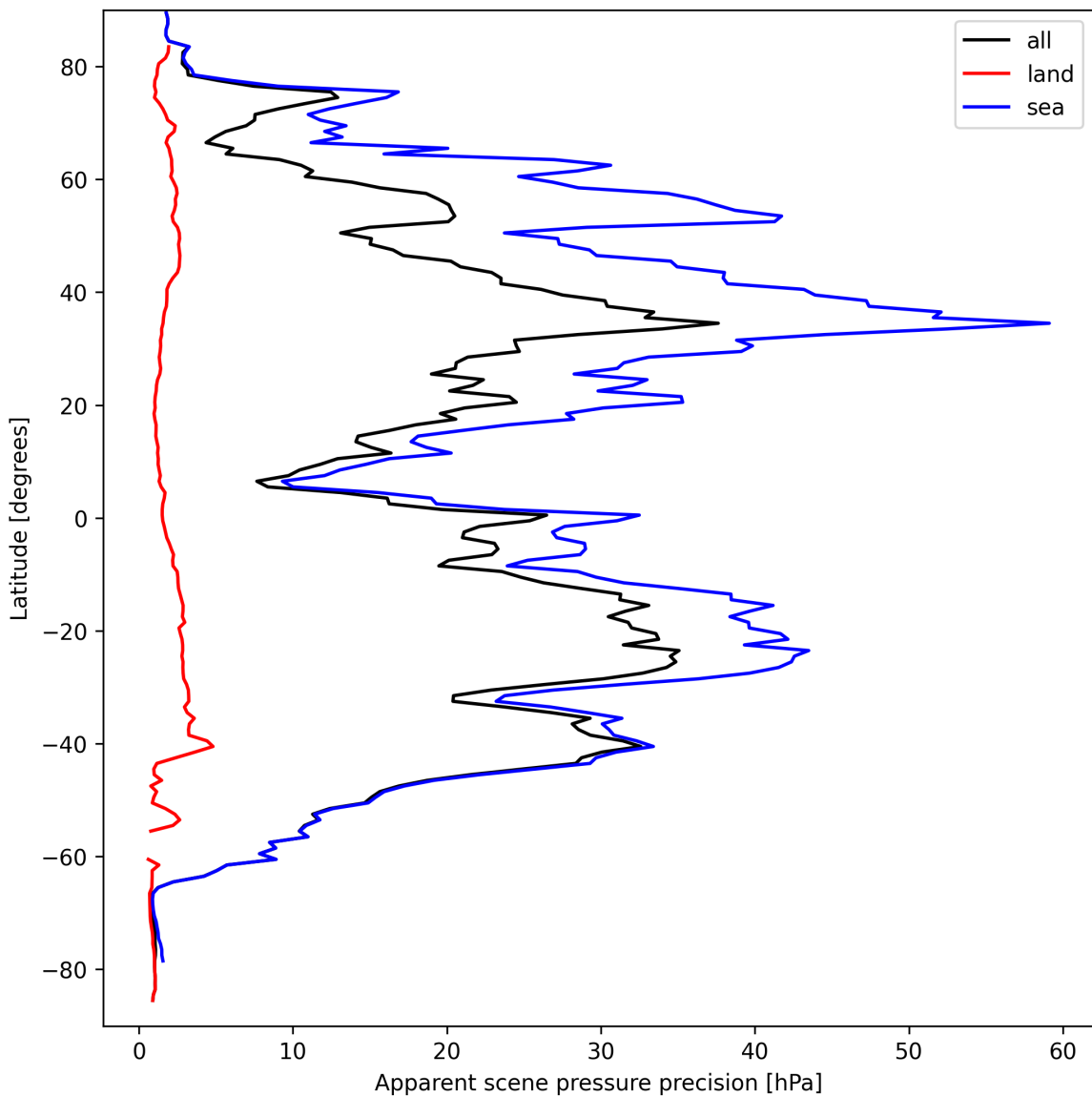


Figure 20: Zonal average of “Apparent scene pressure precision” for 2024-09-14 to 2024-09-16.

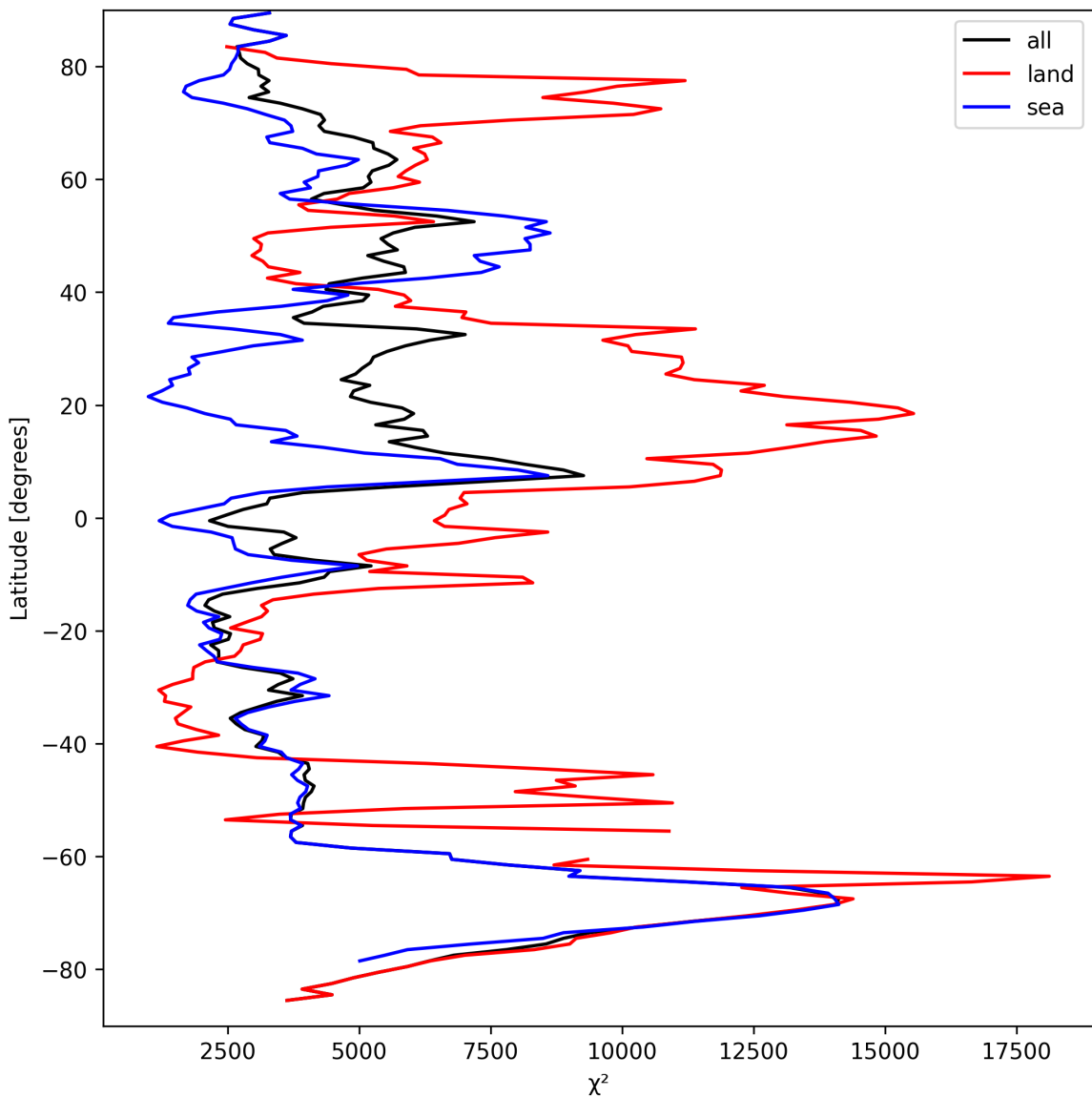


Figure 21: Zonal average of “ $\chi^2$ ” for 2024-09-14 to 2024-09-16.

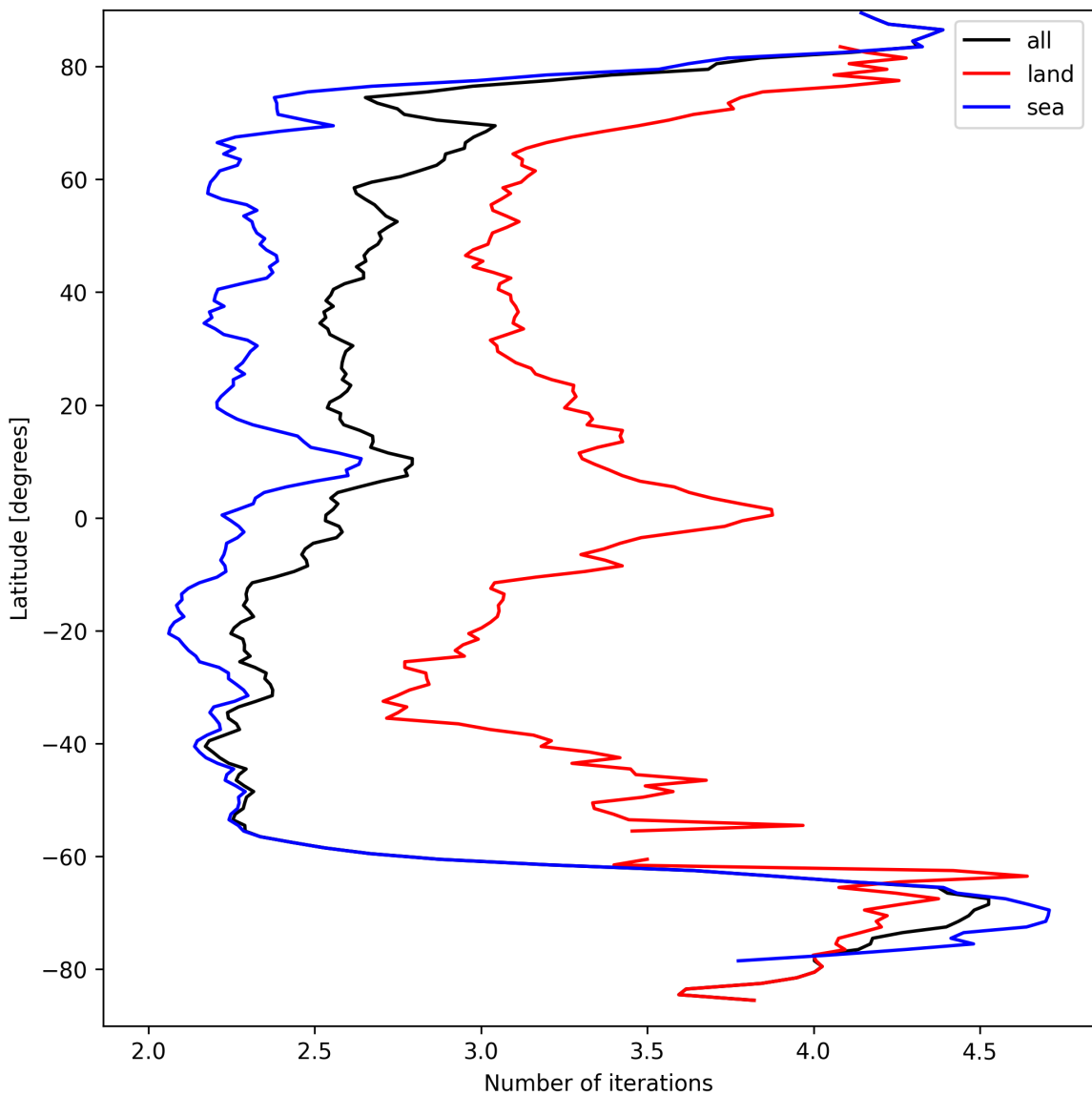


Figure 22: Zonal average of “Number of iterations” for 2024-09-14 to 2024-09-16.

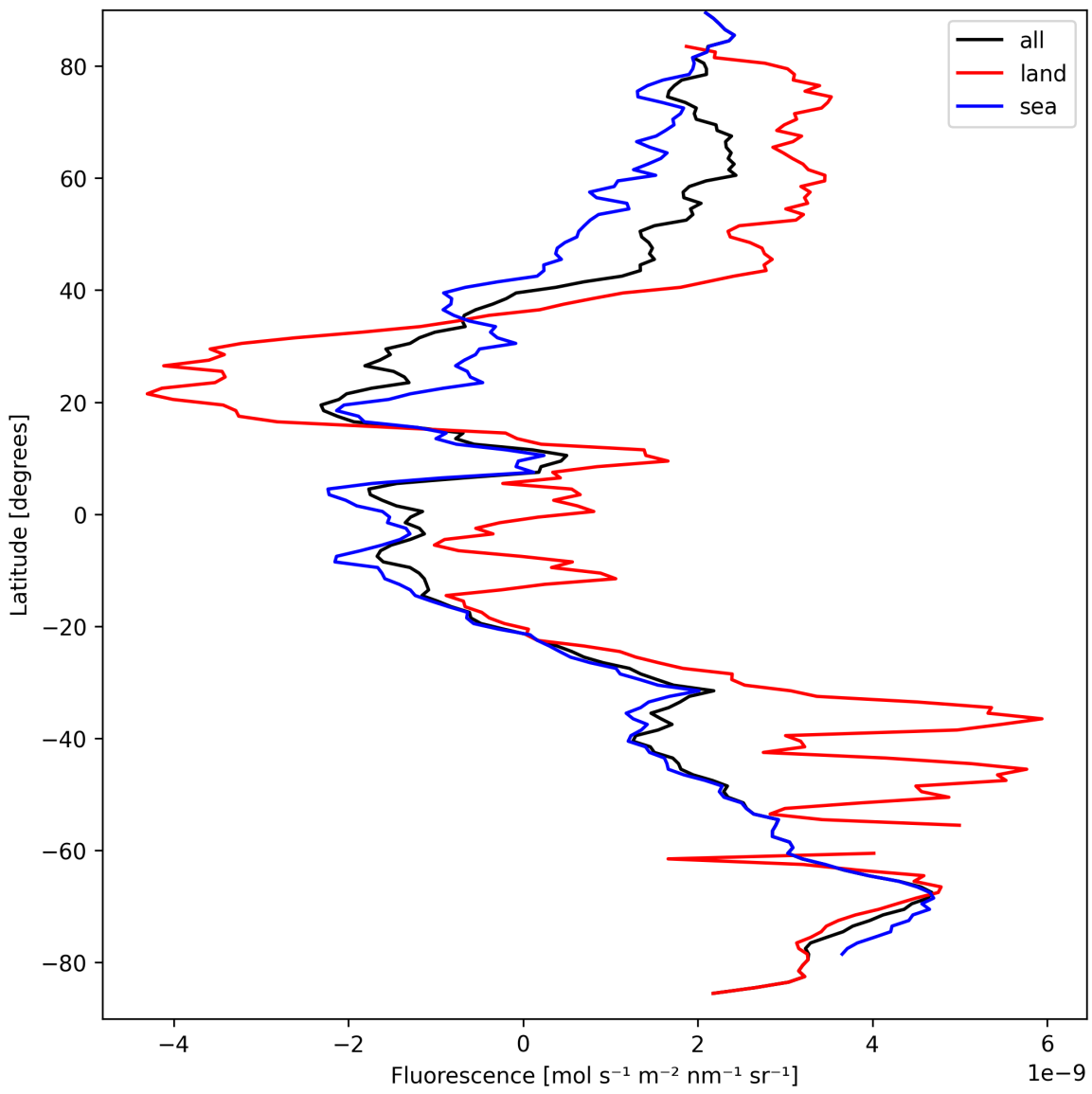


Figure 23: Zonal average of “Fluorescence” for 2024-09-14 to 2024-09-16.

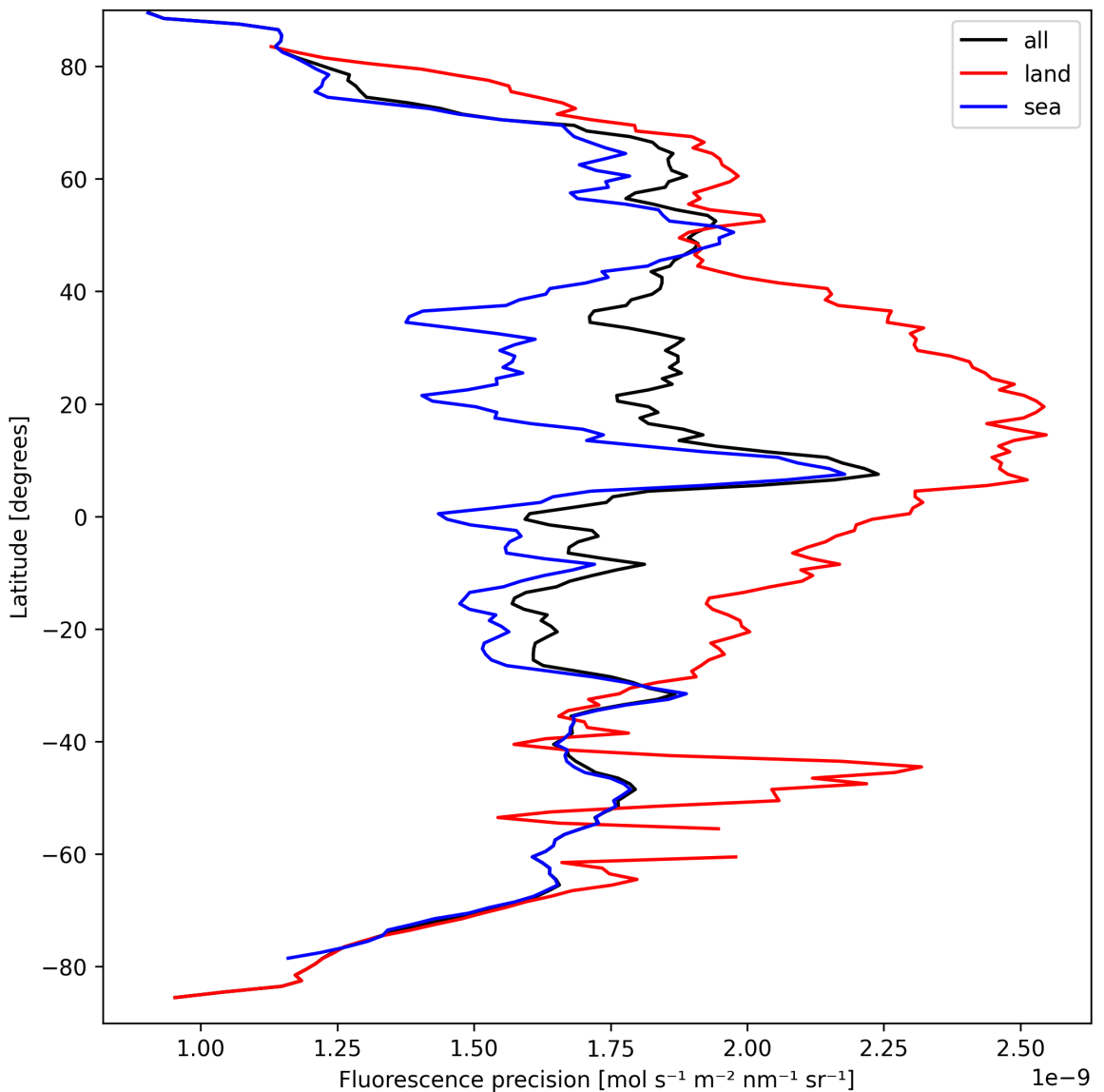


Figure 24: Zonal average of “Fluorescence precision” for 2024-09-14 to 2024-09-16.

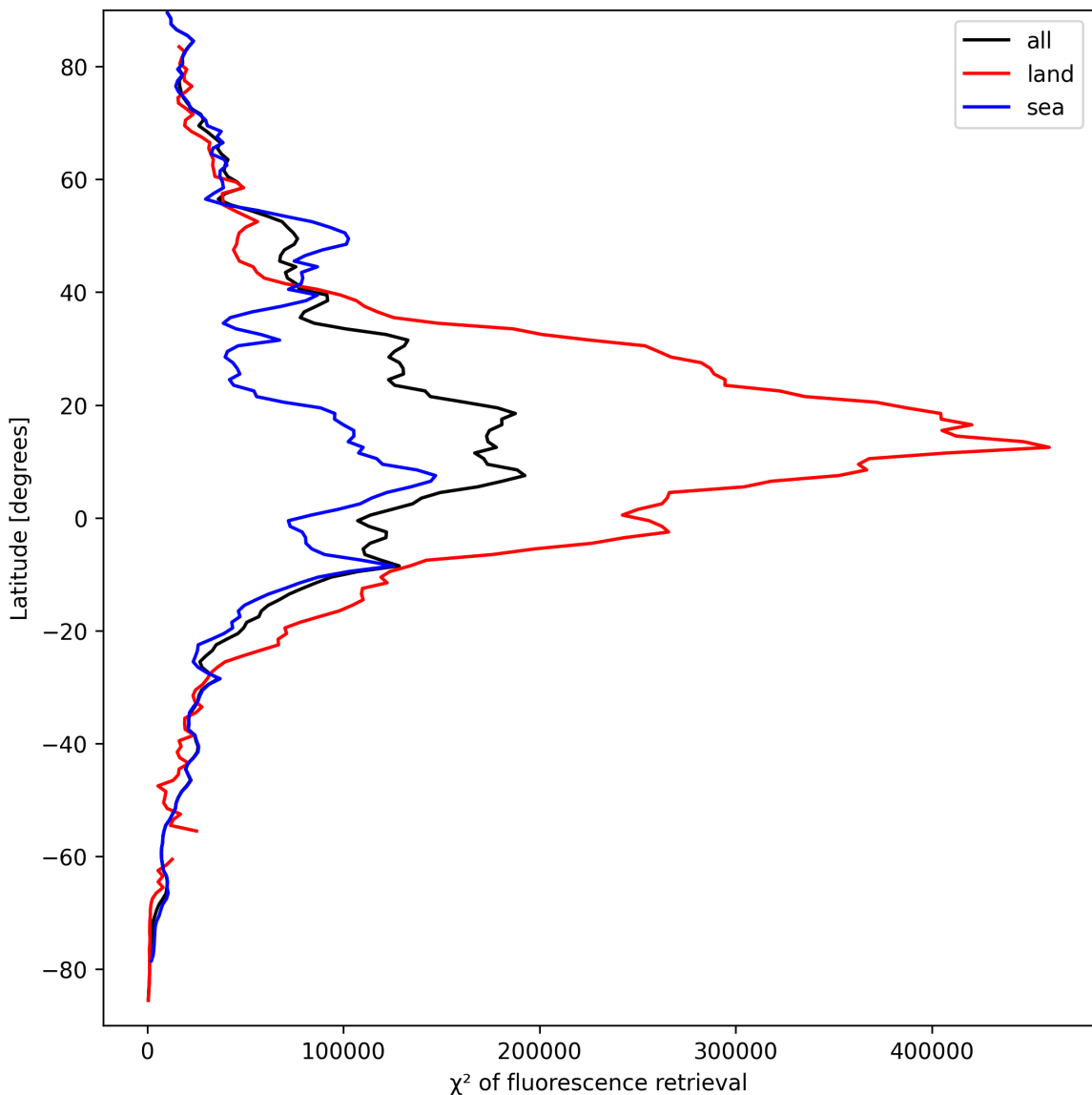


Figure 25: Zonal average of “ $\chi^2$  of fluorescence retrieval” for 2024-09-14 to 2024-09-16.

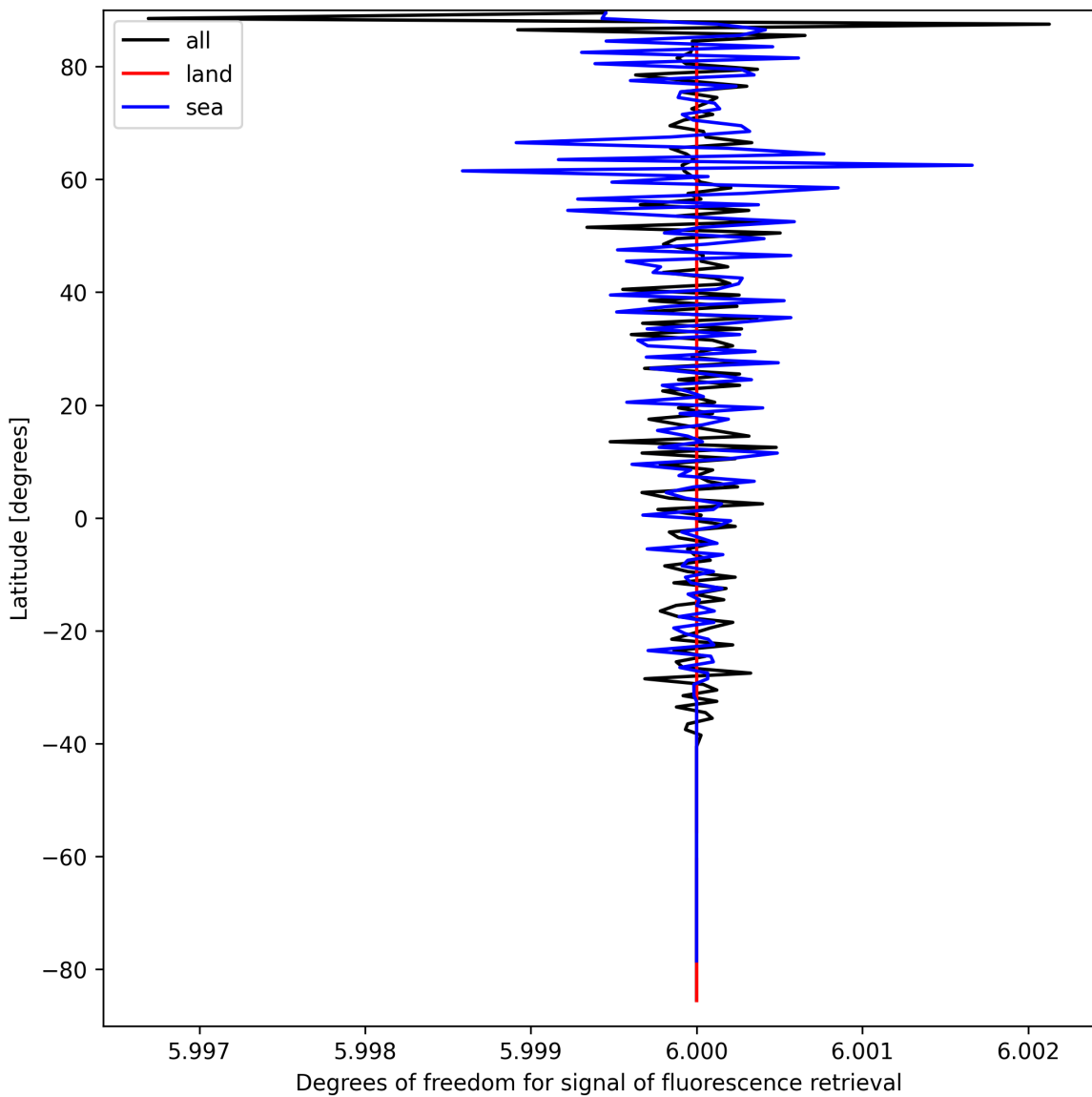


Figure 26: Zonal average of “Degrees of freedom for signal of fluorescence retrieval” for 2024-09-14 to 2024-09-16.

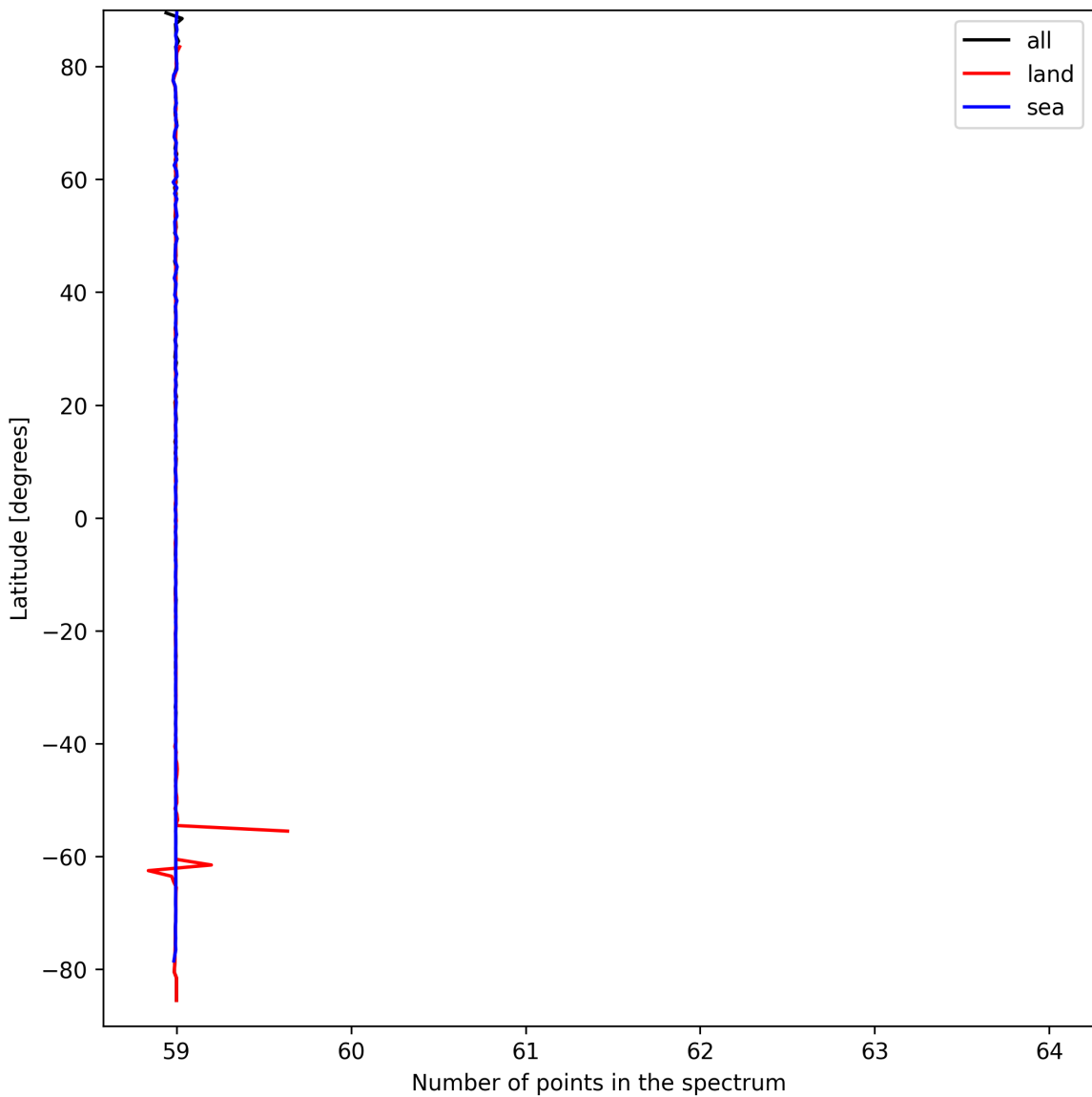


Figure 27: Zonal average of “Number of points in the spectrum” for 2024-09-14 to 2024-09-16.

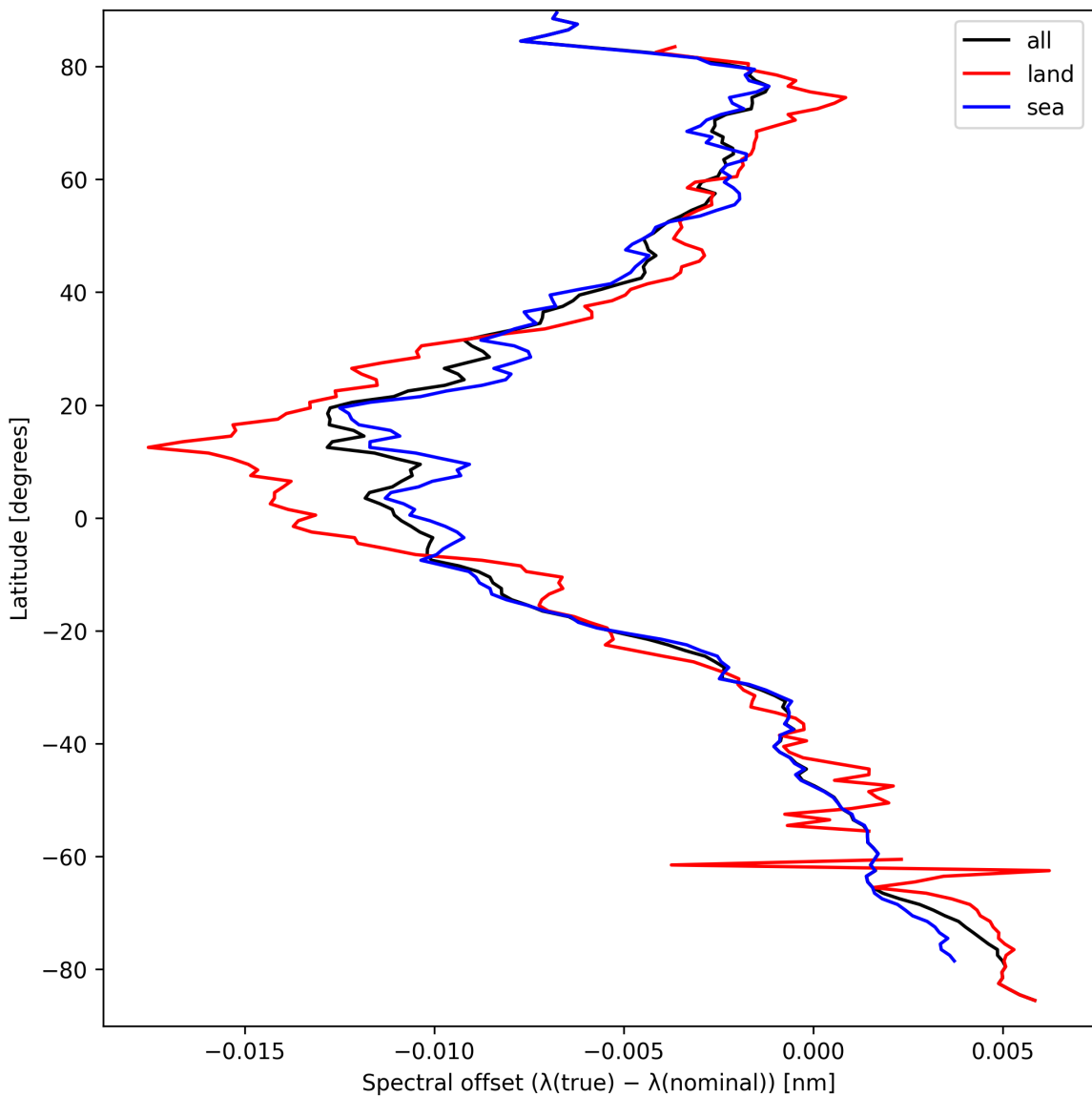


Figure 28: Zonal average of “Spectral offset ( $\lambda_{\text{true}} - \lambda_{\text{nominal}}$ )” for 2024-09-14 to 2024-09-16.

## 8 Histograms

The definitions of the parameters given in this section can be found in section 2.

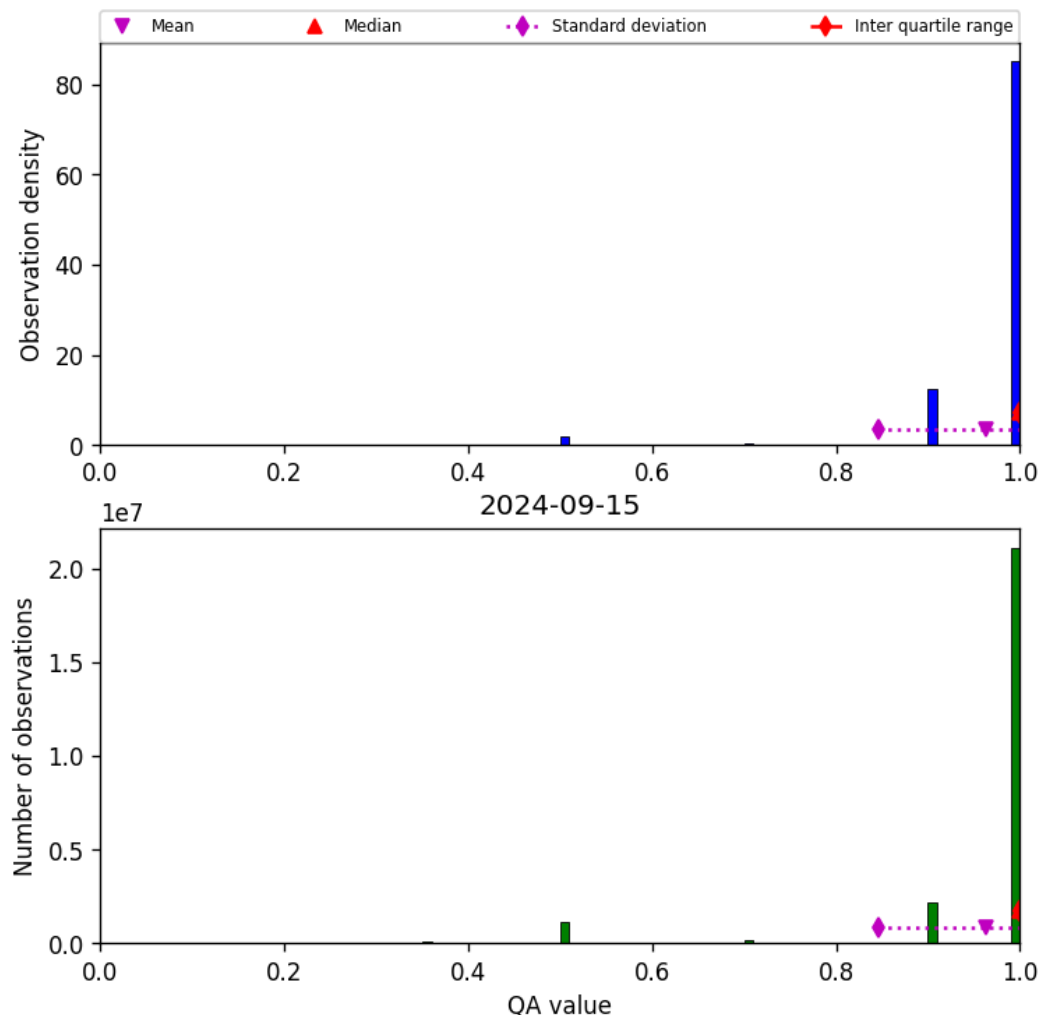


Figure 29: Histogram of “QA value” for 2024-09-14 to 2024-09-16

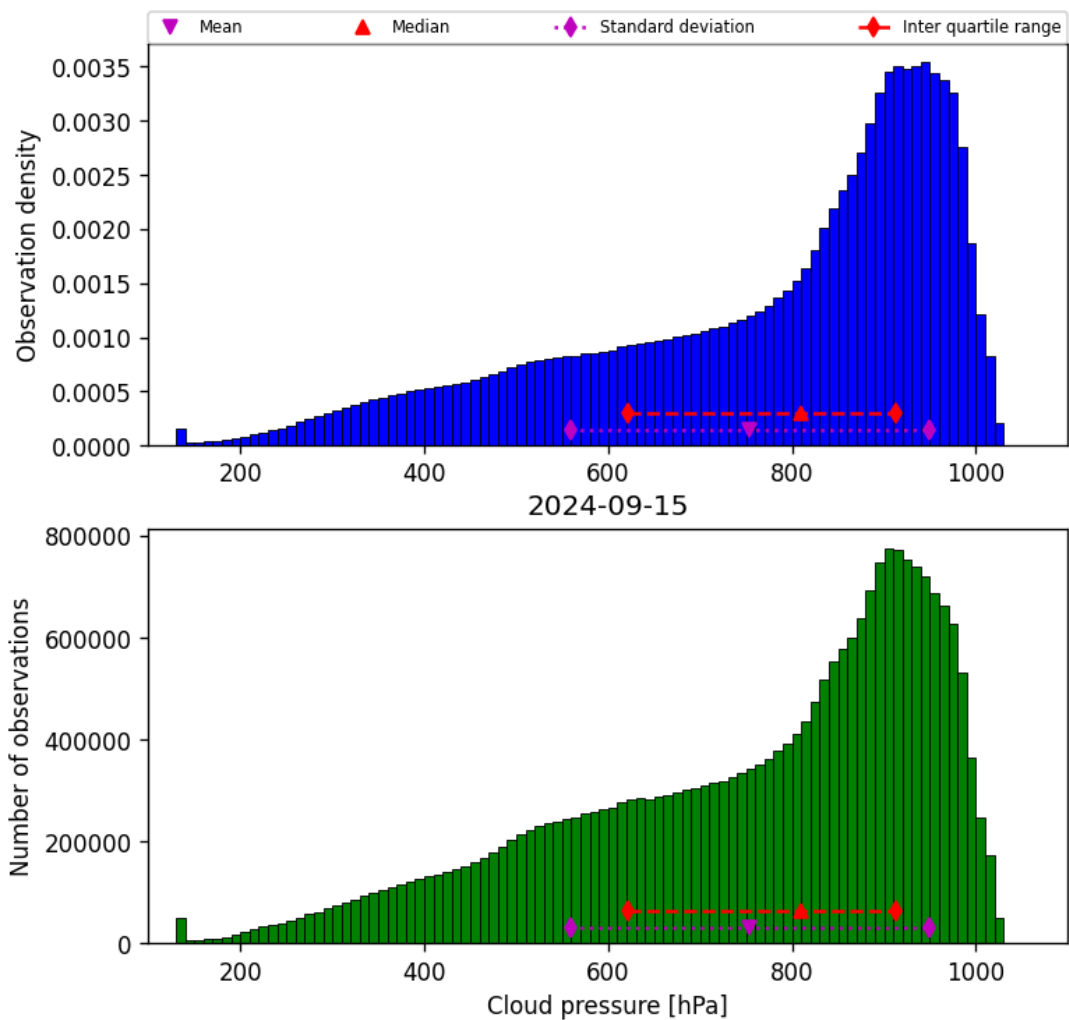


Figure 30: Histogram of “Cloud pressure” for 2024-09-14 to 2024-09-16

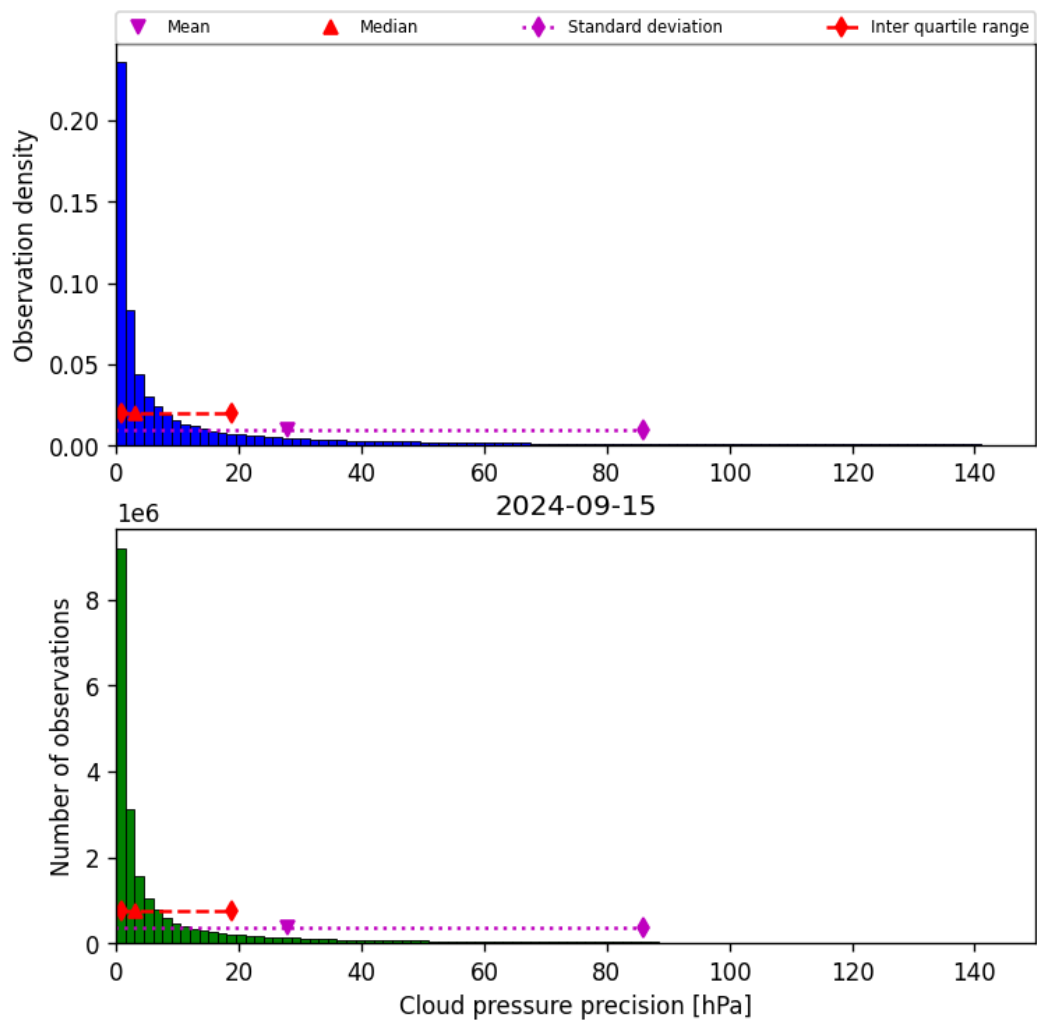


Figure 31: Histogram of “Cloud pressure precision” for 2024-09-14 to 2024-09-16

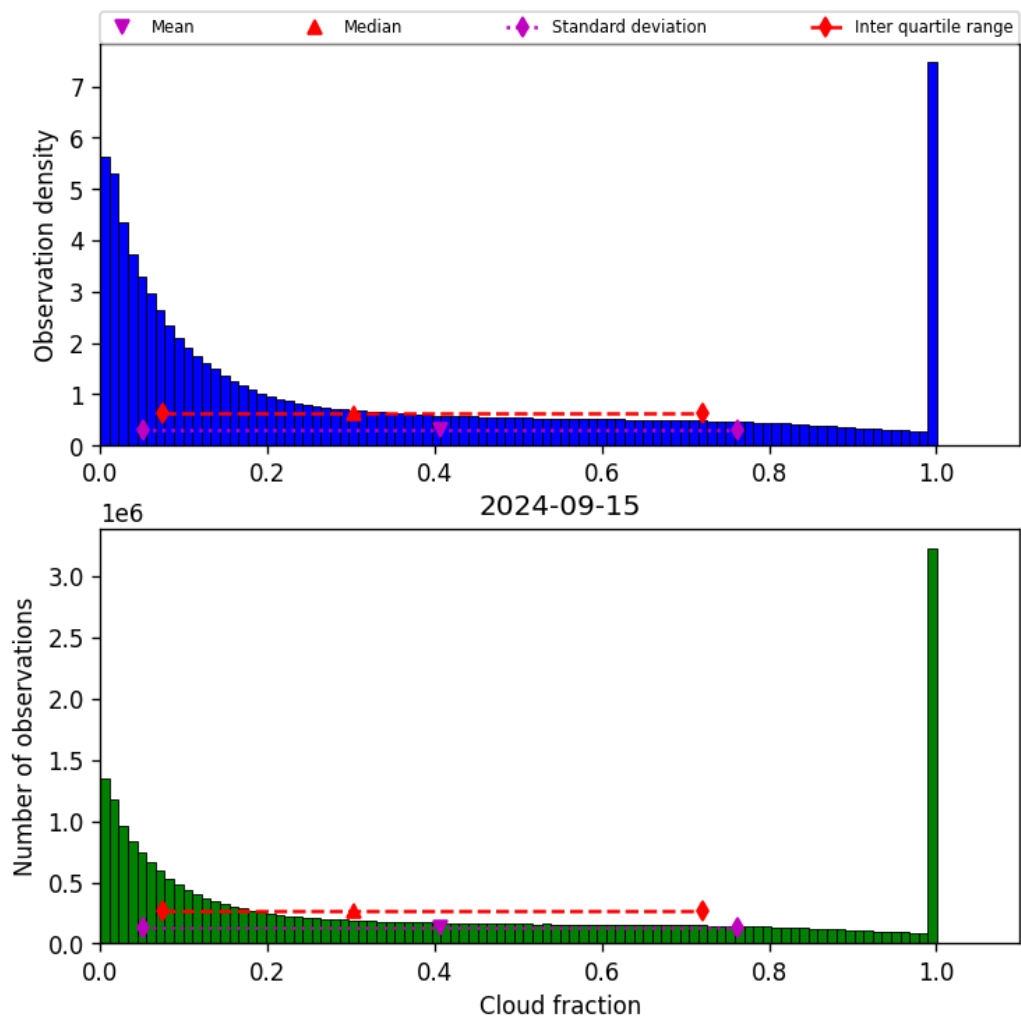


Figure 32: Histogram of “Cloud fraction” for 2024-09-14 to 2024-09-16

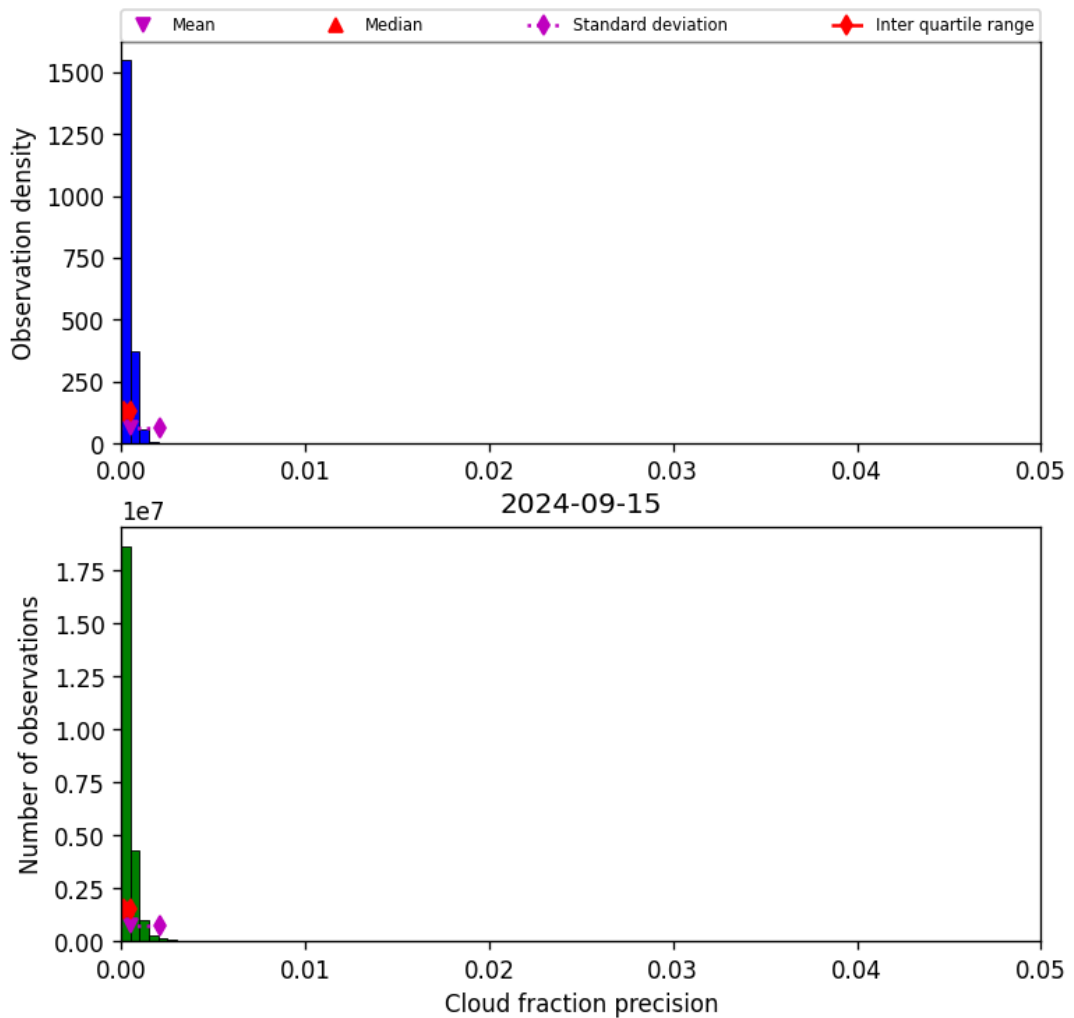


Figure 33: Histogram of “Cloud fraction precision” for 2024-09-14 to 2024-09-16

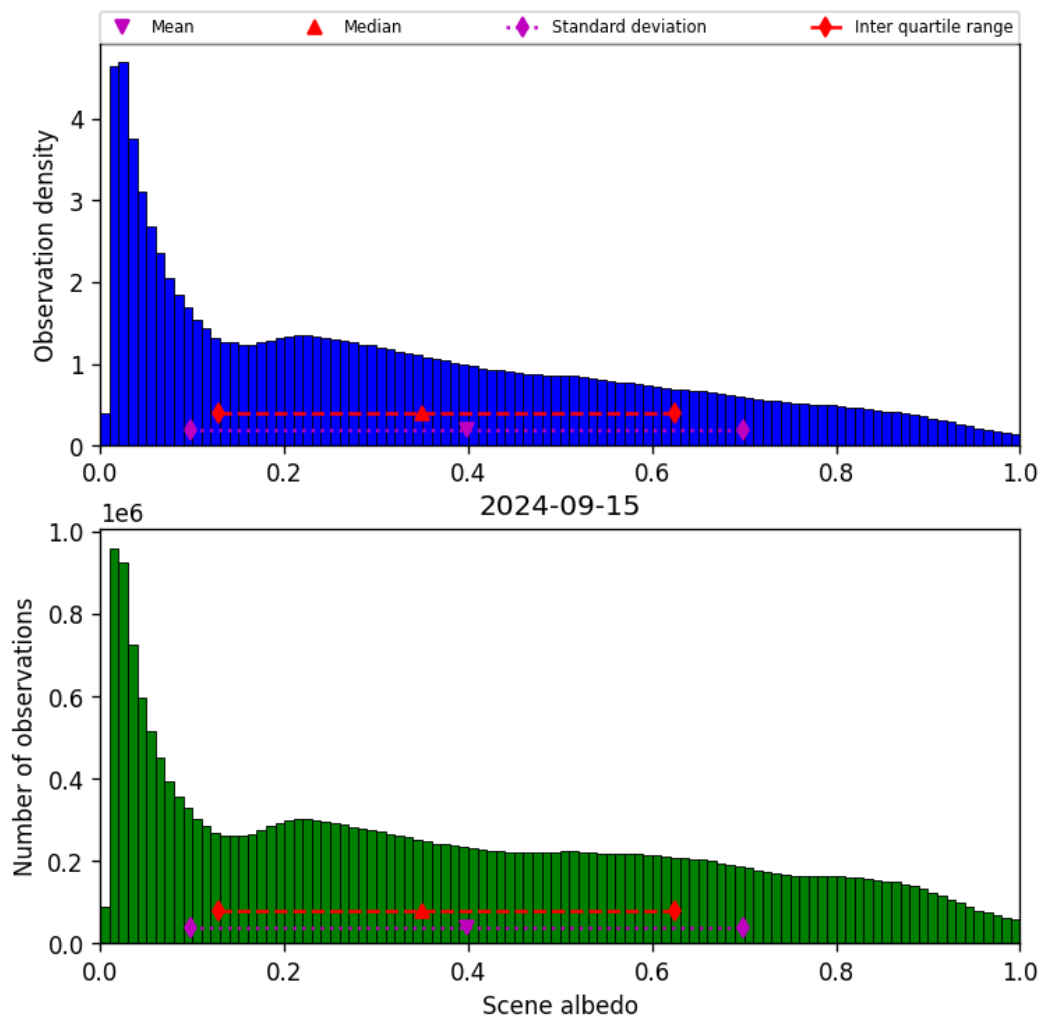


Figure 34: Histogram of “Scene albedo” for 2024-09-14 to 2024-09-16

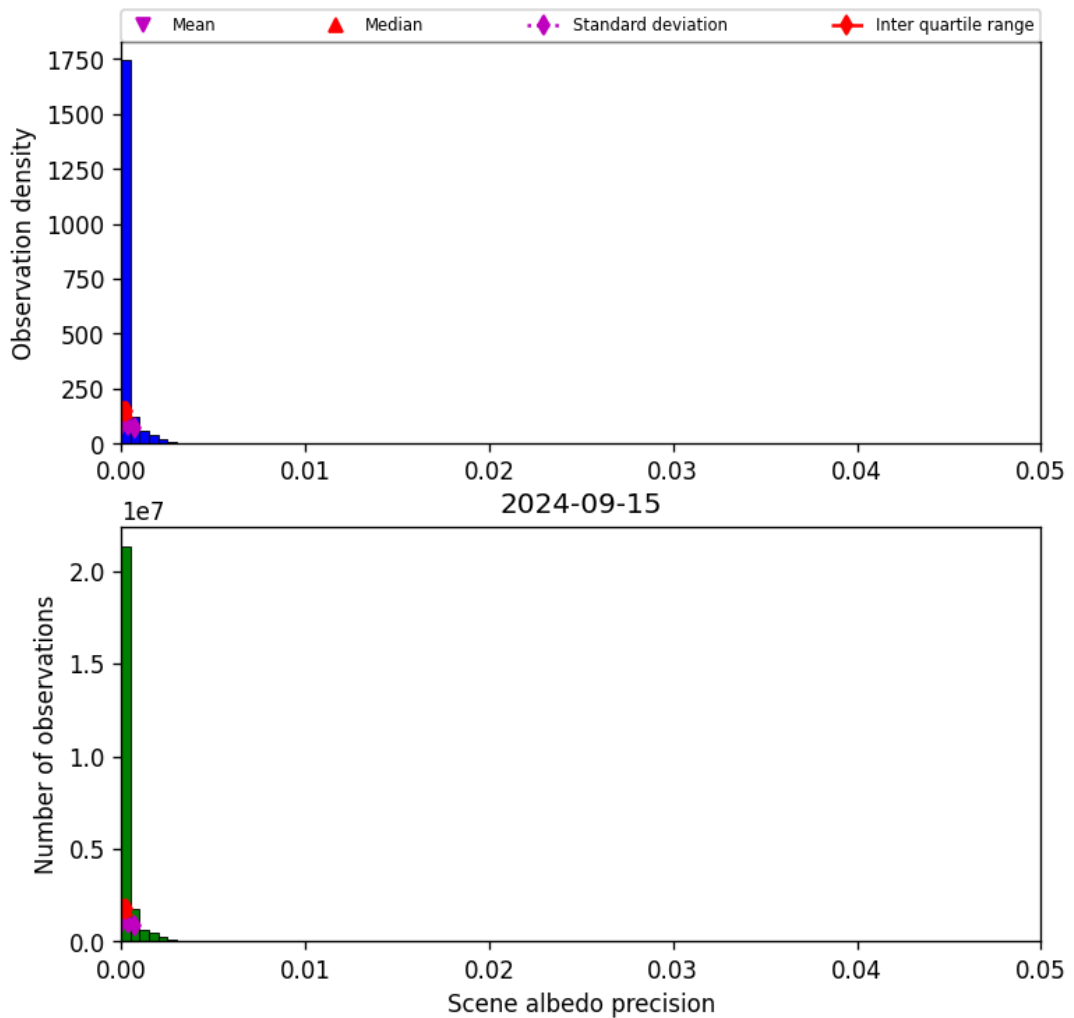


Figure 35: Histogram of “Scene albedo precision” for 2024-09-14 to 2024-09-16

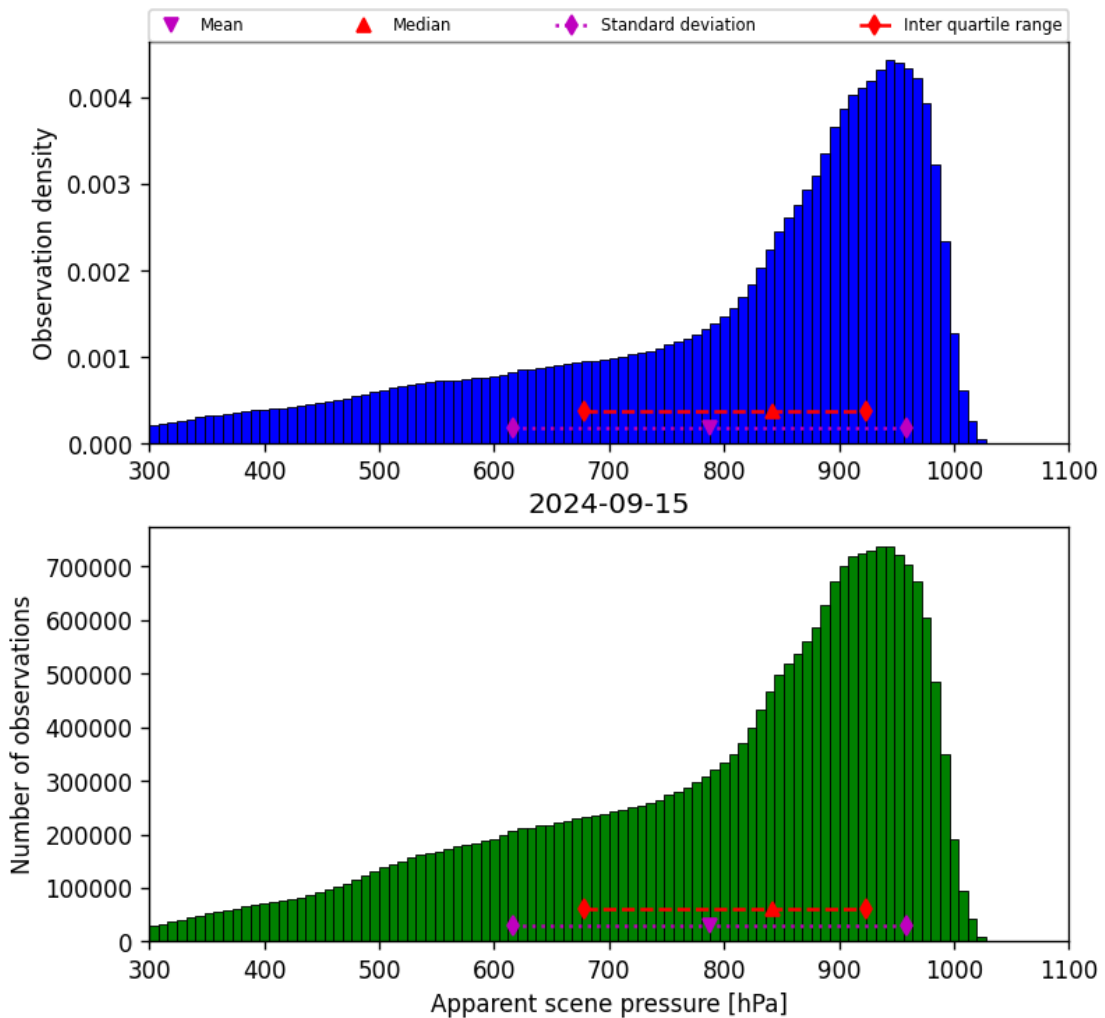


Figure 36: Histogram of “Apparent scene pressure” for 2024-09-14 to 2024-09-16

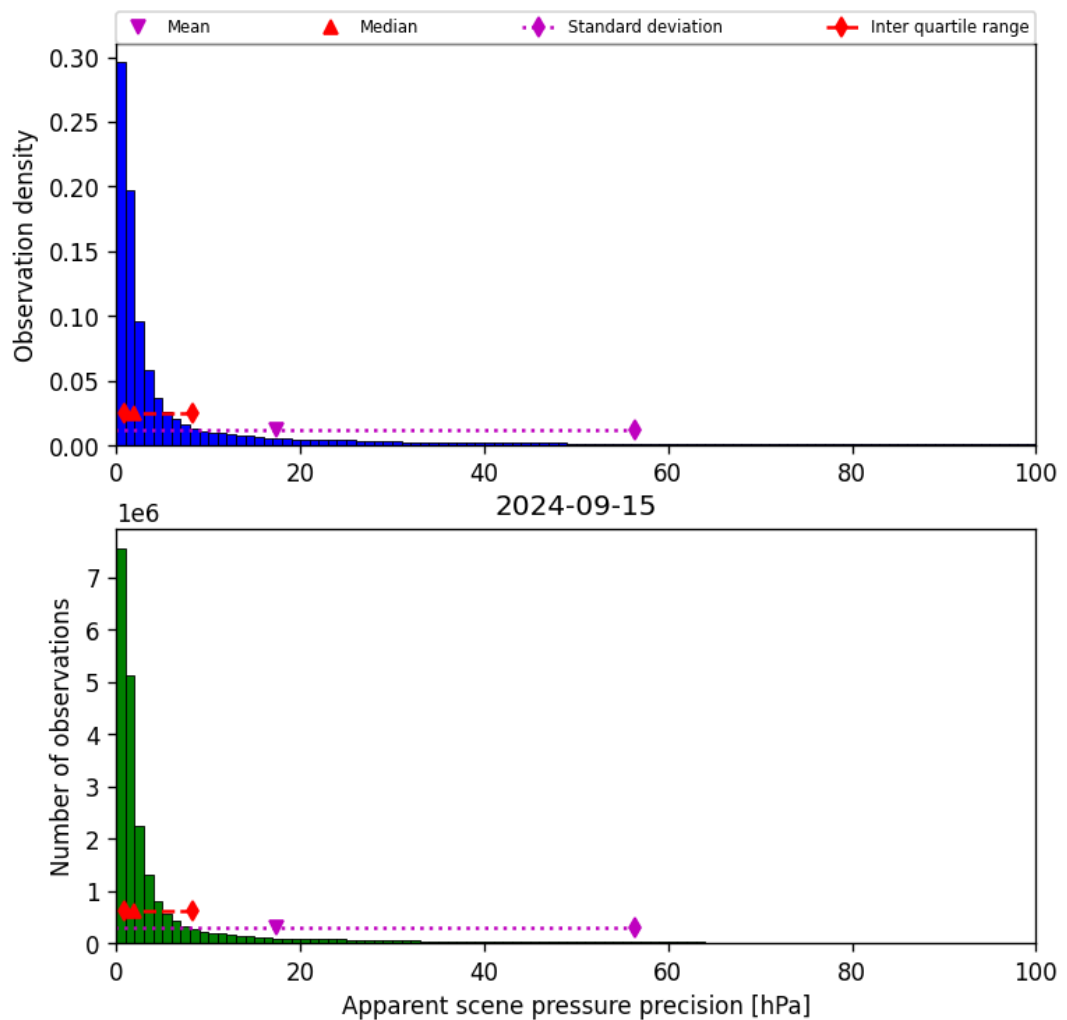


Figure 37: Histogram of “Apparent scene pressure precision” for 2024-09-14 to 2024-09-16

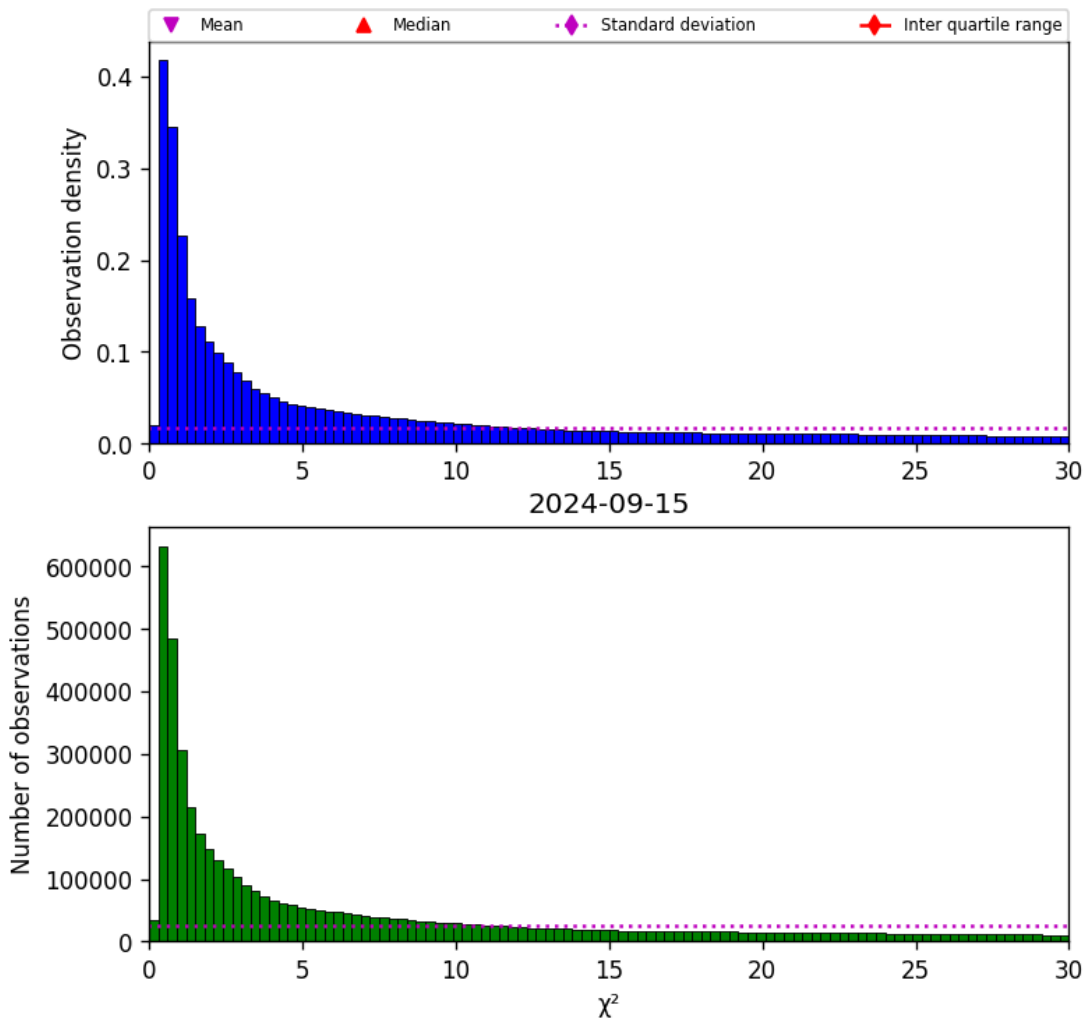


Figure 38: Histogram of “ $\chi^2$ ” for 2024-09-14 to 2024-09-16

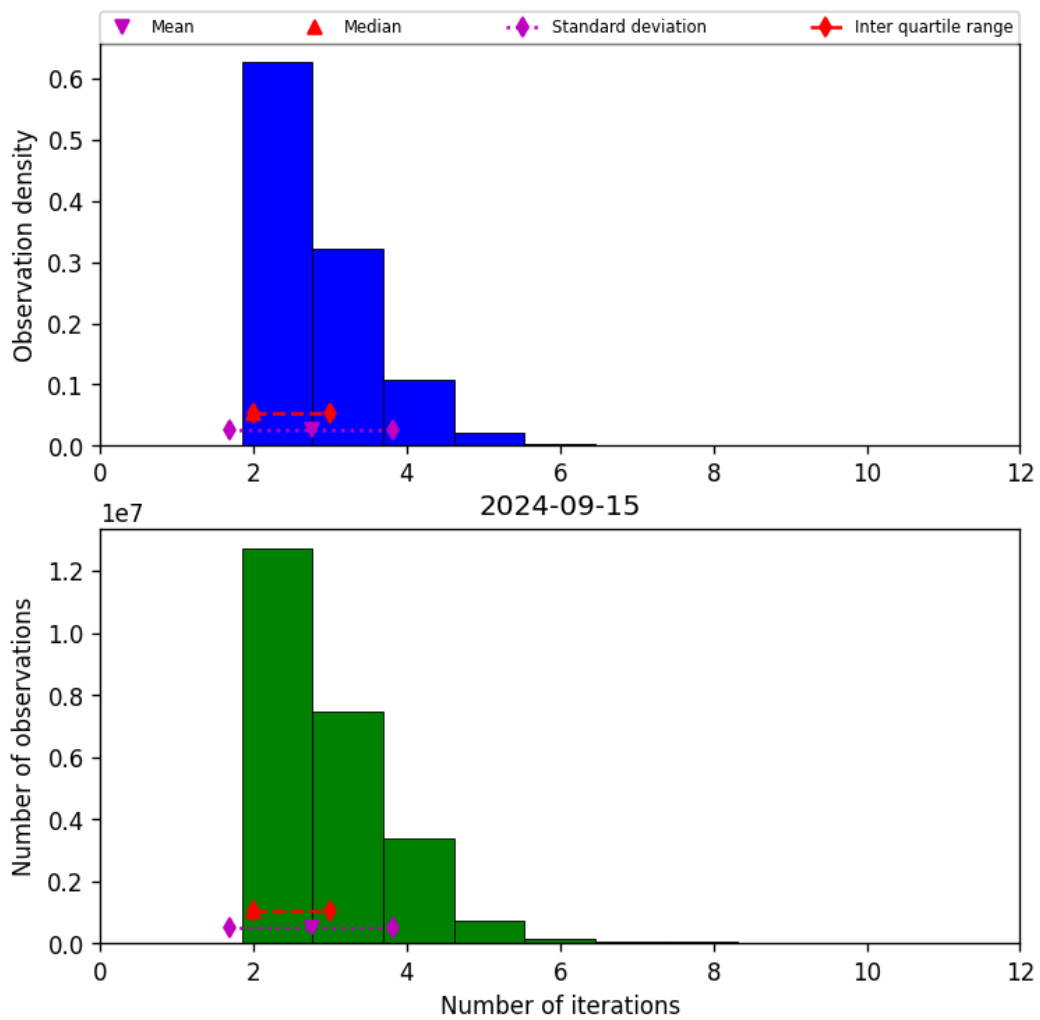


Figure 39: Histogram of “Number of iterations” for 2024-09-14 to 2024-09-16

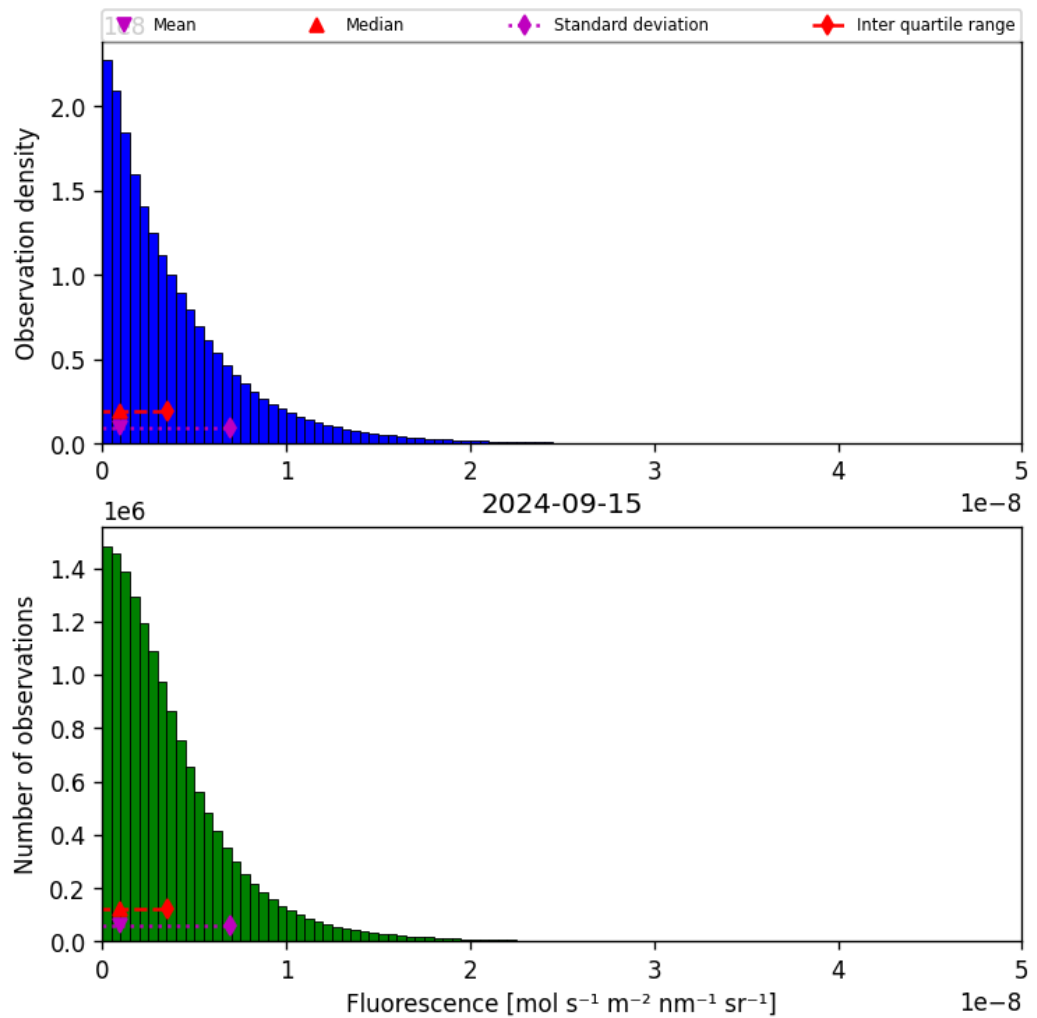


Figure 40: Histogram of “Fluorescence” for 2024-09-14 to 2024-09-16

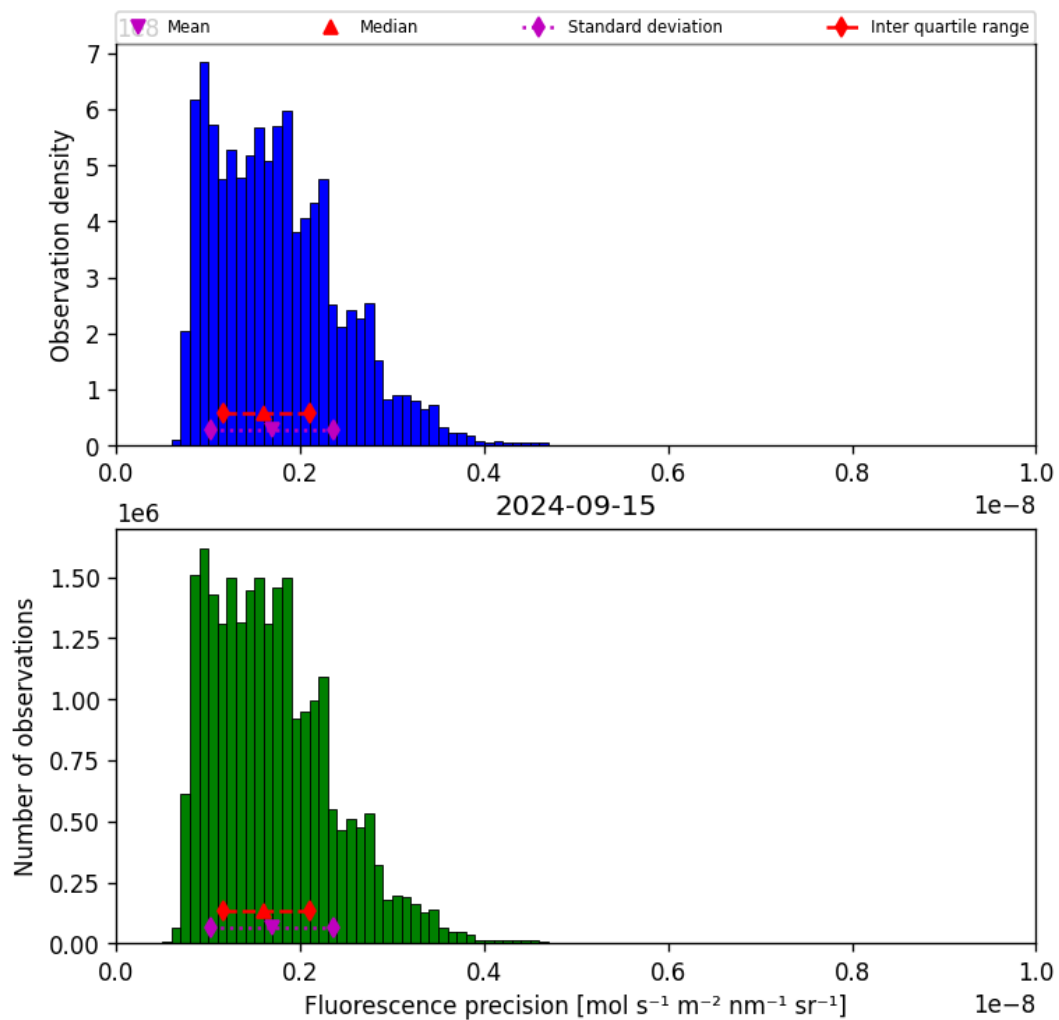


Figure 41: Histogram of “Fluorescence precision” for 2024-09-14 to 2024-09-16

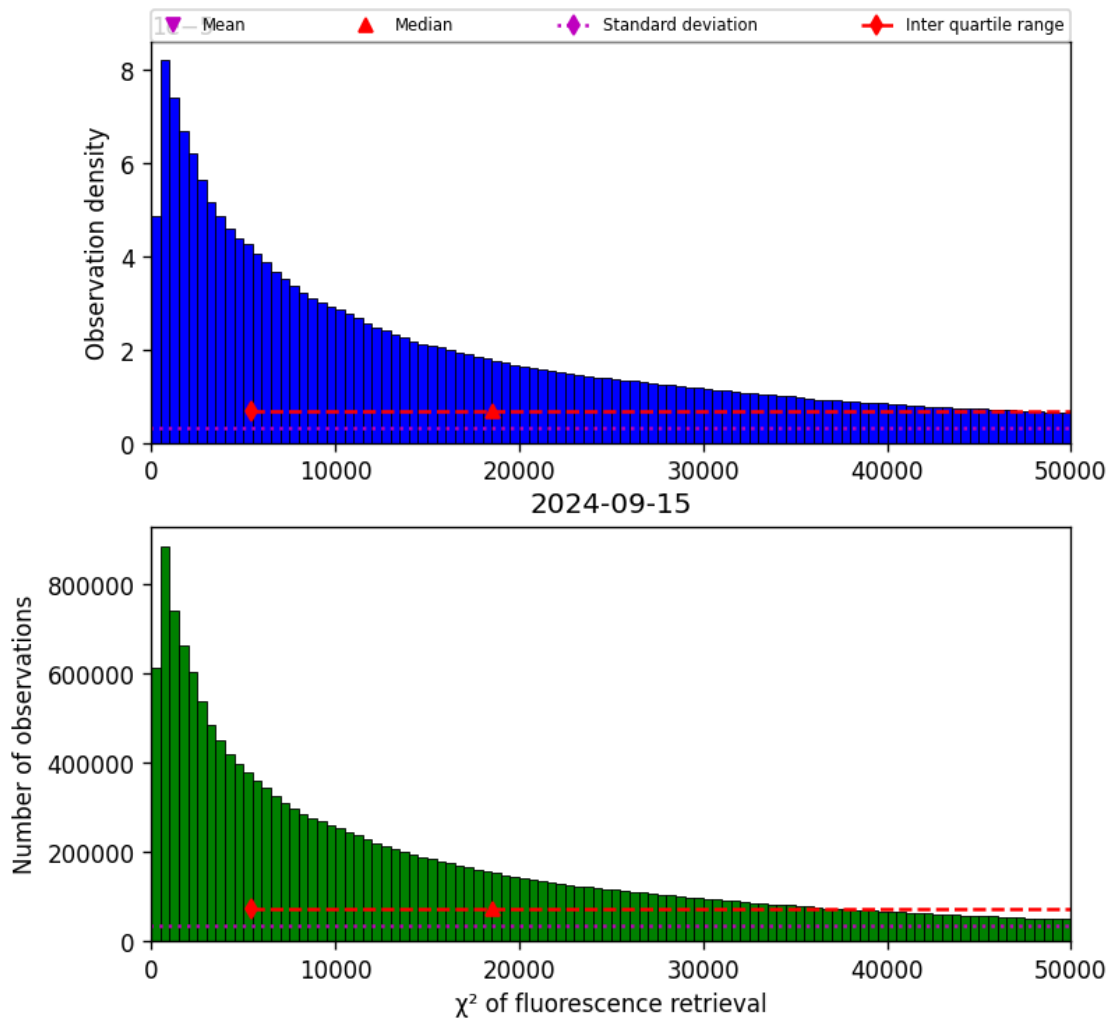


Figure 42: Histogram of “ $\chi^2$  of fluorescence retrieval” for 2024-09-14 to 2024-09-16

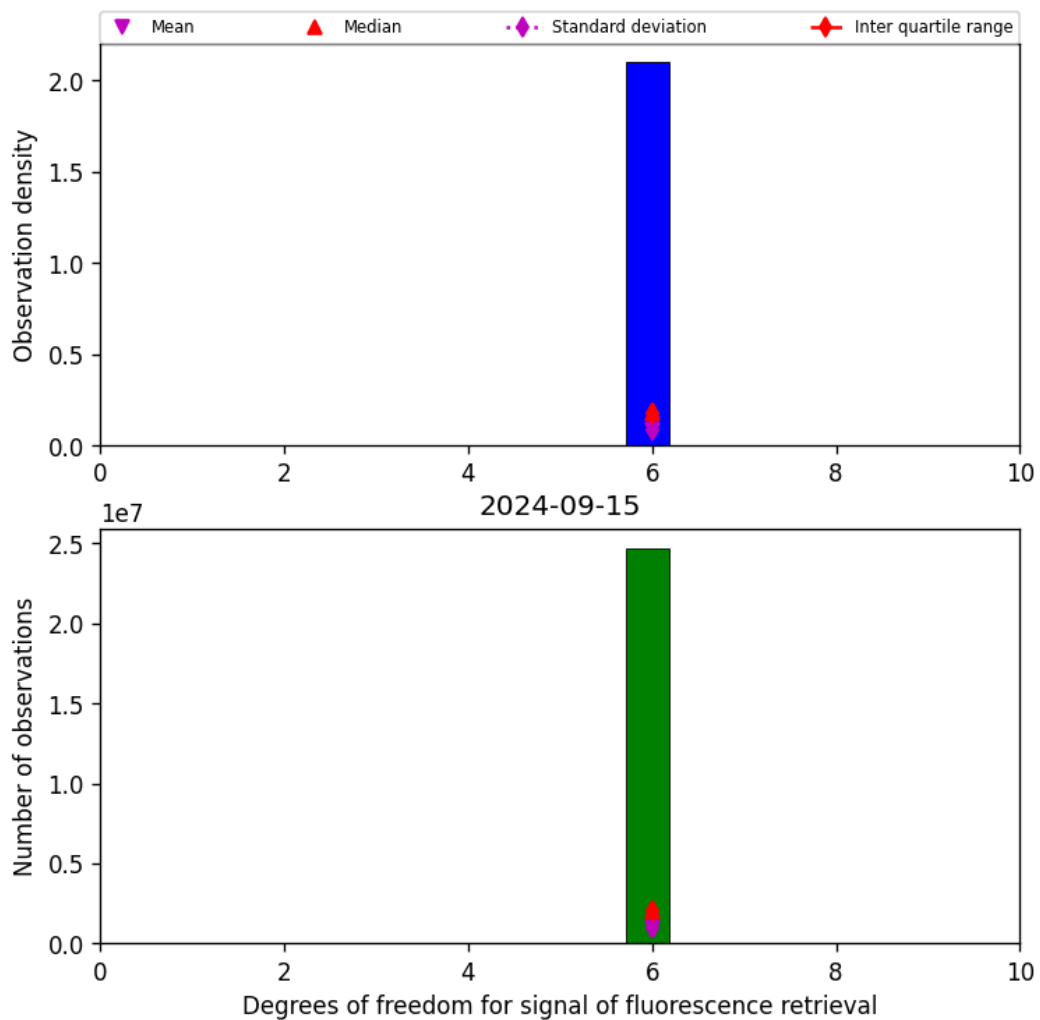


Figure 43: Histogram of “Degrees of freedom for signal of fluorescence retrieval” for 2024-09-14 to 2024-09-16

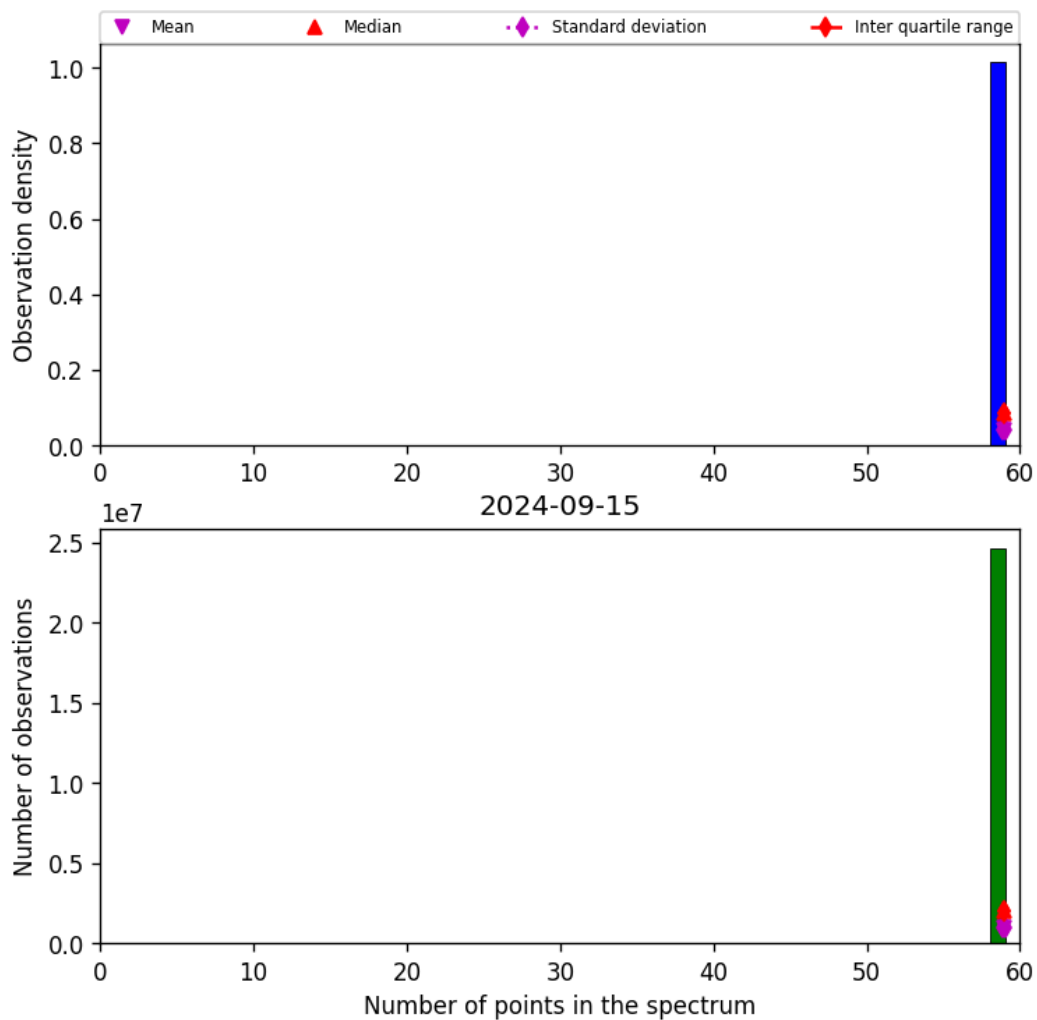


Figure 44: Histogram of “Number of points in the spectrum” for 2024-09-14 to 2024-09-16

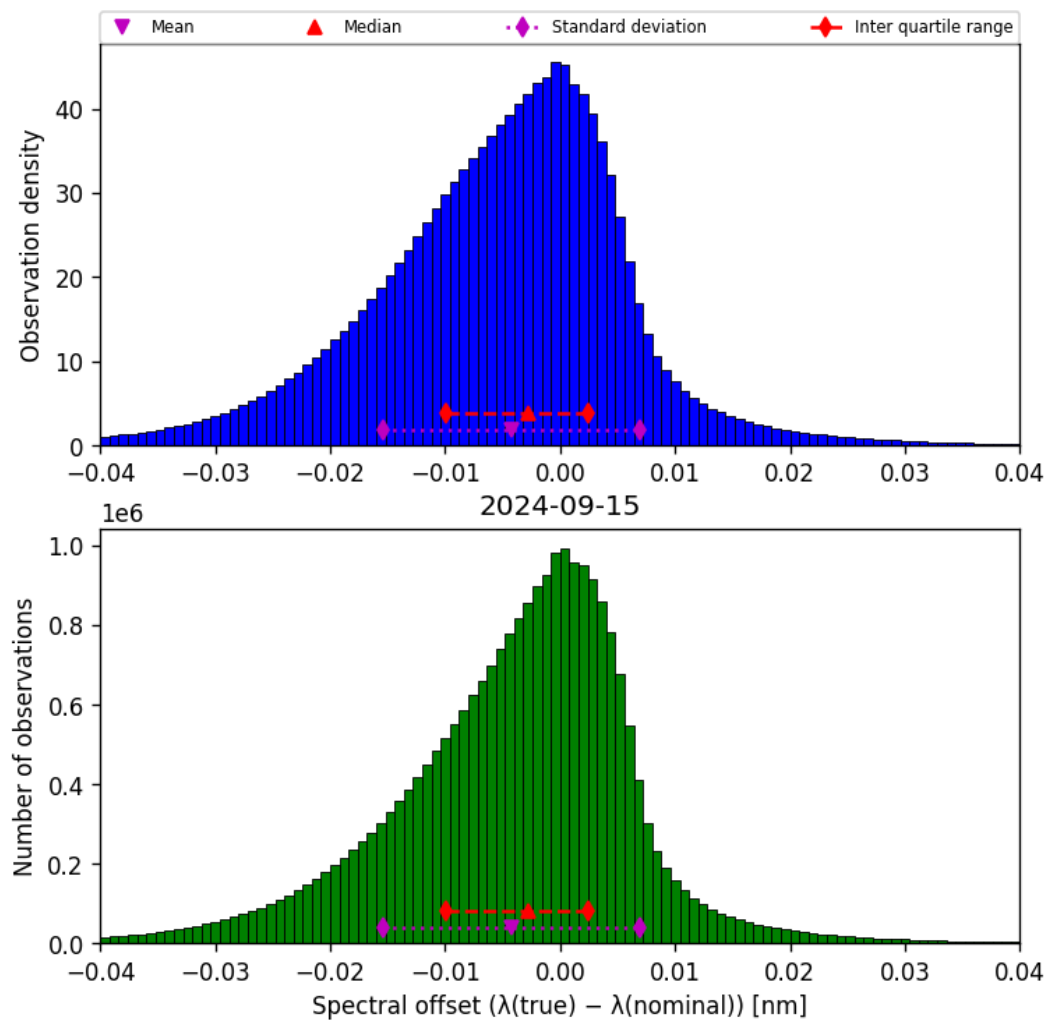


Figure 45: Histogram of “Spectral offset ( $\lambda_{\text{true}} - \lambda_{\text{nominal}}$ )” for 2024-09-14 to 2024-09-16

## 9 Along track statistics

The TROPOMI instrument uses different binned detector rows for different viewing directions. In this section statistics are presented for each of the binned rows in the instrument.

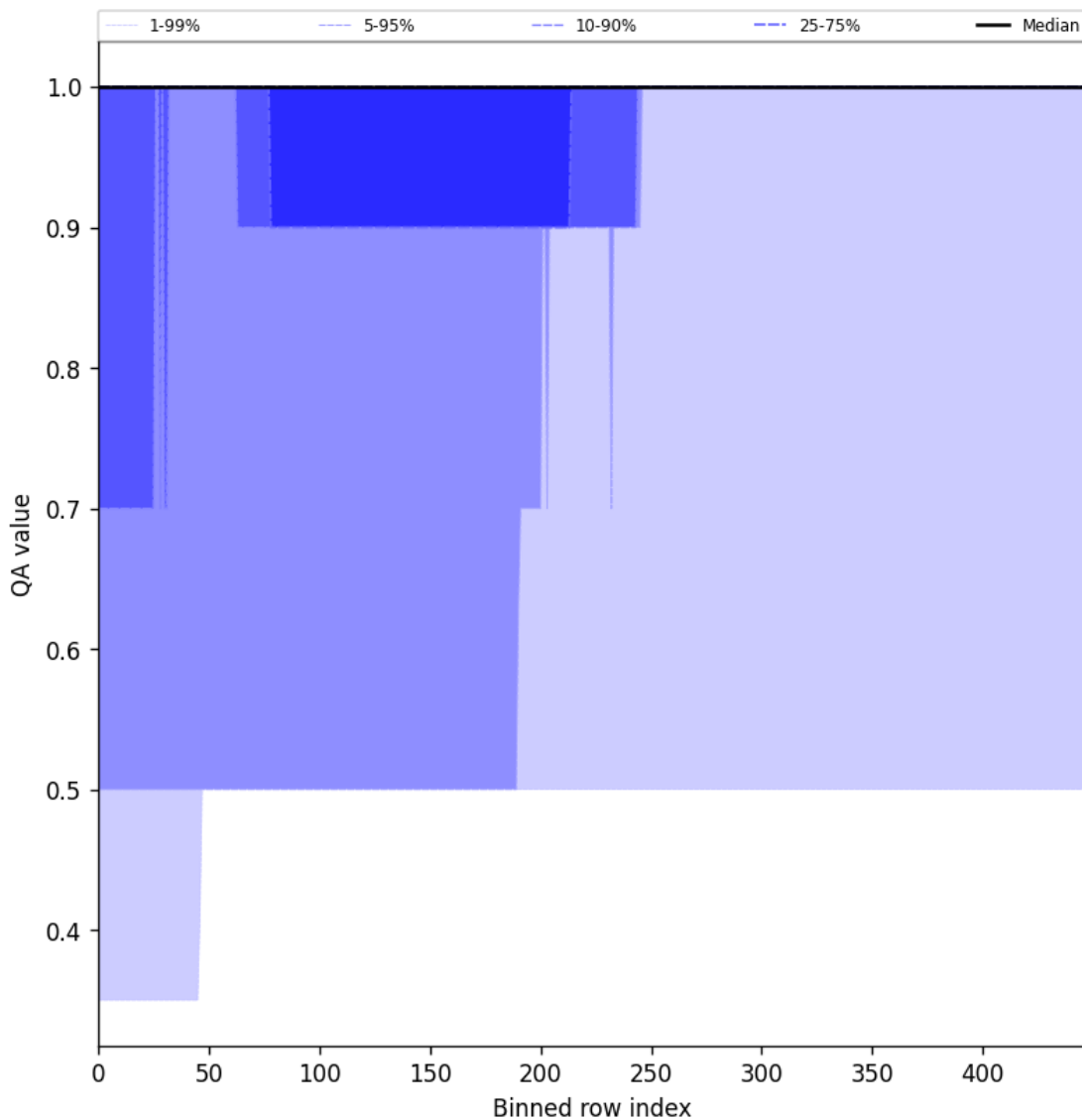


Figure 46: Along track statistics of “QA value” for 2024-09-14 to 2024-09-16

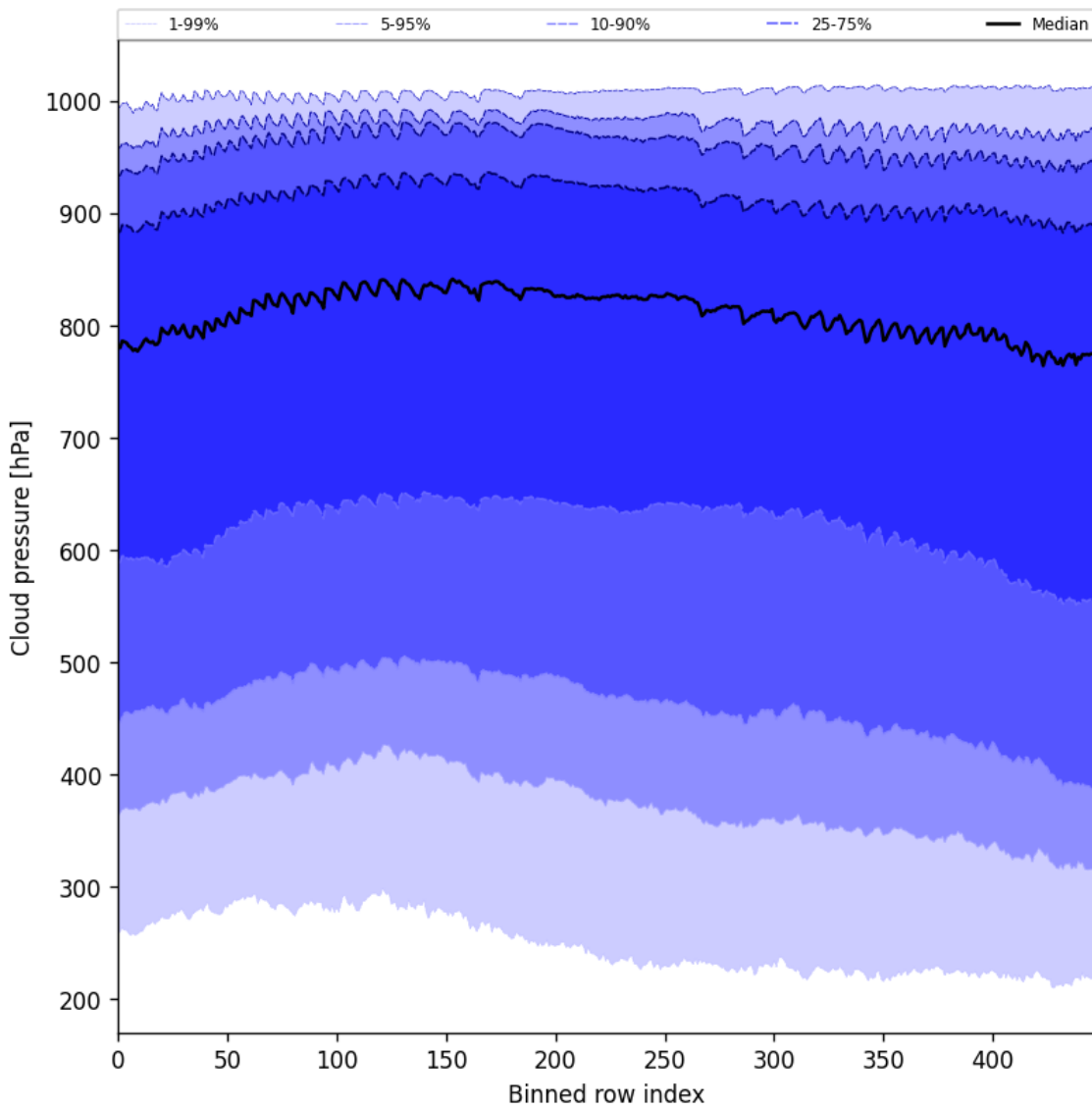


Figure 47: Along track statistics of “Cloud pressure” for 2024-09-14 to 2024-09-16

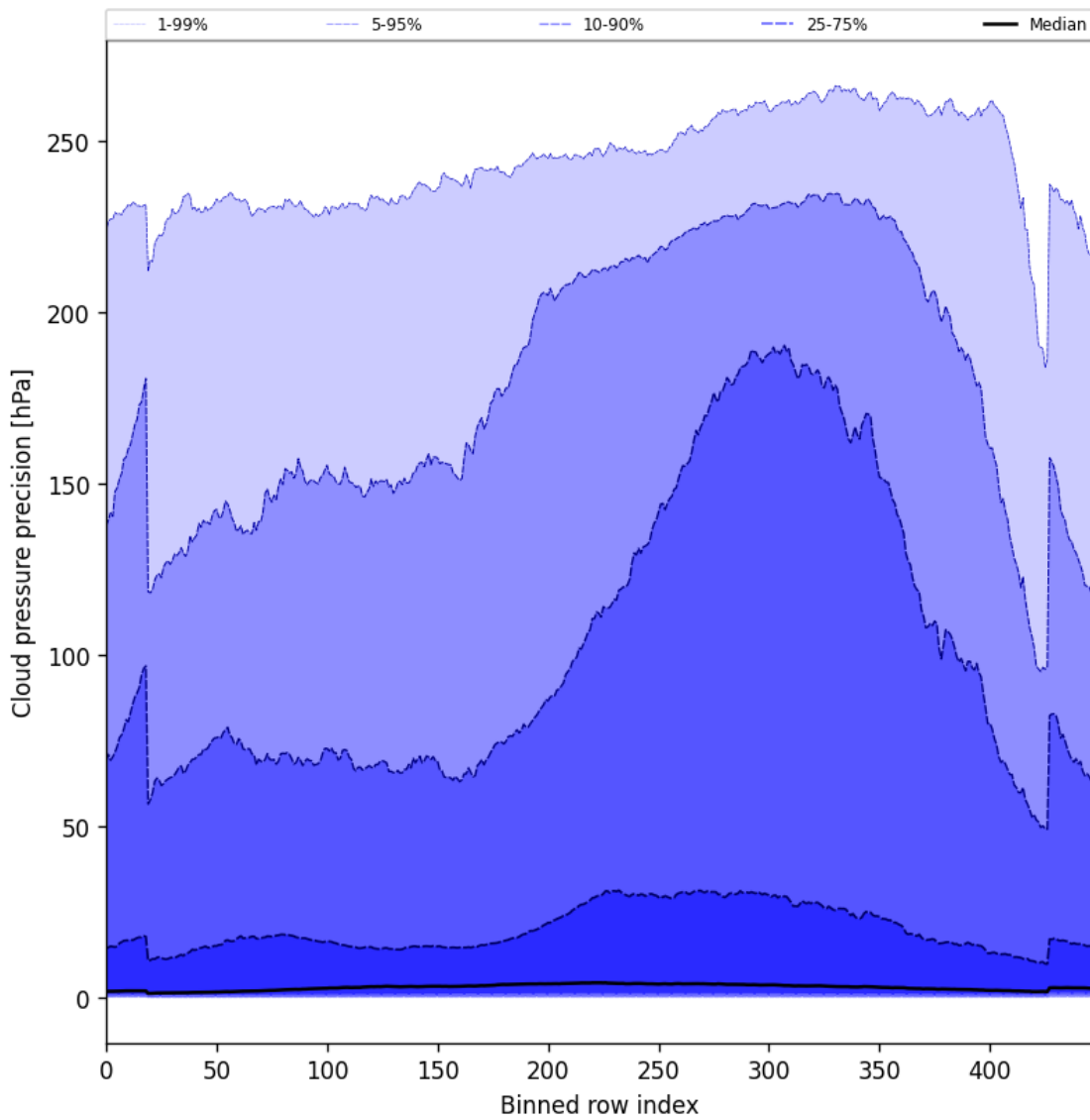


Figure 48: Along track statistics of “Cloud pressure precision” for 2024-09-14 to 2024-09-16

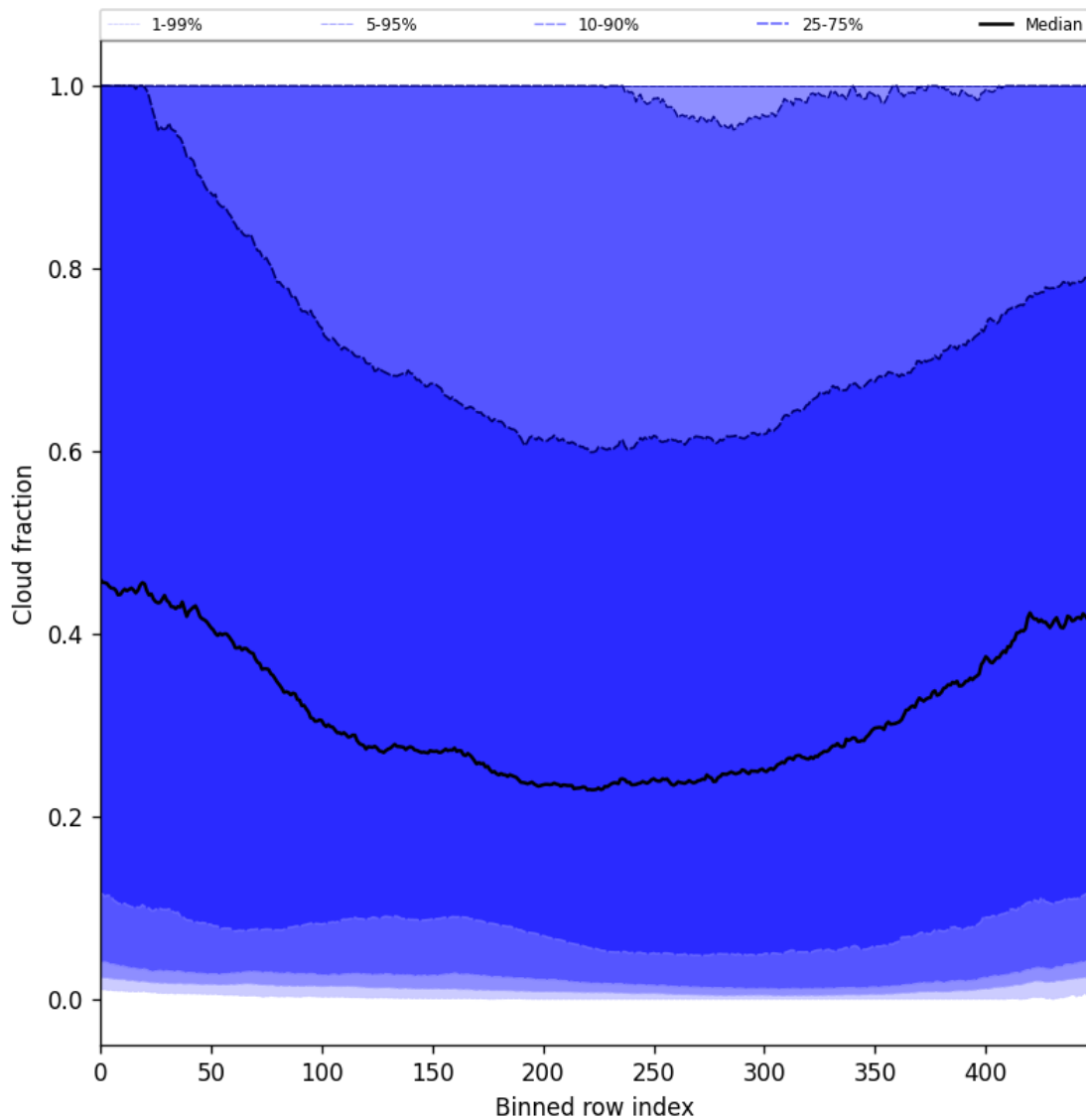


Figure 49: Along track statistics of “Cloud fraction” for 2024-09-14 to 2024-09-16

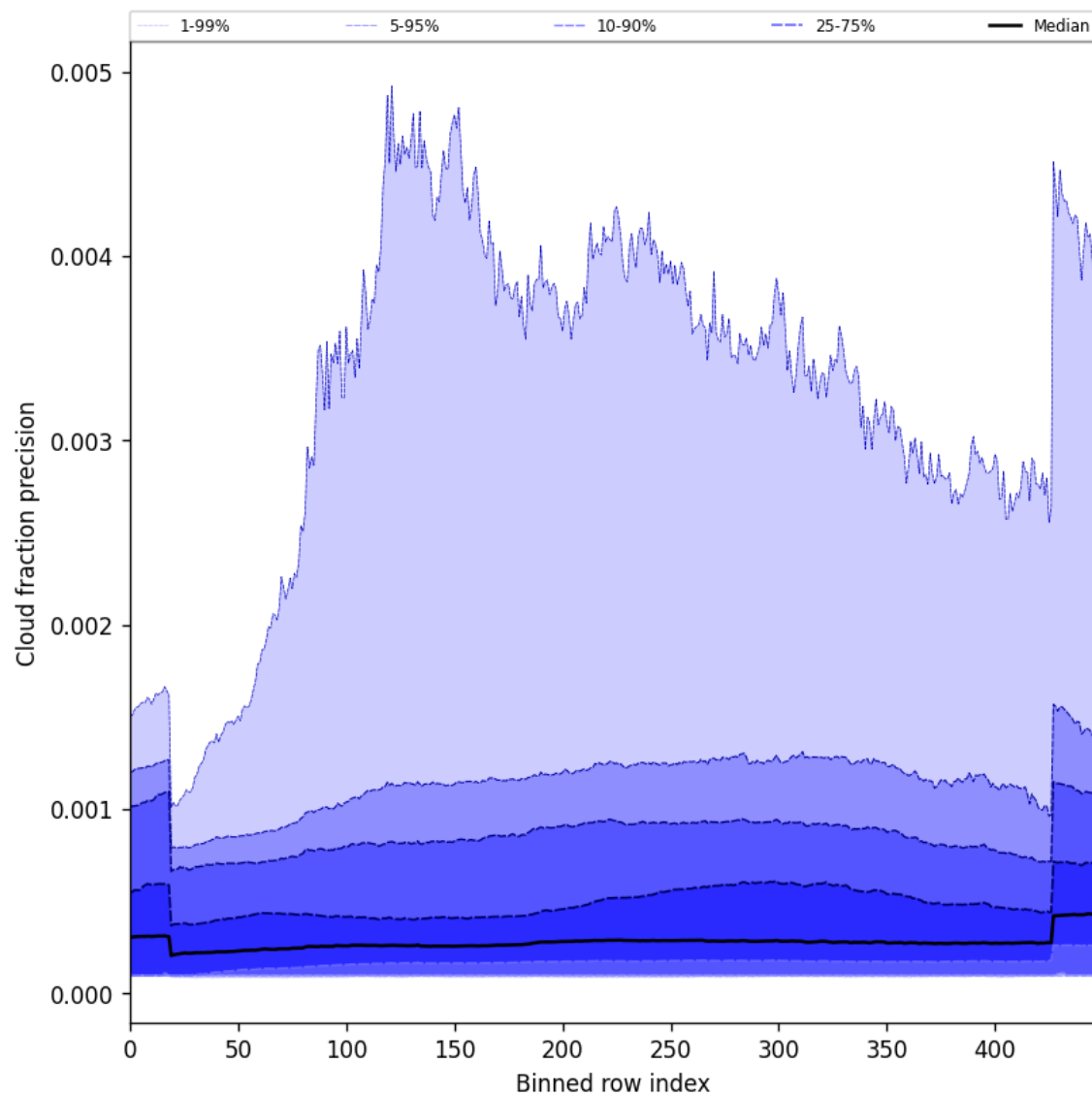


Figure 50: Along track statistics of “Cloud fraction precision” for 2024-09-14 to 2024-09-16

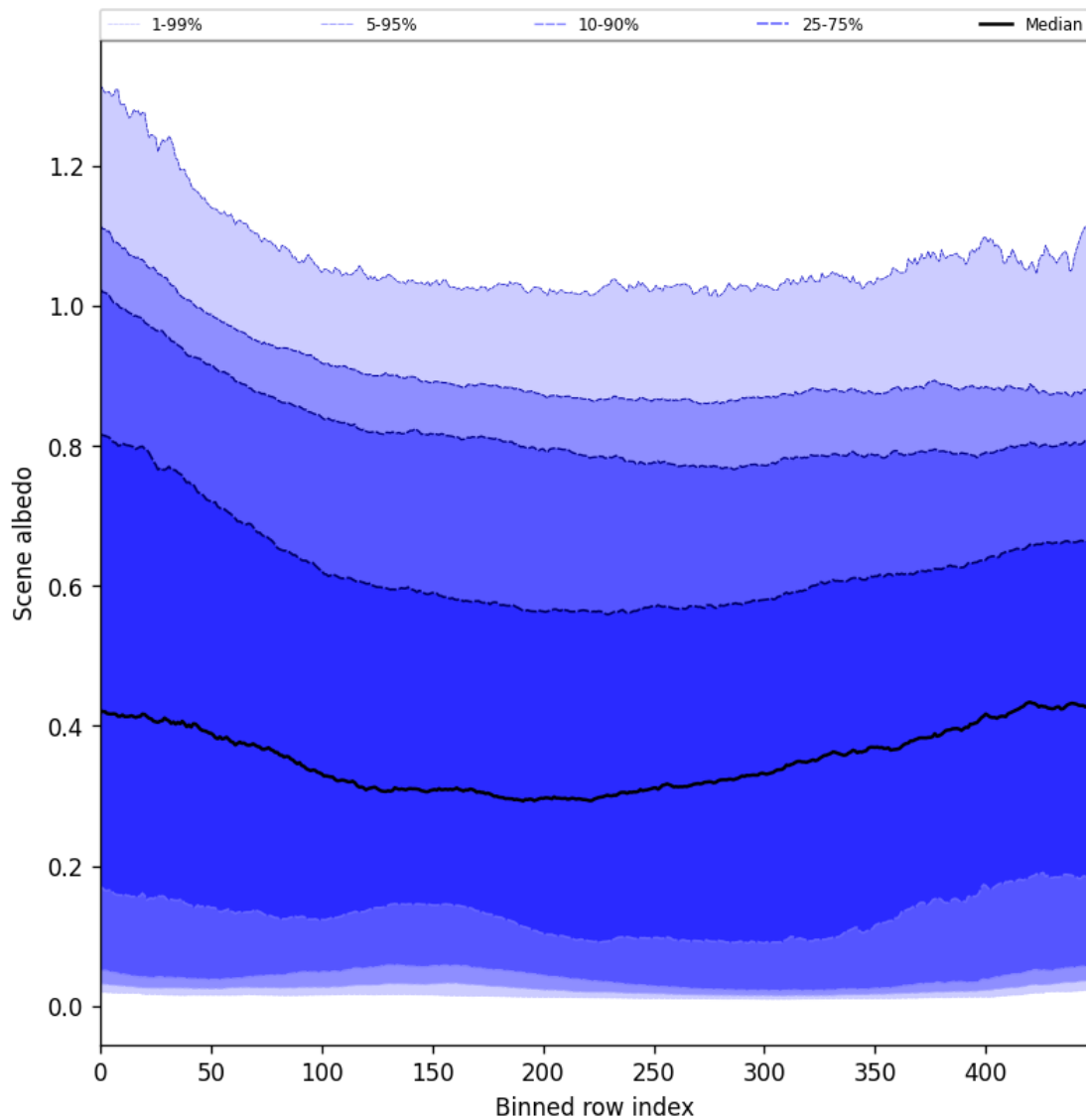


Figure 51: Along track statistics of “Scene albedo” for 2024-09-14 to 2024-09-16

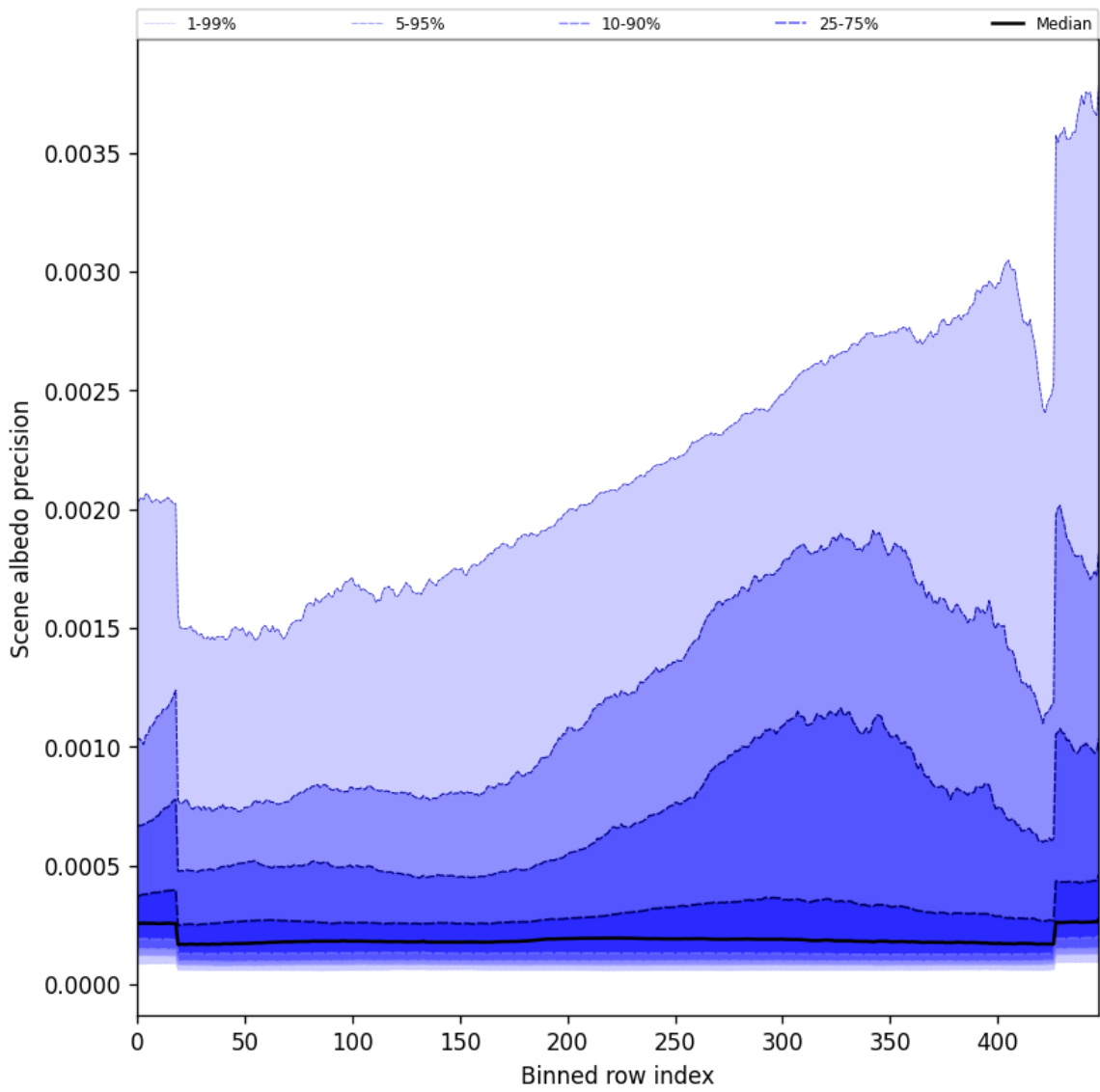


Figure 52: Along track statistics of “Scene albedo precision” for 2024-09-14 to 2024-09-16

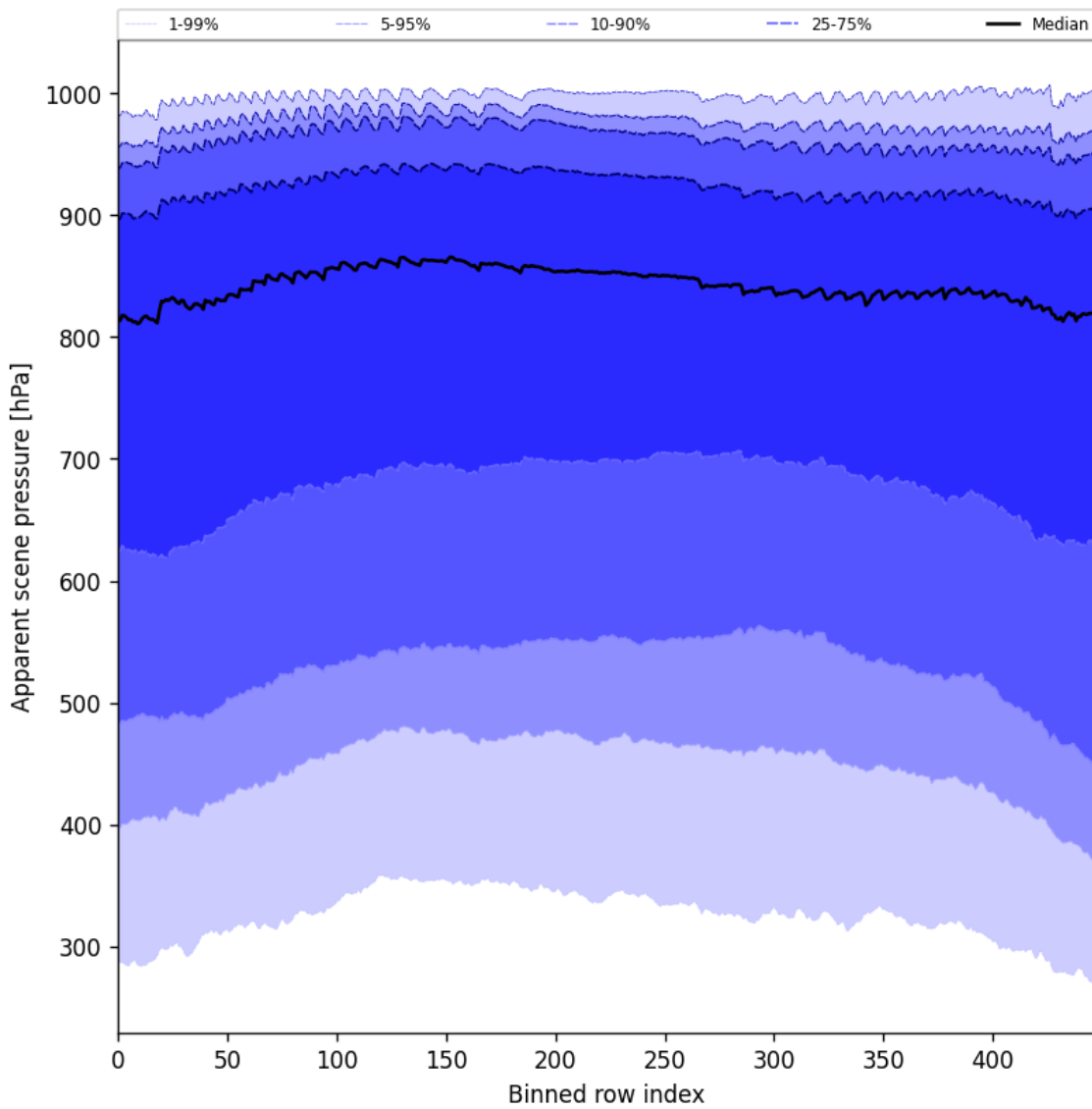


Figure 53: Along track statistics of “Apparent scene pressure” for 2024-09-14 to 2024-09-16

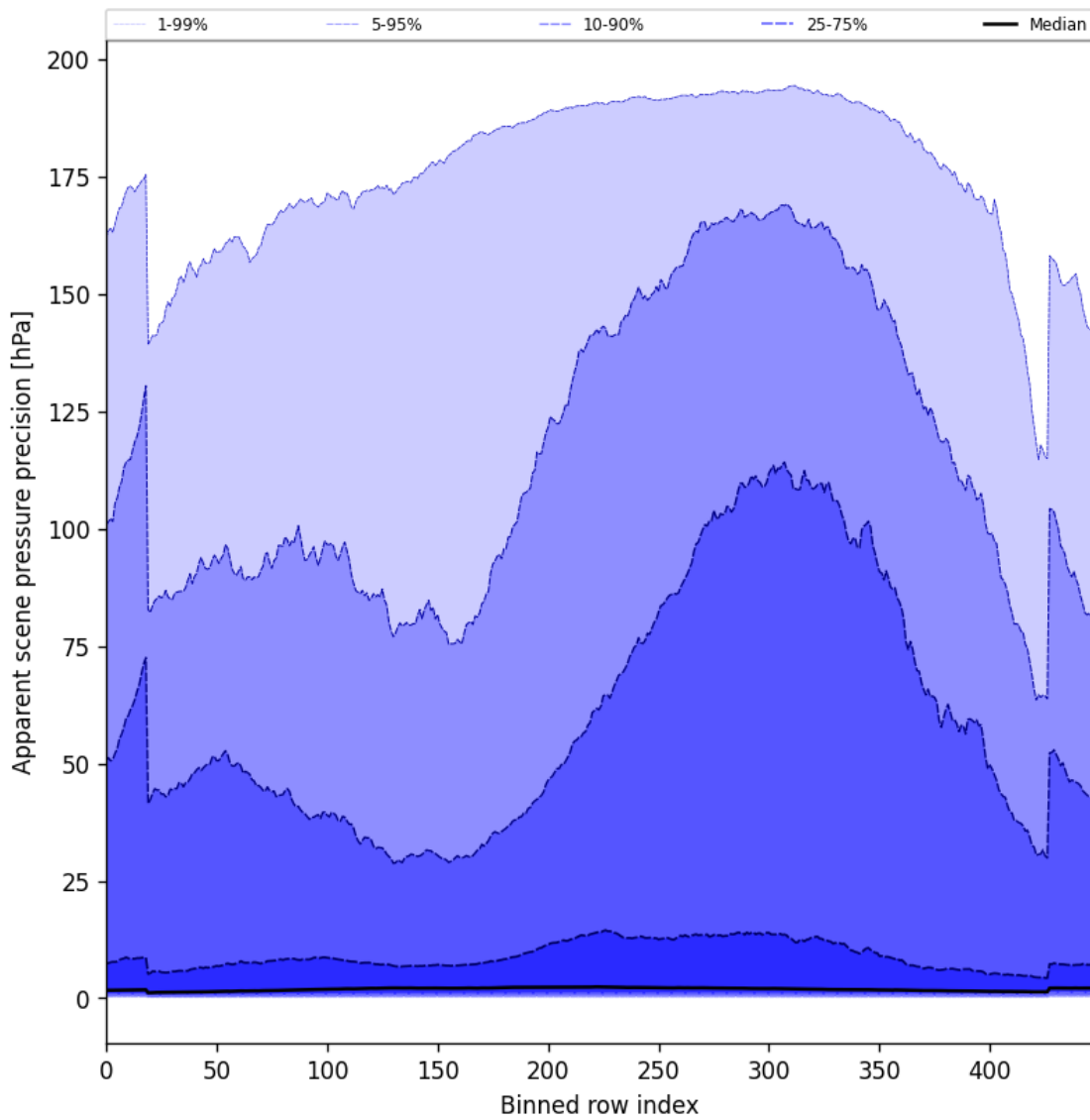


Figure 54: Along track statistics of “Apparent scene pressure precision” for 2024-09-14 to 2024-09-16

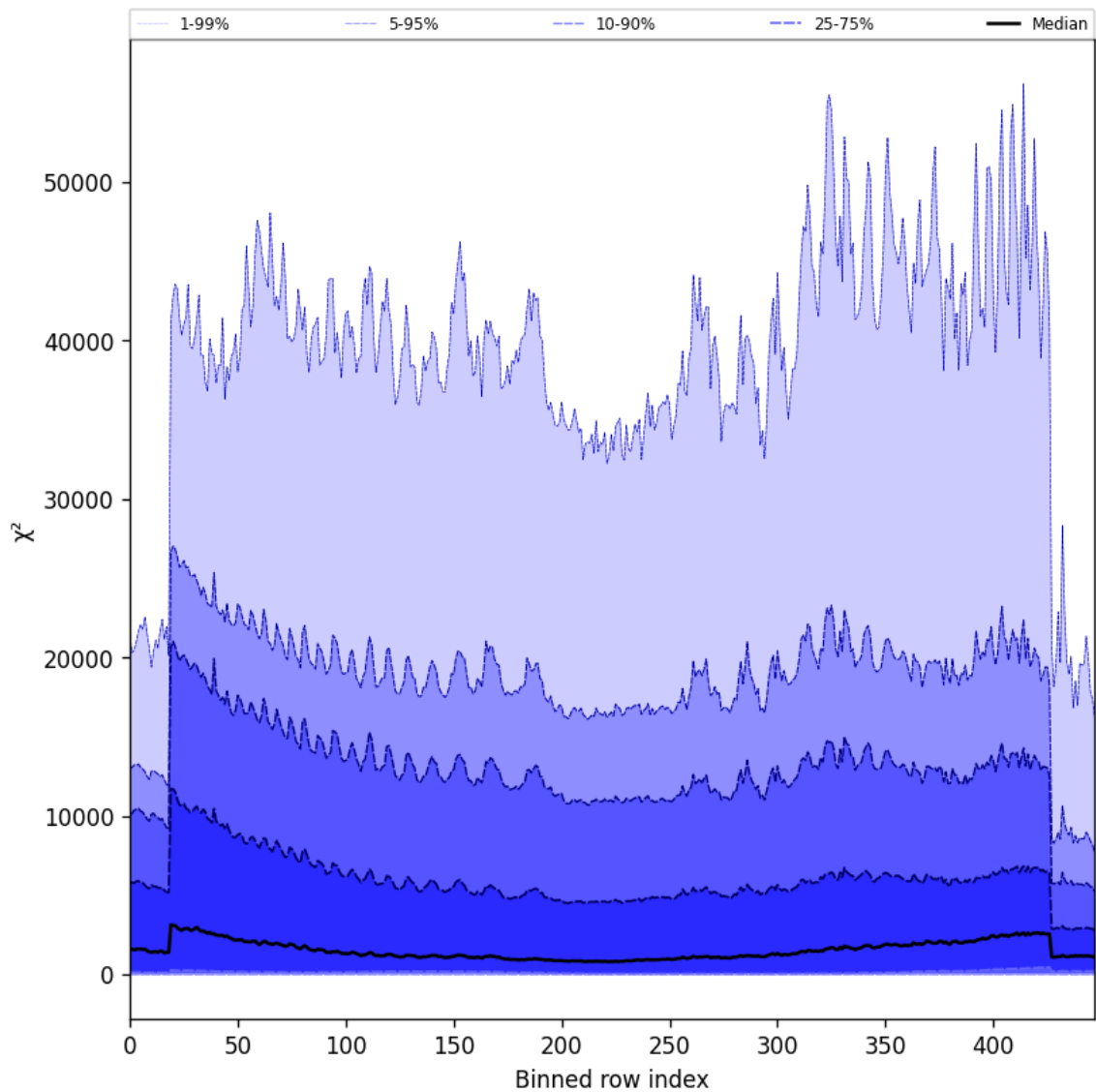


Figure 55: Along track statistics of “ $\chi^2$ ” for 2024-09-14 to 2024-09-16

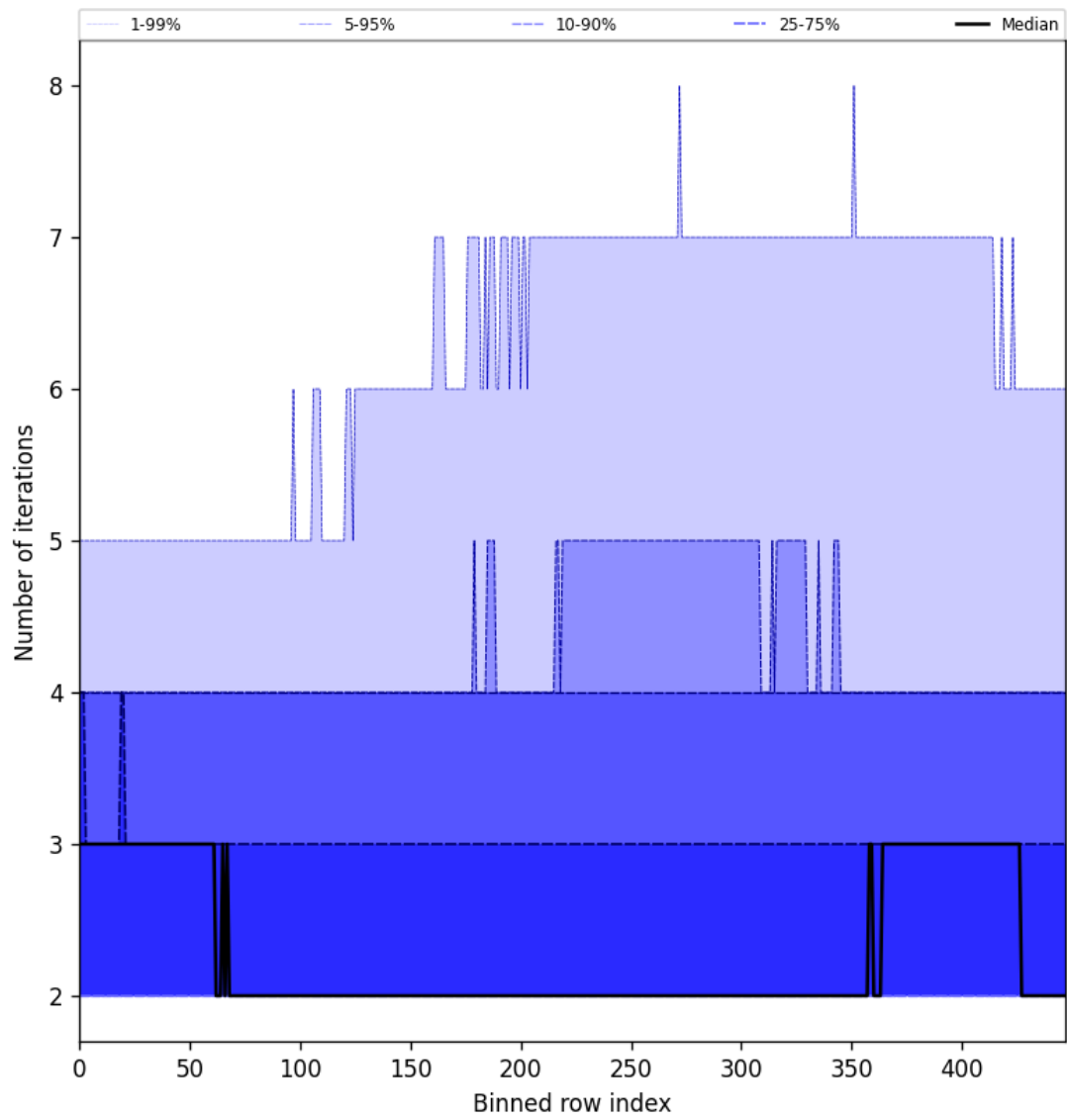


Figure 56: Along track statistics of “Number of iterations” for 2024-09-14 to 2024-09-16

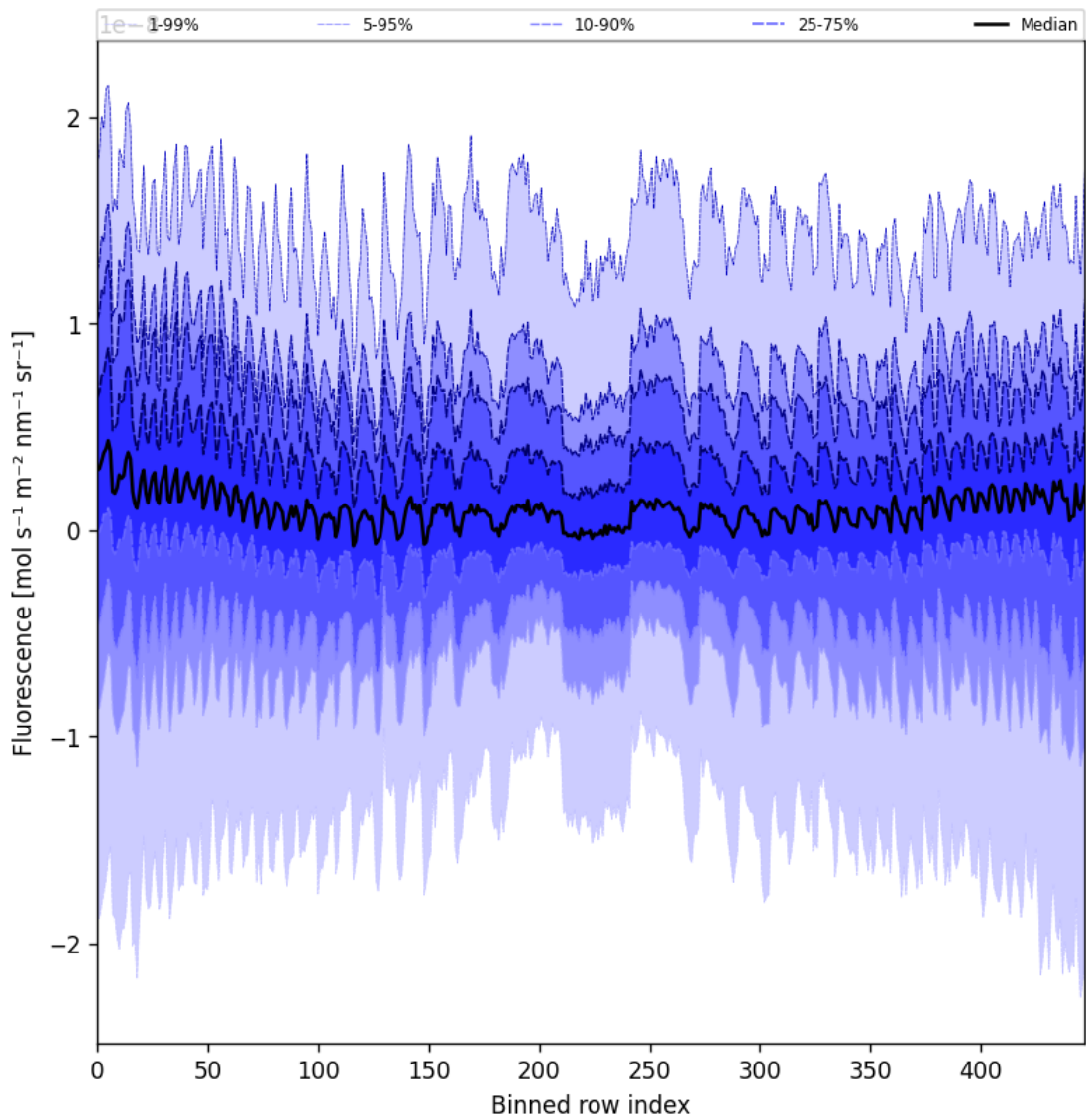


Figure 57: Along track statistics of “Fluorescence” for 2024-09-14 to 2024-09-16

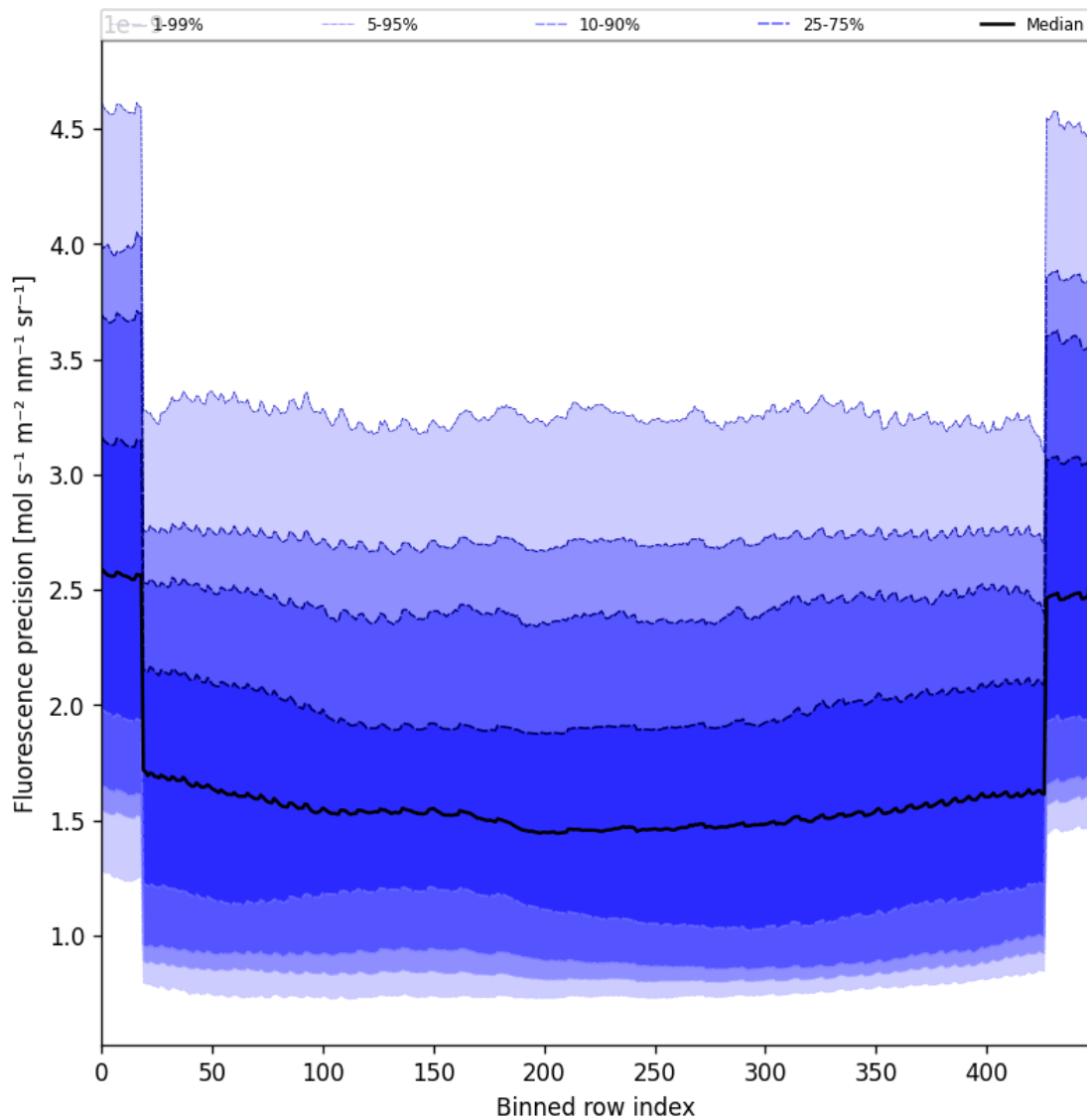


Figure 58: Along track statistics of “Fluorescence precision” for 2024-09-14 to 2024-09-16

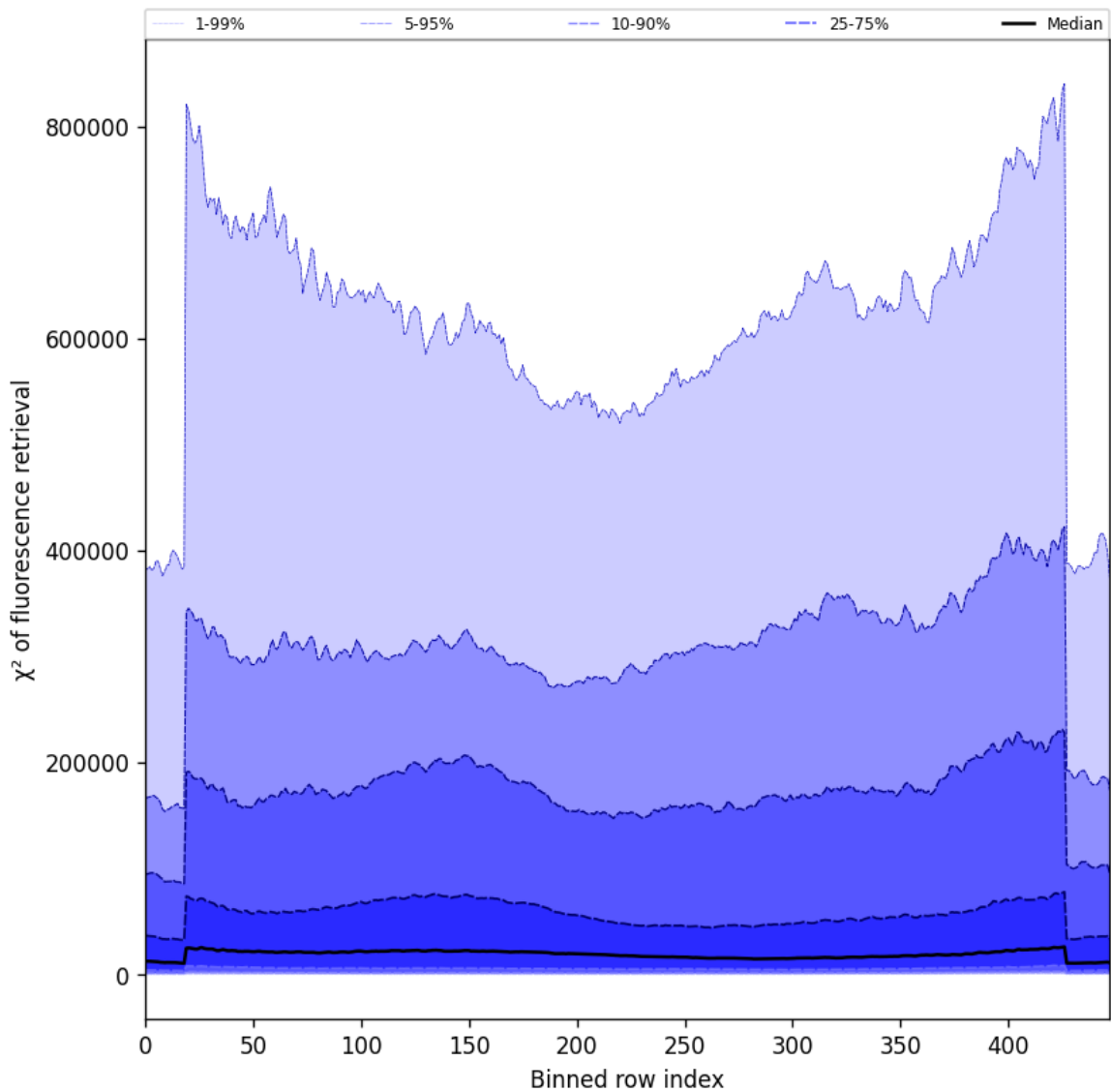


Figure 59: Along track statistics of “ $\chi^2$  of fluorescence retrieval” for 2024-09-14 to 2024-09-16



Figure 60: Along track statistics of “Degrees of freedom for signal of fluorescence retrieval” for 2024-09-14 to 2024-09-16

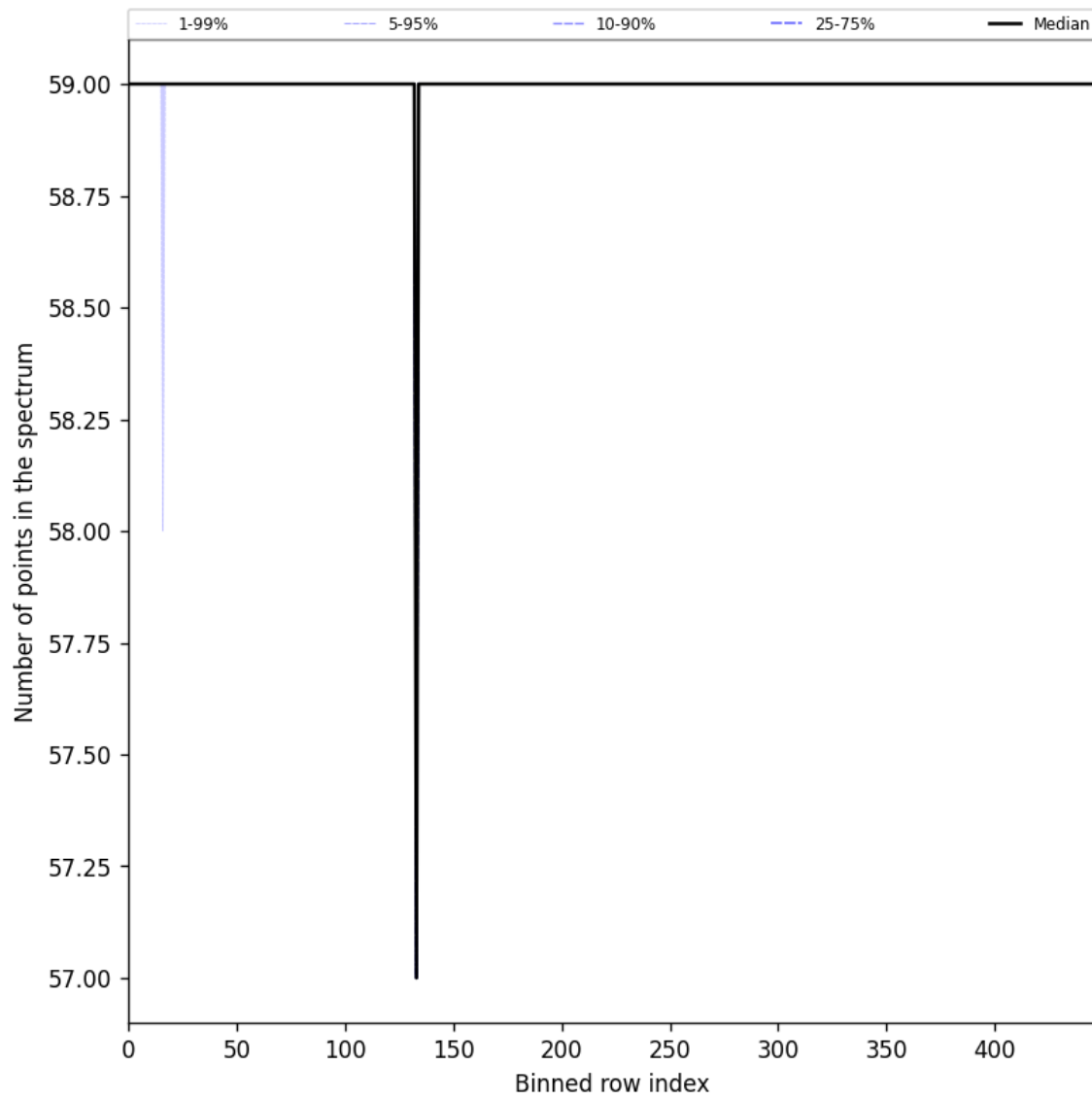


Figure 61: Along track statistics of “Number of points in the spectrum” for 2024-09-14 to 2024-09-16

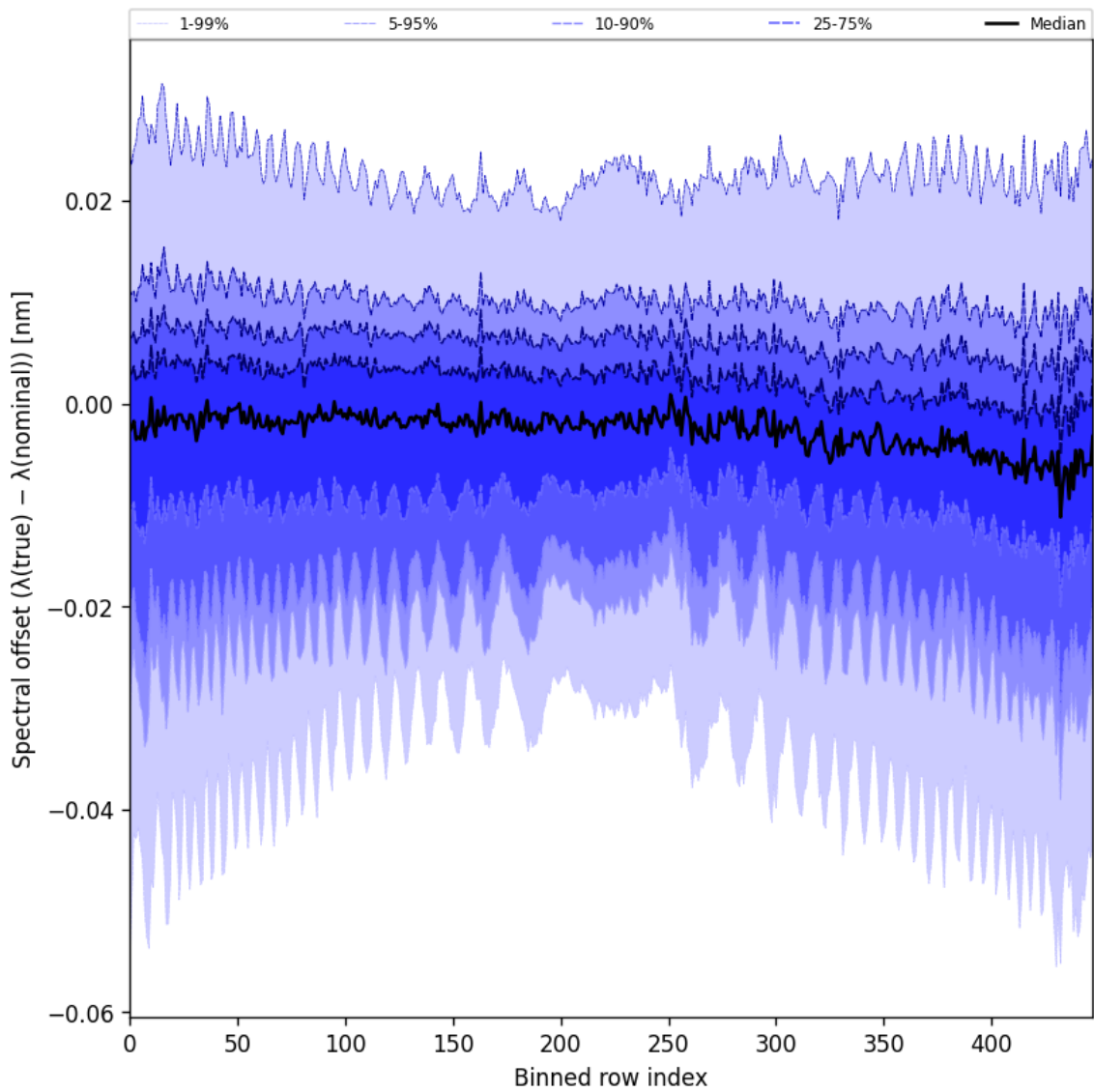


Figure 62: Along track statistics of “Spectral offset ( $\lambda_{\text{true}} - \lambda_{\text{nominal}}$ )” for 2024-09-14 to 2024-09-16

## 10 Coincidence density

To investigate the relation between parameters scatter density plots are produced. These include some ‘hidden’ parameters, latitude and the solar- and viewing geometries, in addition to all configured parameters. All combinations of pairs of parameters are included *once*, in one direction alone.

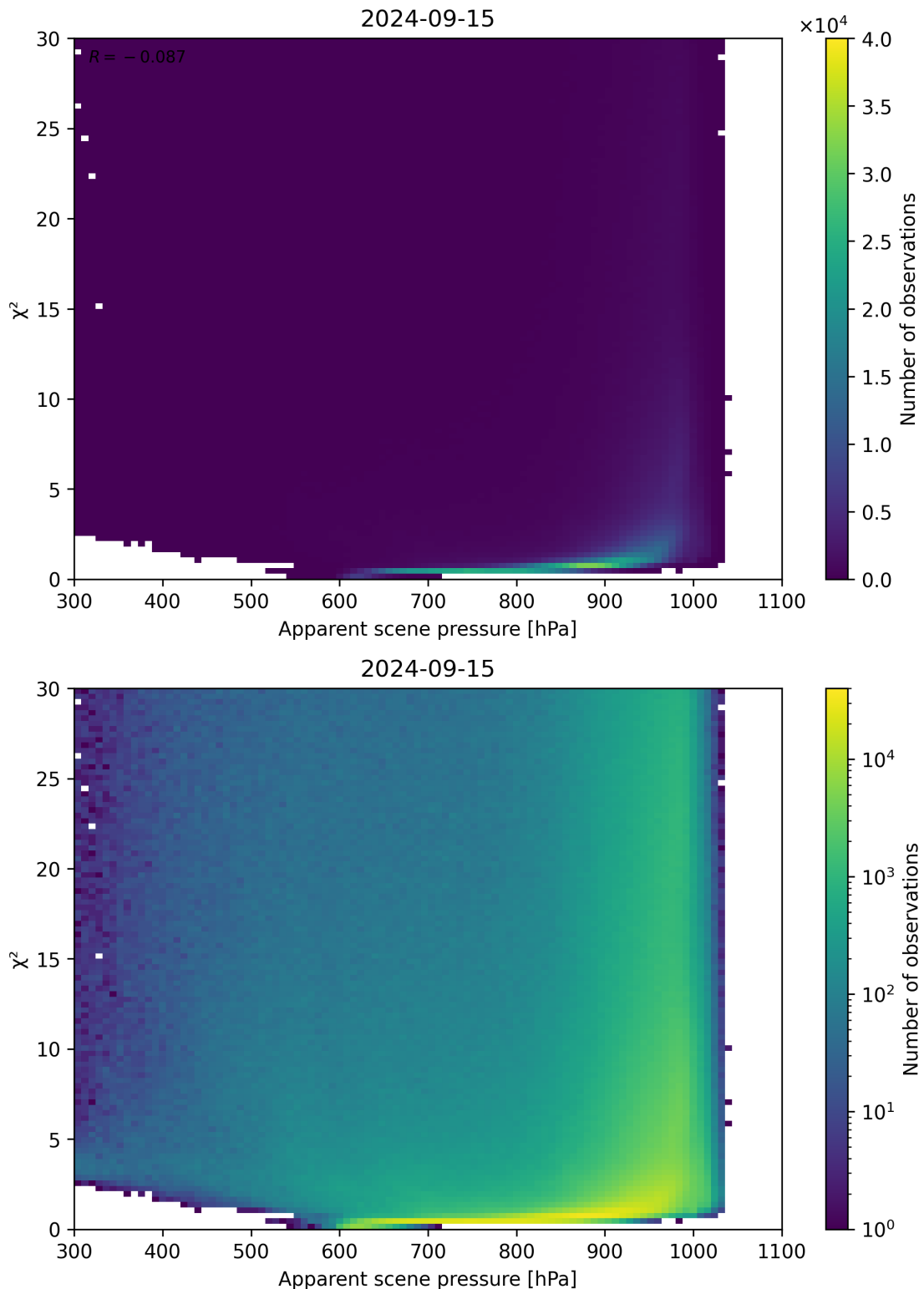


Figure 63: Scatter density plot of “Apparent scene pressure” against “ $\chi^2$ ” for 2024-09-14 to 2024-09-16.

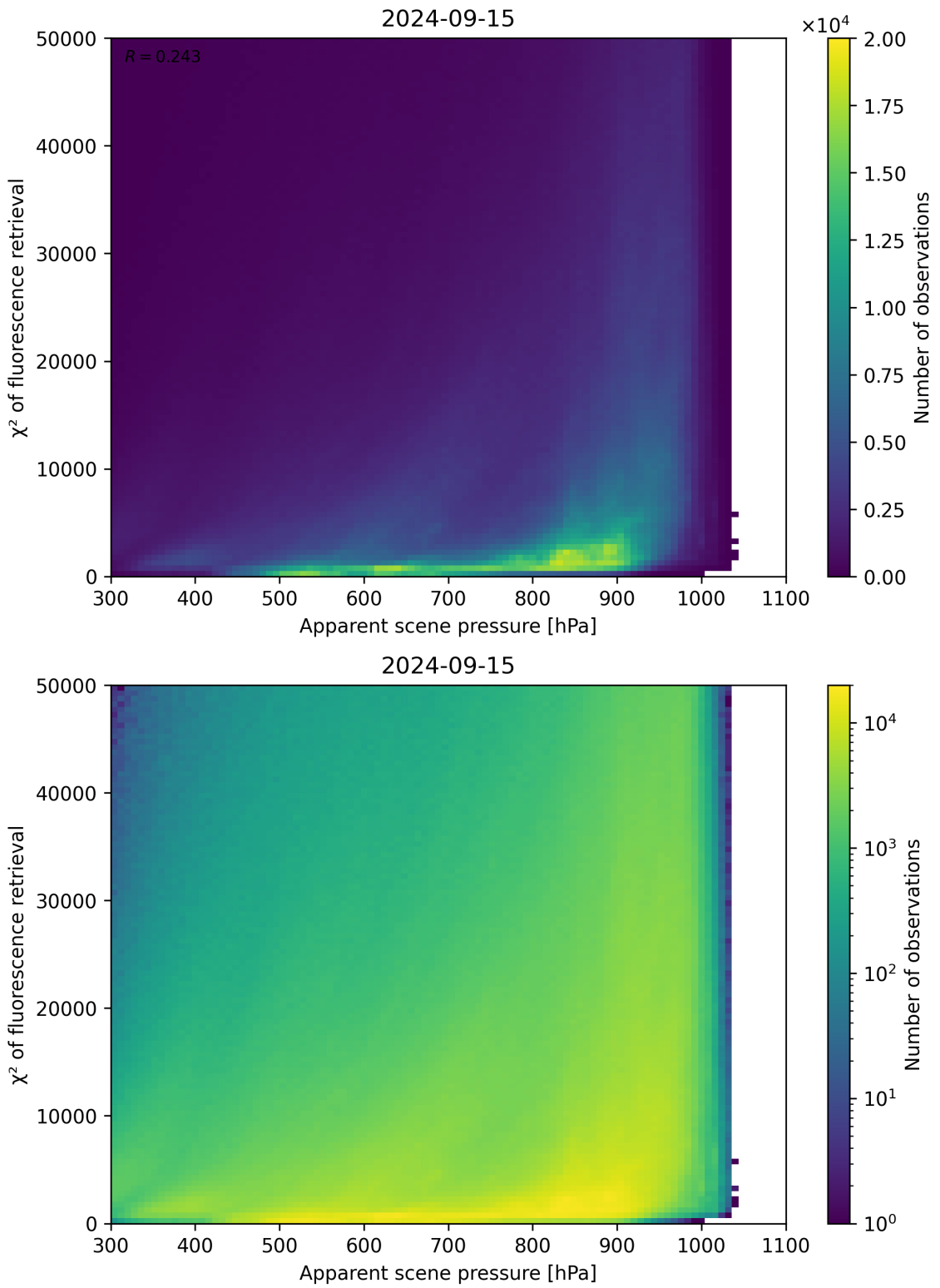


Figure 64: Scatter density plot of “Apparent scene pressure” against “ $\chi^2$  of fluorescence retrieval” for 2024-09-14 to 2024-09-16.

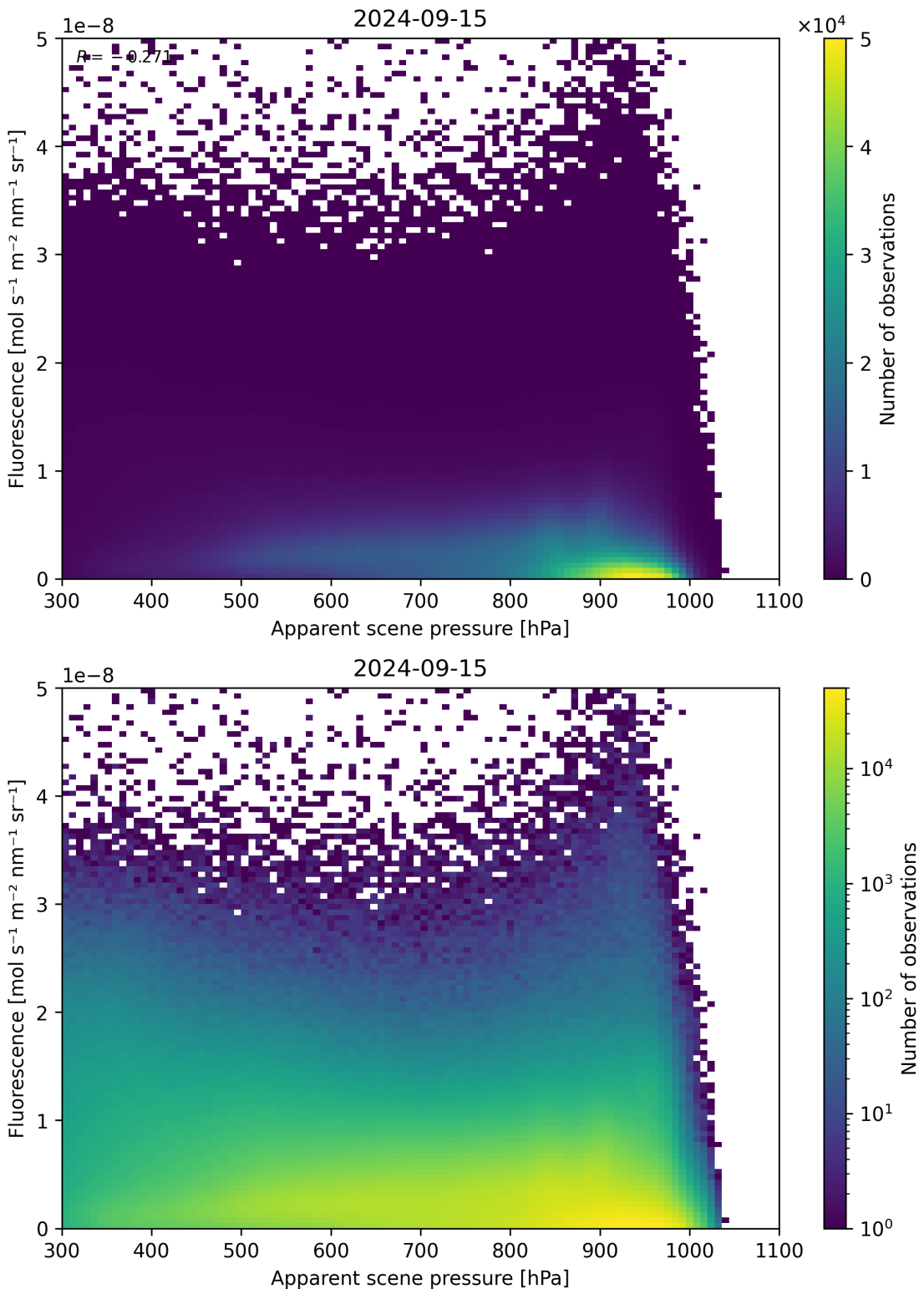


Figure 65: Scatter density plot of “Apparent scene pressure” against “Fluorescence” for 2024-09-14 to 2024-09-16.

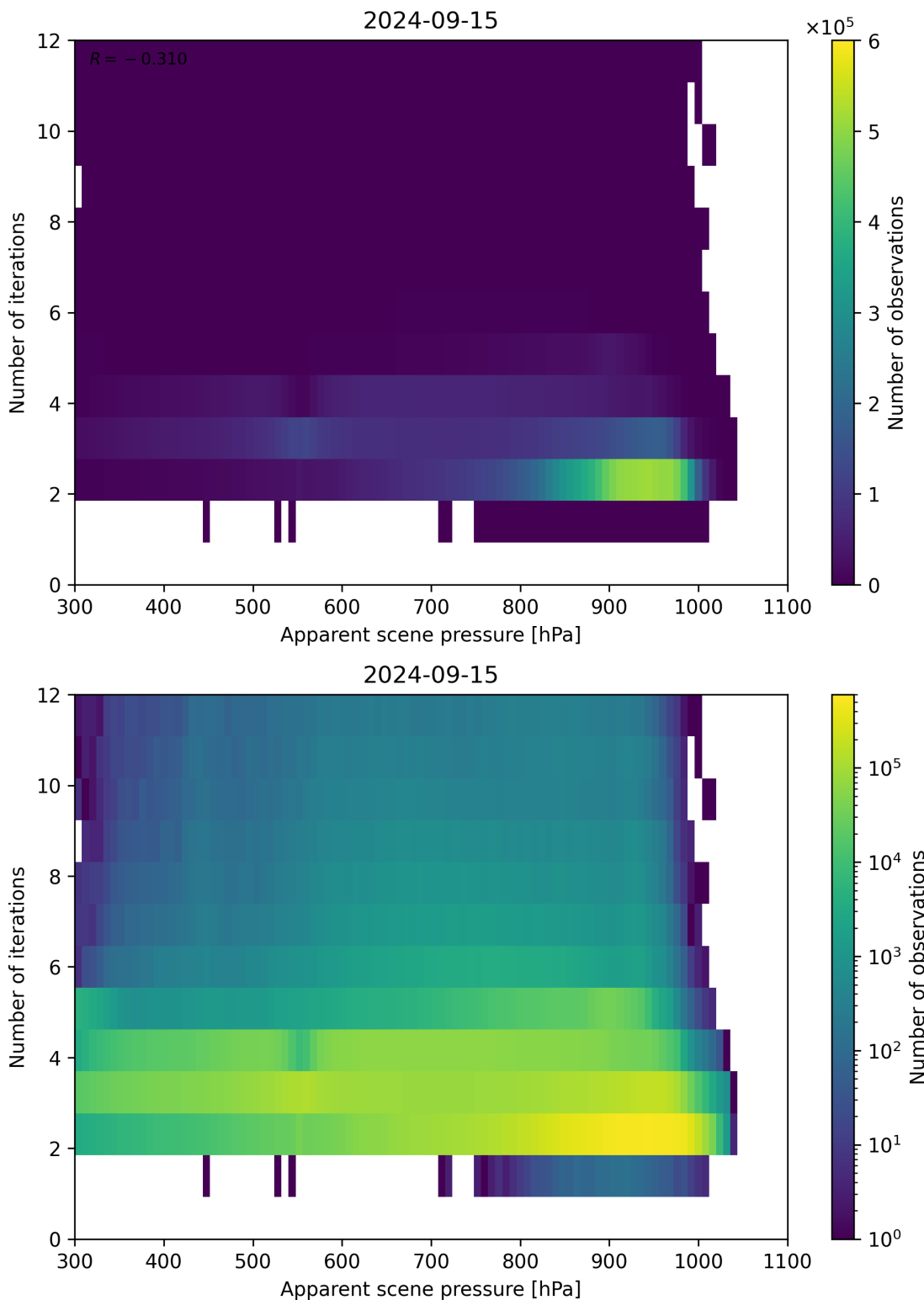


Figure 66: Scatter density plot of “Apparent scene pressure” against “Number of iterations” for 2024-09-14 to 2024-09-16.

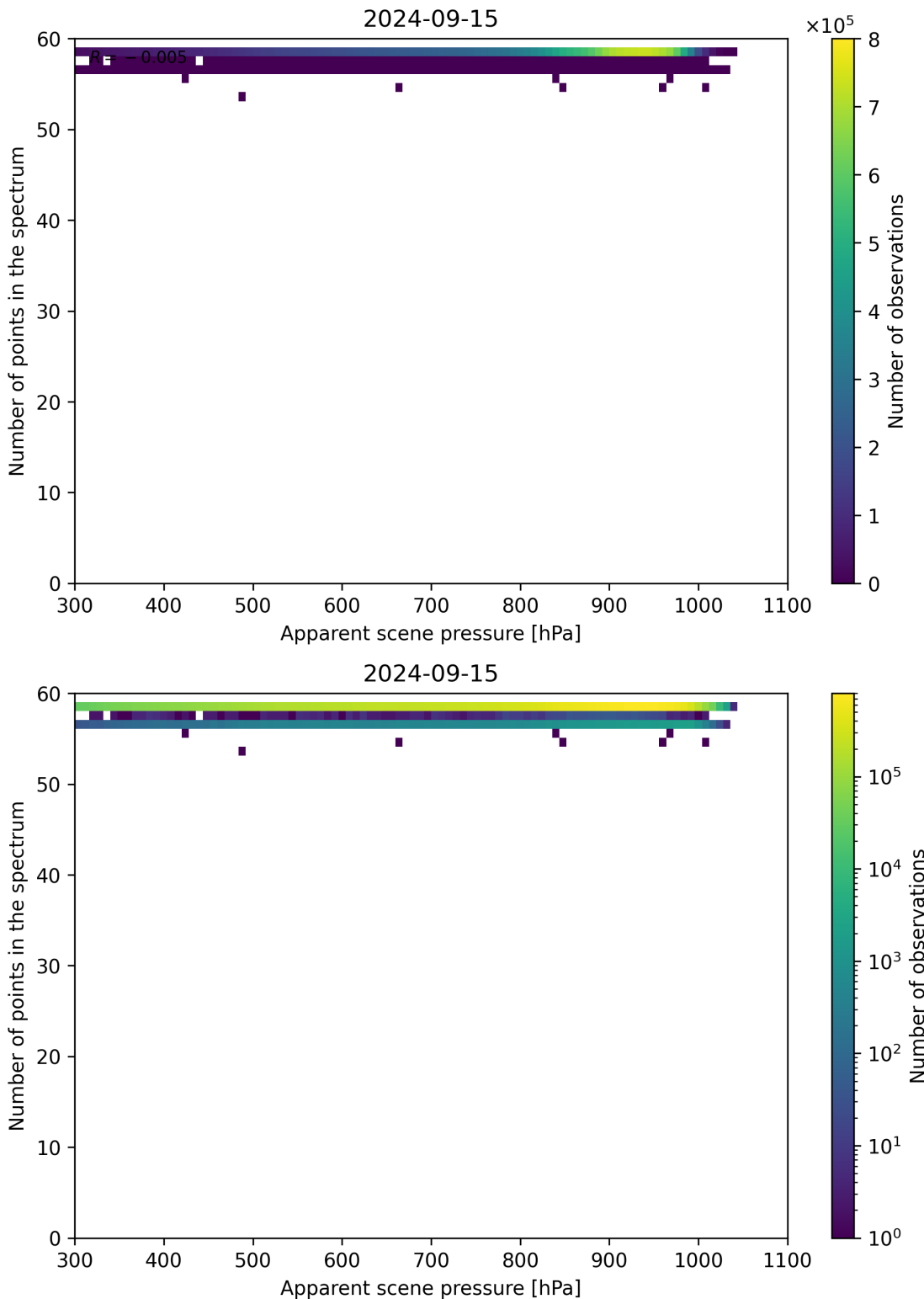


Figure 67: Scatter density plot of “Apparent scene pressure” against “Number of points in the spectrum” for 2024-09-14 to 2024-09-16.

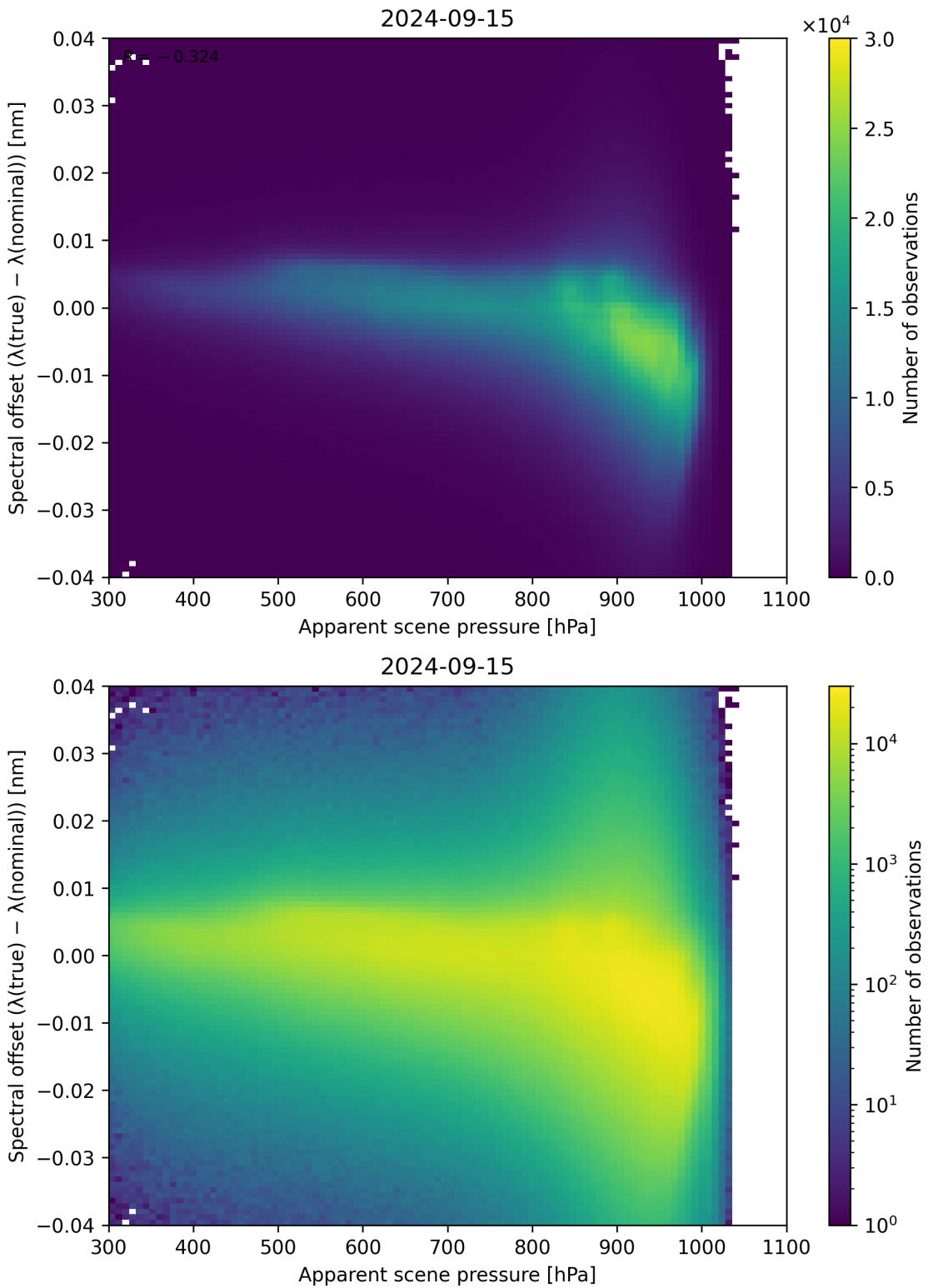


Figure 68: Scatter density plot of “Apparent scene pressure” against “Spectral offset ( $\lambda_{\text{true}} - \lambda_{\text{nominal}}$ )” for 2024-09-14 to 2024-09-16.

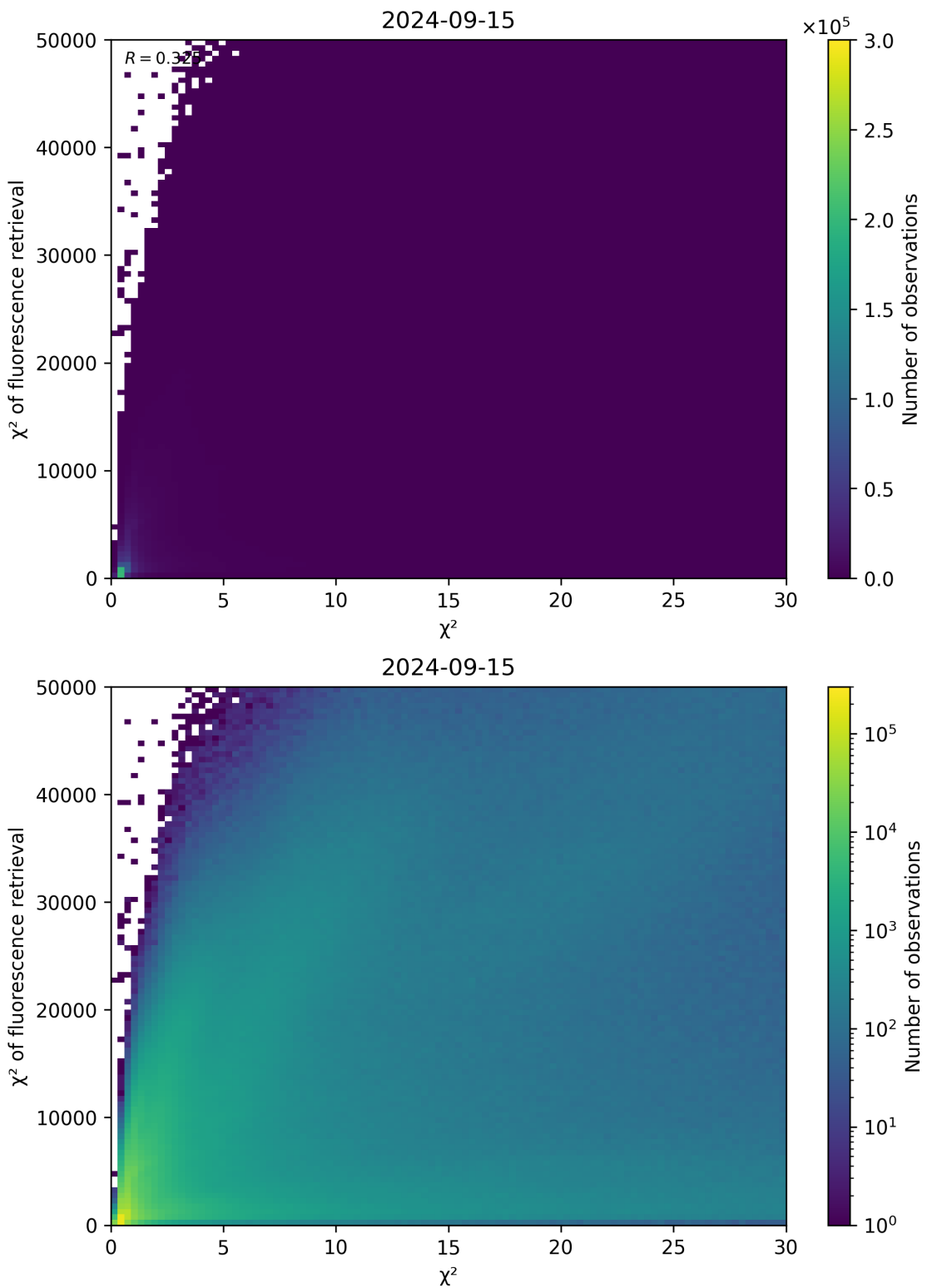


Figure 69: Scatter density plot of “ $\chi^2$ ” against “ $\chi^2$  of fluorescence retrieval” for 2024-09-14 to 2024-09-16.

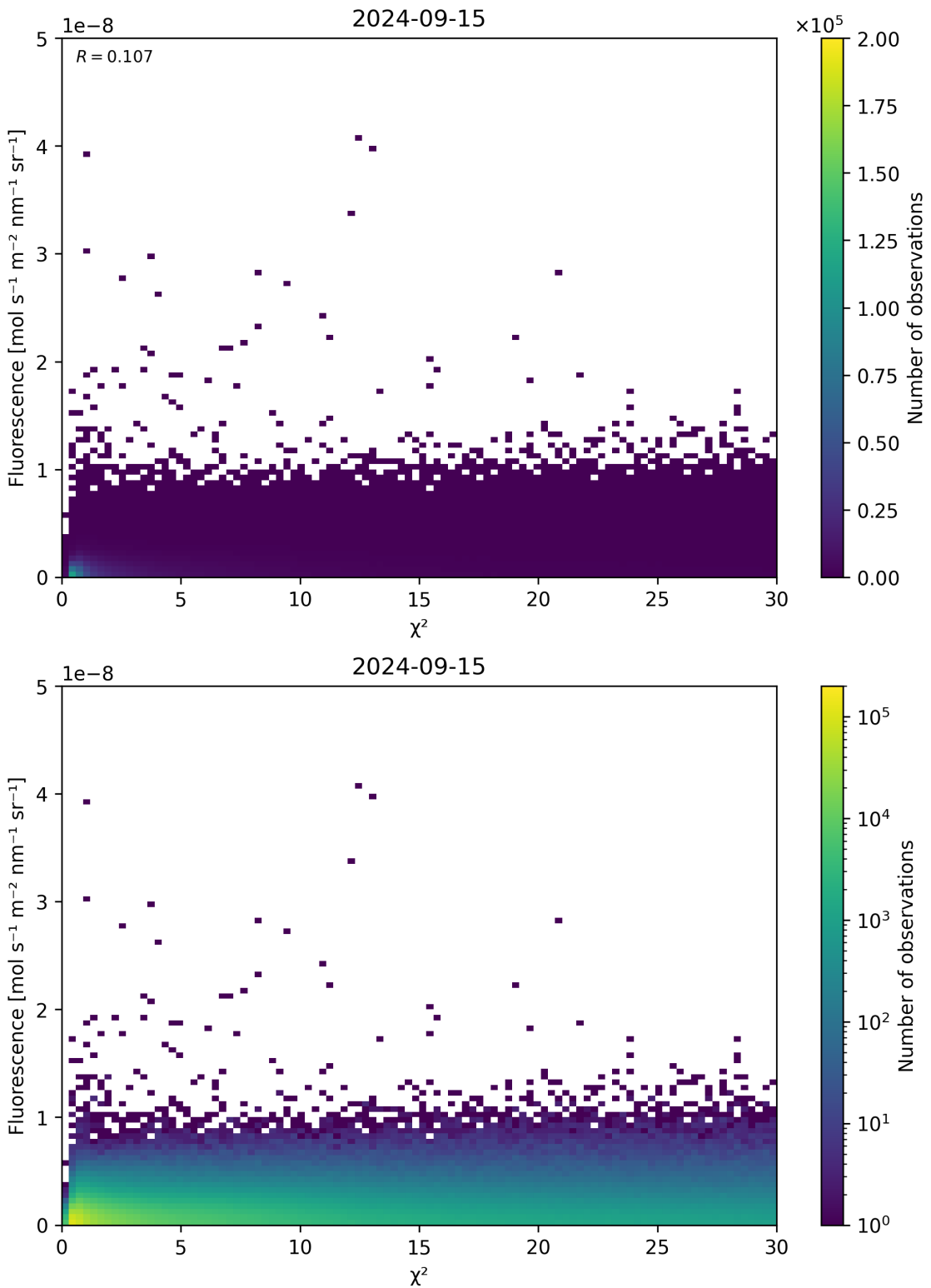


Figure 70: Scatter density plot of “ $\chi^2$ ” against “Fluorescence” for 2024-09-14 to 2024-09-16.

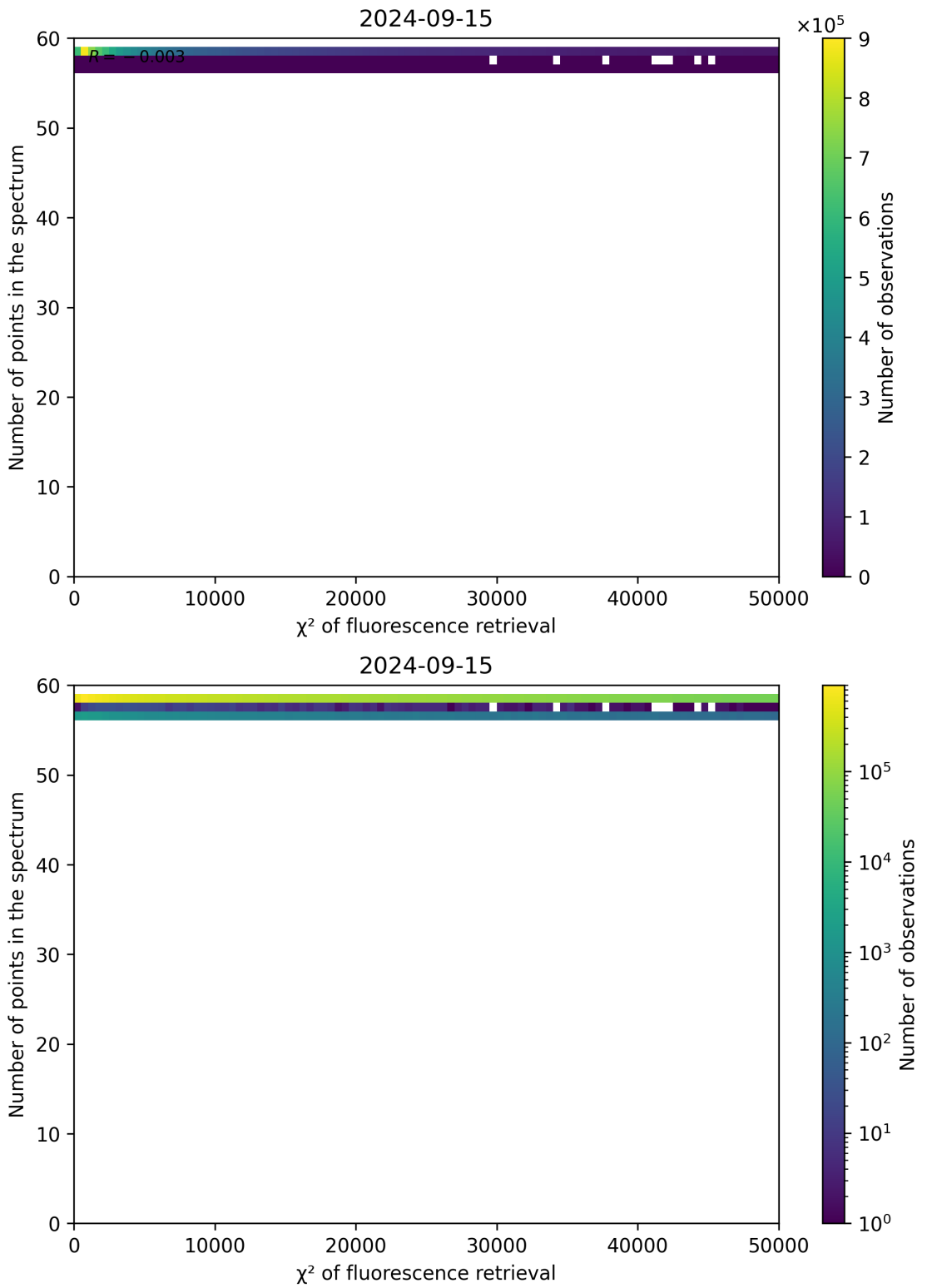


Figure 71: Scatter density plot of “ $\chi^2$  of fluorescence retrieval” against “Number of points in the spectrum” for 2024-09-14 to 2024-09-16.

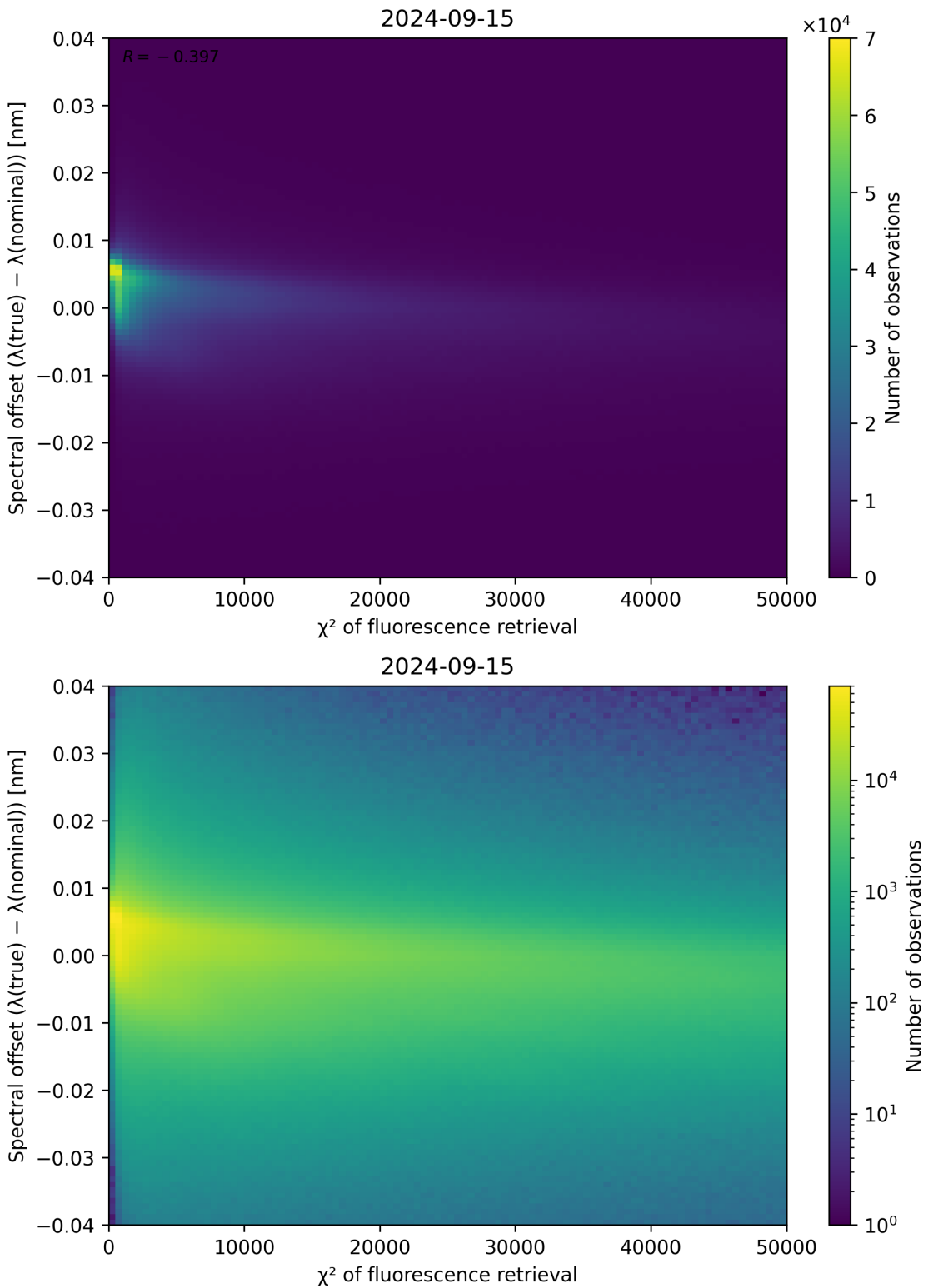


Figure 72: Scatter density plot of “ $\chi^2$  of fluorescence retrieval” against “Spectral offset ( $\lambda_{\text{true}} - \lambda_{\text{nominal}}$ )” for 2024-09-14 to 2024-09-16.

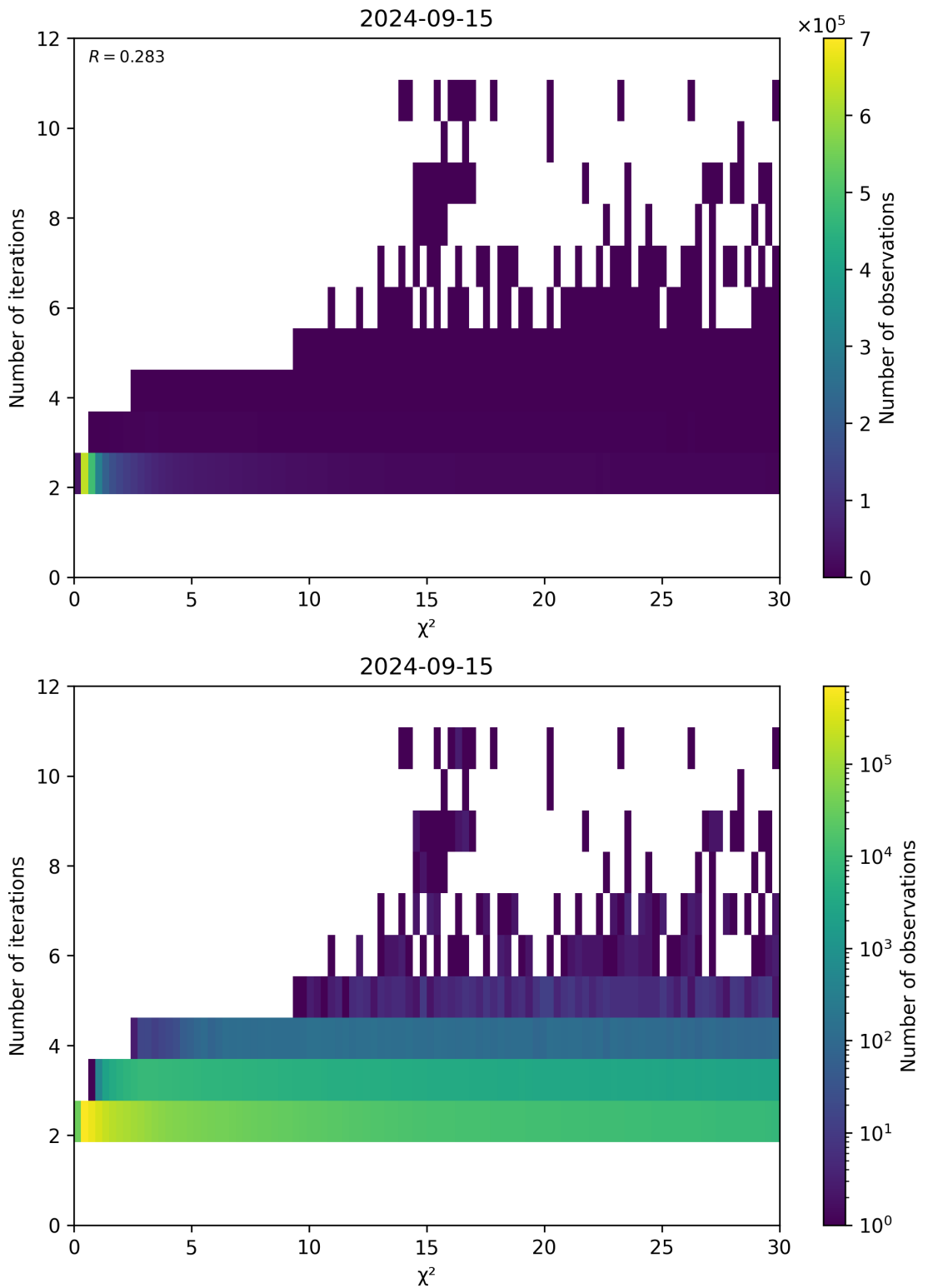


Figure 73: Scatter density plot of “ $\chi^2$ ” against “Number of iterations” for 2024-09-14 to 2024-09-16.

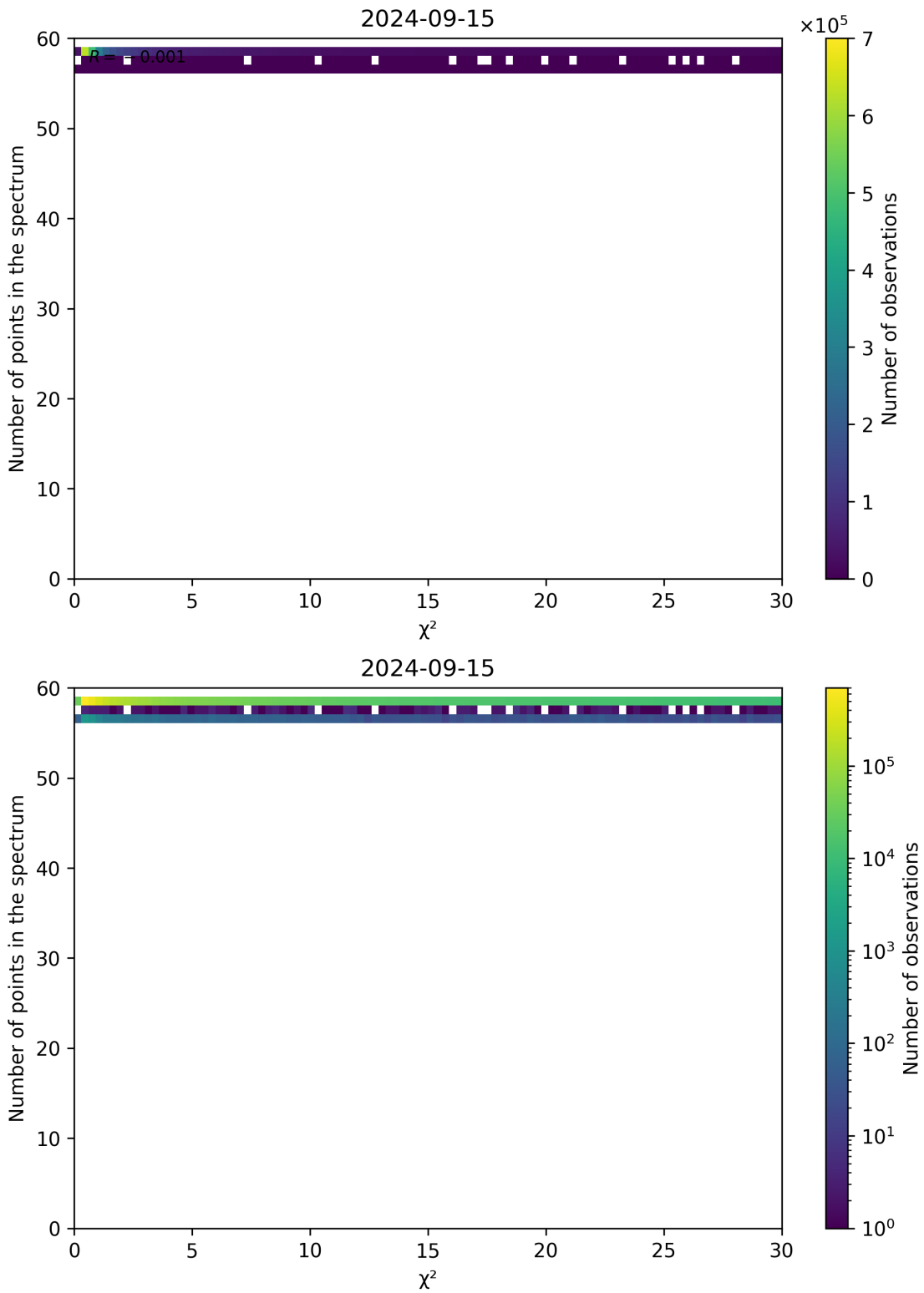


Figure 74: Scatter density plot of “ $\chi^2$ ” against “Number of points in the spectrum” for 2024-09-14 to 2024-09-16.

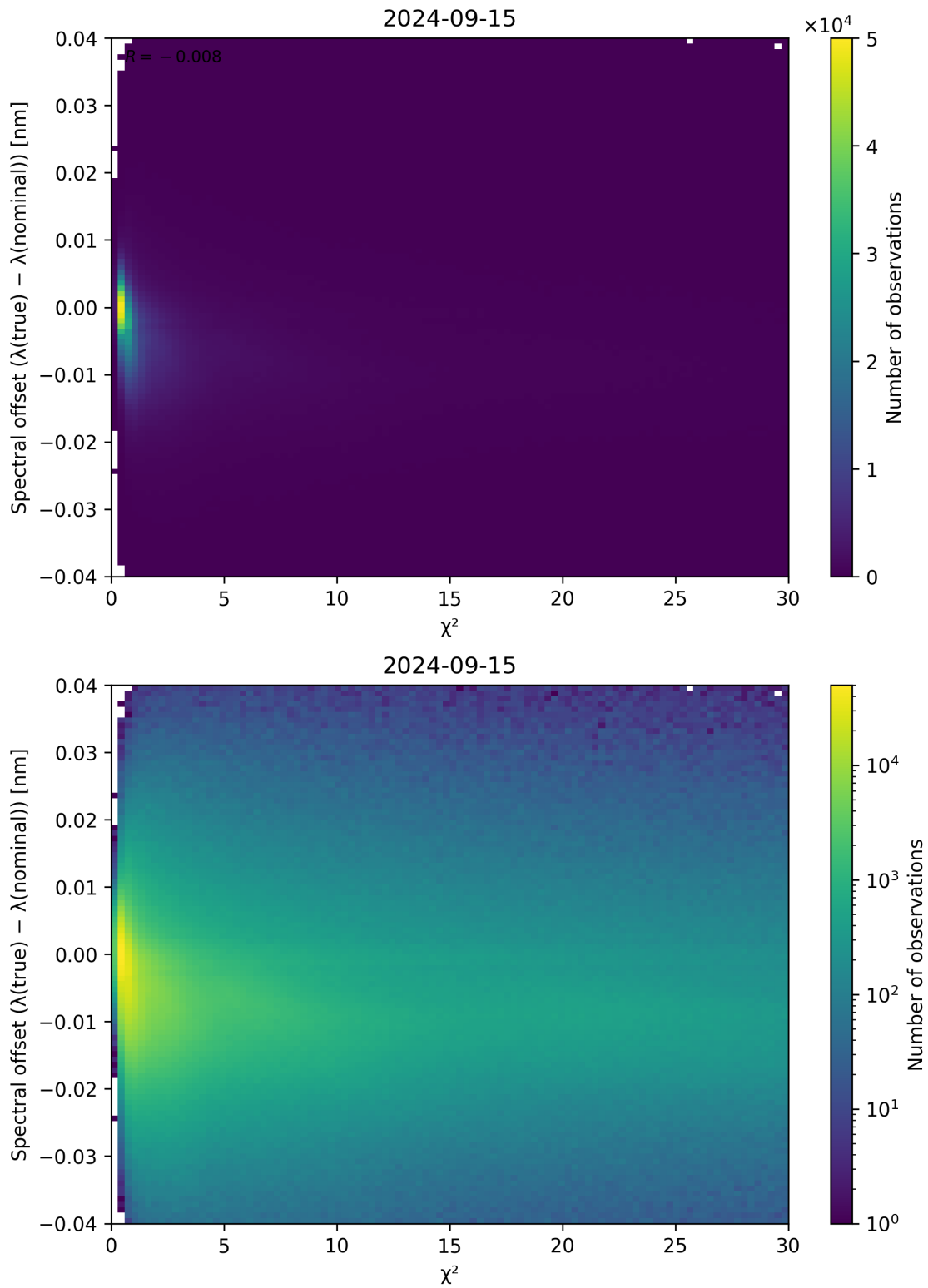


Figure 75: Scatter density plot of “ $\chi^2$ ” against “Spectral offset ( $\lambda_{\text{true}} - \lambda_{\text{nominal}}$ )” for 2024-09-14 to 2024-09-16.

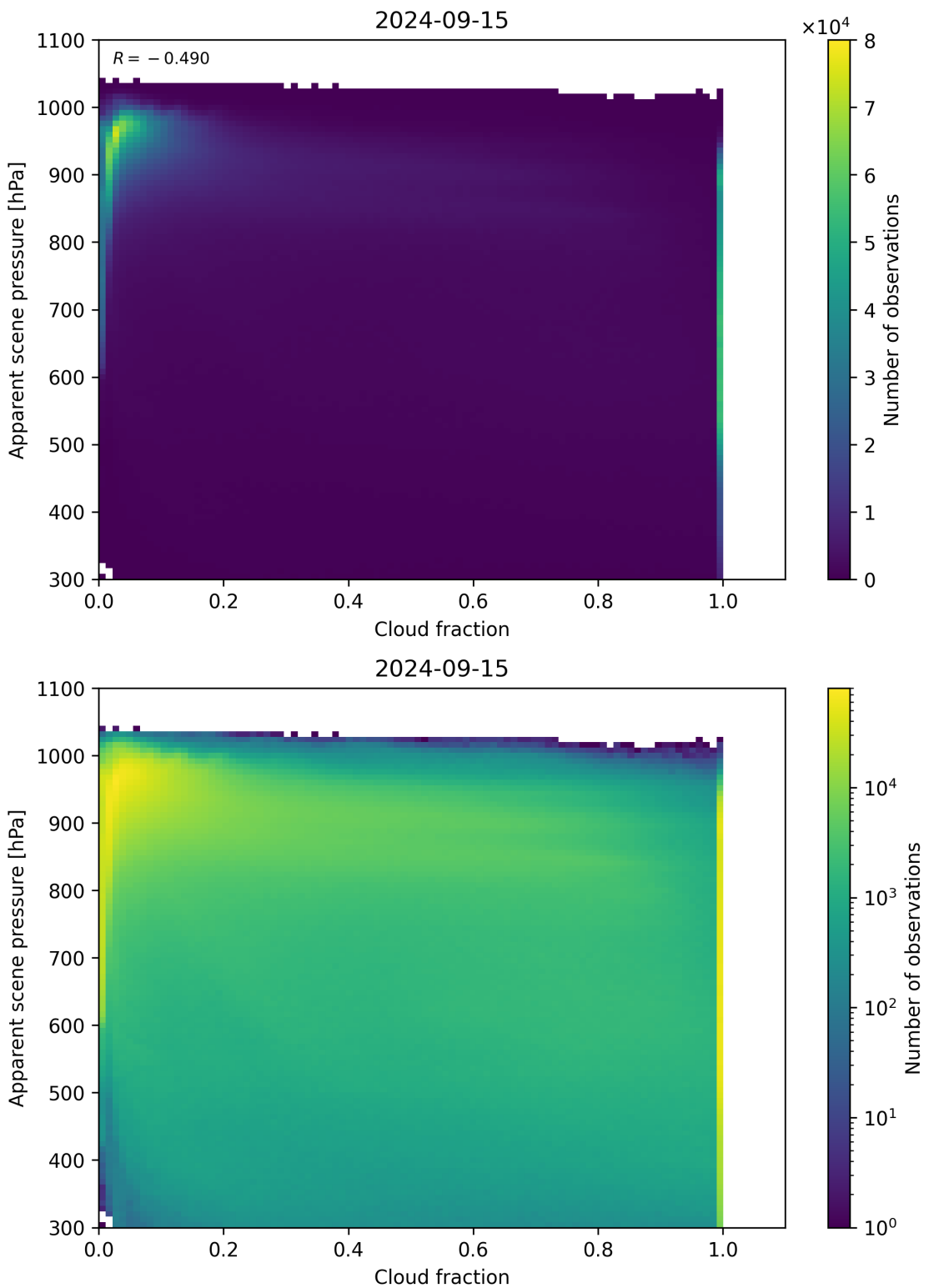


Figure 76: Scatter density plot of “Cloud fraction” against “Apparent scene pressure” for 2024-09-14 to 2024-09-16.

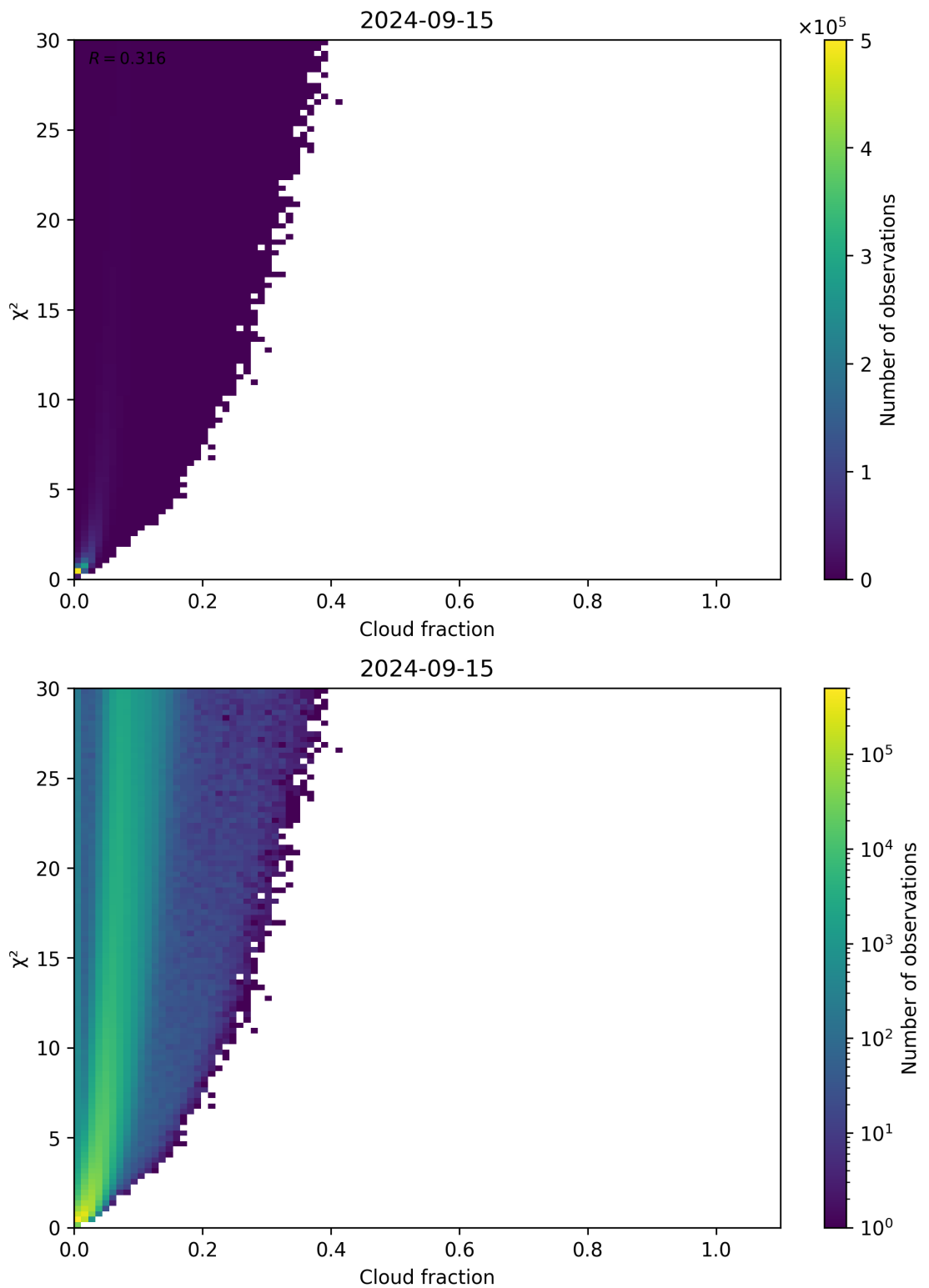


Figure 77: Scatter density plot of “Cloud fraction” against “ $\chi^2$ ” for 2024-09-14 to 2024-09-16.

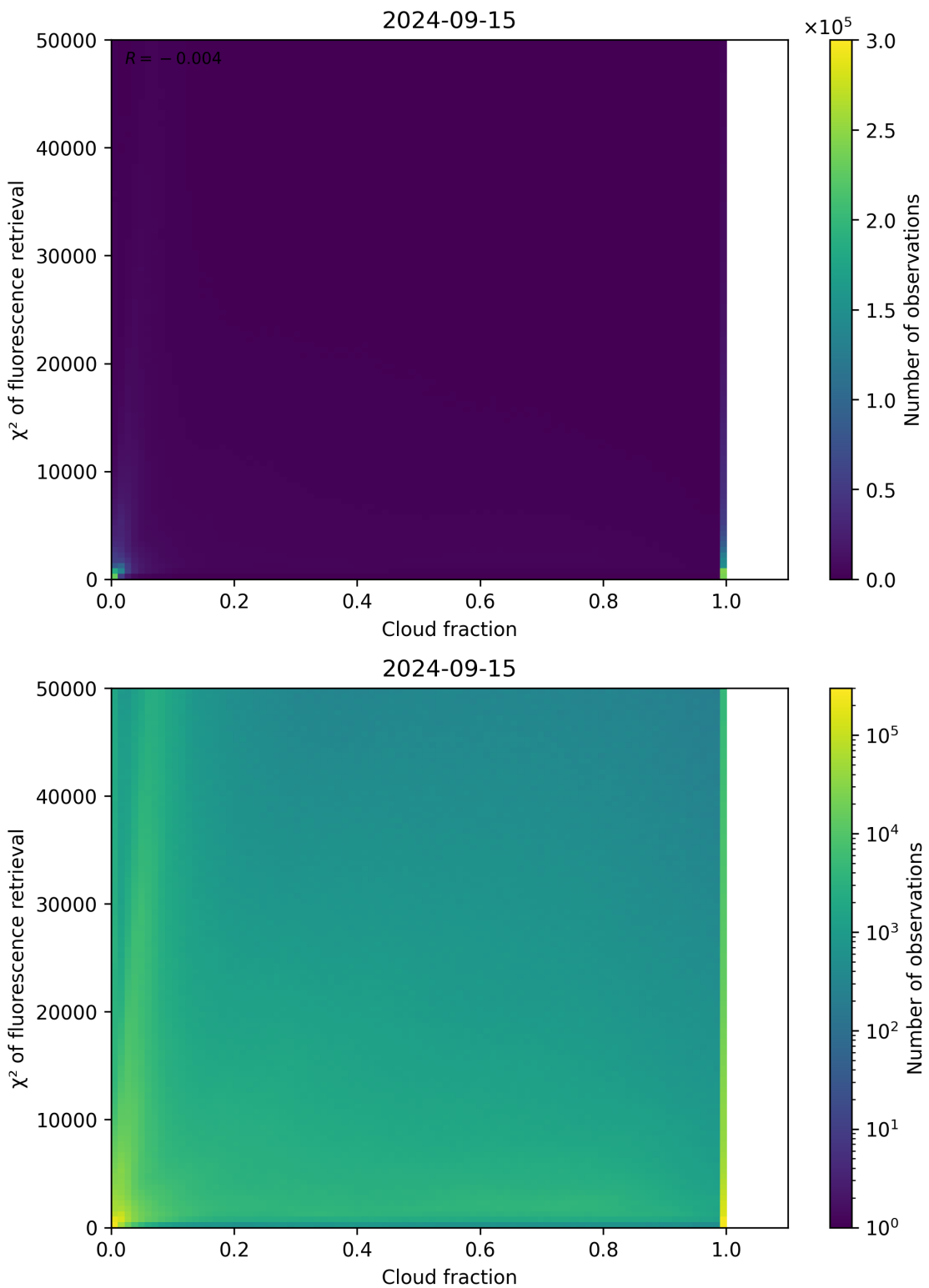


Figure 78: Scatter density plot of “Cloud fraction” against “ $\chi^2$  of fluorescence retrieval” for 2024-09-14 to 2024-09-16.

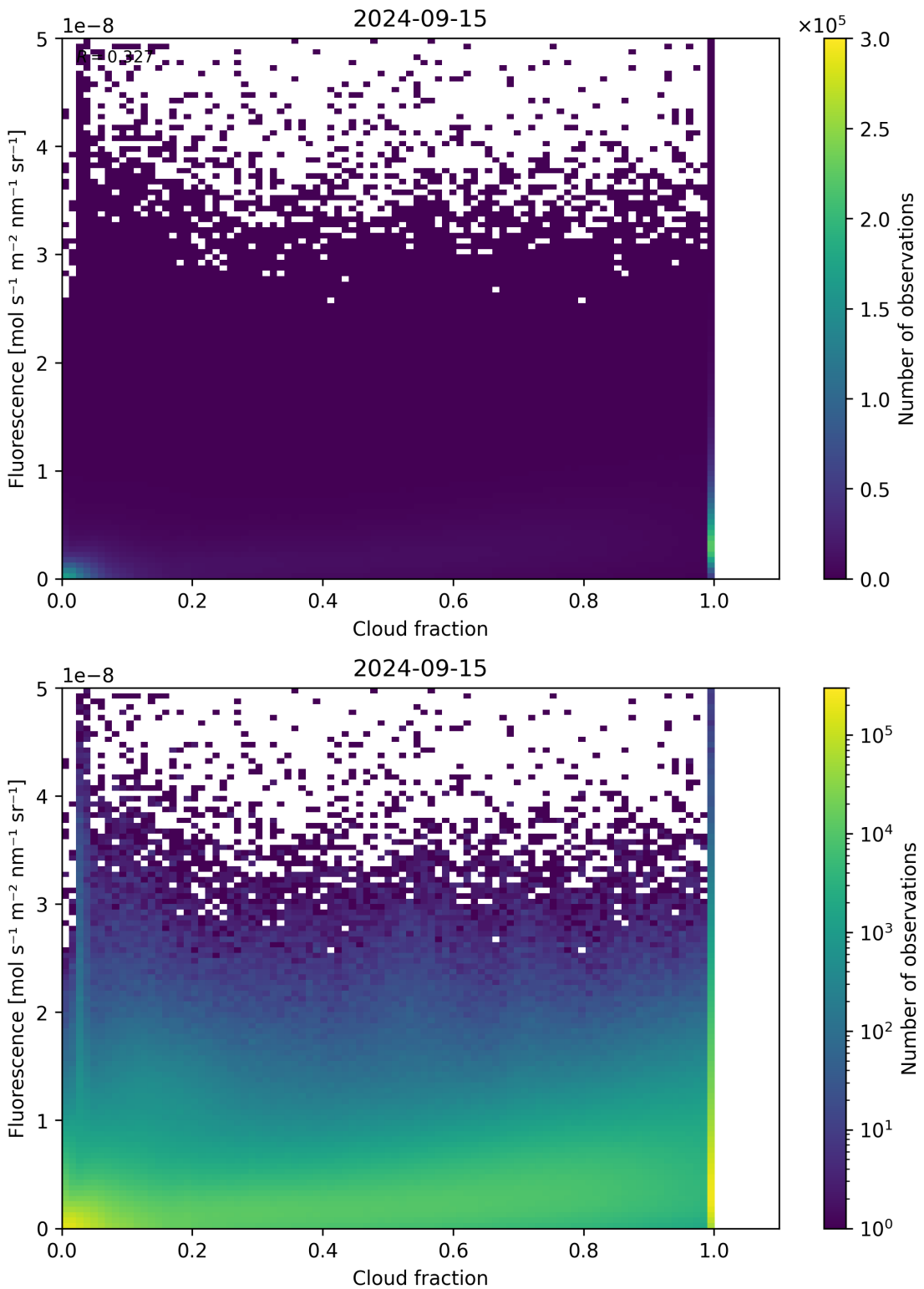


Figure 79: Scatter density plot of “Cloud fraction” against “Fluorescence” for 2024-09-14 to 2024-09-16.

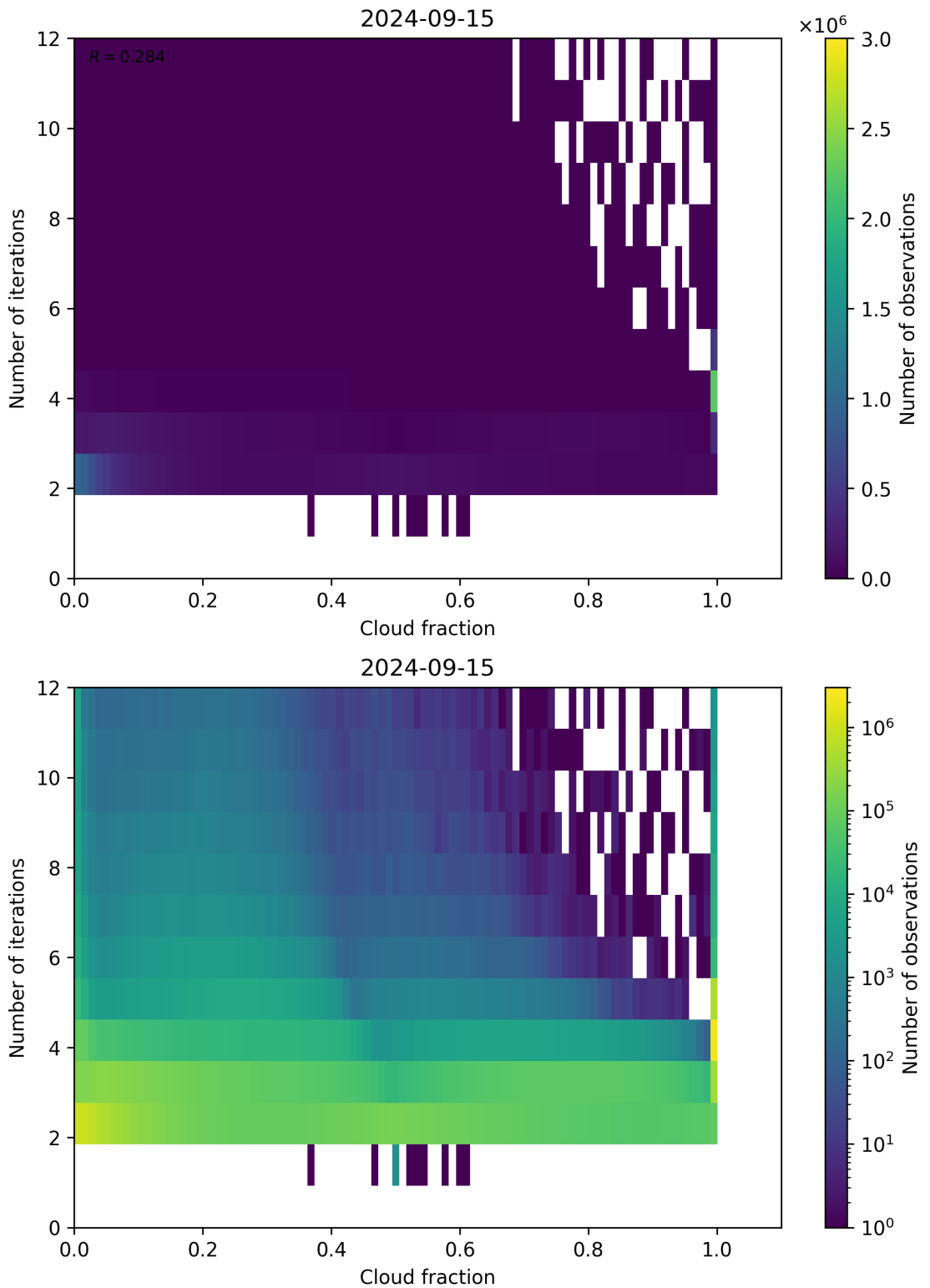


Figure 80: Scatter density plot of “Cloud fraction” against “Number of iterations” for 2024-09-14 to 2024-09-16.

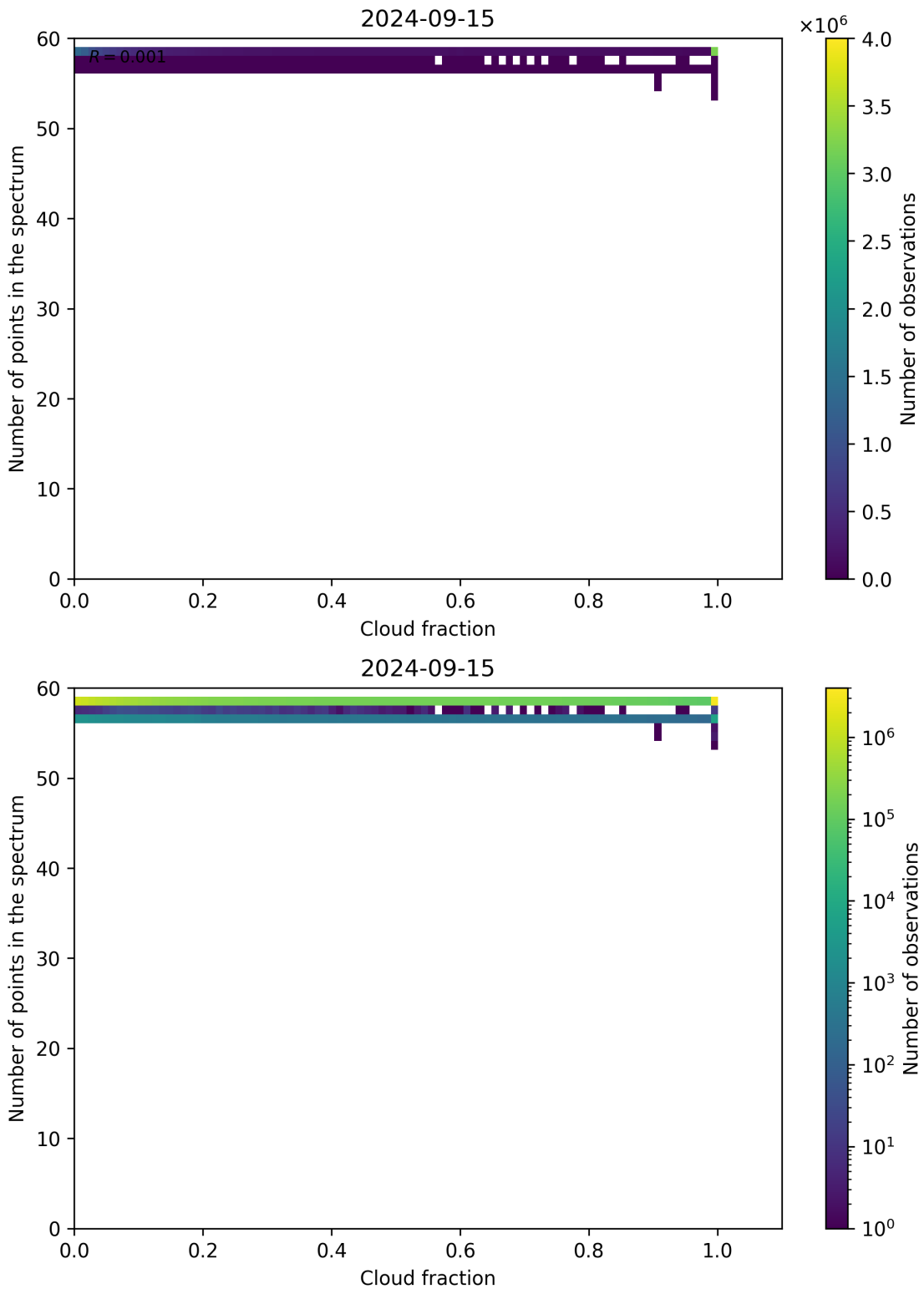


Figure 81: Scatter density plot of “Cloud fraction” against “Number of points in the spectrum” for 2024-09-14 to 2024-09-16.

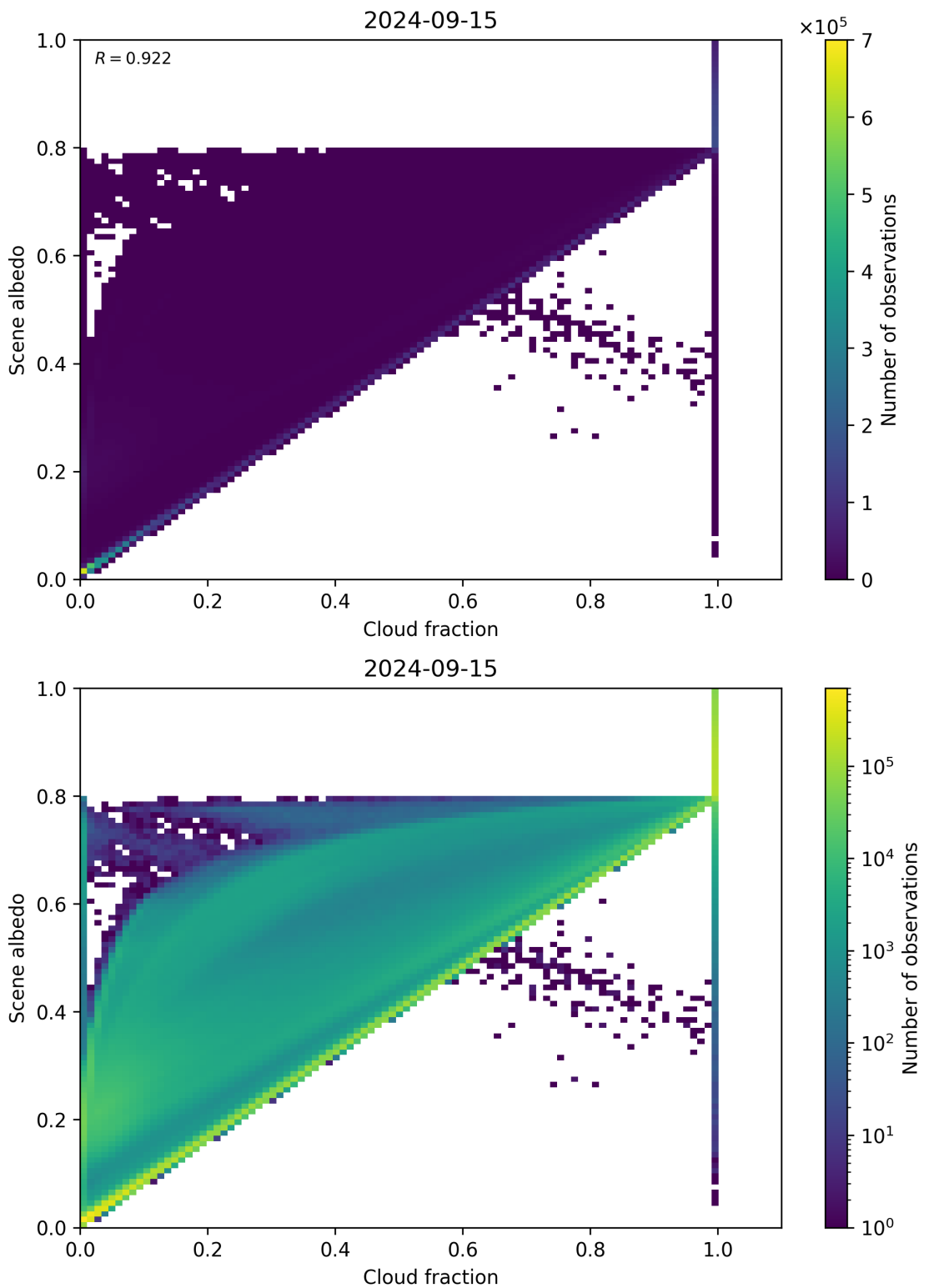


Figure 82: Scatter density plot of “Cloud fraction” against “Scene albedo” for 2024-09-14 to 2024-09-16.

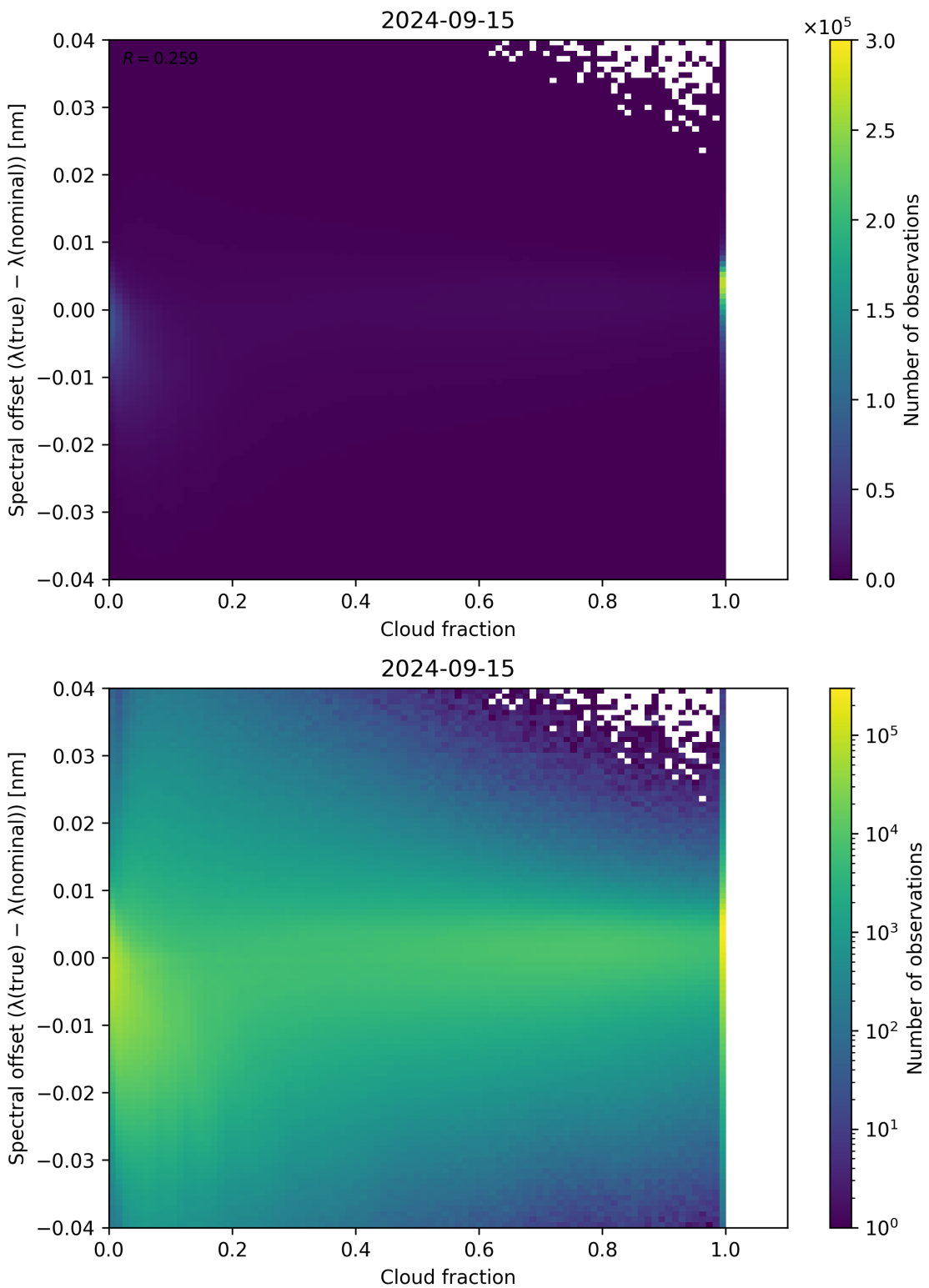


Figure 83: Scatter density plot of “Cloud fraction” against “Spectral offset ( $\lambda_{\text{true}} - \lambda_{\text{nominal}}$ )” for 2024-09-14 to 2024-09-16.

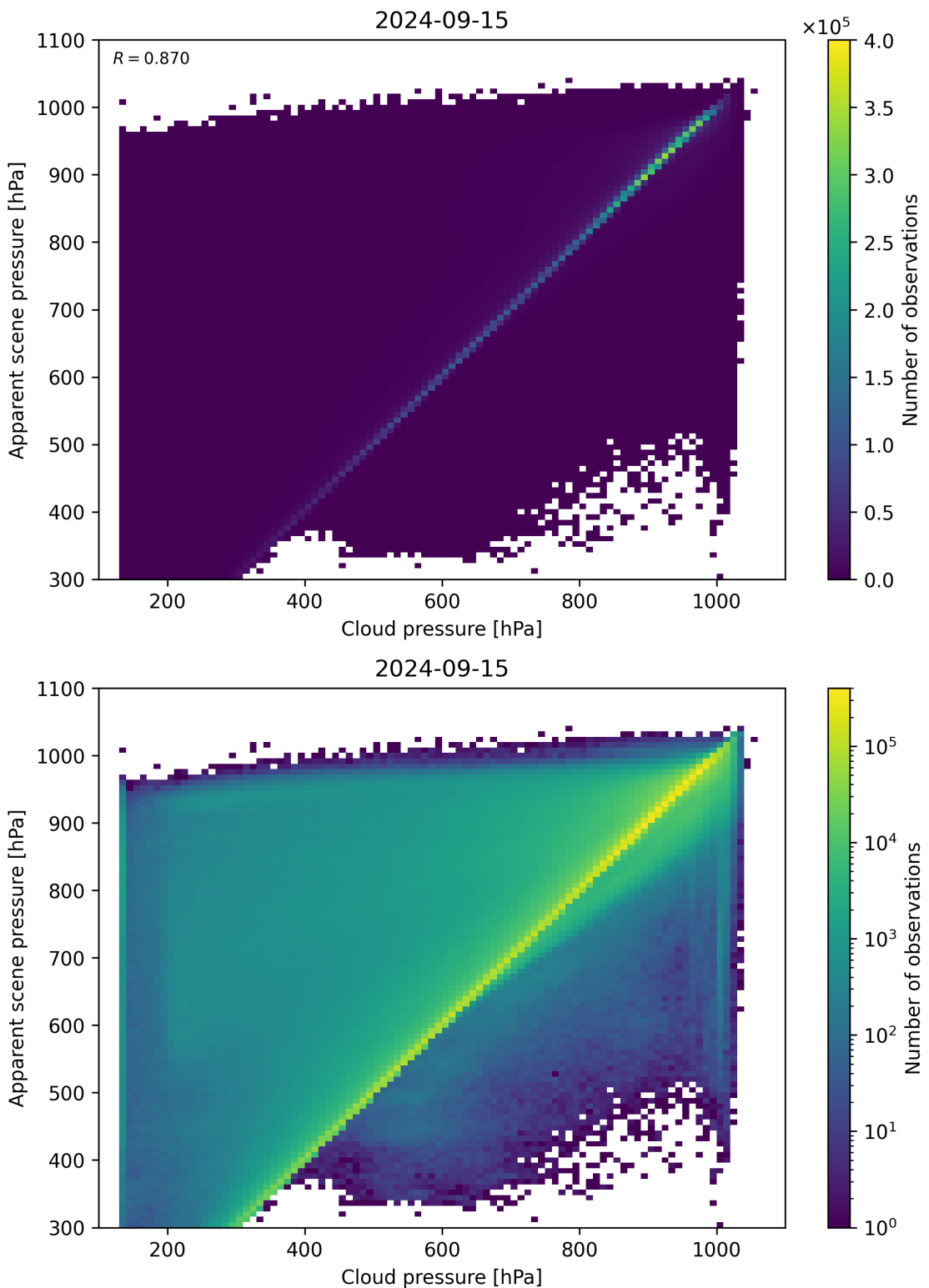


Figure 84: Scatter density plot of “Cloud pressure” against “Apparent scene pressure” for 2024-09-14 to 2024-09-16.

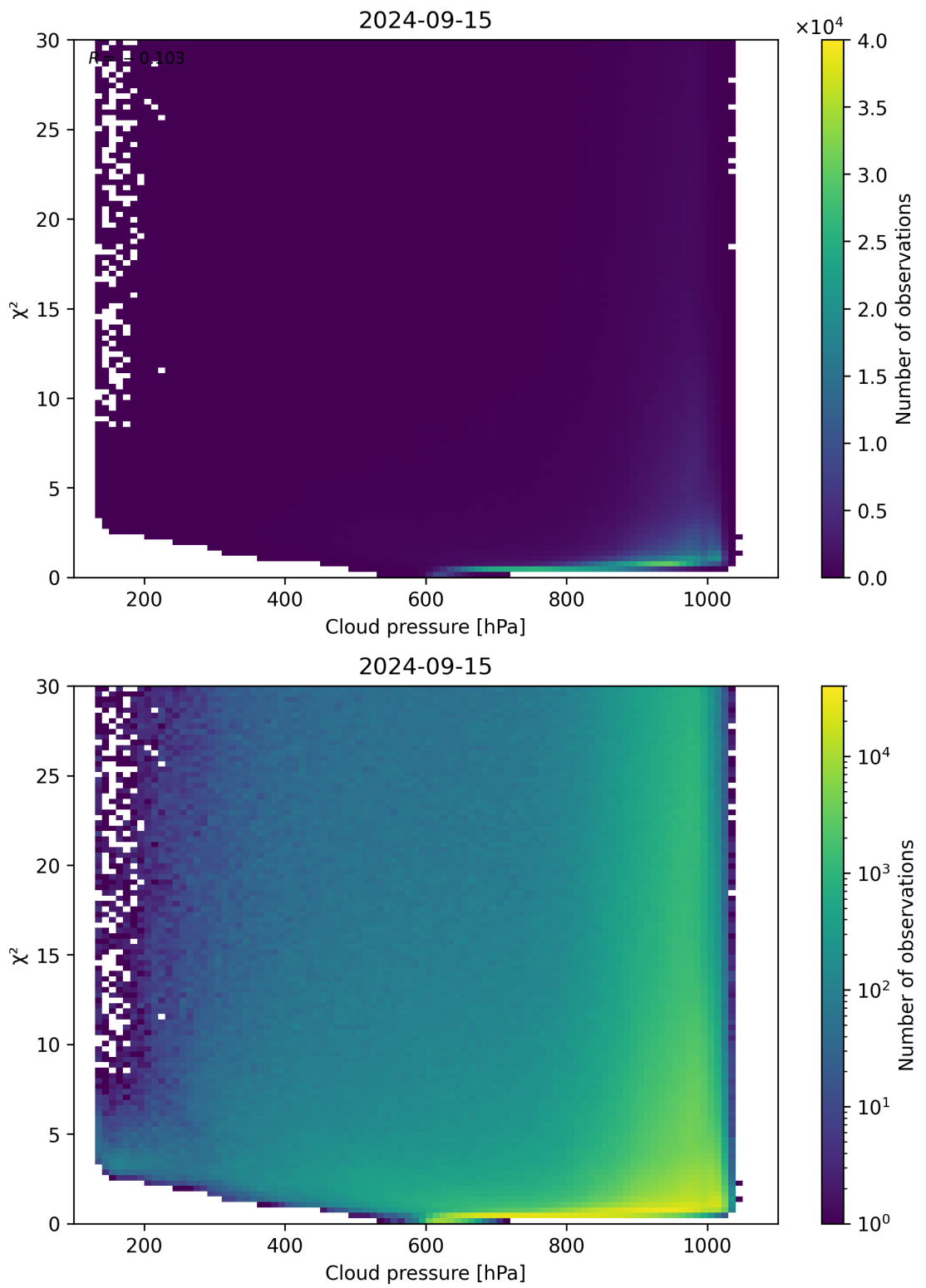


Figure 85: Scatter density plot of “Cloud pressure” against “ $\chi^2$ ” for 2024-09-14 to 2024-09-16.

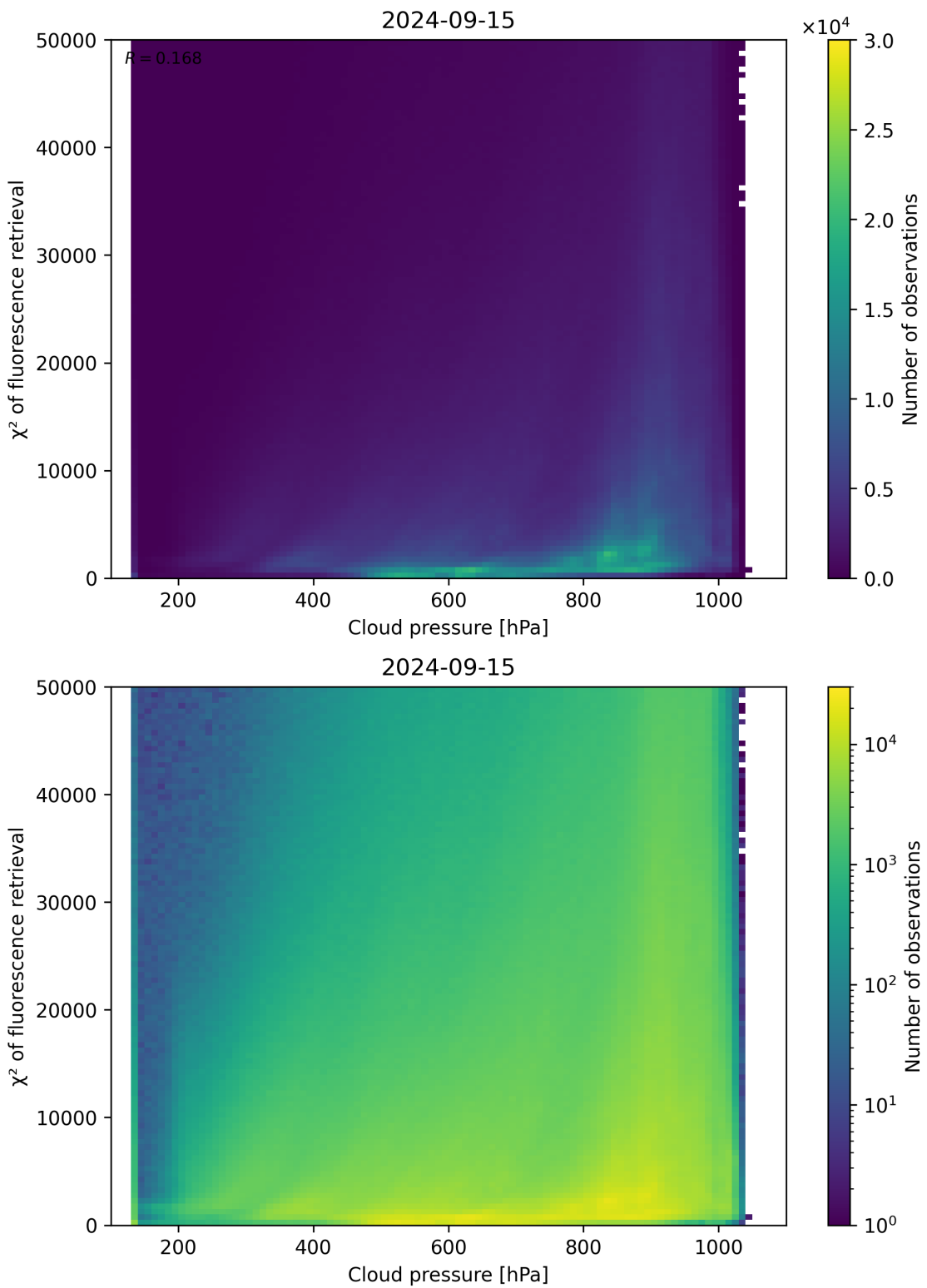


Figure 86: Scatter density plot of “Cloud pressure” against “ $\chi^2$  of fluorescence retrieval” for 2024-09-14 to 2024-09-16.

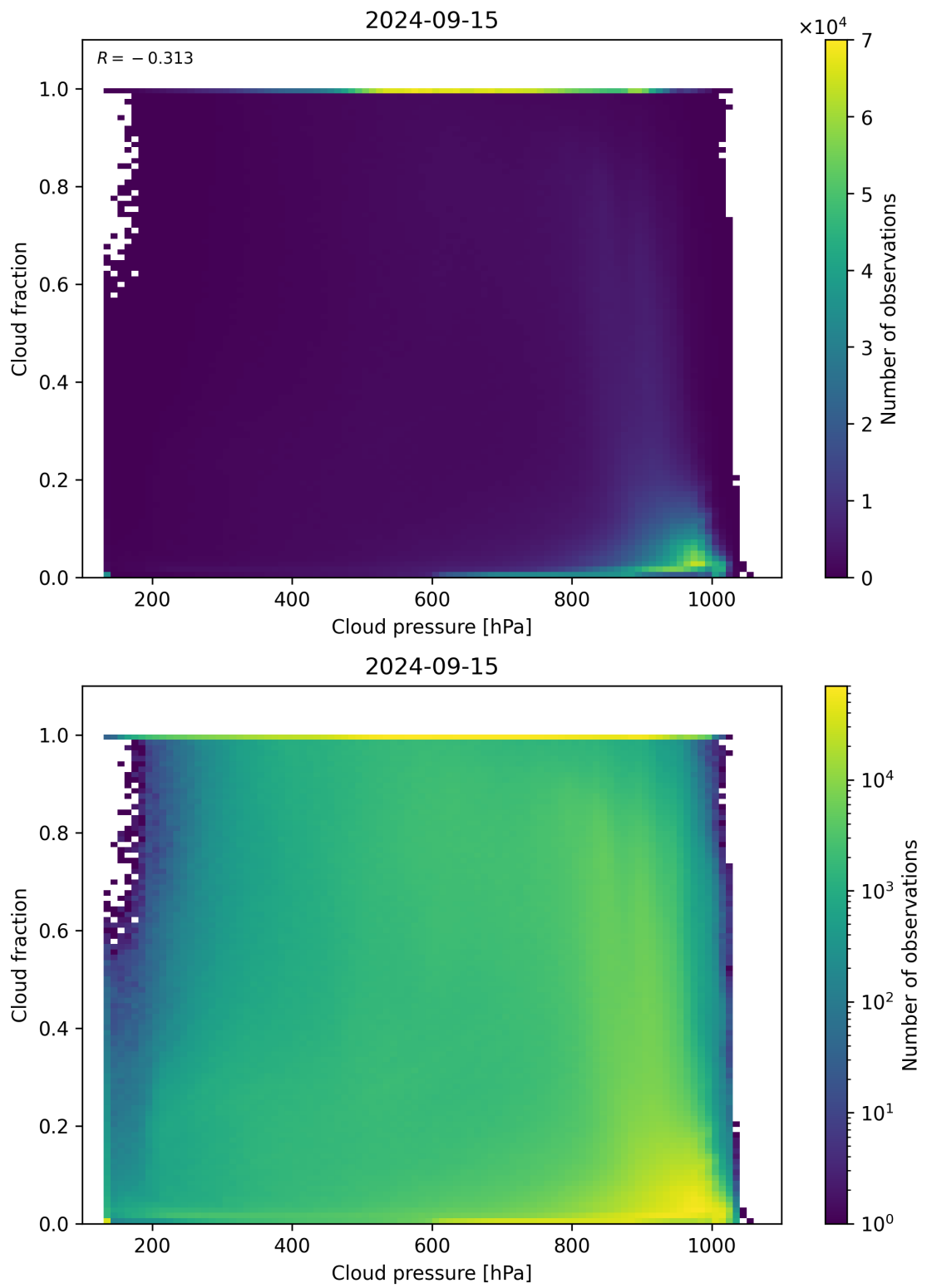


Figure 87: Scatter density plot of “Cloud pressure” against “Cloud fraction” for 2024-09-14 to 2024-09-16.

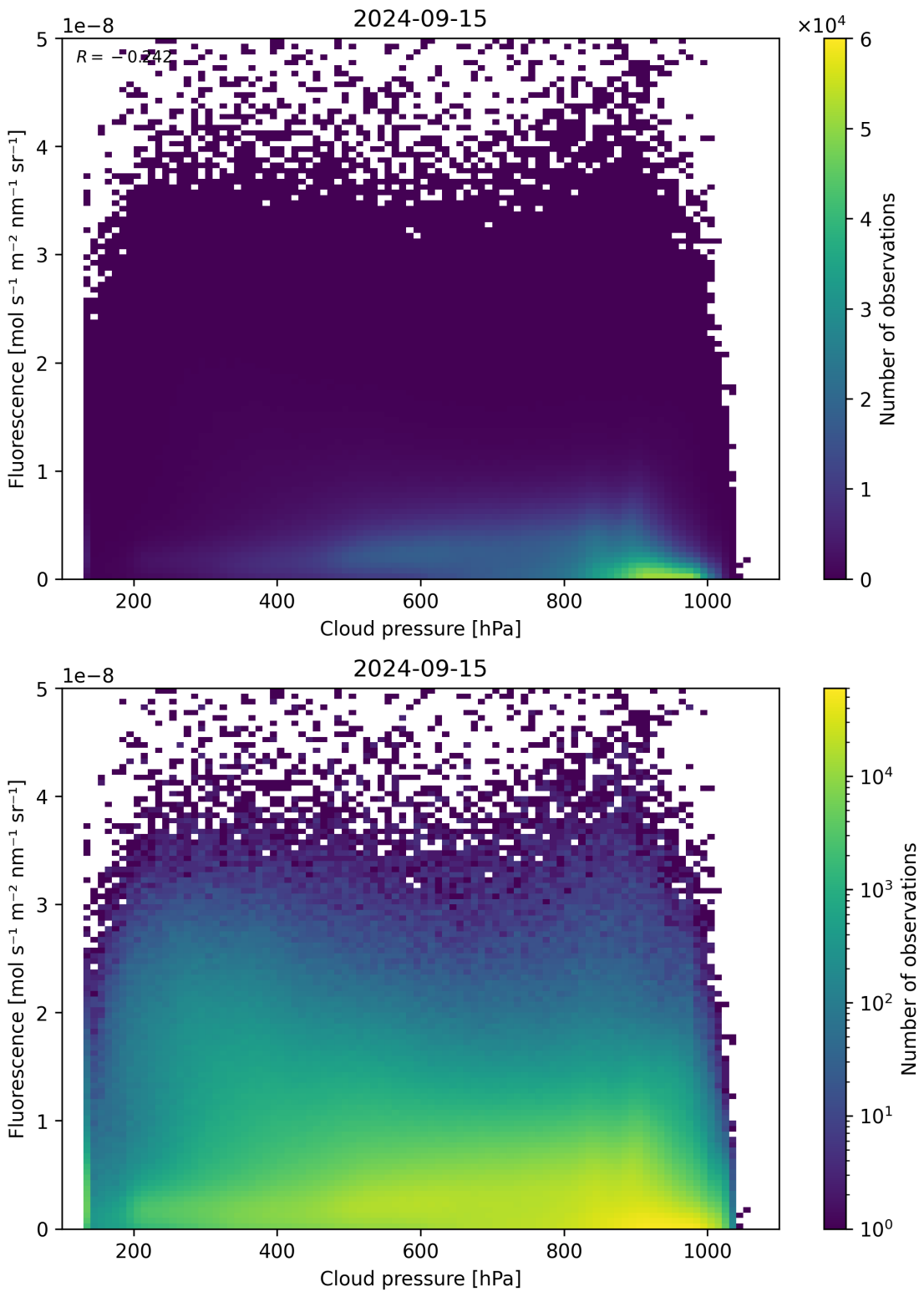


Figure 88: Scatter density plot of “Cloud pressure” against “Fluorescence” for 2024-09-14 to 2024-09-16.

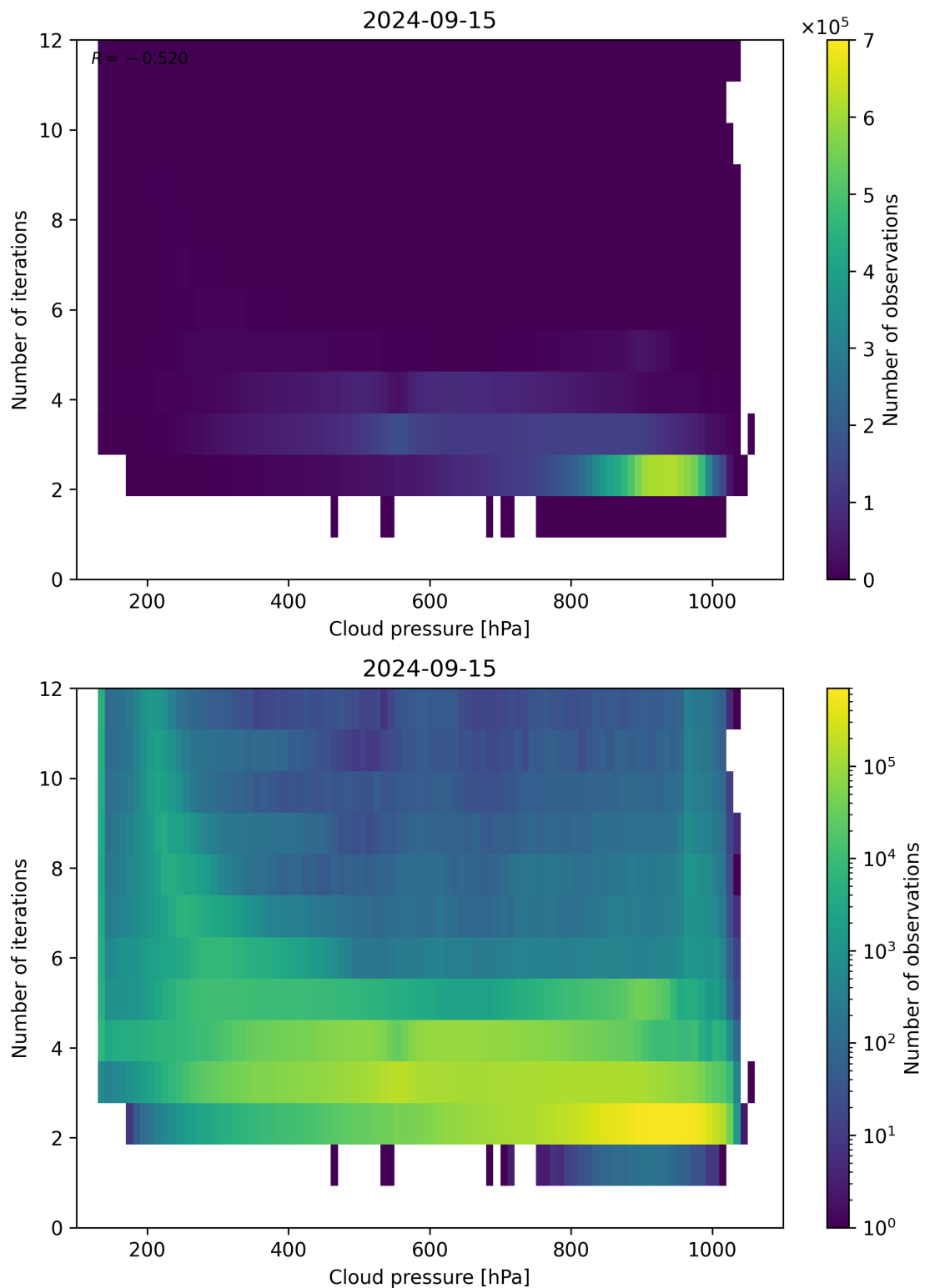


Figure 89: Scatter density plot of “Cloud pressure” against “Number of iterations” for 2024-09-14 to 2024-09-16.

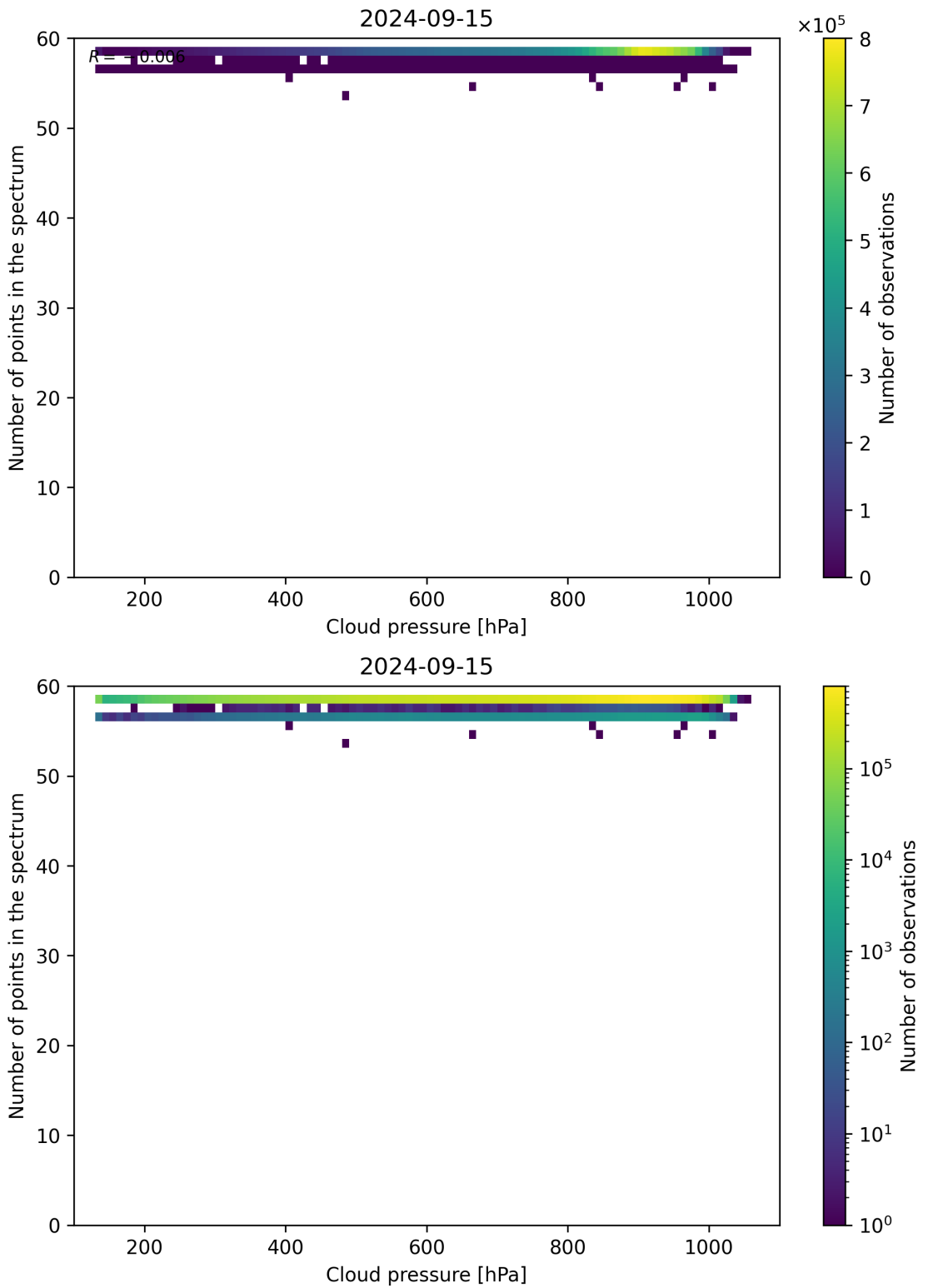


Figure 90: Scatter density plot of “Cloud pressure” against “Number of points in the spectrum” for 2024-09-14 to 2024-09-16.

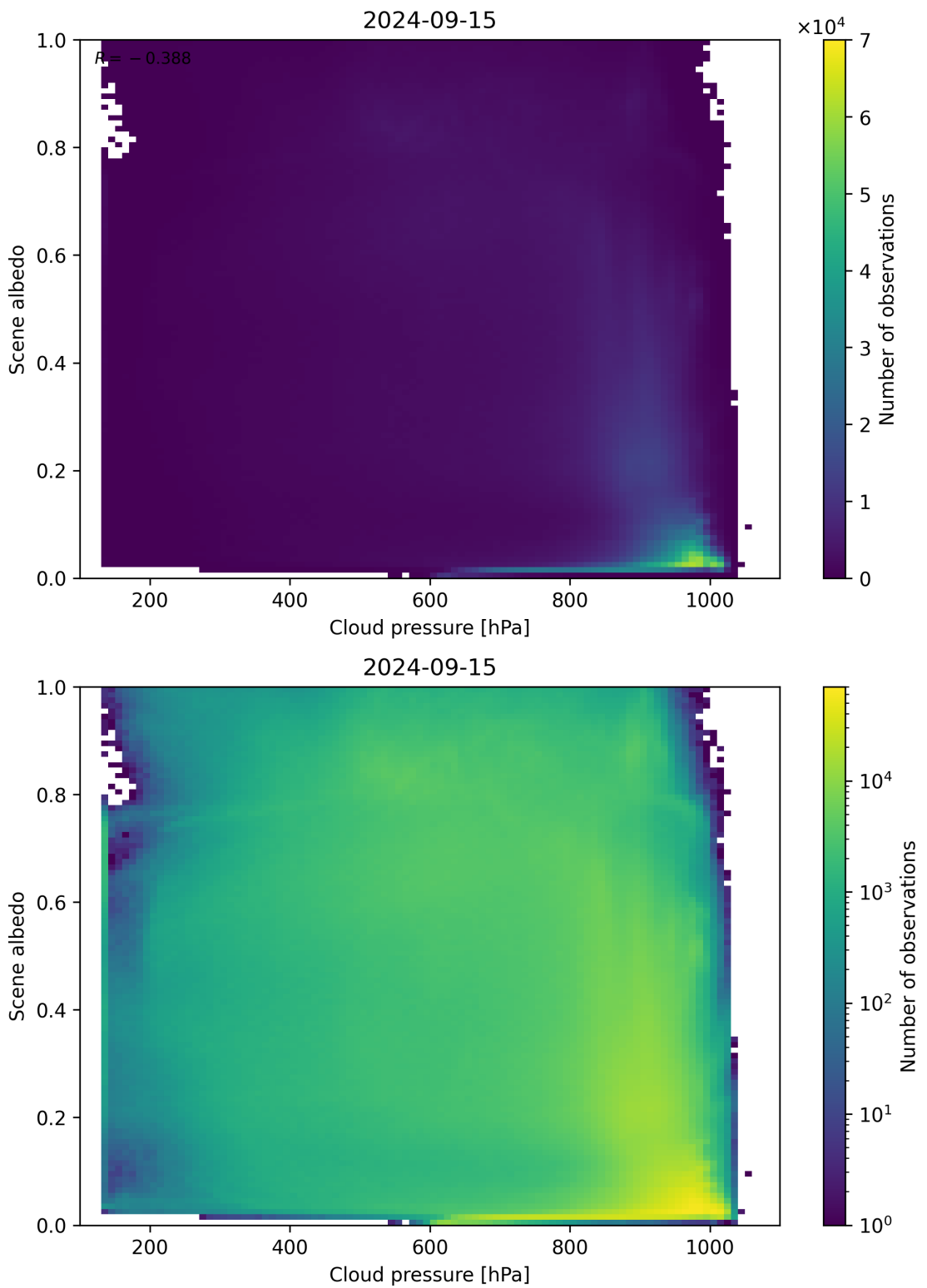


Figure 91: Scatter density plot of “Cloud pressure” against “Scene albedo” for 2024-09-14 to 2024-09-16.

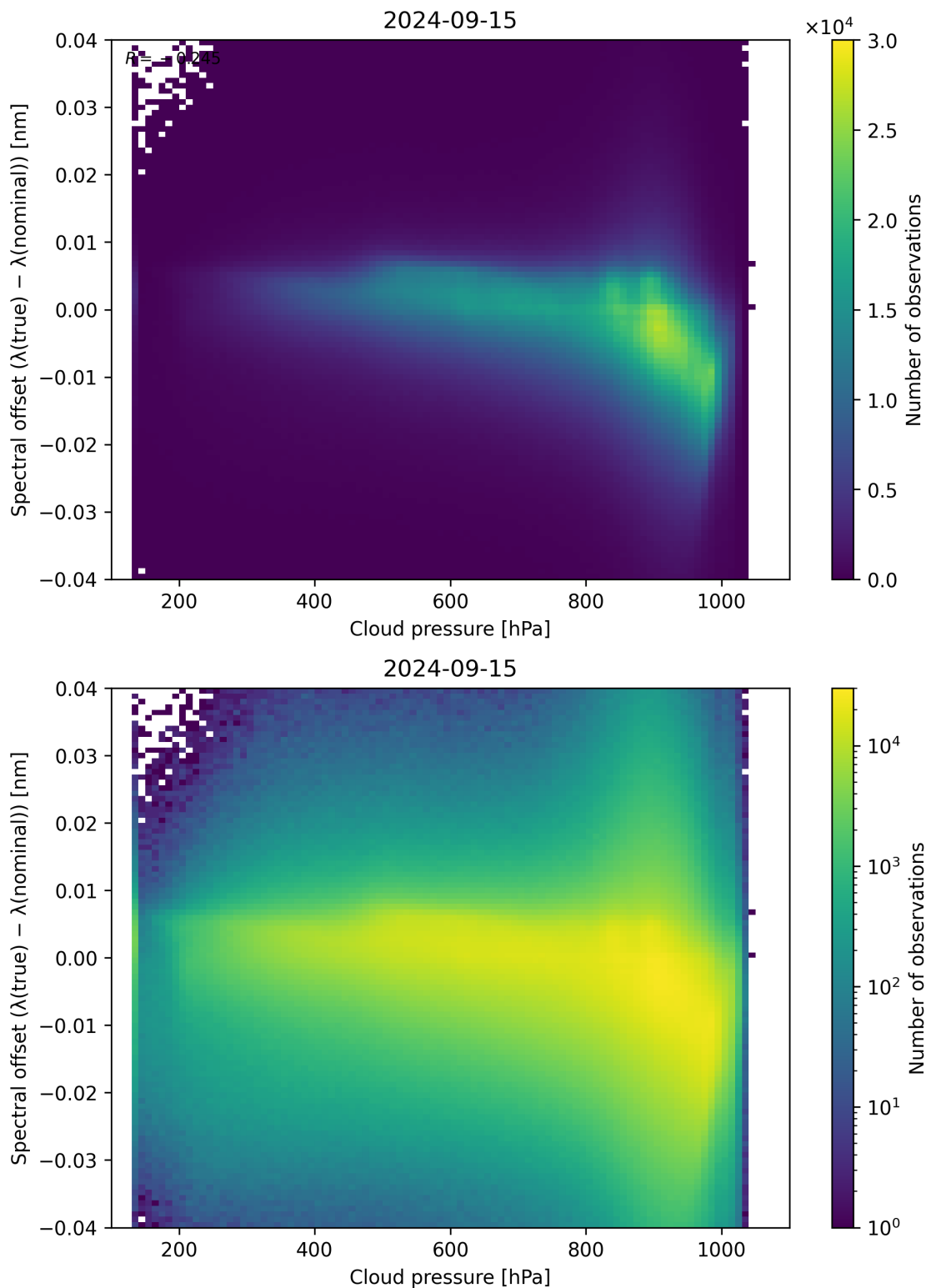


Figure 92: Scatter density plot of “Cloud pressure” against “Spectral offset ( $\lambda_{\text{true}} - \lambda_{\text{nominal}}$ )” for 2024-09-14 to 2024-09-16.

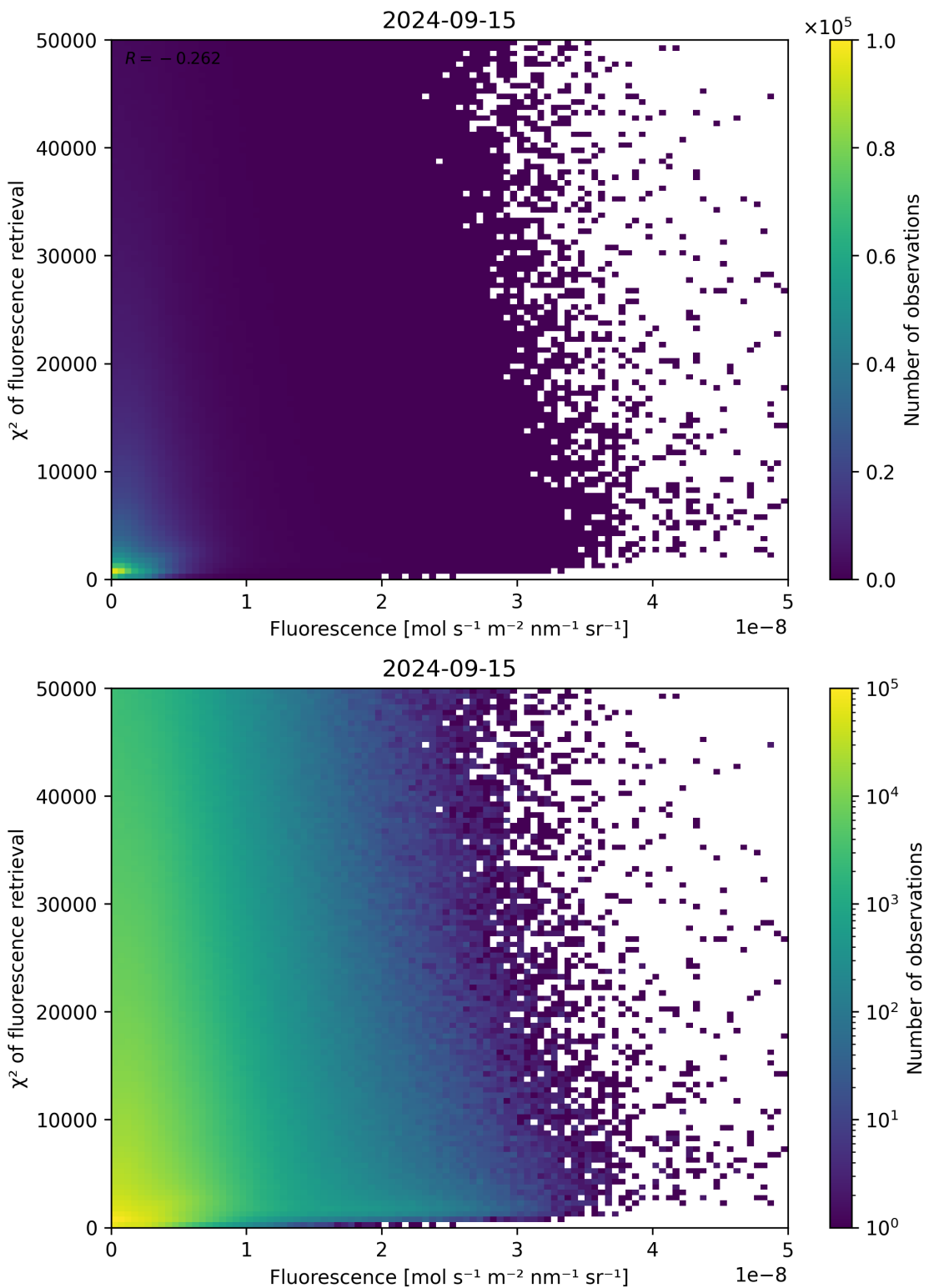


Figure 93: Scatter density plot of “Fluorescence” against “ $\chi^2$  of fluorescence retrieval” for 2024-09-14 to 2024-09-16.

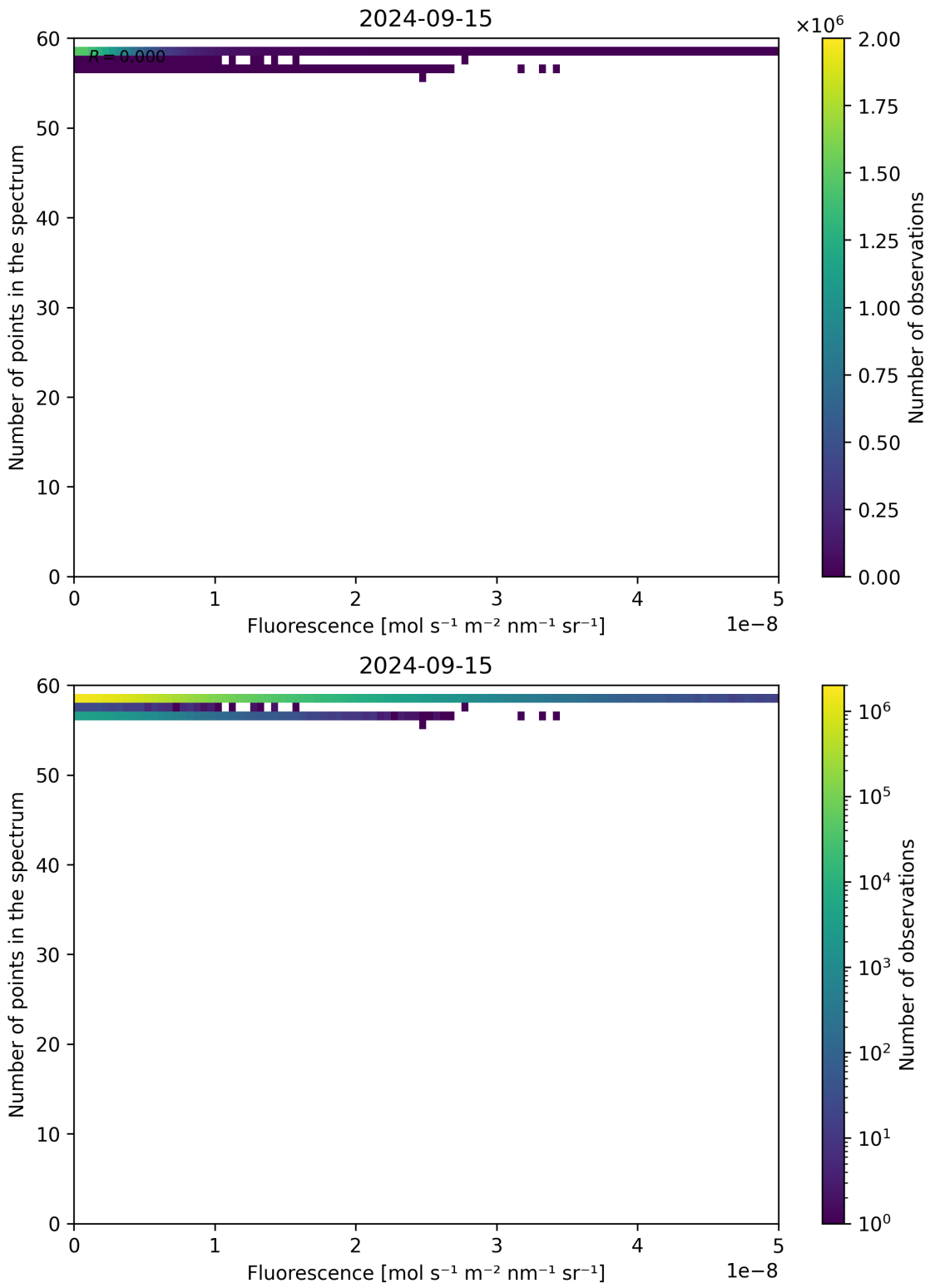


Figure 94: Scatter density plot of “Fluorescence” against “Number of points in the spectrum” for 2024-09-14 to 2024-09-16.

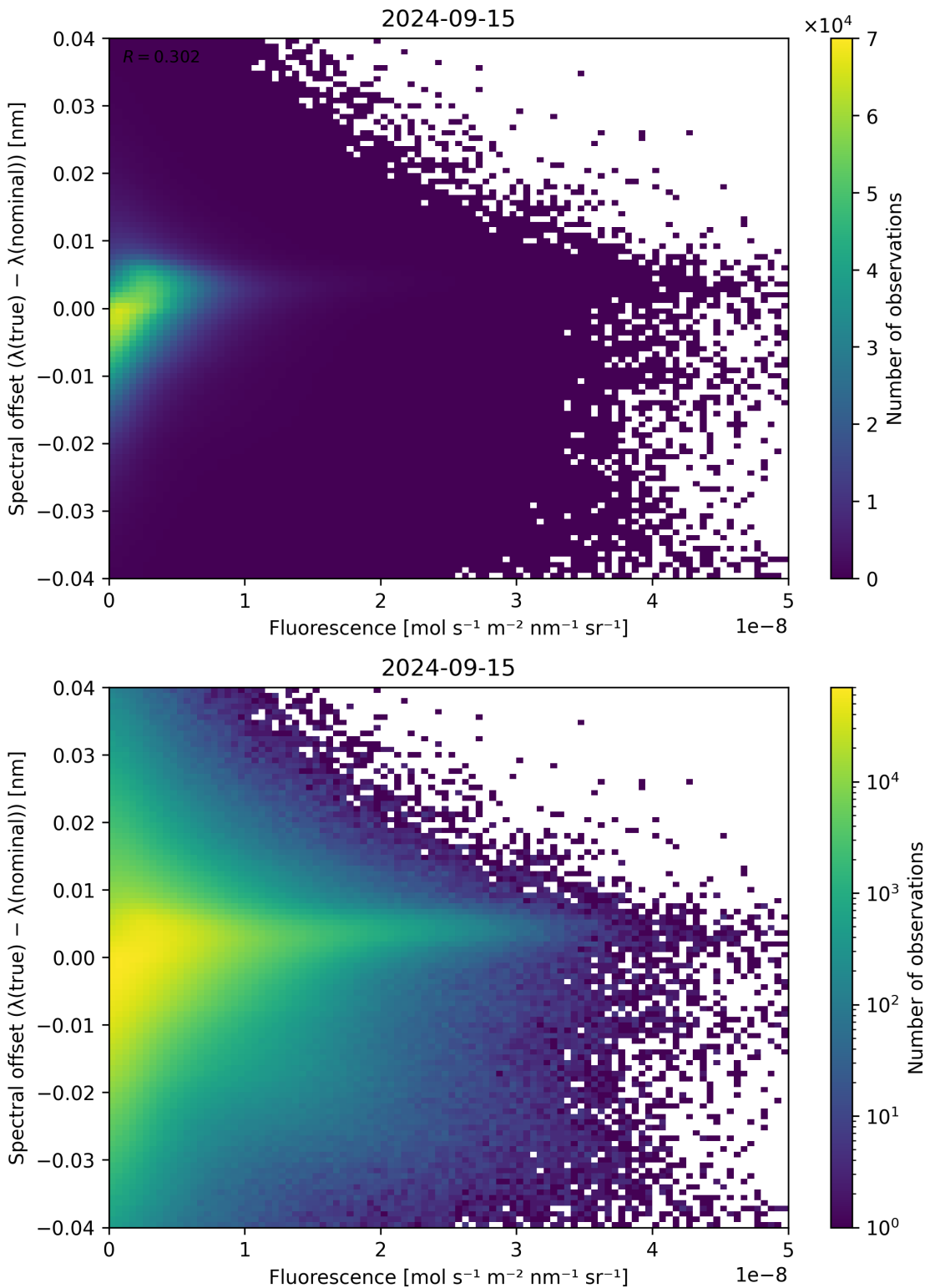


Figure 95: Scatter density plot of “Fluorescence” against “Spectral offset ( $\lambda_{\text{true}} - \lambda_{\text{nominal}}$ )” for 2024-09-14 to 2024-09-16.

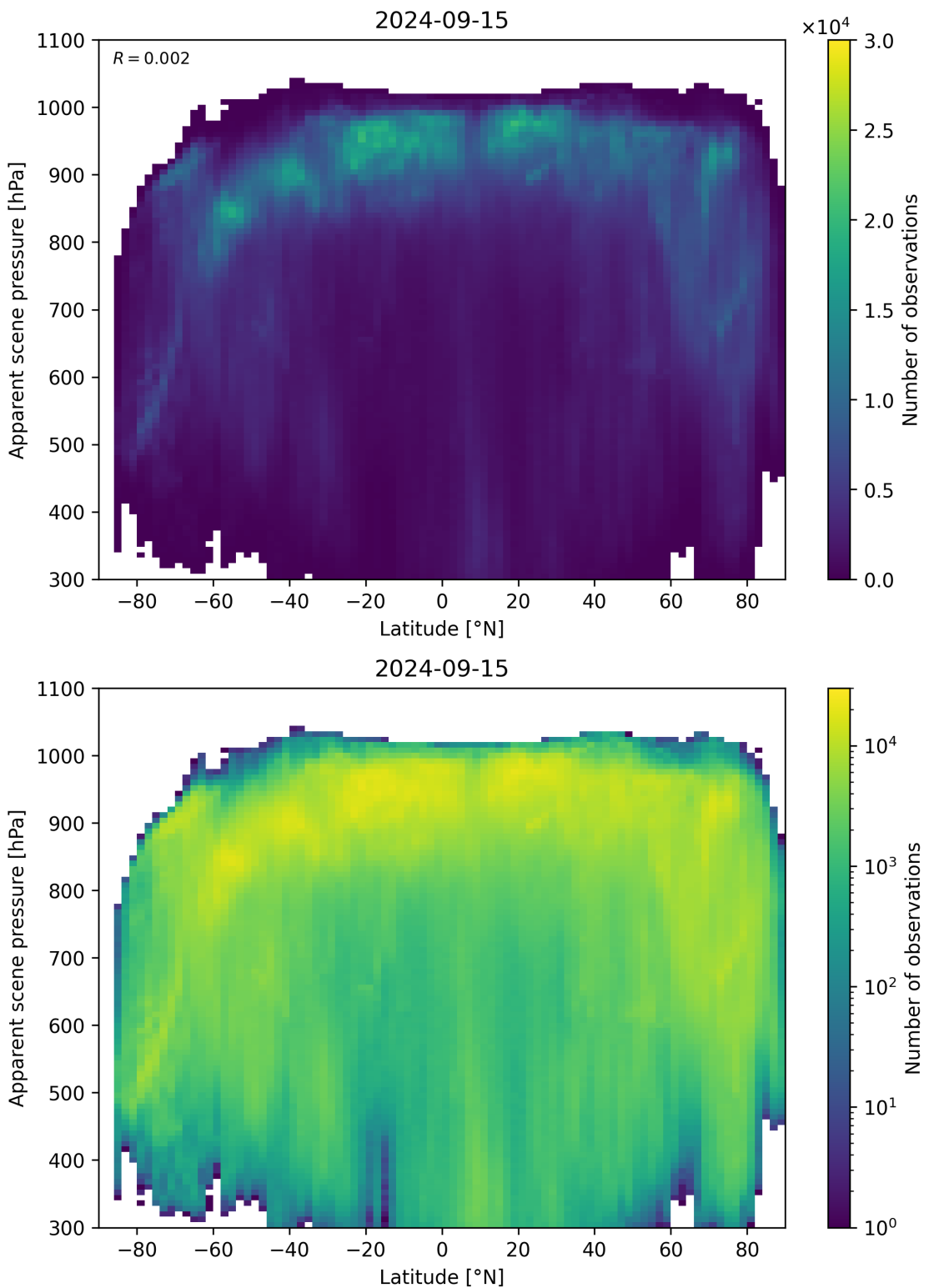


Figure 96: Scatter density plot of “Latitude” against “Apparent scene pressure” for 2024-09-14 to 2024-09-16.

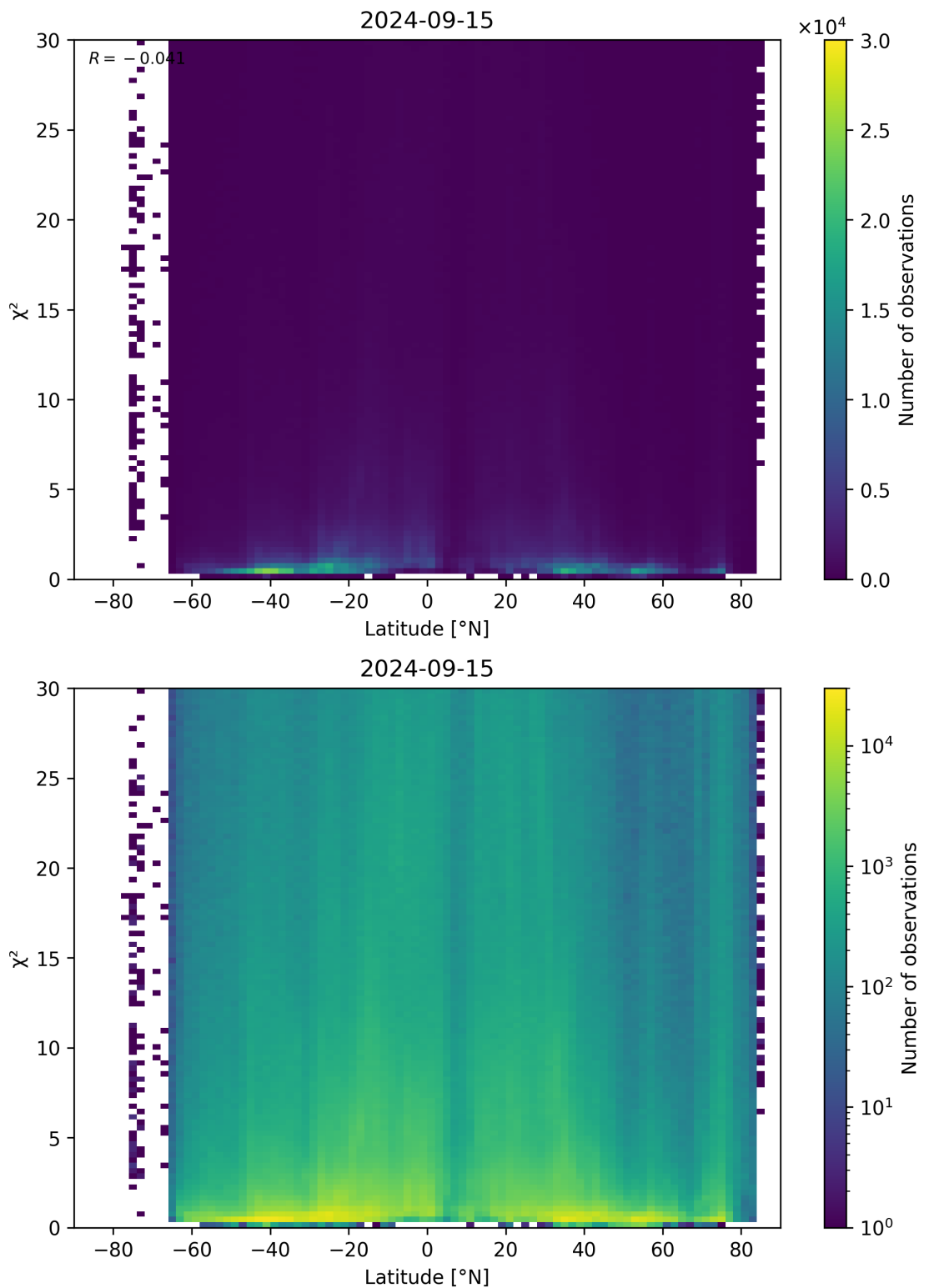


Figure 97: Scatter density plot of “Latitude” against “ $\chi^2$ ” for 2024-09-14 to 2024-09-16.

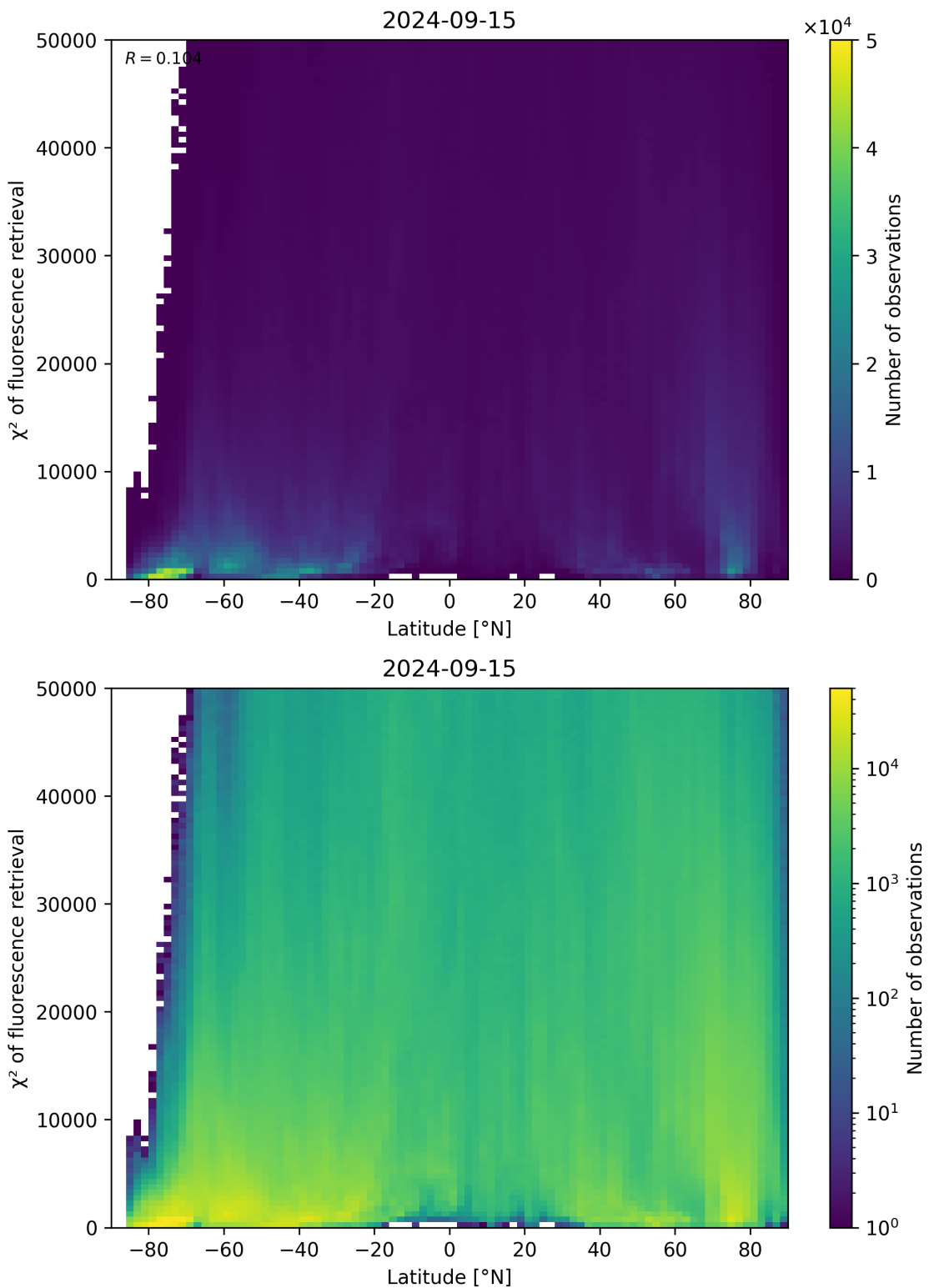


Figure 98: Scatter density plot of “Latitude” against “ $\chi^2$  of fluorescence retrieval” for 2024-09-14 to 2024-09-16.

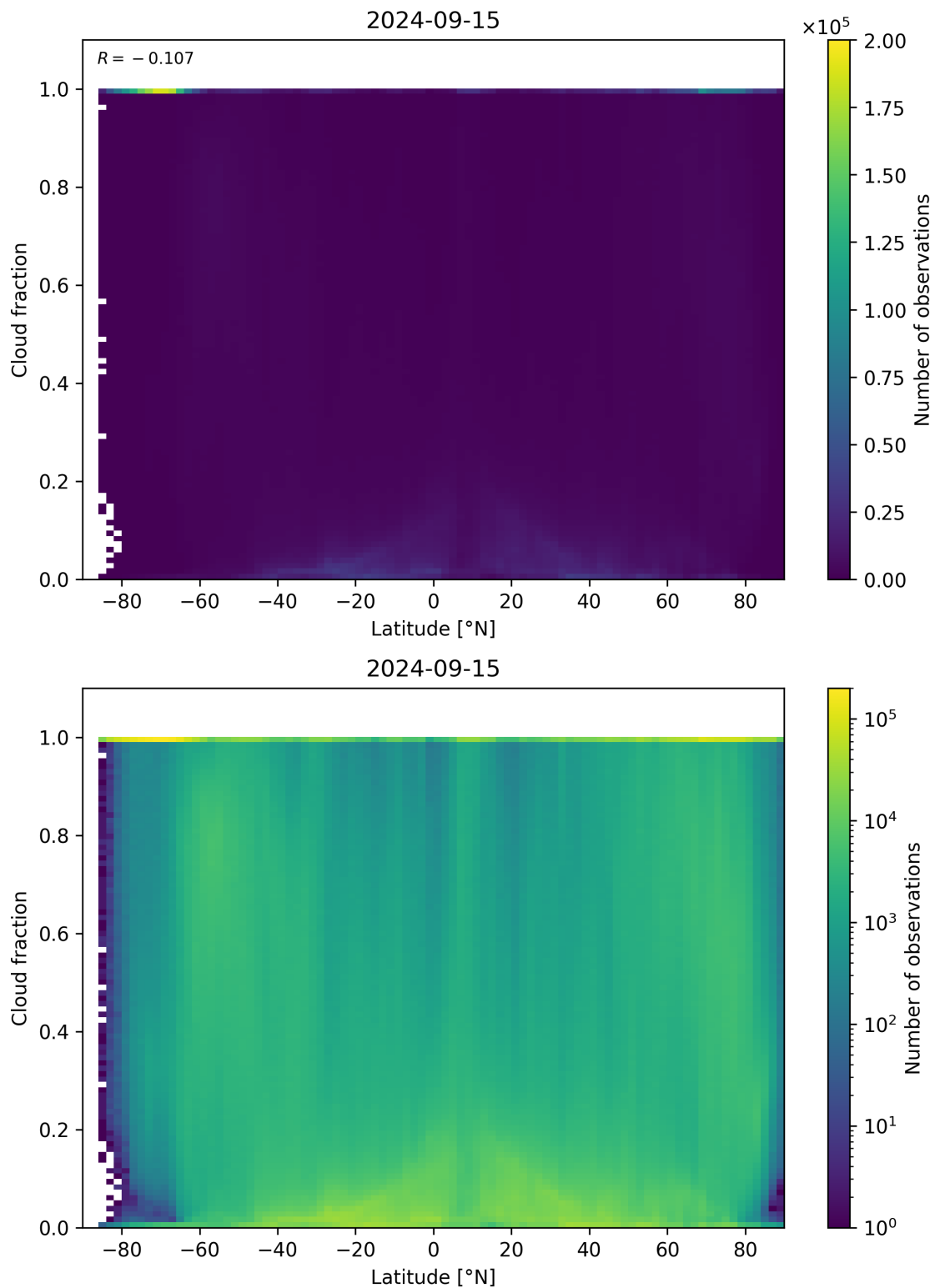


Figure 99: Scatter density plot of “Latitude” against “Cloud fraction” for 2024-09-14 to 2024-09-16.

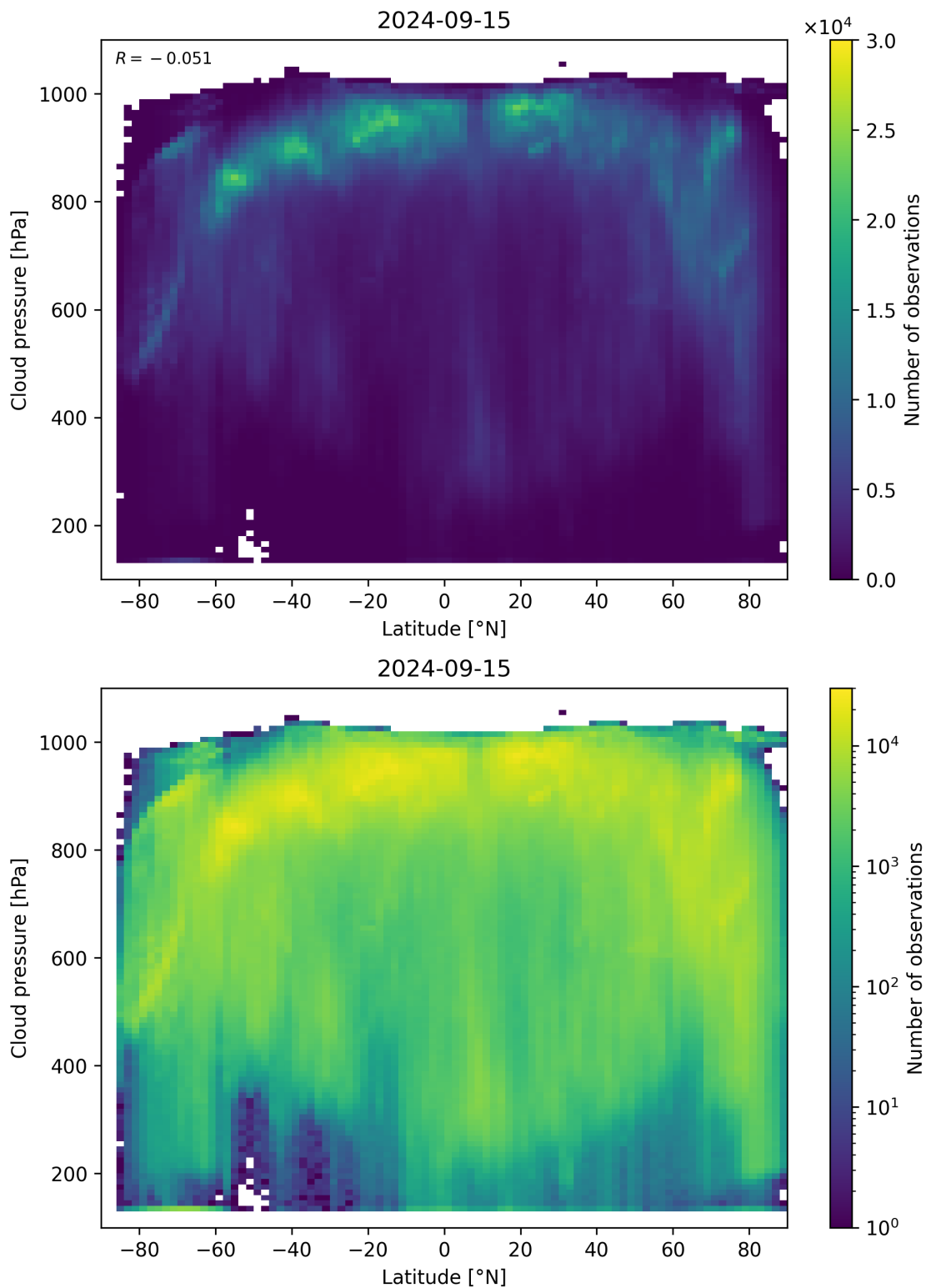


Figure 100: Scatter density plot of “Latitude” against “Cloud pressure” for 2024-09-14 to 2024-09-16.

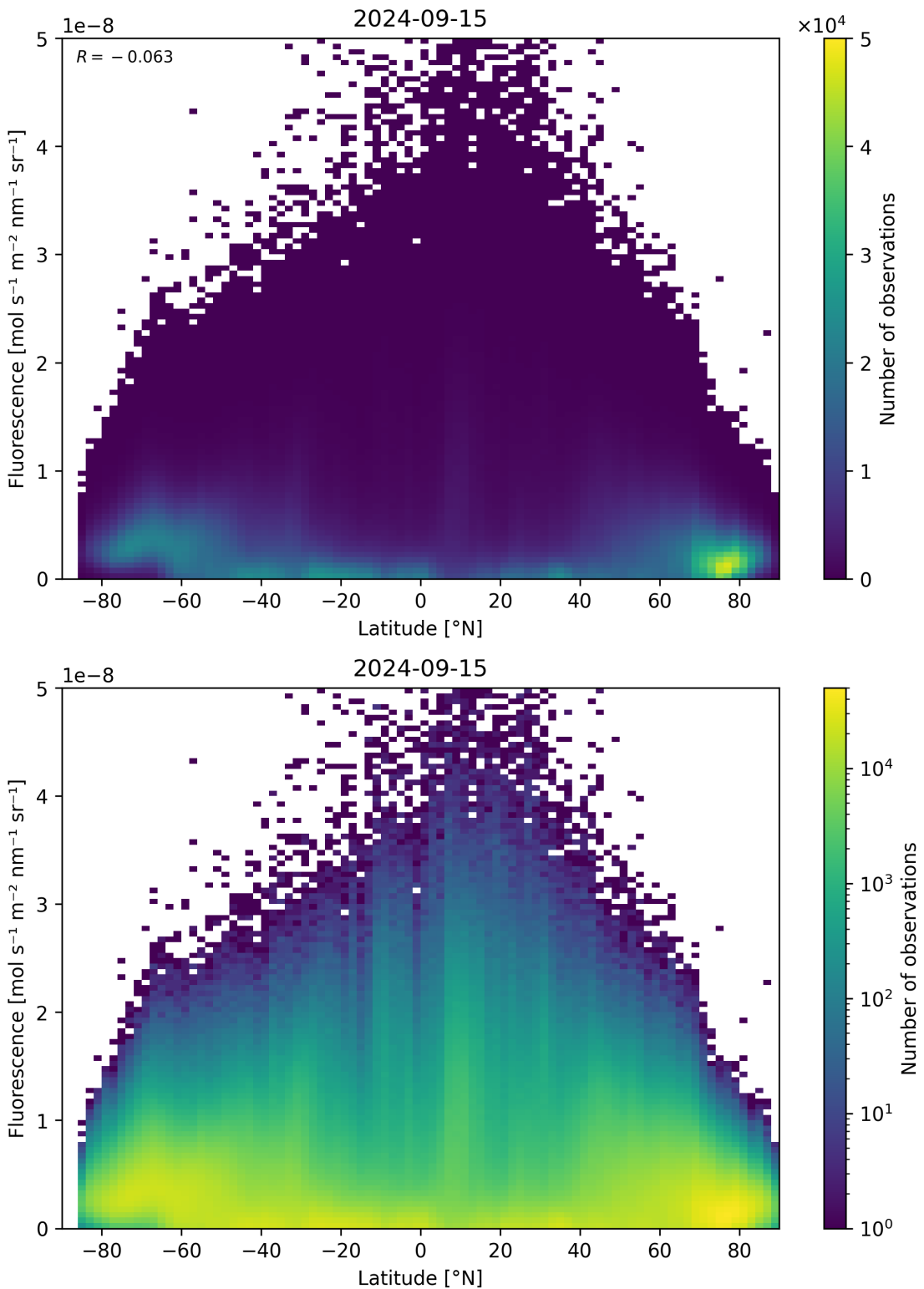


Figure 101: Scatter density plot of “Latitude” against “Fluorescence” for 2024-09-14 to 2024-09-16.

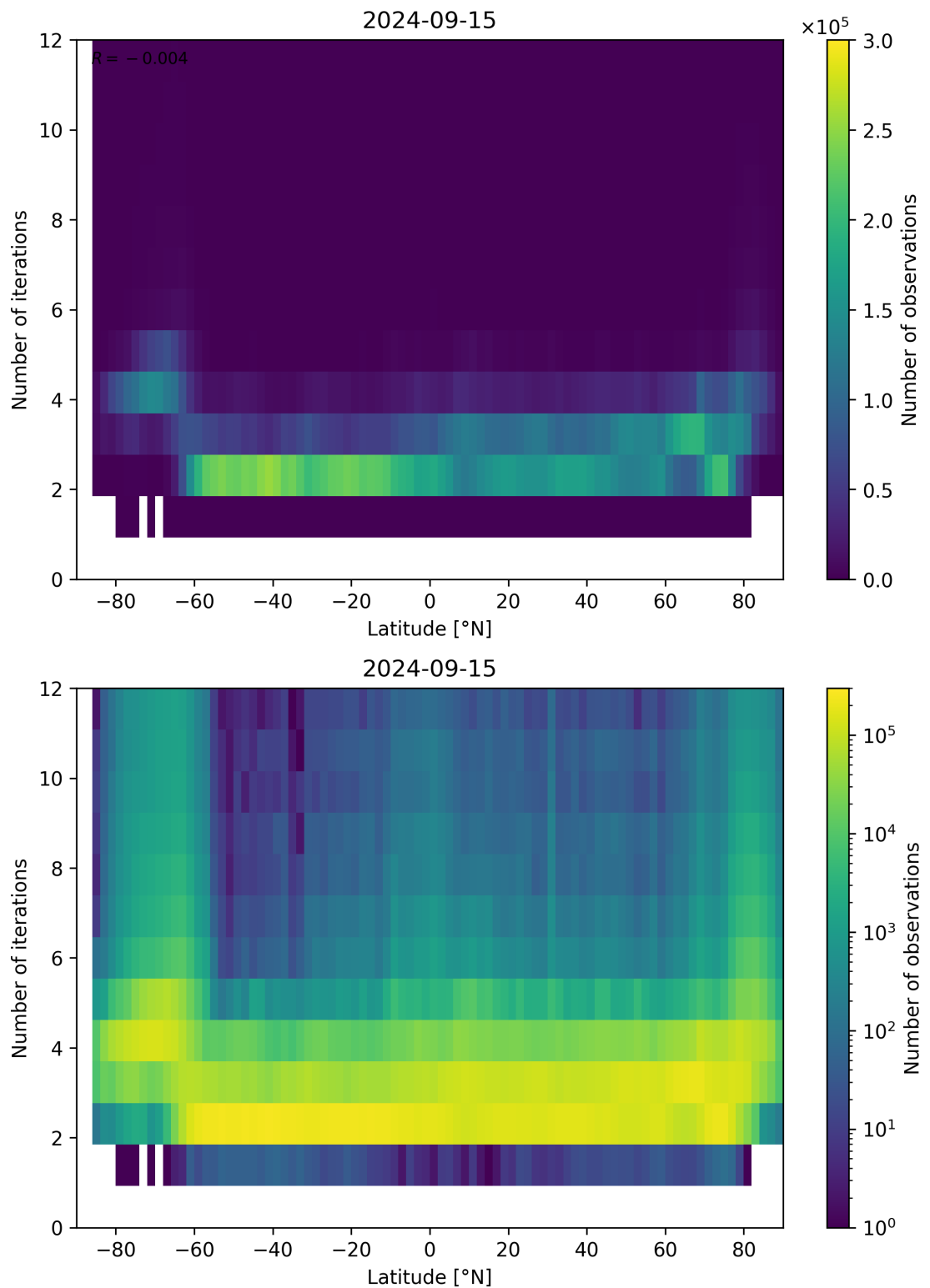


Figure 102: Scatter density plot of “Latitude” against “Number of iterations” for 2024-09-14 to 2024-09-16.

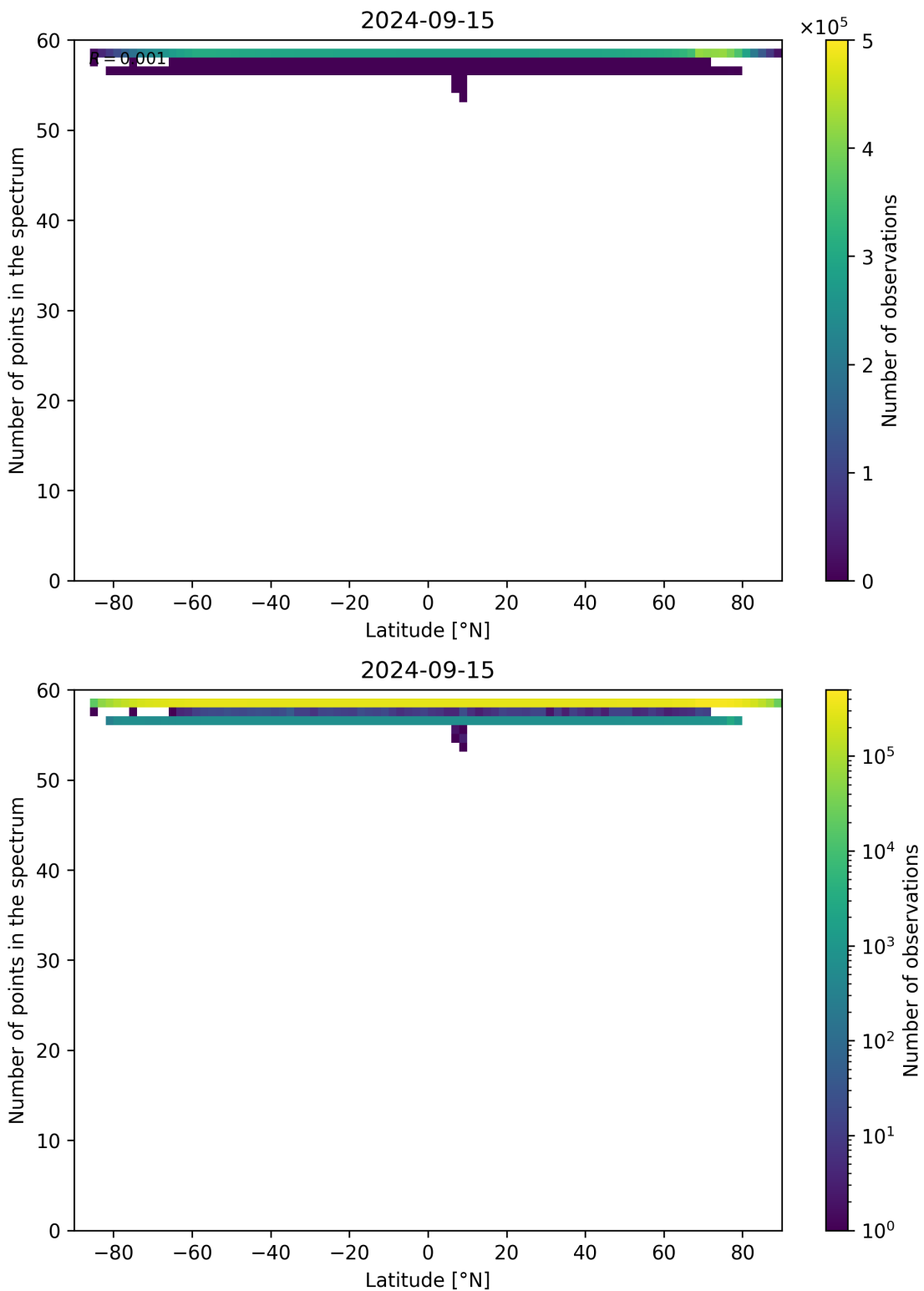


Figure 103: Scatter density plot of “Latitude” against “Number of points in the spectrum” for 2024-09-14 to 2024-09-16.

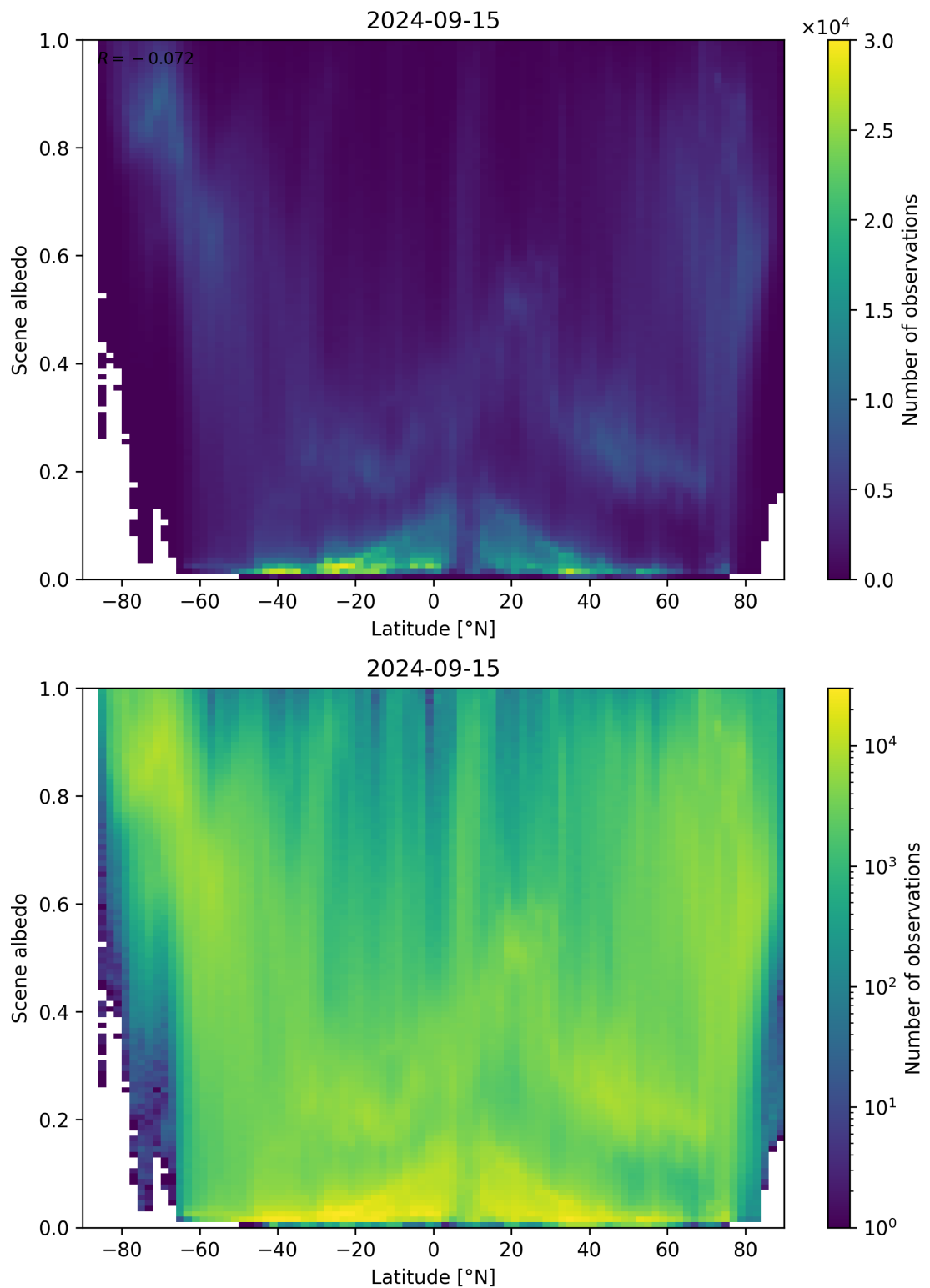


Figure 104: Scatter density plot of “Latitude” against “Scene albedo” for 2024-09-14 to 2024-09-16.

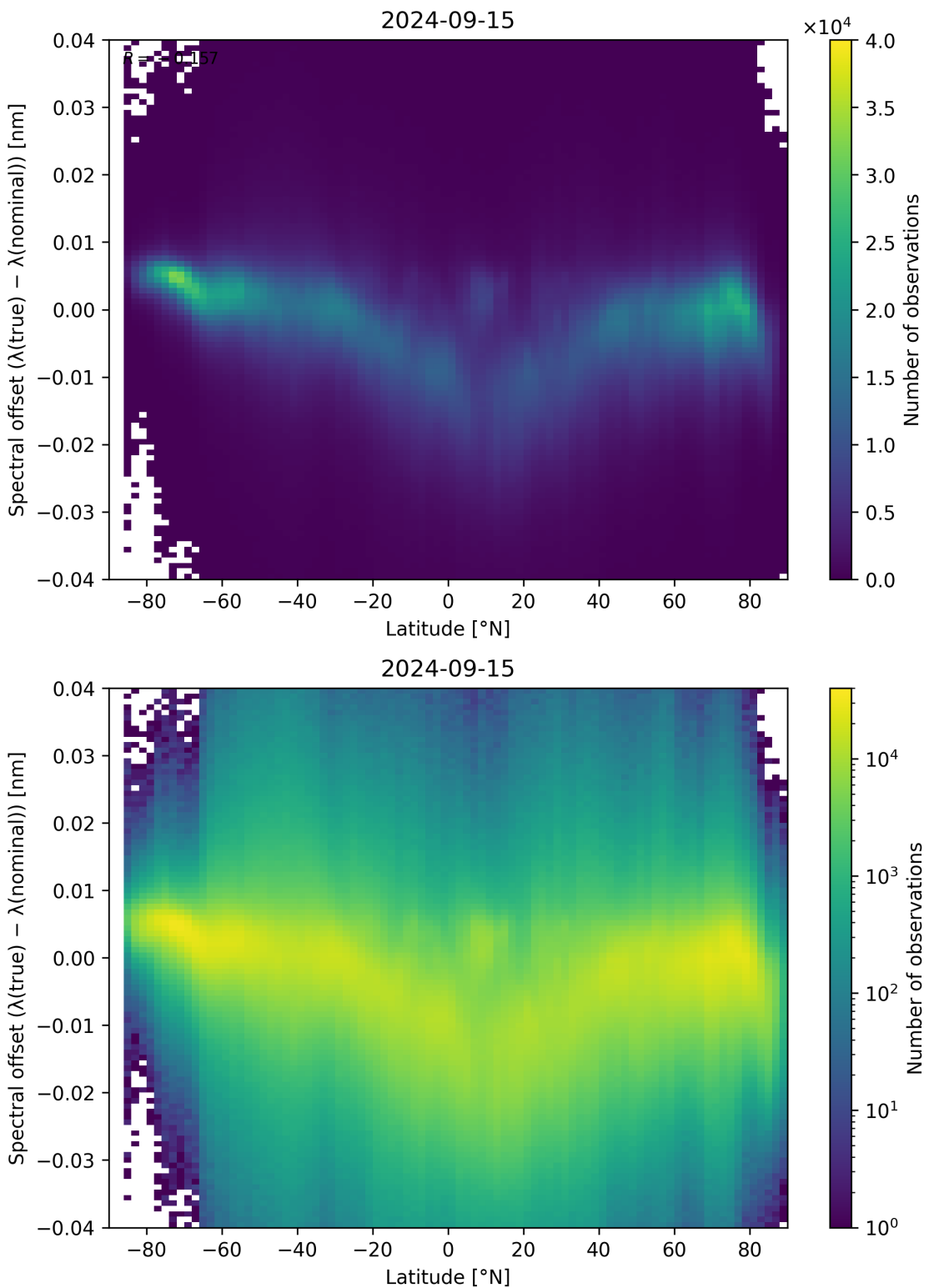


Figure 105: Scatter density plot of “Latitude” against “Spectral offset ( $\lambda_{\text{true}} - \lambda_{\text{nominal}}$ )” for 2024-09-14 to 2024-09-16.

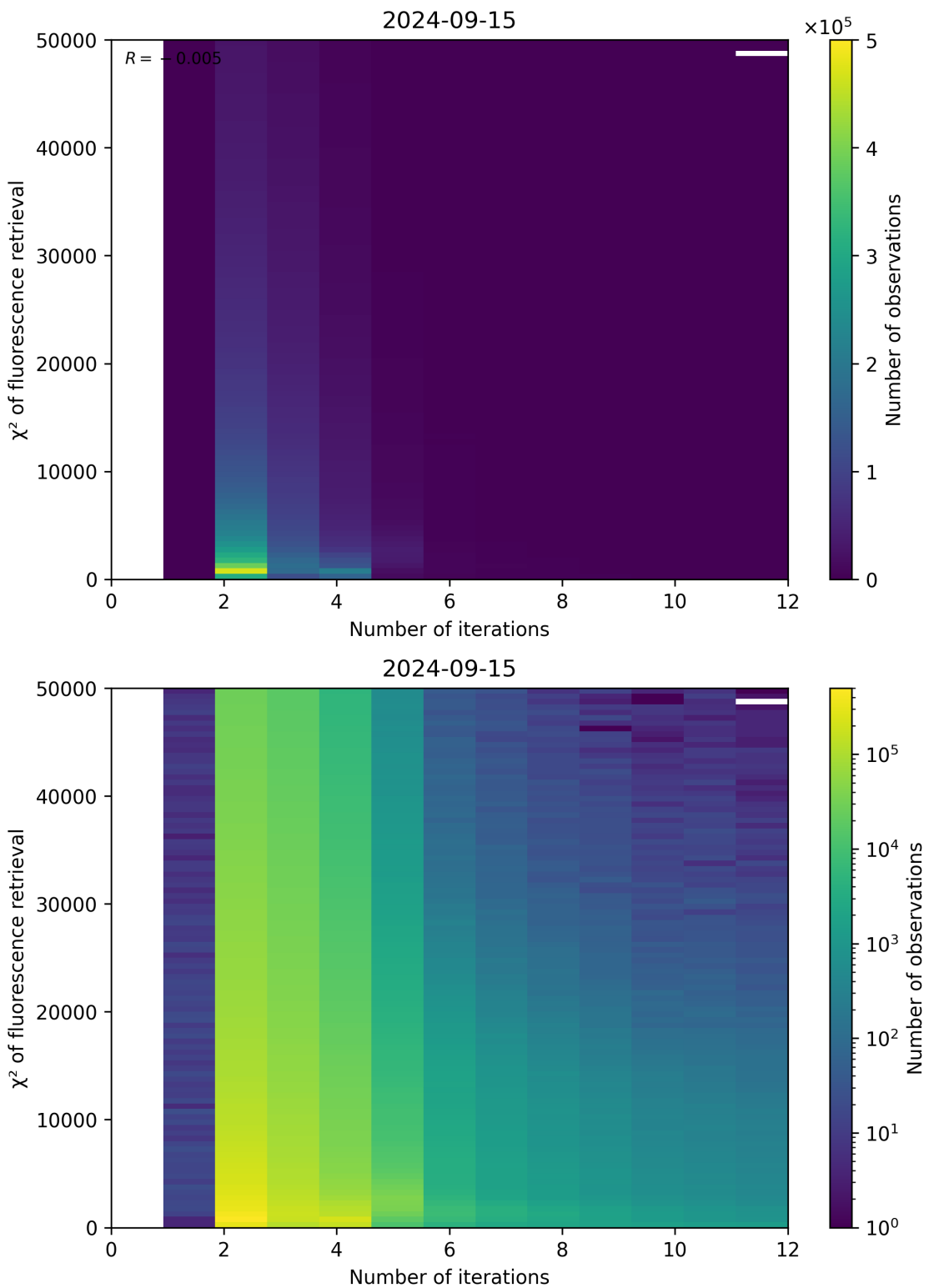


Figure 106: Scatter density plot of “Number of iterations” against “ $\chi^2$  of fluorescence retrieval” for 2024-09-14 to 2024-09-16.

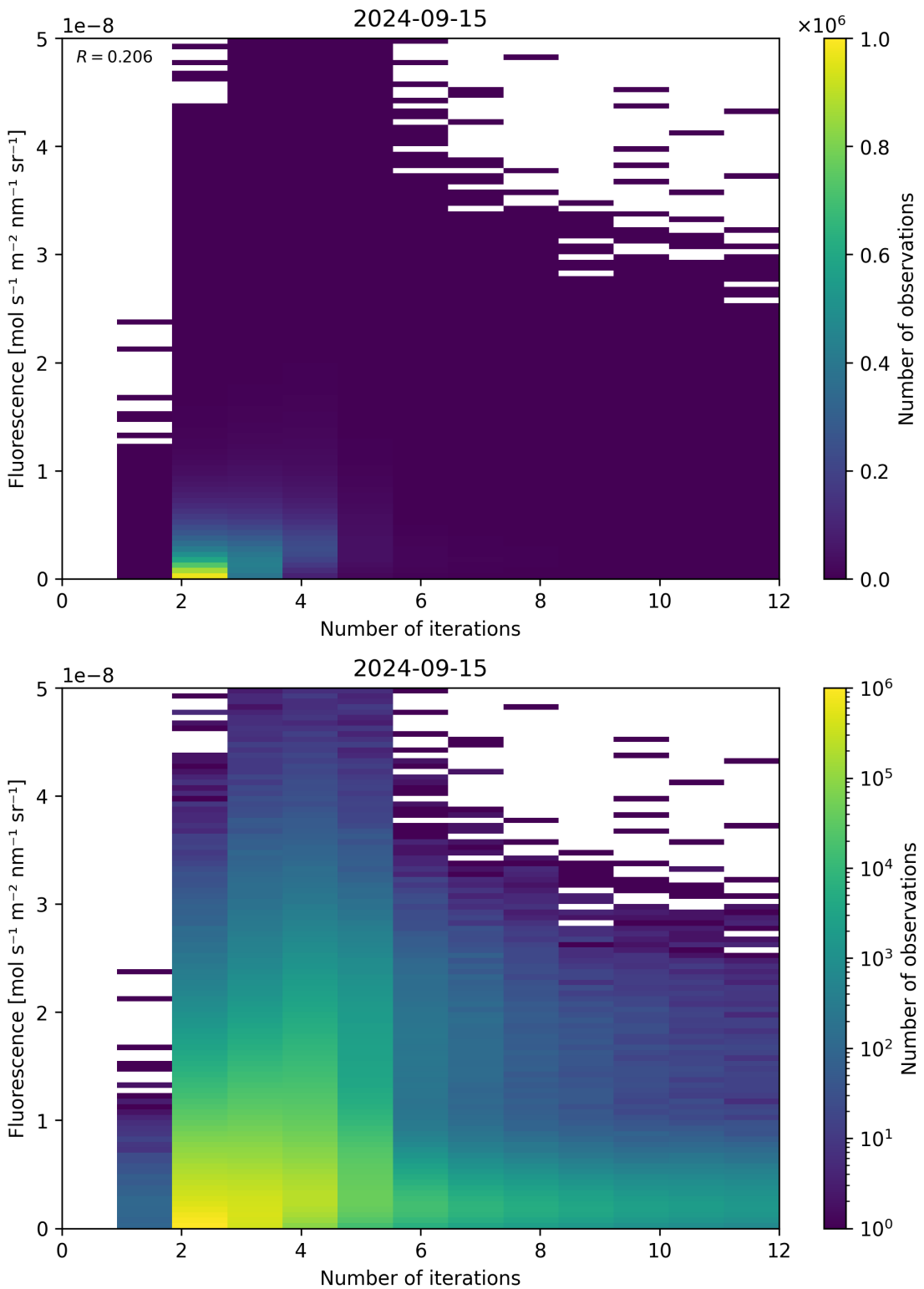


Figure 107: Scatter density plot of “Number of iterations” against “Fluorescence” for 2024-09-14 to 2024-09-16.

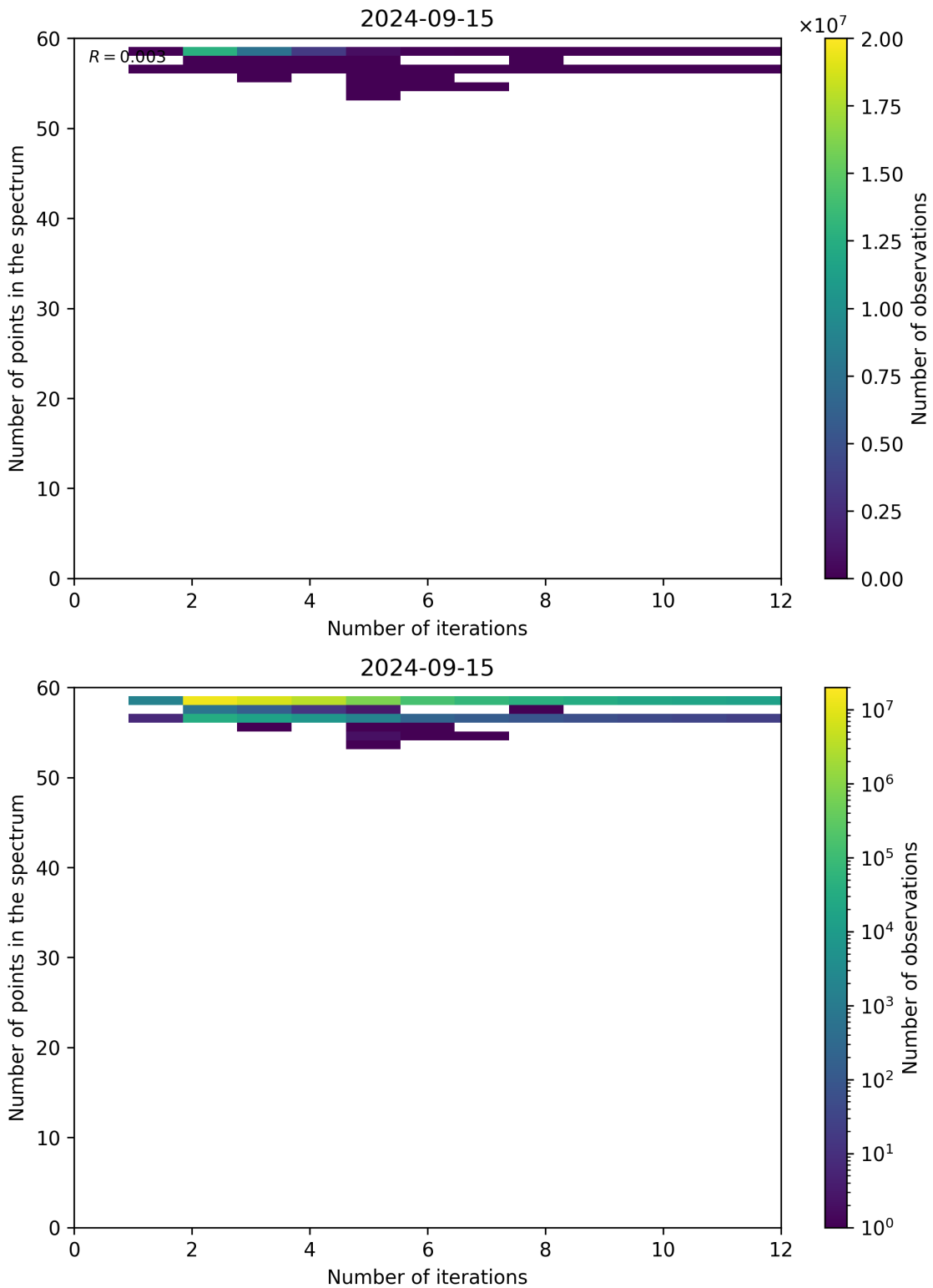


Figure 108: Scatter density plot of “Number of iterations” against “Number of points in the spectrum” for 2024-09-14 to 2024-09-16.

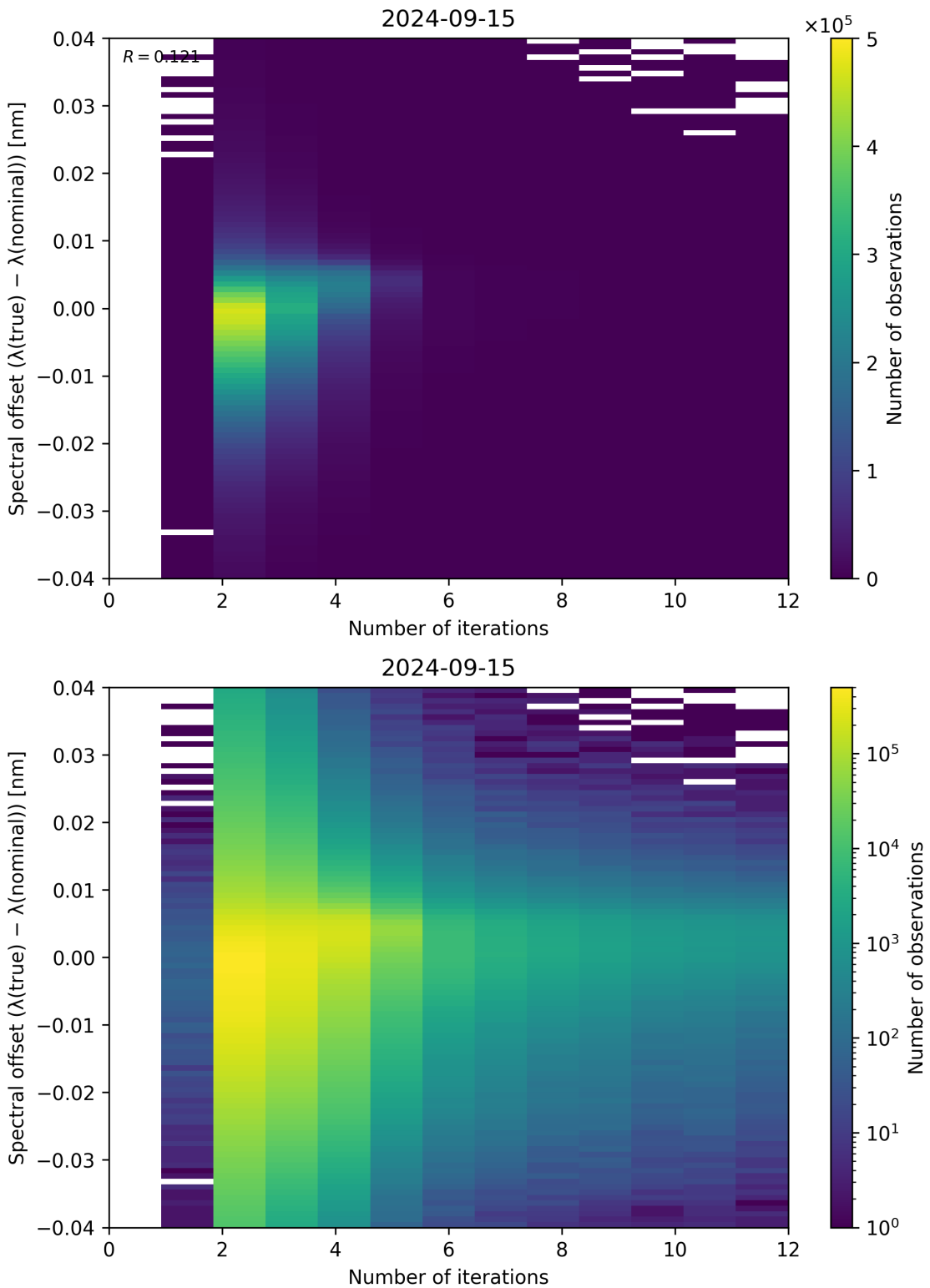


Figure 109: Scatter density plot of “Number of iterations” against “Spectral offset ( $\lambda_{\text{true}} - \lambda_{\text{nominal}}$ )” for 2024-09-14 to 2024-09-16.

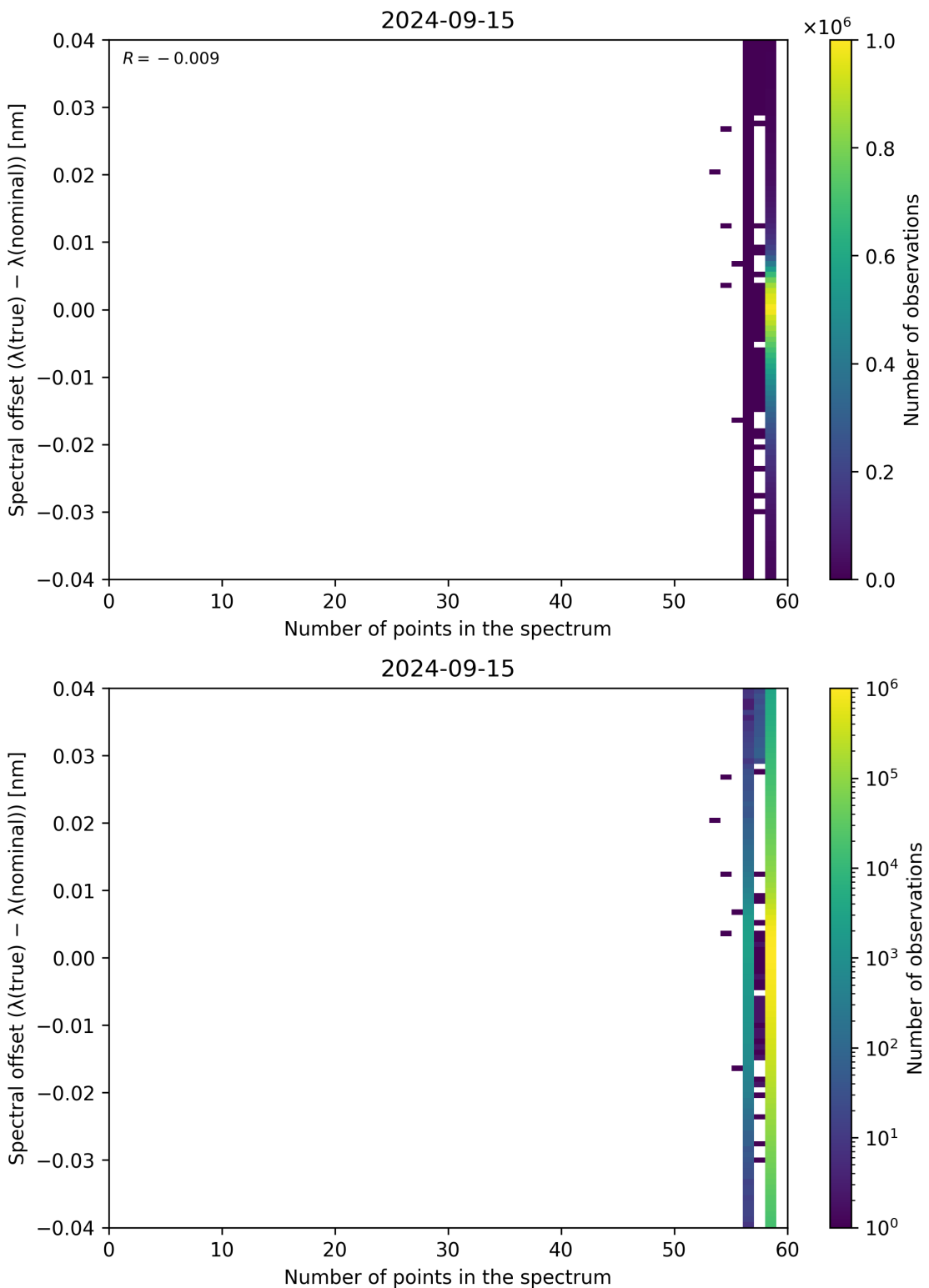


Figure 110: Scatter density plot of “Number of points in the spectrum” against “Spectral offset ( $\lambda_{\text{true}} - \lambda_{\text{nominal}}$ )” for 2024-09-14 to 2024-09-16.

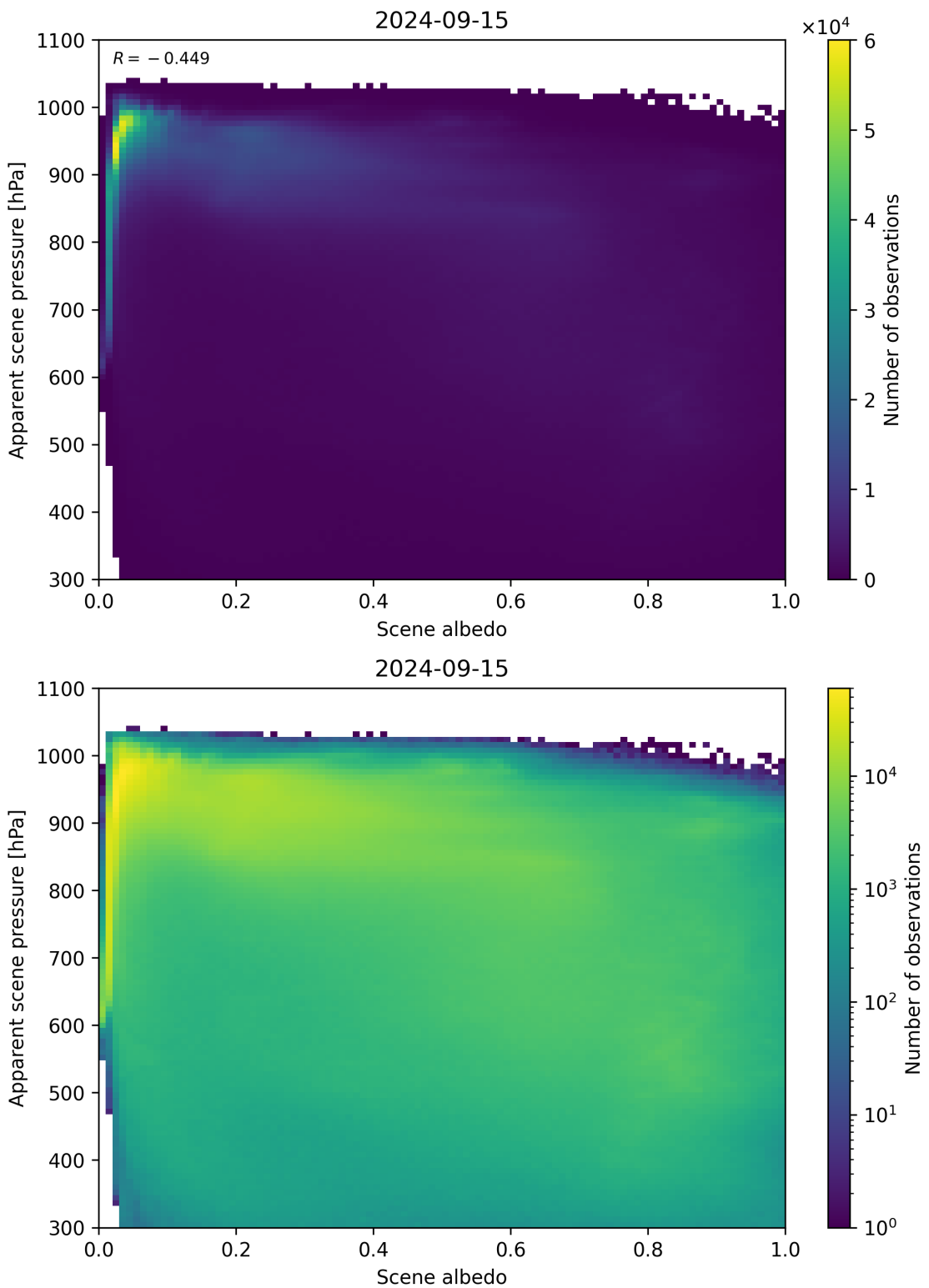


Figure 111: Scatter density plot of “Scene albedo” against “Apparent scene pressure” for 2024-09-14 to 2024-09-16.

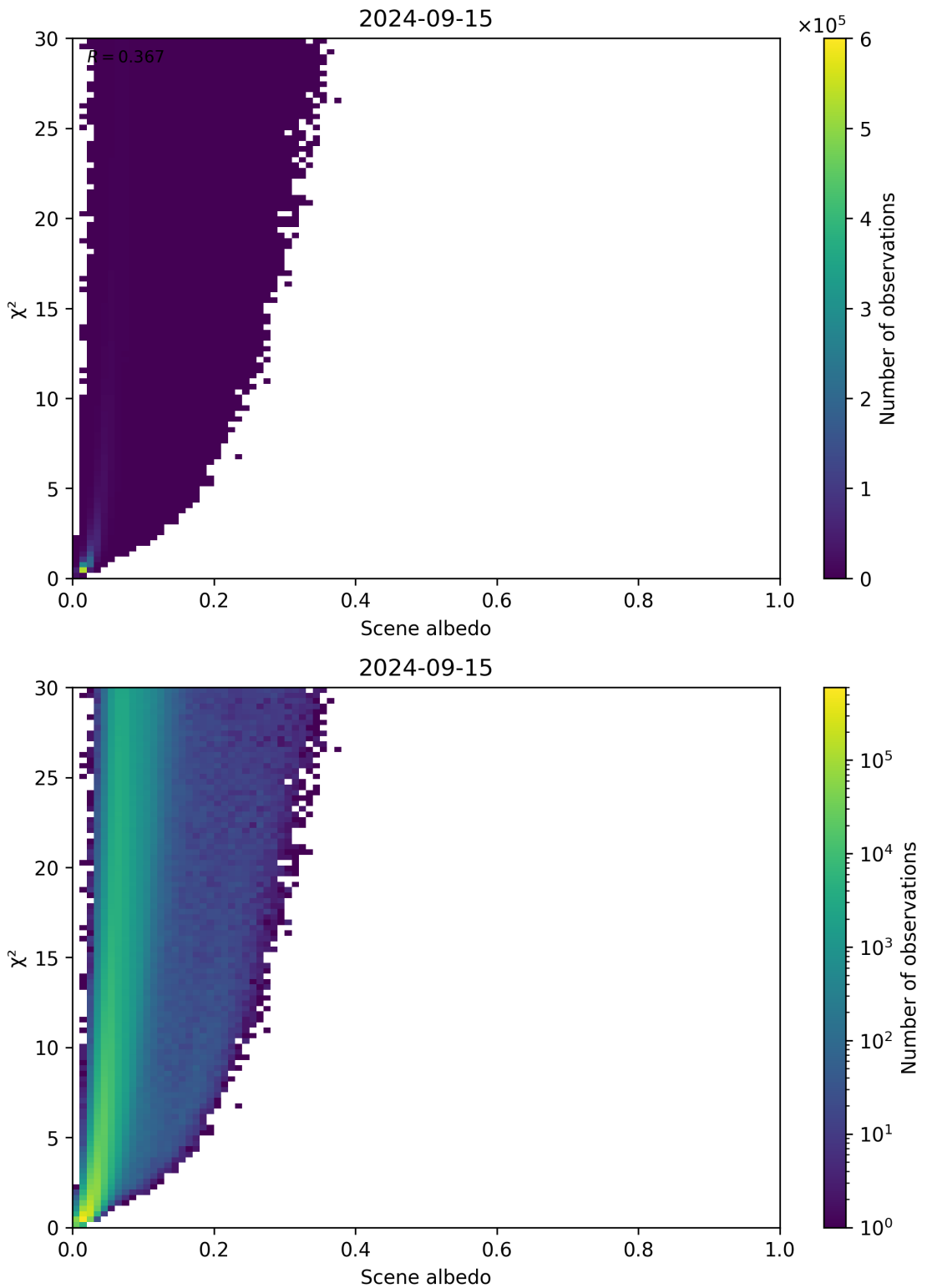


Figure 112: Scatter density plot of “Scene albedo” against “ $\chi^2$ ” for 2024-09-14 to 2024-09-16.

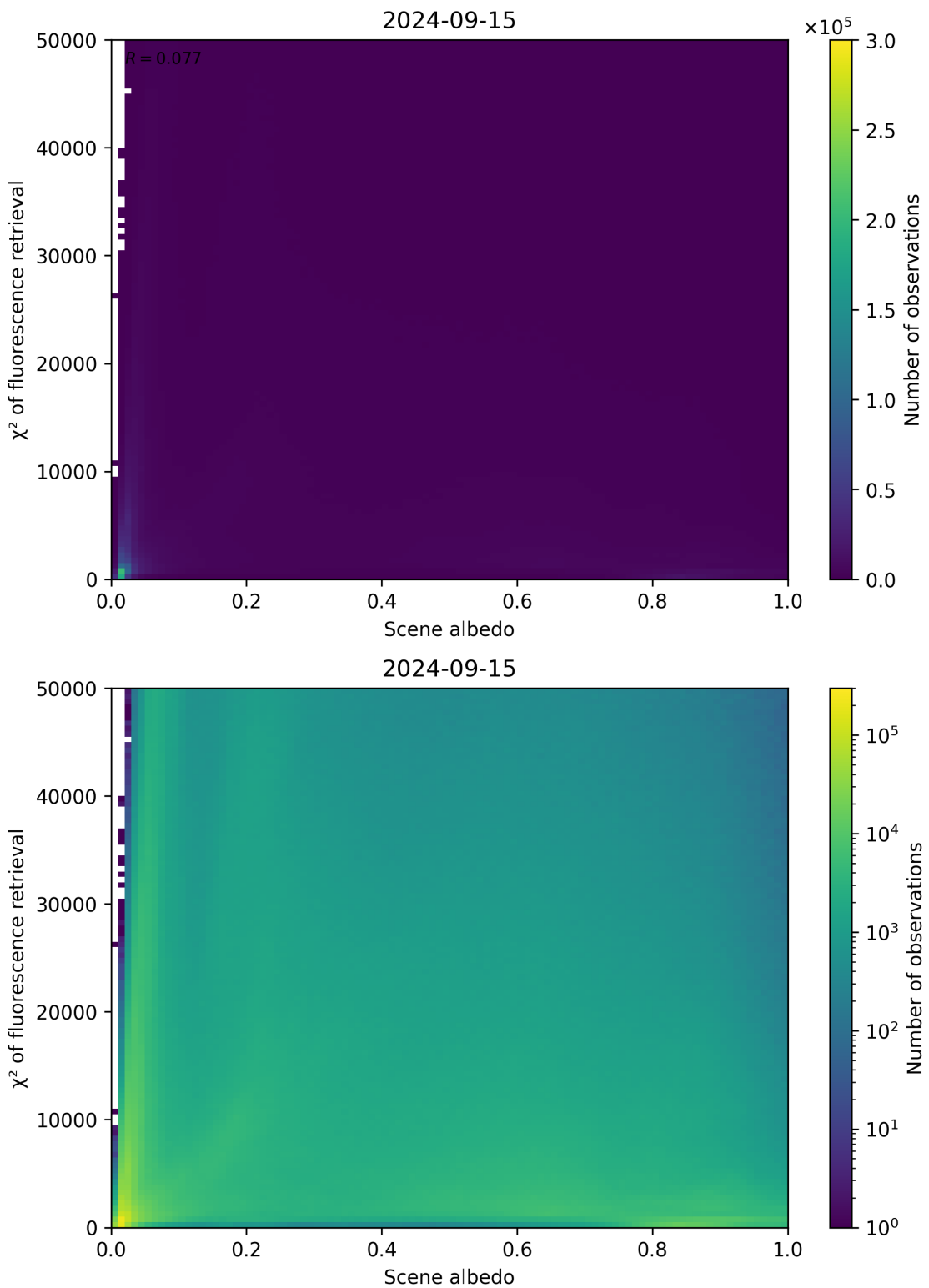


Figure 113: Scatter density plot of “Scene albedo” against “ $\chi^2$  of fluorescence retrieval” for 2024-09-14 to 2024-09-16.

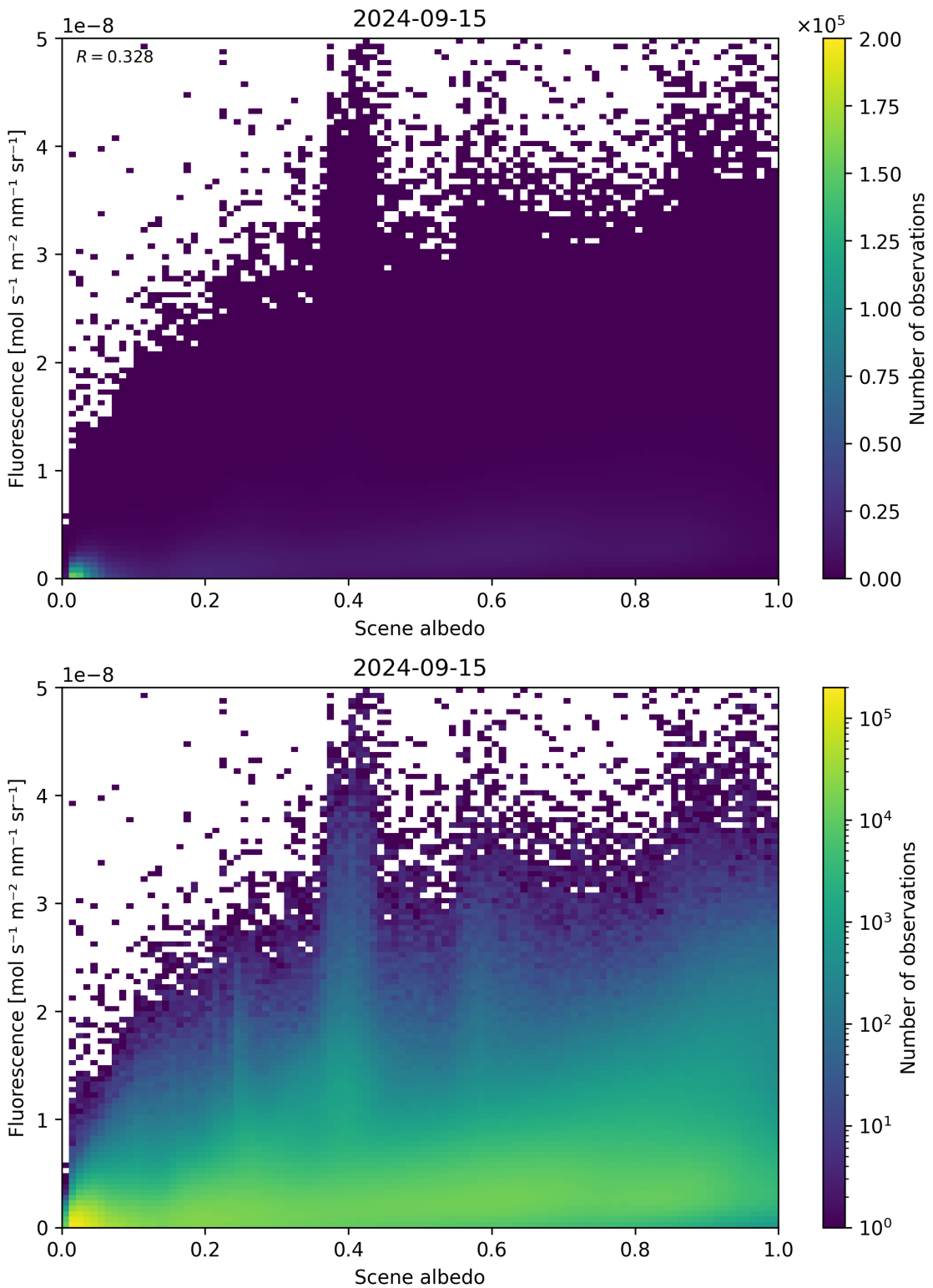


Figure 114: Scatter density plot of “Scene albedo” against “Fluorescence” for 2024-09-14 to 2024-09-16.

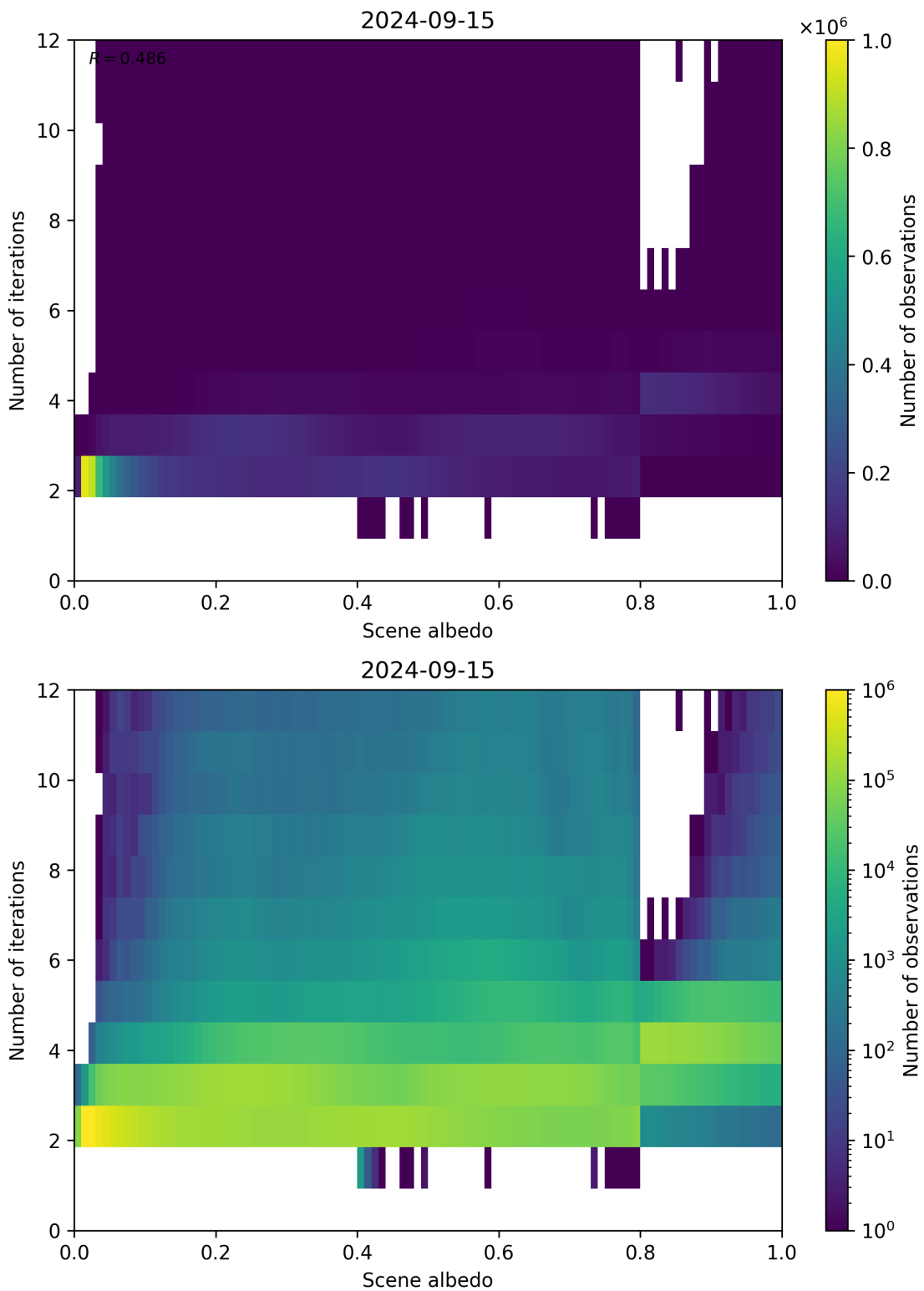


Figure 115: Scatter density plot of “Scene albedo” against “Number of iterations” for 2024-09-14 to 2024-09-16.

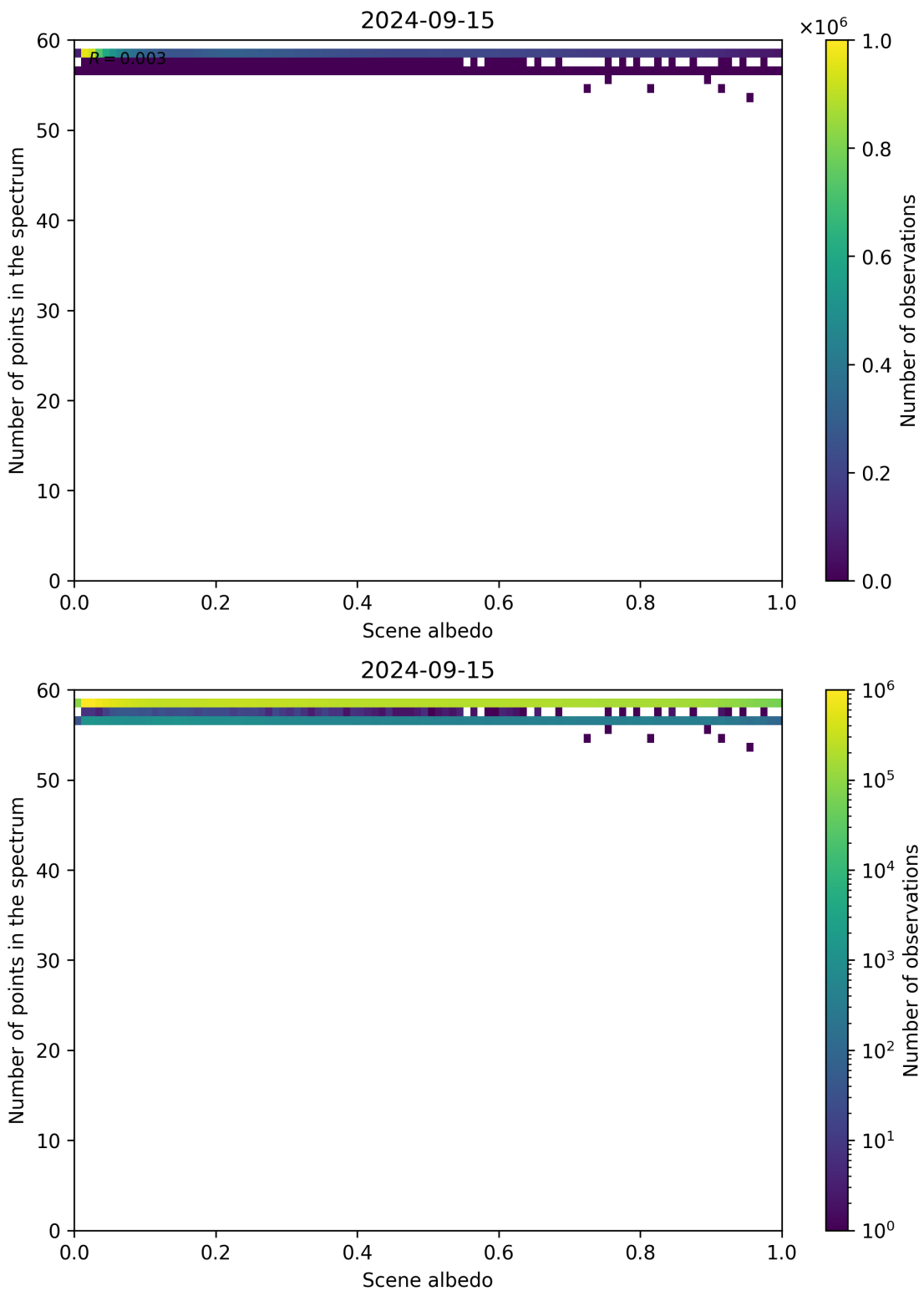


Figure 116: Scatter density plot of “Scene albedo” against “Number of points in the spectrum” for 2024-09-14 to 2024-09-16.

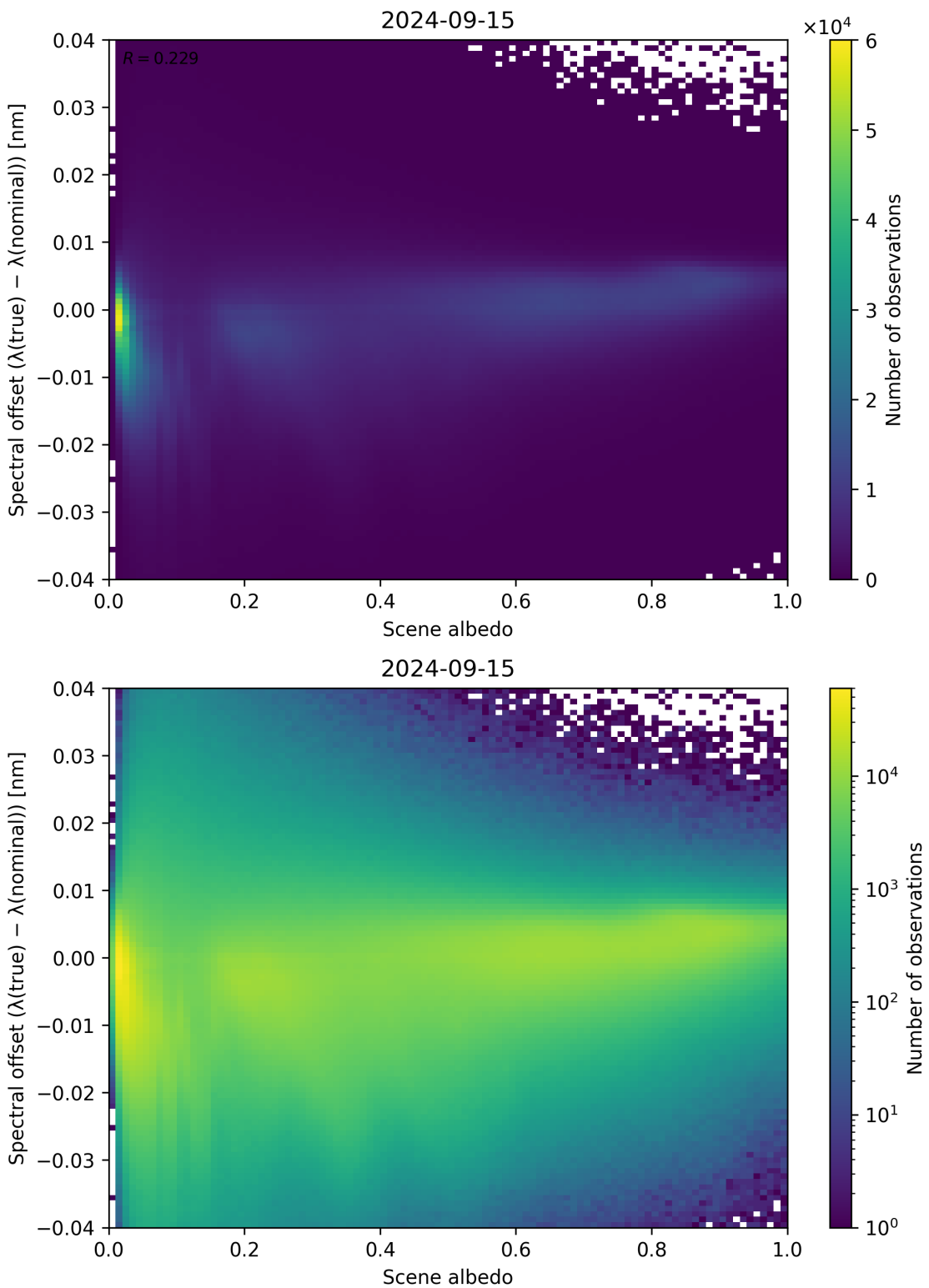


Figure 117: Scatter density plot of “Scene albedo” against “Spectral offset ( $\lambda_{\text{true}} - \lambda_{\text{nominal}}$ )” for 2024-09-14 to 2024-09-16.

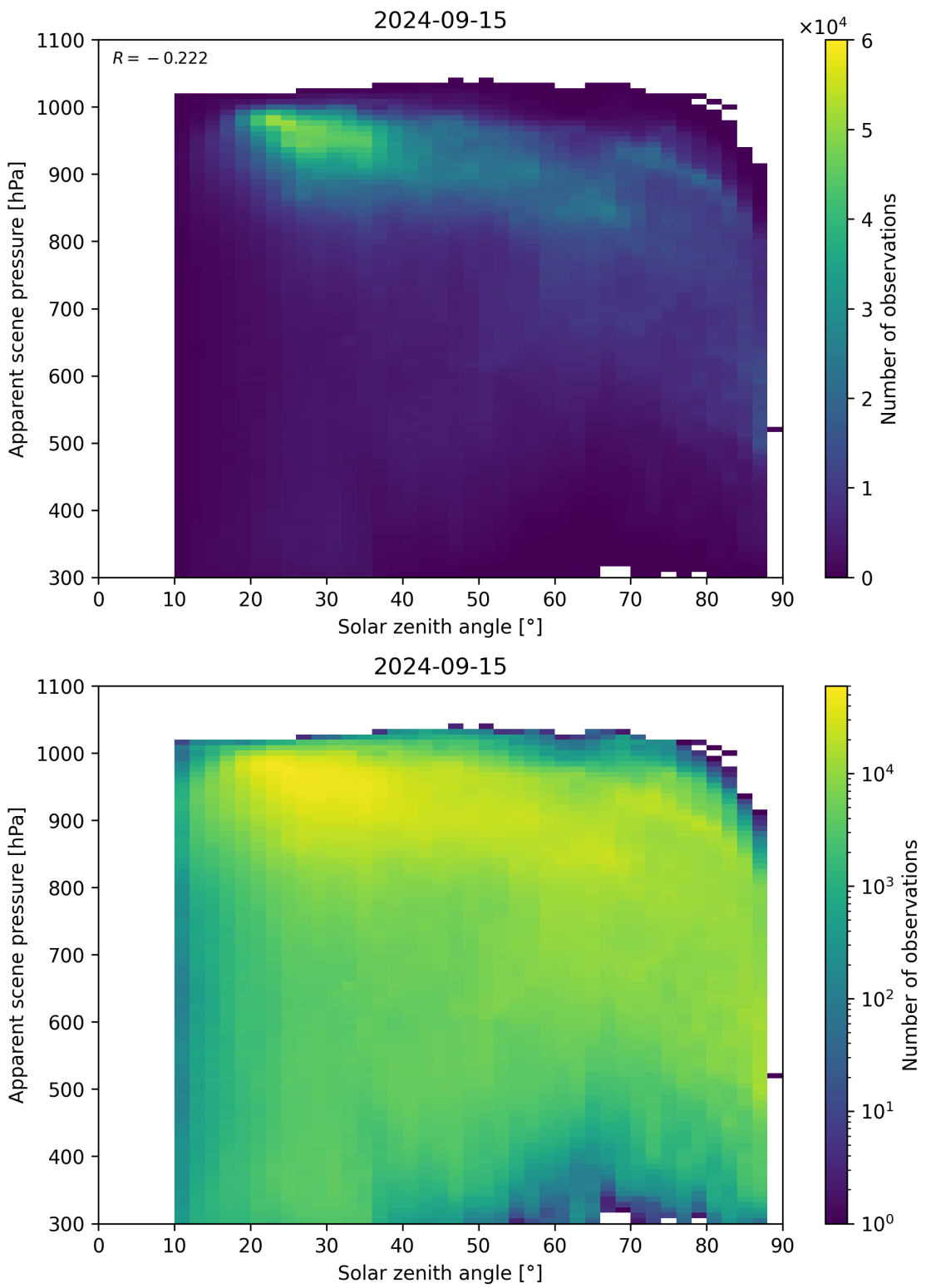


Figure 118: Scatter density plot of “Solar zenith angle” against “Apparent scene pressure” for 2024-09-14 to 2024-09-16.

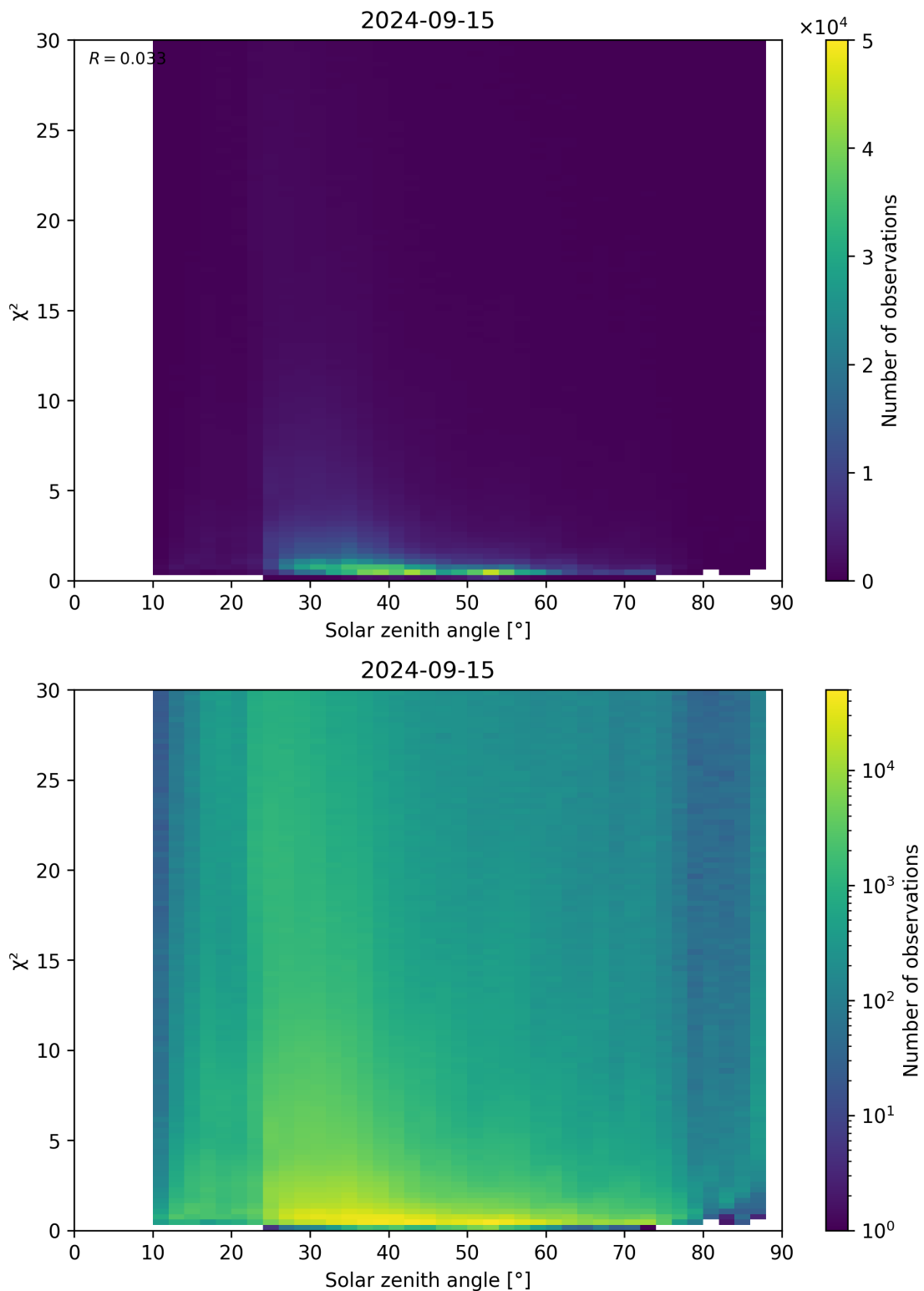


Figure 119: Scatter density plot of “Solar zenith angle” against “ $\chi^2$ ” for 2024-09-14 to 2024-09-16.

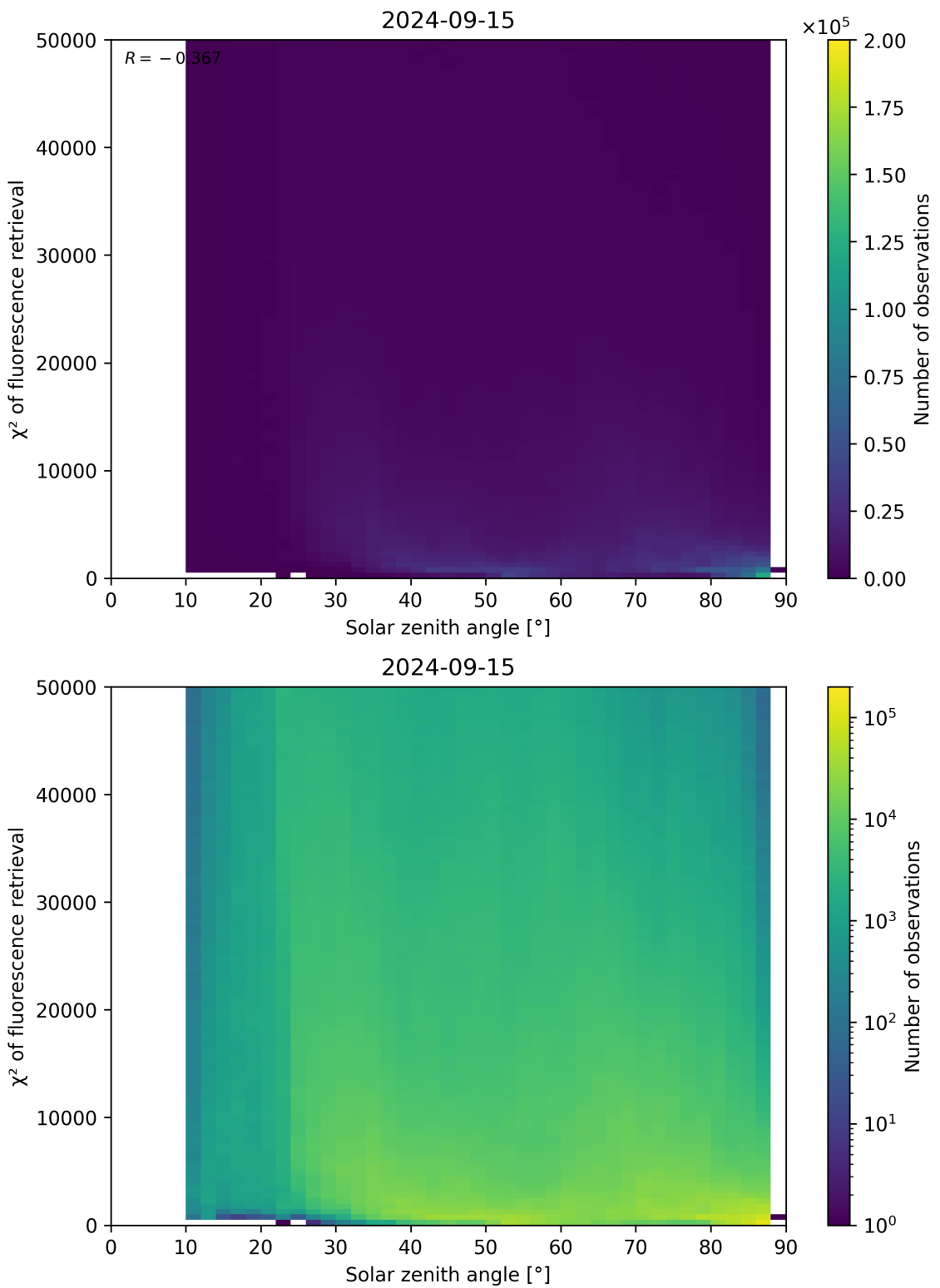


Figure 120: Scatter density plot of “Solar zenith angle” against “ $\chi^2$  of fluorescence retrieval” for 2024-09-14 to 2024-09-16.

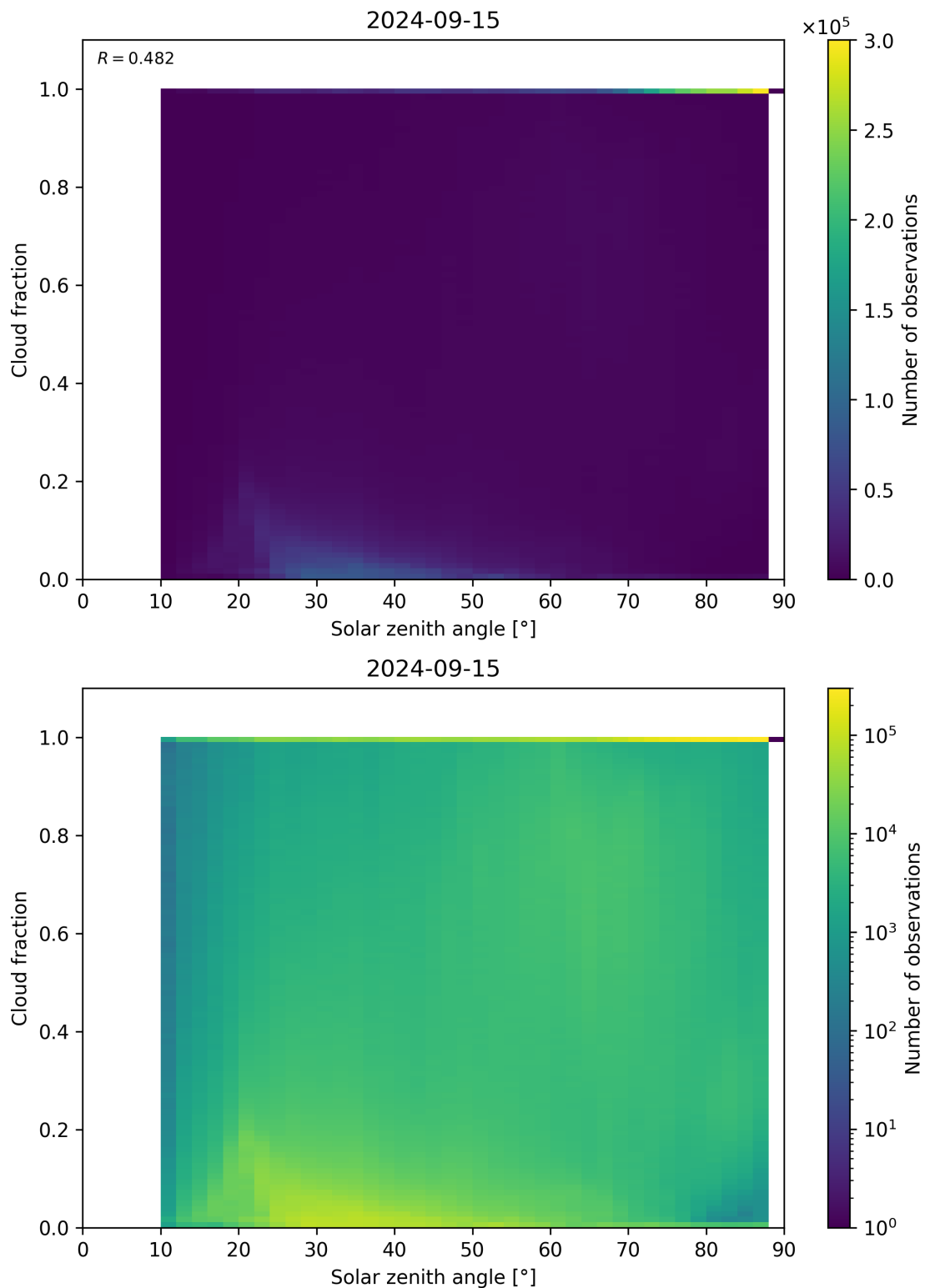


Figure 121: Scatter density plot of “Solar zenith angle” against “Cloud fraction” for 2024-09-14 to 2024-09-16.

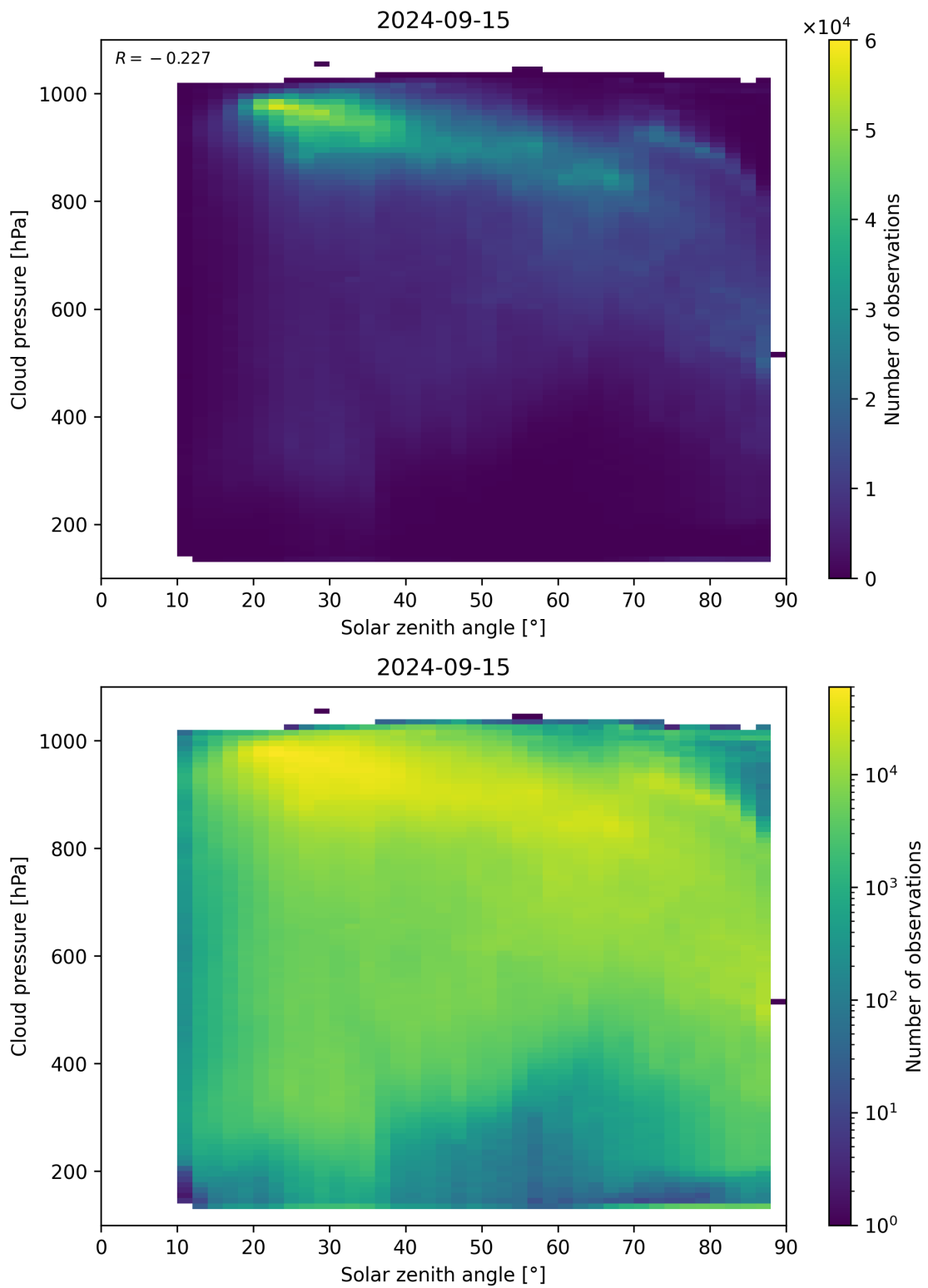


Figure 122: Scatter density plot of “Solar zenith angle” against “Cloud pressure” for 2024-09-14 to 2024-09-16.

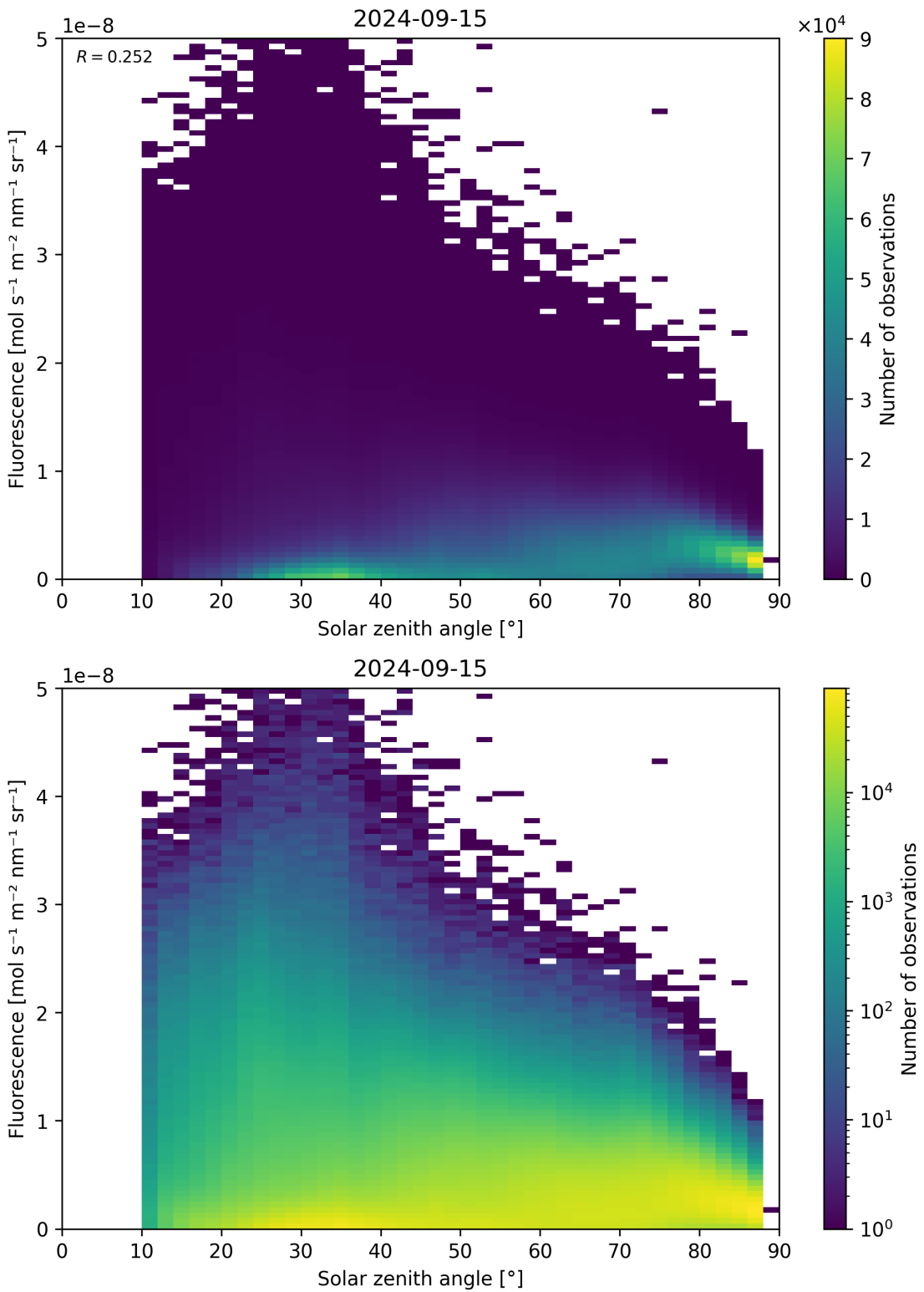


Figure 123: Scatter density plot of “Solar zenith angle” against “Fluorescence” for 2024-09-14 to 2024-09-16.

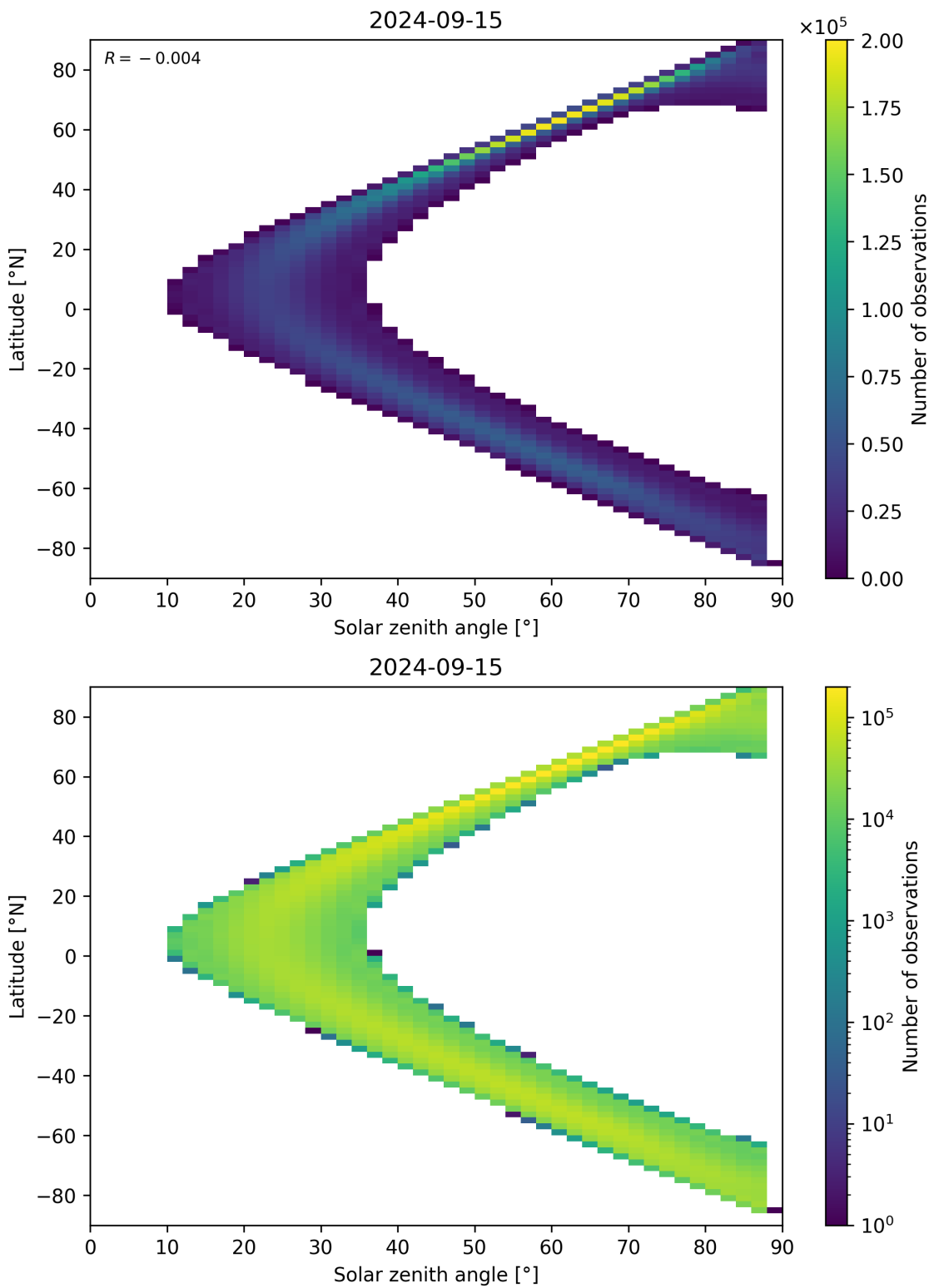


Figure 124: Scatter density plot of “Solar zenith angle” against “Latitude” for 2024-09-14 to 2024-09-16.

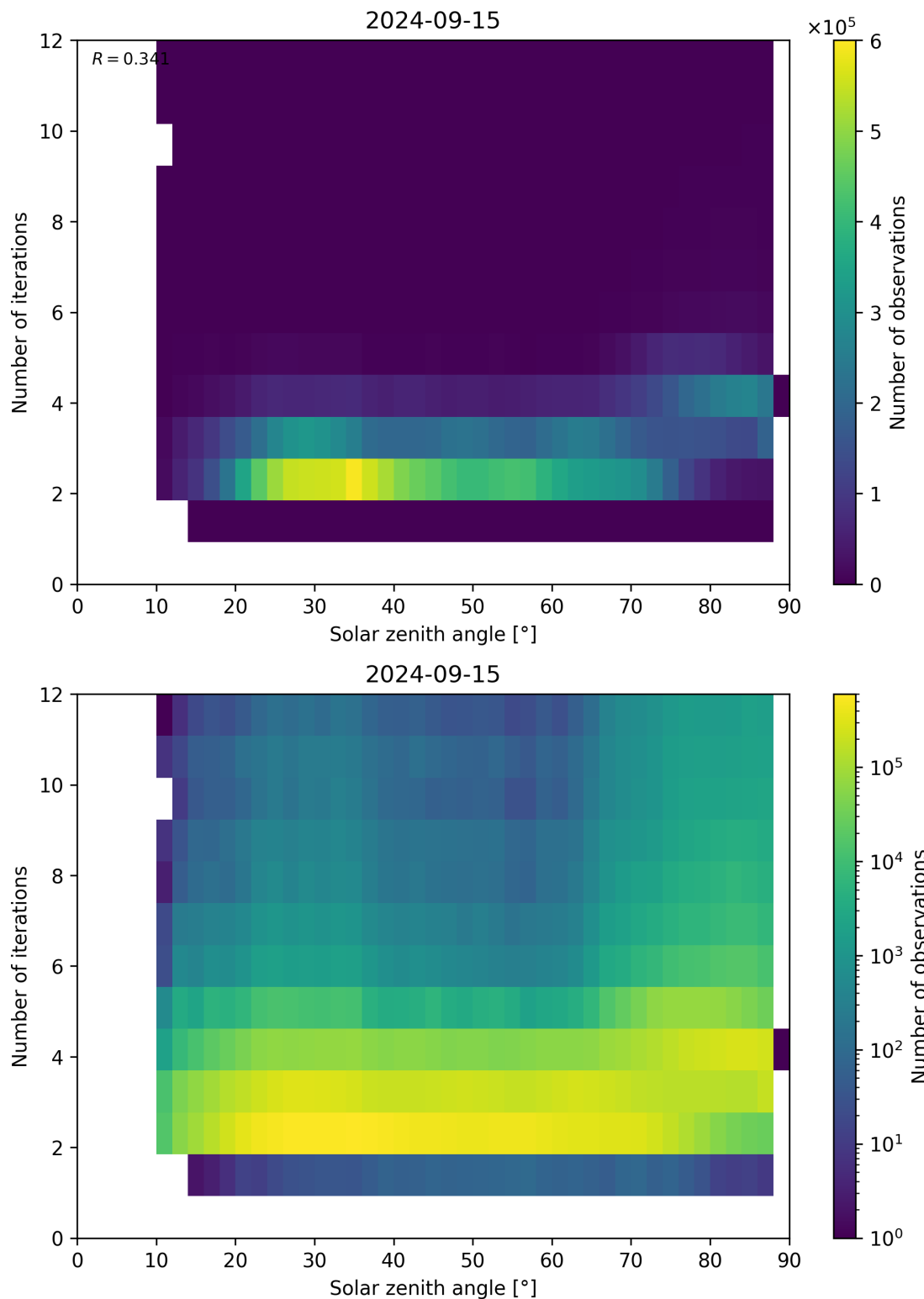


Figure 125: Scatter density plot of “Solar zenith angle” against “Number of iterations” for 2024-09-14 to 2024-09-16.

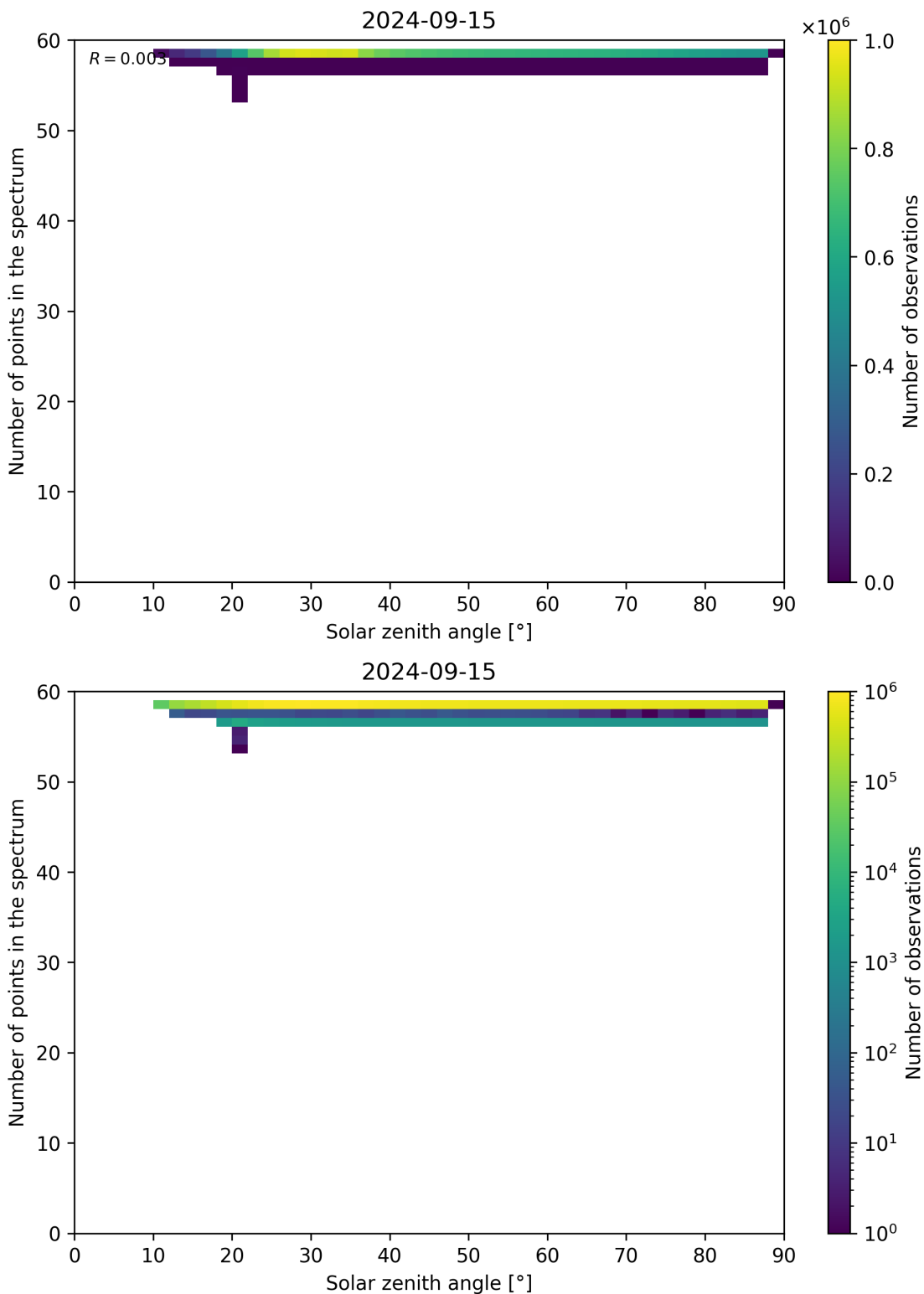


Figure 126: Scatter density plot of “Solar zenith angle” against “Number of points in the spectrum” for 2024-09-14 to 2024-09-16.

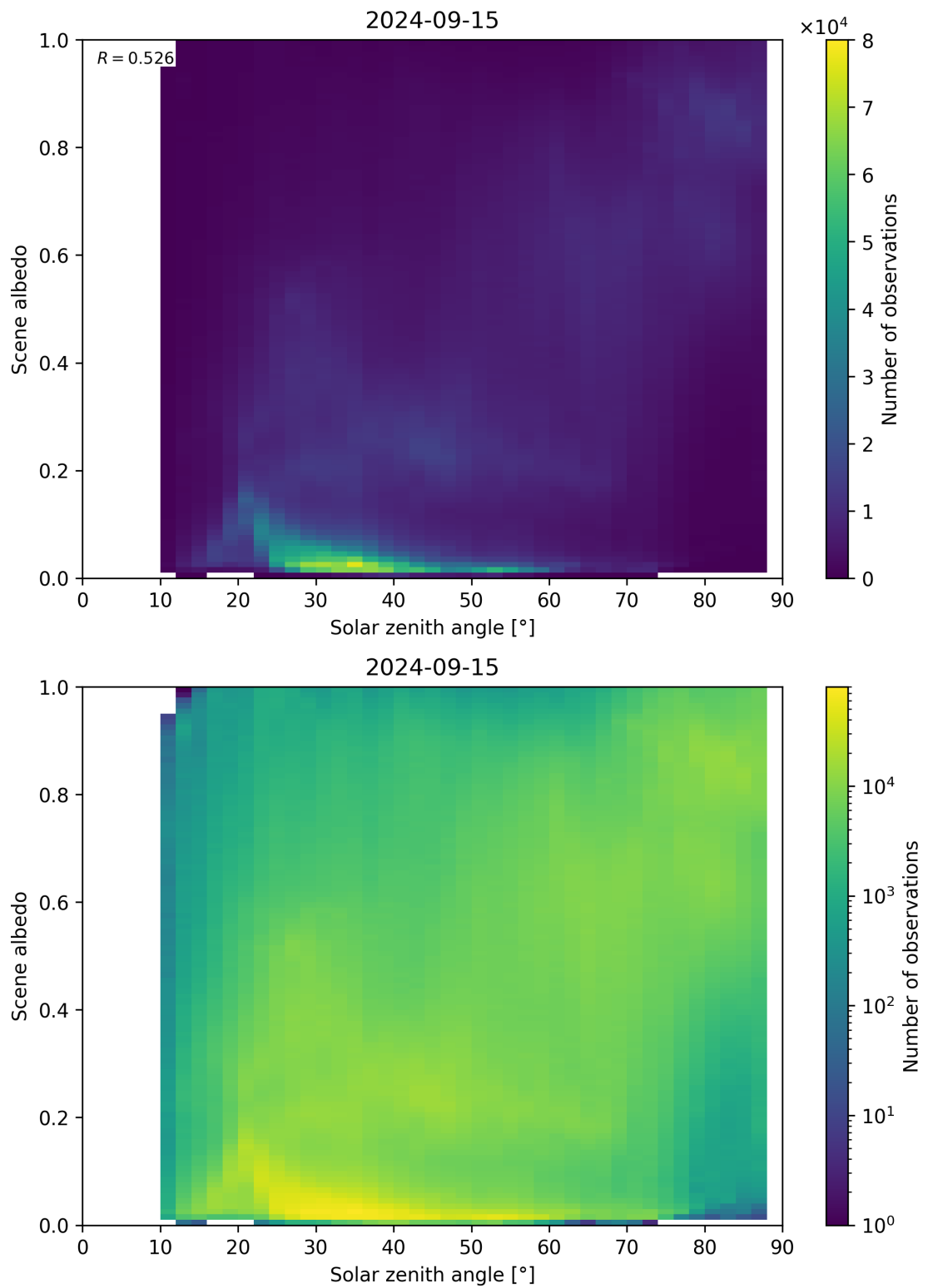


Figure 127: Scatter density plot of “Solar zenith angle” against “Scene albedo” for 2024-09-14 to 2024-09-16.

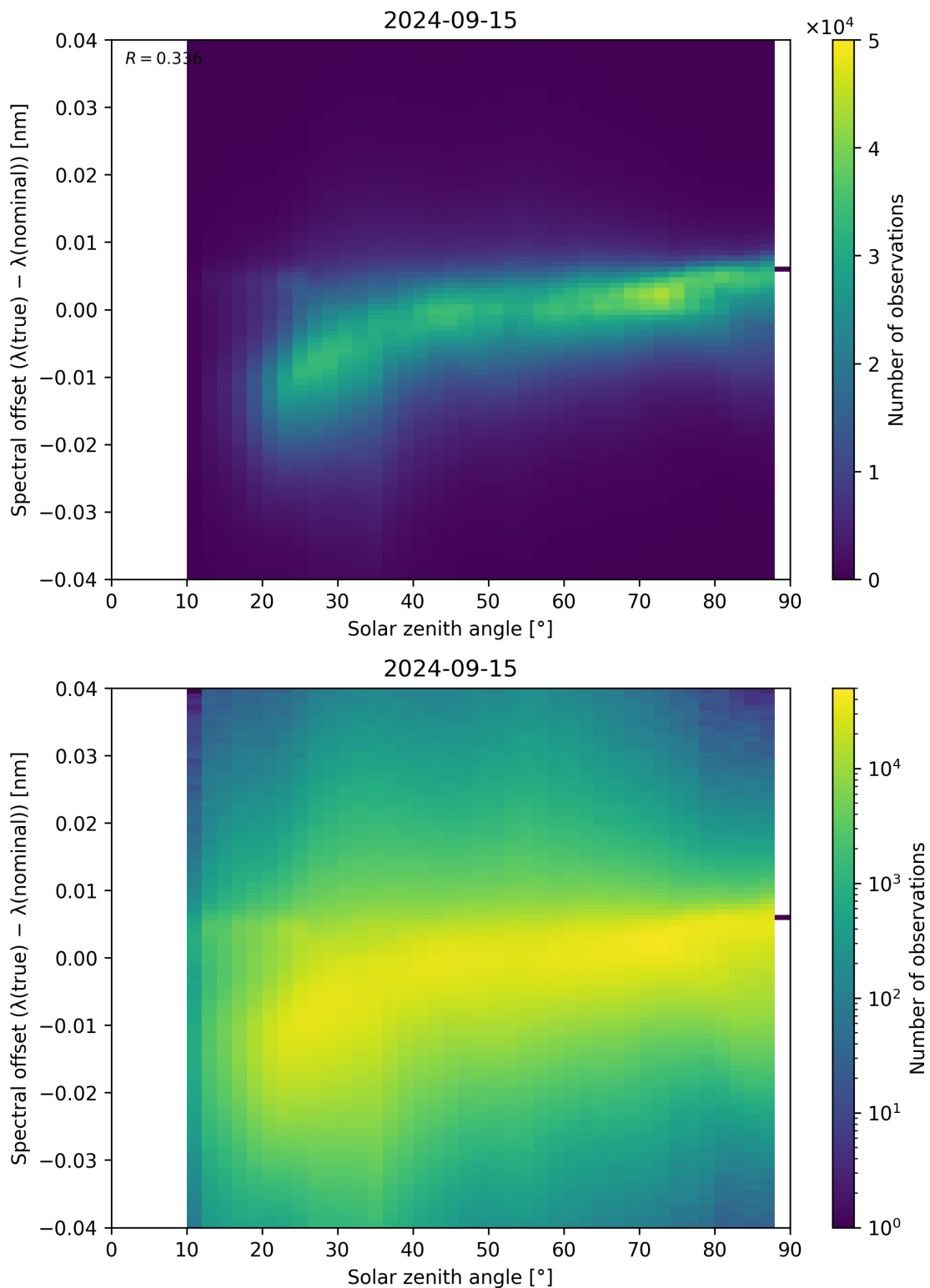


Figure 128: Scatter density plot of “Solar zenith angle” against “Spectral offset ( $\lambda_{\text{true}} - \lambda_{\text{nominal}}$ )” for 2024-09-14 to 2024-09-16.

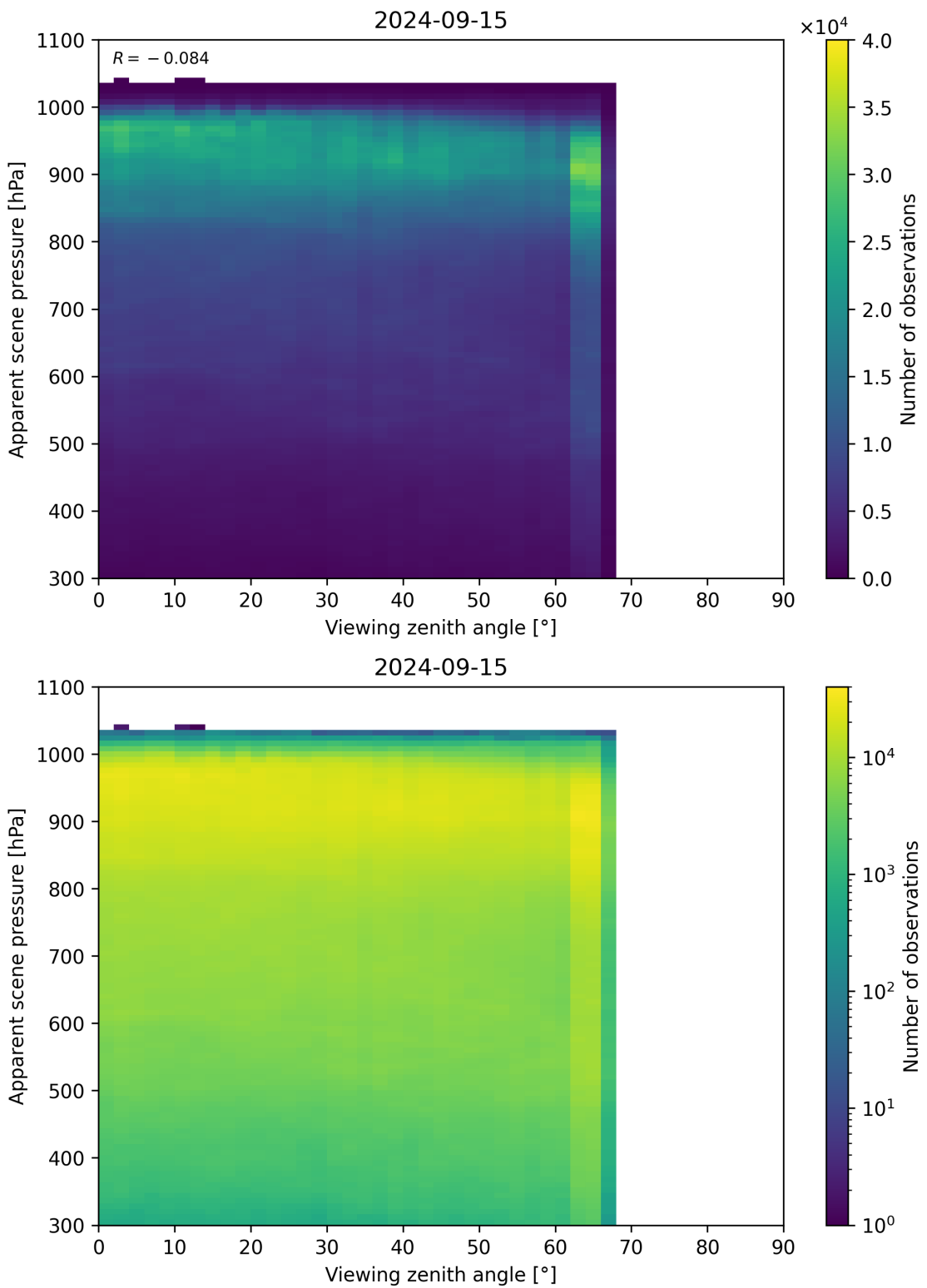


Figure 129: Scatter density plot of “Viewing zenith angle” against “Apparent scene pressure” for 2024-09-14 to 2024-09-16.

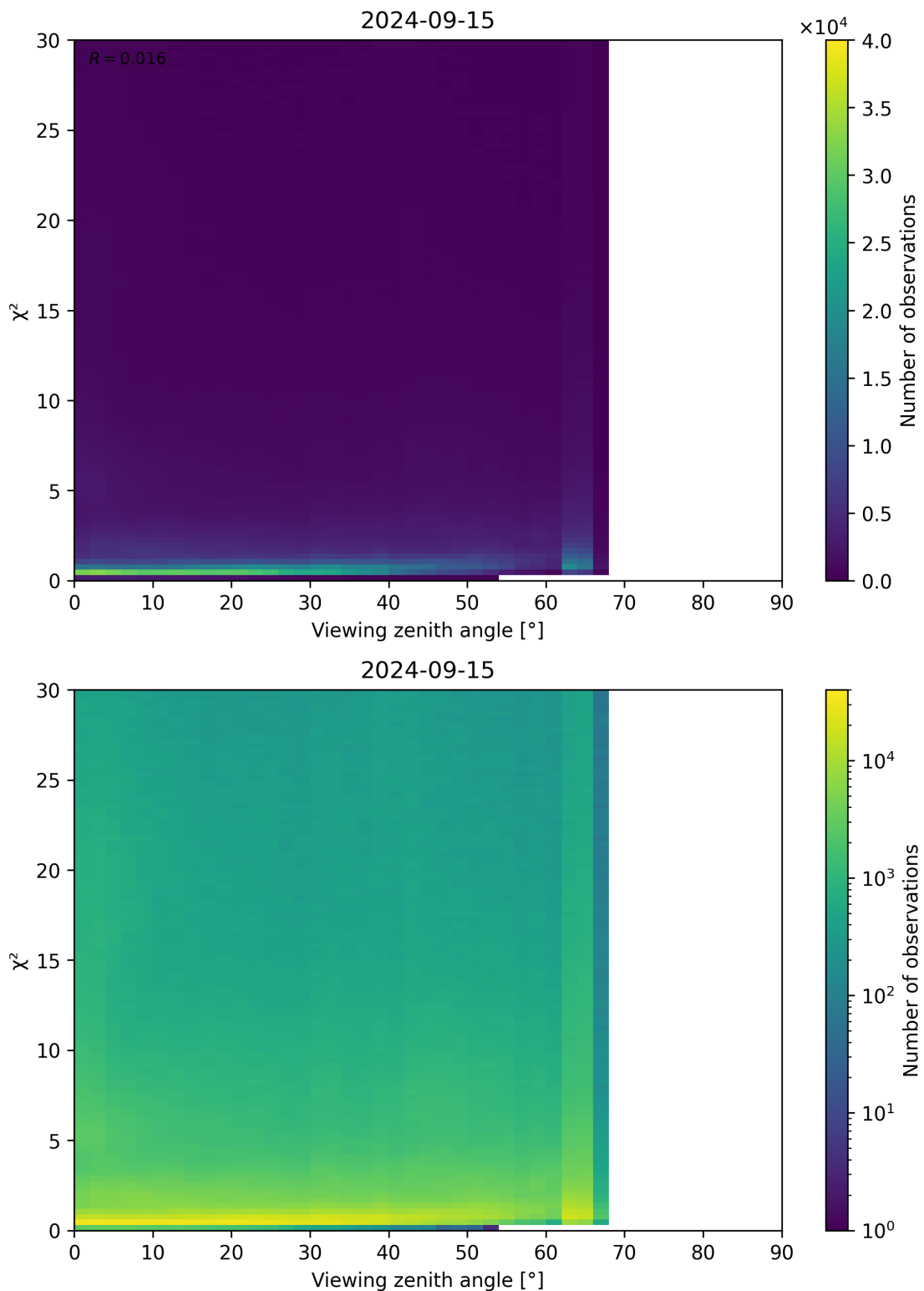


Figure 130: Scatter density plot of “Viewing zenith angle” against “ $\chi^2$ ” for 2024-09-14 to 2024-09-16.

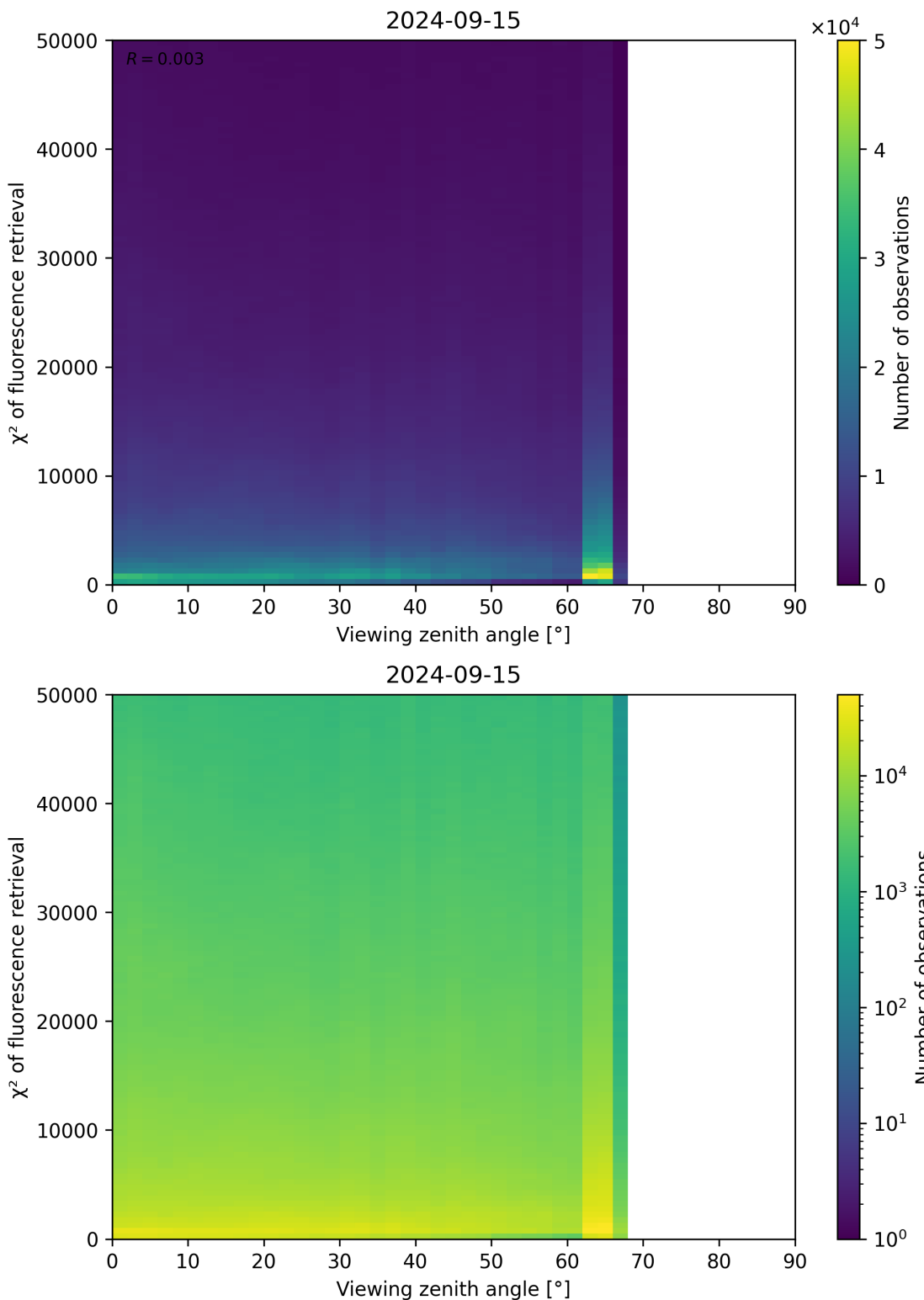


Figure 131: Scatter density plot of “Viewing zenith angle” against “ $\chi^2$  of fluorescence retrieval” for 2024-09-14 to 2024-09-16.

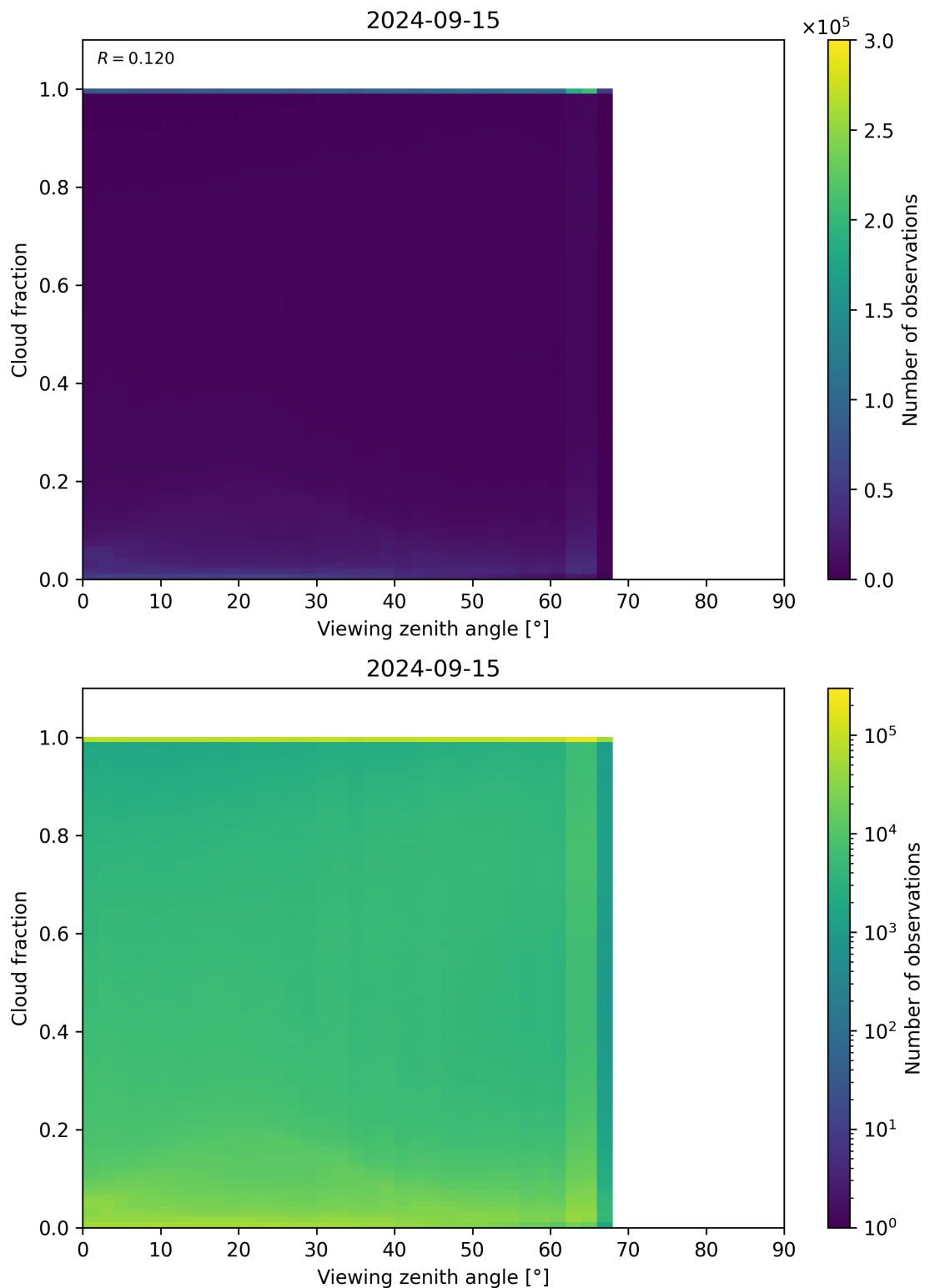


Figure 132: Scatter density plot of “Viewing zenith angle” against “Cloud fraction” for 2024-09-14 to 2024-09-16.

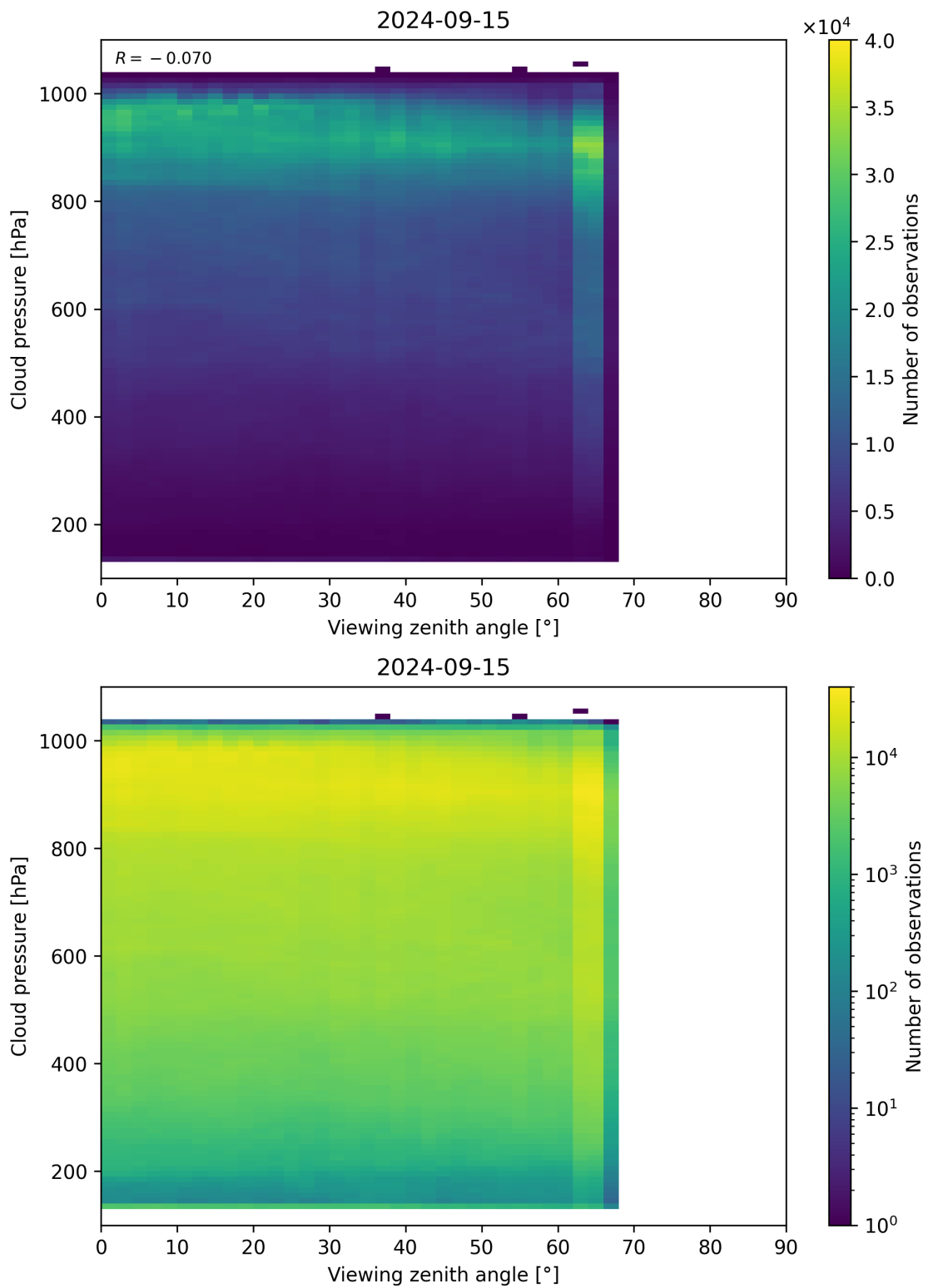


Figure 133: Scatter density plot of “Viewing zenith angle” against “Cloud pressure” for 2024-09-14 to 2024-09-16.

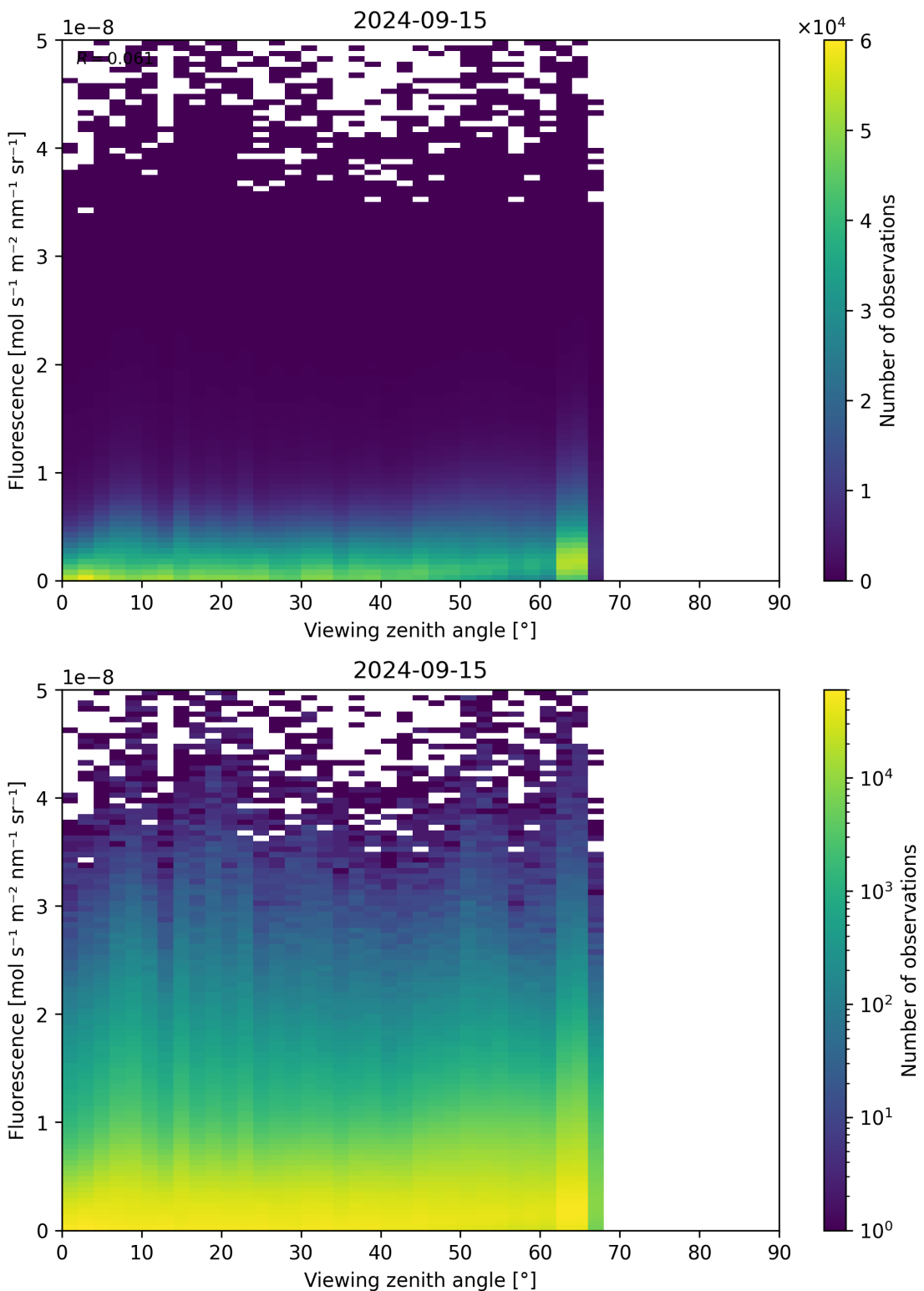


Figure 134: Scatter density plot of “Viewing zenith angle” against “Fluorescence” for 2024-09-14 to 2024-09-16.

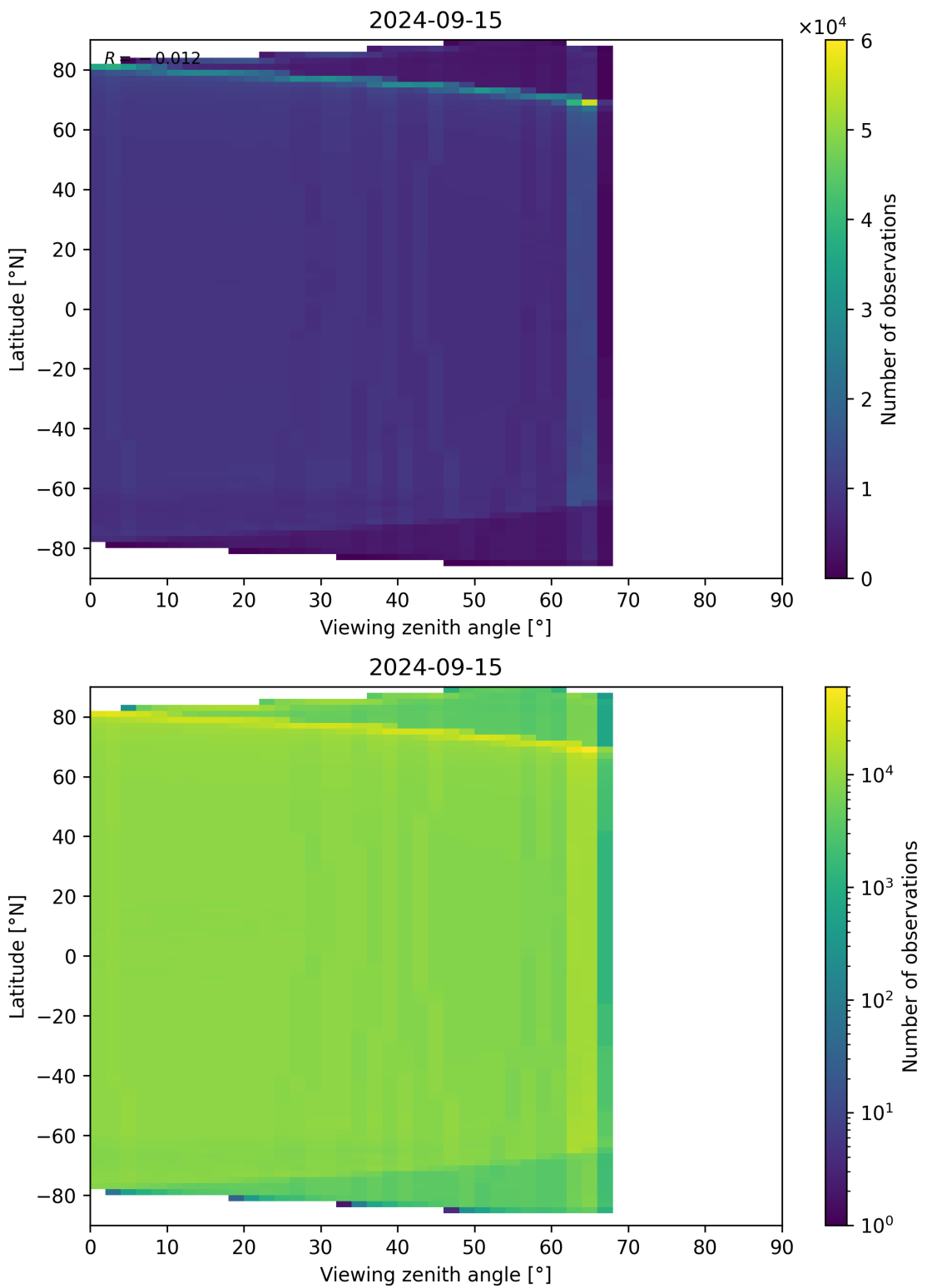


Figure 135: Scatter density plot of “Viewing zenith angle” against “Latitude” for 2024-09-14 to 2024-09-16.

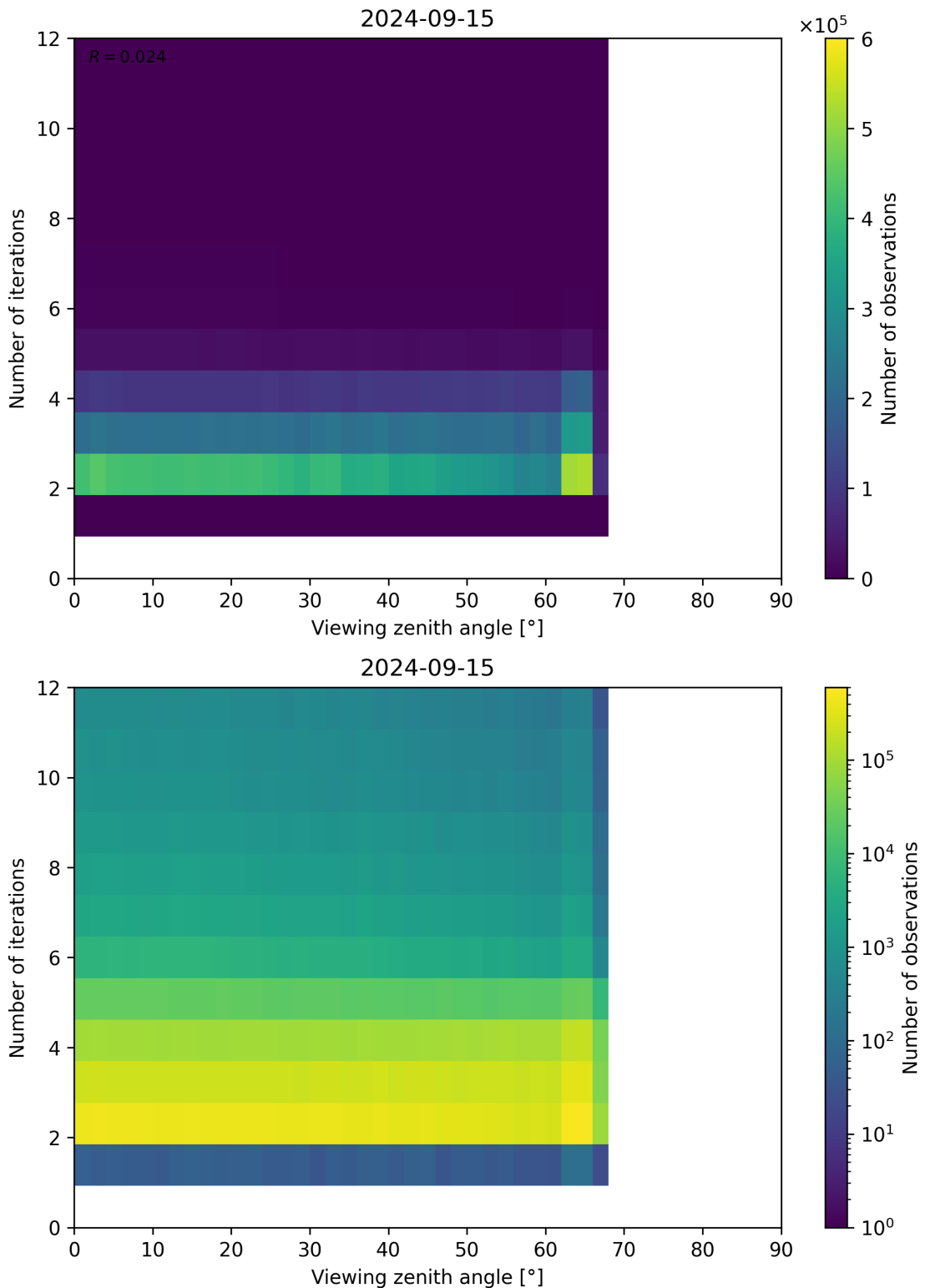


Figure 136: Scatter density plot of “Viewing zenith angle” against “Number of iterations” for 2024-09-14 to 2024-09-16.

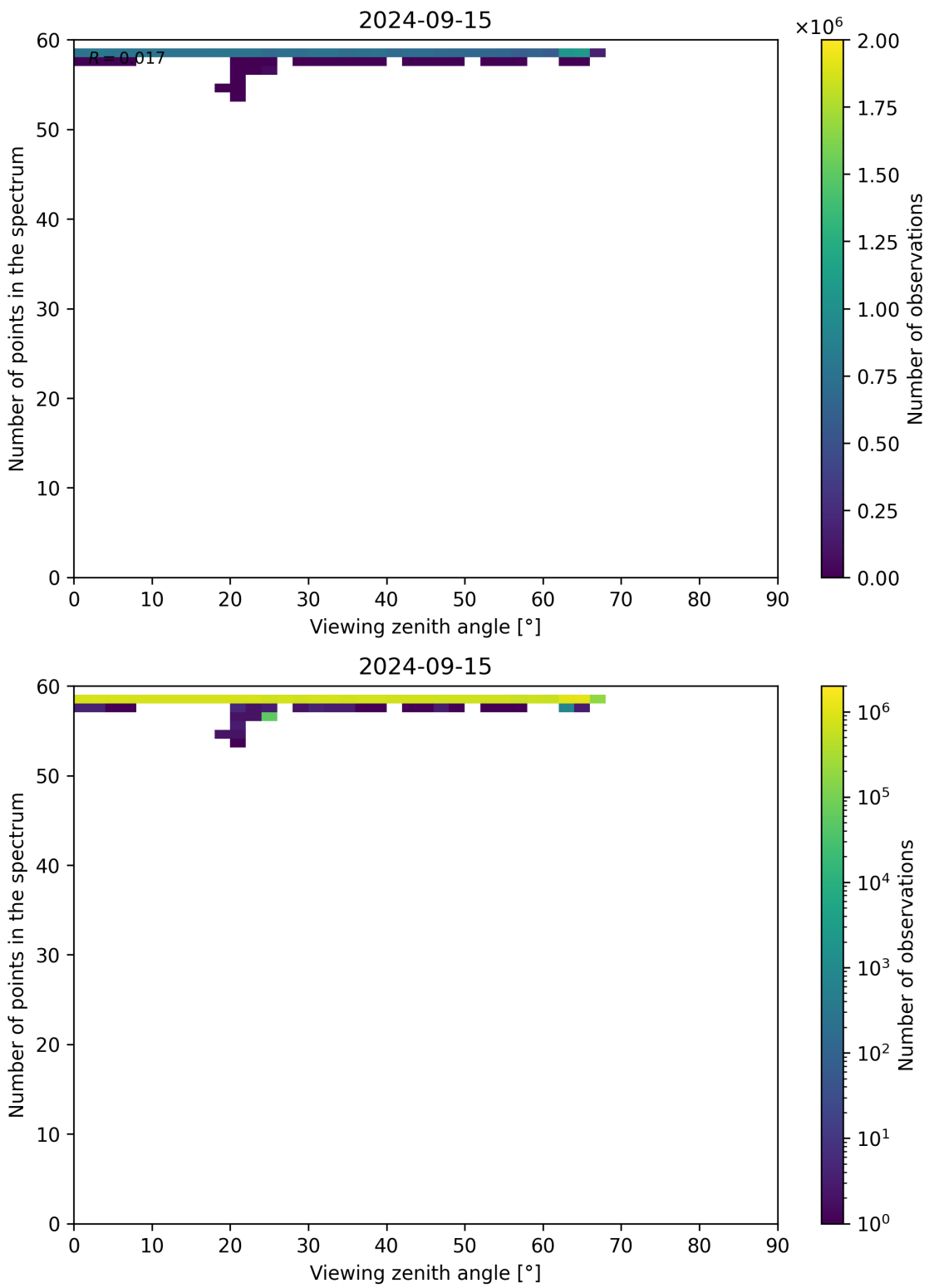


Figure 137: Scatter density plot of “Viewing zenith angle” against “Number of points in the spectrum” for 2024-09-14 to 2024-09-16.

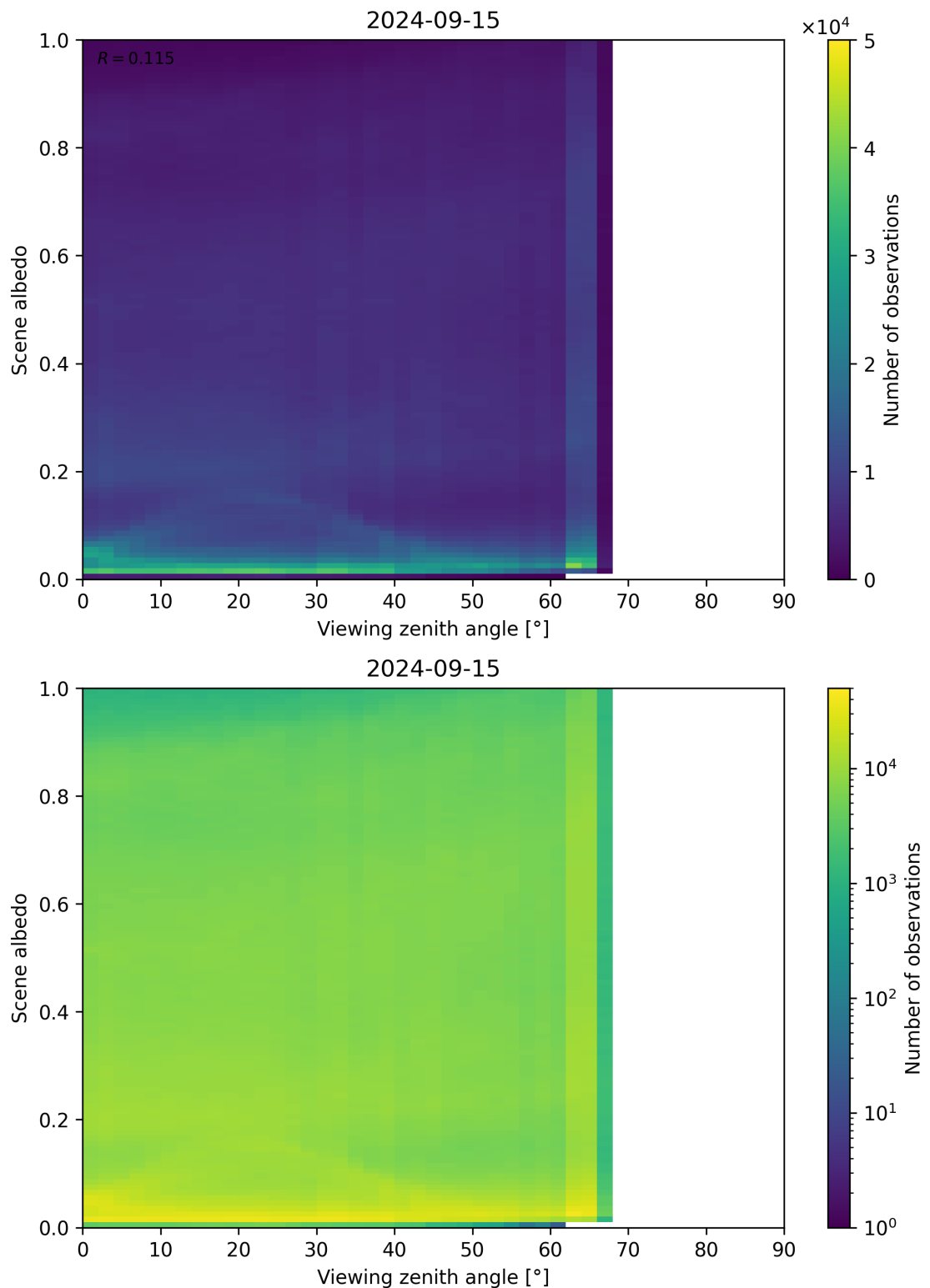


Figure 138: Scatter density plot of “Viewing zenith angle” against “Scene albedo” for 2024-09-14 to 2024-09-16.

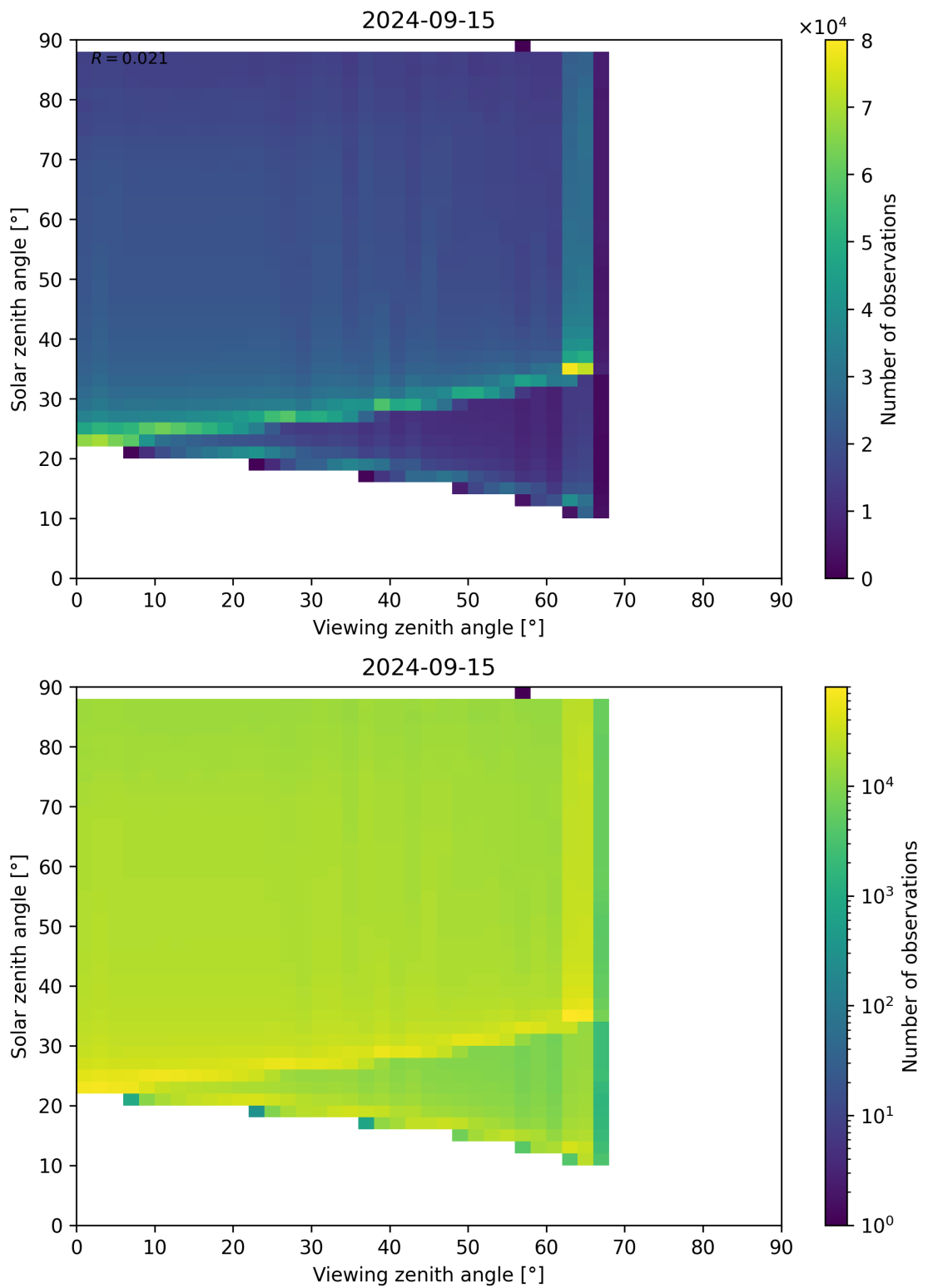


Figure 139: Scatter density plot of “Viewing zenith angle” against “Solar zenith angle” for 2024-09-14 to 2024-09-16.

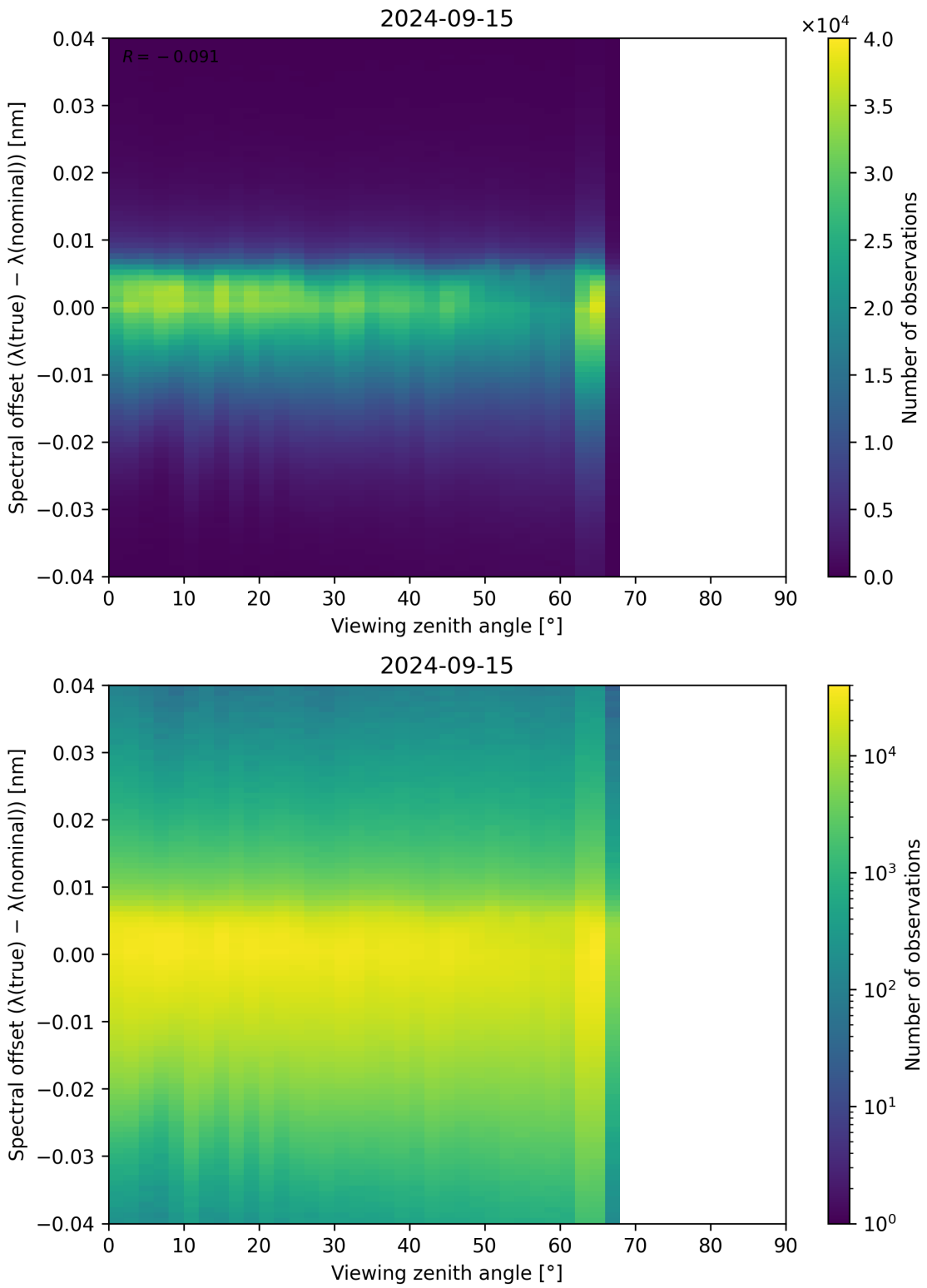


Figure 140: Scatter density plot of “Viewing zenith angle” against “Spectral offset ( $\lambda_{\text{true}} - \lambda_{\text{nominal}}$ )” for 2024-09-14 to 2024-09-16.

# Contents

<b>1</b>	<b>Short Introduction</b>	<b>1</b>
1.1	The list of parameters . . . . .	1
<b>2</b>	<b>Definitions</b>	<b>1</b>
<b>3</b>	<b>Granule outlines</b>	<b>12</b>
<b>4</b>	<b>Input data monitoring</b>	<b>13</b>
<b>5</b>	<b>Warnings and errors</b>	<b>14</b>
<b>6</b>	<b>World maps</b>	<b>15</b>
<b>7</b>	<b>Zonal average</b>	<b>21</b>
<b>8</b>	<b>Histograms</b>	<b>38</b>
<b>9</b>	<b>Along track statistics</b>	<b>55</b>
<b>10</b>	<b>Coincidence density</b>	<b>72</b>
<b>11</b>	<b>Copyright information of ‘PyCAMA’</b>	<b>150</b>

## List of Figures

1	Map of correlation graph for 2024-09-14 to 2024-09-16. . . . .	10
2	Map of correlation matrix for 2024-09-14 to 2024-09-16. . . . .	11
3	Outline of the granules. . . . .	12
4	Input data per granule . . . . .	13
5	Fraction of pixels with specific warnings and errors during processing . . . . .	14
6	Map of “Cloud pressure” for 2024-09-14 to 2024-09-16 . . . . .	15
7	Map of “Cloud fraction” for 2024-09-14 to 2024-09-16 . . . . .	16
8	Map of “Scene albedo” for 2024-09-14 to 2024-09-16 . . . . .	17
9	Map of “Apparent scene pressure” for 2024-09-14 to 2024-09-16 . . . . .	18
10	Map of “Fluorescence” for 2024-09-14 to 2024-09-16 . . . . .	19
11	Map of the number of observations for 2024-09-14 to 2024-09-16 . . . . .	20
12	Zonal average of “QA value” for 2024-09-14 to 2024-09-16. . . . .	21
13	Zonal average of “Cloud pressure” for 2024-09-14 to 2024-09-16. . . . .	22
14	Zonal average of “Cloud pressure precision” for 2024-09-14 to 2024-09-16. . . . .	23
15	Zonal average of “Cloud fraction” for 2024-09-14 to 2024-09-16. . . . .	24
16	Zonal average of “Cloud fraction precision” for 2024-09-14 to 2024-09-16. . . . .	25
17	Zonal average of “Scene albedo” for 2024-09-14 to 2024-09-16. . . . .	26
18	Zonal average of “Scene albedo precision” for 2024-09-14 to 2024-09-16. . . . .	27
19	Zonal average of “Apparent scene pressure” for 2024-09-14 to 2024-09-16. . . . .	28
20	Zonal average of “Apparent scene pressure precision” for 2024-09-14 to 2024-09-16. . . . .	29
21	Zonal average of “ $\chi^2$ ” for 2024-09-14 to 2024-09-16. . . . .	30
22	Zonal average of “Number of iterations” for 2024-09-14 to 2024-09-16. . . . .	31
23	Zonal average of “Fluorescence” for 2024-09-14 to 2024-09-16. . . . .	32
24	Zonal average of “Fluorescence precision” for 2024-09-14 to 2024-09-16. . . . .	33
25	Zonal average of “ $\chi^2$ of fluorescence retrieval” for 2024-09-14 to 2024-09-16. . . . .	34
26	Zonal average of “Degrees of freedom for signal of fluorescence retrieval” for 2024-09-14 to 2024-09-16. . . . .	35
27	Zonal average of “Number of points in the spectrum” for 2024-09-14 to 2024-09-16. . . . .	36
28	Zonal average of “Spectral offset ( $\lambda_{\text{true}} - \lambda_{\text{nominal}}$ )” for 2024-09-14 to 2024-09-16. . . . .	37
29	Histogram of “QA value” for 2024-09-14 to 2024-09-16 . . . . .	38
30	Histogram of “Cloud pressure” for 2024-09-14 to 2024-09-16 . . . . .	39
31	Histogram of “Cloud pressure precision” for 2024-09-14 to 2024-09-16 . . . . .	40
32	Histogram of “Cloud fraction” for 2024-09-14 to 2024-09-16 . . . . .	41
33	Histogram of “Cloud fraction precision” for 2024-09-14 to 2024-09-16 . . . . .	42
34	Histogram of “Scene albedo” for 2024-09-14 to 2024-09-16 . . . . .	43
35	Histogram of “Scene albedo precision” for 2024-09-14 to 2024-09-16 . . . . .	44
36	Histogram of “Apparent scene pressure” for 2024-09-14 to 2024-09-16 . . . . .	45

37	Histogram of “Apparent scene pressure precision” for 2024-09-14 to 2024-09-16 . . . . .	46
38	Histogram of “ $\chi^2$ ” for 2024-09-14 to 2024-09-16 . . . . .	47
39	Histogram of “Number of iterations” for 2024-09-14 to 2024-09-16 . . . . .	48
40	Histogram of “Fluorescence” for 2024-09-14 to 2024-09-16 . . . . .	49
41	Histogram of “Fluorescence precision” for 2024-09-14 to 2024-09-16 . . . . .	50
42	Histogram of “ $\chi^2$ of fluorescence retrieval” for 2024-09-14 to 2024-09-16 . . . . .	51
43	Histogram of “Degrees of freedom for signal of fluorescence retrieval” for 2024-09-14 to 2024-09-16 . . . . .	52
44	Histogram of “Number of points in the spectrum” for 2024-09-14 to 2024-09-16 . . . . .	53
45	Histogram of “Spectral offset ( $\lambda_{\text{true}} - \lambda_{\text{nominal}}$ )” for 2024-09-14 to 2024-09-16 . . . . .	54
46	Along track statistics of “QA value” for 2024-09-14 to 2024-09-16 . . . . .	55
47	Along track statistics of “Cloud pressure” for 2024-09-14 to 2024-09-16 . . . . .	56
48	Along track statistics of “Cloud pressure precision” for 2024-09-14 to 2024-09-16 . . . . .	57
49	Along track statistics of “Cloud fraction” for 2024-09-14 to 2024-09-16 . . . . .	58
50	Along track statistics of “Cloud fraction precision” for 2024-09-14 to 2024-09-16 . . . . .	59
51	Along track statistics of “Scene albedo” for 2024-09-14 to 2024-09-16 . . . . .	60
52	Along track statistics of “Scene albedo precision” for 2024-09-14 to 2024-09-16 . . . . .	61
53	Along track statistics of “Apparent scene pressure” for 2024-09-14 to 2024-09-16 . . . . .	62
54	Along track statistics of “Apparent scene pressure precision” for 2024-09-14 to 2024-09-16 . . . . .	63
55	Along track statistics of “ $\chi^2$ ” for 2024-09-14 to 2024-09-16 . . . . .	64
56	Along track statistics of “Number of iterations” for 2024-09-14 to 2024-09-16 . . . . .	65
57	Along track statistics of “Fluorescence” for 2024-09-14 to 2024-09-16 . . . . .	66
58	Along track statistics of “Fluorescence precision” for 2024-09-14 to 2024-09-16 . . . . .	67
59	Along track statistics of “ $\chi^2$ of fluorescence retrieval” for 2024-09-14 to 2024-09-16 . . . . .	68
60	Along track statistics of “Degrees of freedom for signal of fluorescence retrieval” for 2024-09-14 to 2024-09-16	69
61	Along track statistics of “Number of points in the spectrum” for 2024-09-14 to 2024-09-16 . . . . .	70
62	Along track statistics of “Spectral offset ( $\lambda_{\text{true}} - \lambda_{\text{nominal}}$ )” for 2024-09-14 to 2024-09-16 . . . . .	71
63	Scatter density plot of “Apparent scene pressure” against “ $\chi^2$ ” for 2024-09-14 to 2024-09-16. . . . .	72
64	Scatter density plot of “Apparent scene pressure” against “ $\chi^2$ of fluorescence retrieval” for 2024-09-14 to 2024-09-16. . . . .	73
65	Scatter density plot of “Apparent scene pressure” against “Fluorescence” for 2024-09-14 to 2024-09-16. . . . .	74
66	Scatter density plot of “Apparent scene pressure” against “Number of iterations” for 2024-09-14 to 2024-09-16. . . . .	75
67	Scatter density plot of “Apparent scene pressure” against “Number of points in the spectrum” for 2024-09-14 to 2024-09-16. . . . .	76
68	Scatter density plot of “Apparent scene pressure” against “Spectral offset ( $\lambda_{\text{true}} - \lambda_{\text{nominal}}$ )” for 2024-09-14 to 2024-09-16. . . . .	77
69	Scatter density plot of “ $\chi^2$ ” against “ $\chi^2$ of fluorescence retrieval” for 2024-09-14 to 2024-09-16. . . . .	78
70	Scatter density plot of “ $\chi^2$ ” against “Fluorescence” for 2024-09-14 to 2024-09-16. . . . .	79
71	Scatter density plot of “ $\chi^2$ of fluorescence retrieval” against “Number of points in the spectrum” for 2024-09-14 to 2024-09-16. . . . .	80
72	Scatter density plot of “ $\chi^2$ of fluorescence retrieval” against “Spectral offset ( $\lambda_{\text{true}} - \lambda_{\text{nominal}}$ )” for 2024-09-14 to 2024-09-16. . . . .	81
73	Scatter density plot of “ $\chi^2$ ” against “Number of iterations” for 2024-09-14 to 2024-09-16. . . . .	82
74	Scatter density plot of “ $\chi^2$ ” against “Number of points in the spectrum” for 2024-09-14 to 2024-09-16. . . . .	83
75	Scatter density plot of “ $\chi^2$ ” against “Spectral offset ( $\lambda_{\text{true}} - \lambda_{\text{nominal}}$ )” for 2024-09-14 to 2024-09-16. . . . .	84
76	Scatter density plot of “Cloud fraction” against “Apparent scene pressure” for 2024-09-14 to 2024-09-16. . . . .	85
77	Scatter density plot of “Cloud fraction” against “ $\chi^2$ ” for 2024-09-14 to 2024-09-16. . . . .	86
78	Scatter density plot of “Cloud fraction” against “ $\chi^2$ of fluorescence retrieval” for 2024-09-14 to 2024-09-16. . . . .	87
79	Scatter density plot of “Cloud fraction” against “Fluorescence” for 2024-09-14 to 2024-09-16. . . . .	88
80	Scatter density plot of “Cloud fraction” against “Number of iterations” for 2024-09-14 to 2024-09-16. . . . .	89
81	Scatter density plot of “Cloud fraction” against “Number of points in the spectrum” for 2024-09-14 to 2024-09-16. . . . .	90
82	Scatter density plot of “Cloud fraction” against “Scene albedo” for 2024-09-14 to 2024-09-16. . . . .	91
83	Scatter density plot of “Cloud fraction” against “Spectral offset ( $\lambda_{\text{true}} - \lambda_{\text{nominal}}$ )” for 2024-09-14 to 2024-09-16. . . . .	92
84	Scatter density plot of “Cloud pressure” against “Apparent scene pressure” for 2024-09-14 to 2024-09-16. . . . .	93
85	Scatter density plot of “Cloud pressure” against “ $\chi^2$ ” for 2024-09-14 to 2024-09-16. . . . .	94
86	Scatter density plot of “Cloud pressure” against “ $\chi^2$ of fluorescence retrieval” for 2024-09-14 to 2024-09-16. . . . .	95
87	Scatter density plot of “Cloud pressure” against “Cloud fraction” for 2024-09-14 to 2024-09-16. . . . .	96
88	Scatter density plot of “Cloud pressure” against “Fluorescence” for 2024-09-14 to 2024-09-16. . . . .	97
89	Scatter density plot of “Cloud pressure” against “Number of iterations” for 2024-09-14 to 2024-09-16. . . . .	98
90	Scatter density plot of “Cloud pressure” against “Number of points in the spectrum” for 2024-09-14 to 2024-09-16. . . . .	99

91	Scatter density plot of “Cloud pressure” against “Scene albedo” for 2024-09-14 to 2024-09-16. . . . .	100
92	Scatter density plot of “Cloud pressure” against “Spectral offset ( $\lambda_{\text{true}} - \lambda_{\text{nominal}}$ )” for 2024-09-14 to 2024-09-16. . . . .	101
93	Scatter density plot of “Fluorescence” against “ $\chi^2$ of fluorescence retrieval” for 2024-09-14 to 2024-09-16. . . . .	102
94	Scatter density plot of “Fluorescence” against “Number of points in the spectrum” for 2024-09-14 to 2024-09-16. . . . .	103
95	Scatter density plot of “Fluorescence” against “Spectral offset ( $\lambda_{\text{true}} - \lambda_{\text{nominal}}$ )” for 2024-09-14 to 2024-09-16. . . . .	104
96	Scatter density plot of “Latitude” against “Apparent scene pressure” for 2024-09-14 to 2024-09-16. . . . .	105
97	Scatter density plot of “Latitude” against “ $\chi^2$ ” for 2024-09-14 to 2024-09-16. . . . .	106
98	Scatter density plot of “Latitude” against “ $\chi^2$ of fluorescence retrieval” for 2024-09-14 to 2024-09-16. . . . .	107
99	Scatter density plot of “Latitude” against “Cloud fraction” for 2024-09-14 to 2024-09-16. . . . .	108
100	Scatter density plot of “Latitude” against “Cloud pressure” for 2024-09-14 to 2024-09-16. . . . .	109
101	Scatter density plot of “Latitude” against “Fluorescence” for 2024-09-14 to 2024-09-16. . . . .	110
102	Scatter density plot of “Latitude” against “Number of iterations” for 2024-09-14 to 2024-09-16. . . . .	111
103	Scatter density plot of “Latitude” against “Number of points in the spectrum” for 2024-09-14 to 2024-09-16. . . . .	112
104	Scatter density plot of “Latitude” against “Scene albedo” for 2024-09-14 to 2024-09-16. . . . .	113
105	Scatter density plot of “Latitude” against “Spectral offset ( $\lambda_{\text{true}} - \lambda_{\text{nominal}}$ )” for 2024-09-14 to 2024-09-16. . . . .	114
106	Scatter density plot of “Number of iterations” against “ $\chi^2$ of fluorescence retrieval” for 2024-09-14 to 2024-09-16. . . . .	115
107	Scatter density plot of “Number of iterations” against “Fluorescence” for 2024-09-14 to 2024-09-16. . . . .	116
108	Scatter density plot of “Number of iterations” against “Number of points in the spectrum” for 2024-09-14 to 2024-09-16. . . . .	117
109	Scatter density plot of “Number of iterations” against “Spectral offset ( $\lambda_{\text{true}} - \lambda_{\text{nominal}}$ )” for 2024-09-14 to 2024-09-16. . . . .	118
110	Scatter density plot of “Number of points in the spectrum” against “Spectral offset ( $\lambda_{\text{true}} - \lambda_{\text{nominal}}$ )” for 2024-09-14 to 2024-09-16. . . . .	119
111	Scatter density plot of “Scene albedo” against “Apparent scene pressure” for 2024-09-14 to 2024-09-16. . . . .	120
112	Scatter density plot of “Scene albedo” against “ $\chi^2$ ” for 2024-09-14 to 2024-09-16. . . . .	121
113	Scatter density plot of “Scene albedo” against “ $\chi^2$ of fluorescence retrieval” for 2024-09-14 to 2024-09-16. . . . .	122
114	Scatter density plot of “Scene albedo” against “Fluorescence” for 2024-09-14 to 2024-09-16. . . . .	123
115	Scatter density plot of “Scene albedo” against “Number of iterations” for 2024-09-14 to 2024-09-16. . . . .	124
116	Scatter density plot of “Scene albedo” against “Number of points in the spectrum” for 2024-09-14 to 2024-09-16. . . . .	125
117	Scatter density plot of “Scene albedo” against “Spectral offset ( $\lambda_{\text{true}} - \lambda_{\text{nominal}}$ )” for 2024-09-14 to 2024-09-16. . . . .	126
118	Scatter density plot of “Solar zenith angle” against “Apparent scene pressure” for 2024-09-14 to 2024-09-16. . . . .	127
119	Scatter density plot of “Solar zenith angle” against “ $\chi^2$ ” for 2024-09-14 to 2024-09-16. . . . .	128
120	Scatter density plot of “Solar zenith angle” against “ $\chi^2$ of fluorescence retrieval” for 2024-09-14 to 2024-09-16. . . . .	129
121	Scatter density plot of “Solar zenith angle” against “Cloud fraction” for 2024-09-14 to 2024-09-16. . . . .	130
122	Scatter density plot of “Solar zenith angle” against “Cloud pressure” for 2024-09-14 to 2024-09-16. . . . .	131
123	Scatter density plot of “Solar zenith angle” against “Fluorescence” for 2024-09-14 to 2024-09-16. . . . .	132
124	Scatter density plot of “Solar zenith angle” against “Latitude” for 2024-09-14 to 2024-09-16. . . . .	133
125	Scatter density plot of “Solar zenith angle” against “Number of iterations” for 2024-09-14 to 2024-09-16. . . . .	134
126	Scatter density plot of “Solar zenith angle” against “Number of points in the spectrum” for 2024-09-14 to 2024-09-16. . . . .	135
127	Scatter density plot of “Solar zenith angle” against “Scene albedo” for 2024-09-14 to 2024-09-16. . . . .	136
128	Scatter density plot of “Solar zenith angle” against “Spectral offset ( $\lambda_{\text{true}} - \lambda_{\text{nominal}}$ )” for 2024-09-14 to 2024-09-16. . . . .	137
129	Scatter density plot of “Viewing zenith angle” against “Apparent scene pressure” for 2024-09-14 to 2024-09-16. . . . .	138
130	Scatter density plot of “Viewing zenith angle” against “ $\chi^2$ ” for 2024-09-14 to 2024-09-16. . . . .	139
131	Scatter density plot of “Viewing zenith angle” against “ $\chi^2$ of fluorescence retrieval” for 2024-09-14 to 2024-09-16. . . . .	140
132	Scatter density plot of “Viewing zenith angle” against “Cloud fraction” for 2024-09-14 to 2024-09-16. . . . .	141
133	Scatter density plot of “Viewing zenith angle” against “Cloud pressure” for 2024-09-14 to 2024-09-16. . . . .	142
134	Scatter density plot of “Viewing zenith angle” against “Fluorescence” for 2024-09-14 to 2024-09-16. . . . .	143
135	Scatter density plot of “Viewing zenith angle” against “Latitude” for 2024-09-14 to 2024-09-16. . . . .	144
136	Scatter density plot of “Viewing zenith angle” against “Number of iterations” for 2024-09-14 to 2024-09-16. . . . .	145
137	Scatter density plot of “Viewing zenith angle” against “Number of points in the spectrum” for 2024-09-14 to 2024-09-16. . . . .	146
138	Scatter density plot of “Viewing zenith angle” against “Scene albedo” for 2024-09-14 to 2024-09-16. . . . .	147
139	Scatter density plot of “Viewing zenith angle” against “Solar zenith angle” for 2024-09-14 to 2024-09-16. . . . .	148
140	Scatter density plot of “Viewing zenith angle” against “Spectral offset ( $\lambda_{\text{true}} - \lambda_{\text{nominal}}$ )” for 2024-09-14 to 2024-09-16. . . . .	149

## List of Tables

1	Parameterlist and basic statistics for the analysis . . . . .	2
2	Percentile ranges . . . . .	3
3	Parameterlist and basic statistics for the analysis for observations in the northern hemisphere . . . . .	4
4	Parameterlist and basic statistics for the analysis for observations in the southern hemisphere . . . . .	5
5	Parameterlist and basic statistics for the analysis for observations over water . . . . .	6
6	Parameterlist and basic statistics for the analysis for observations over land . . . . .	7
7	Correlation matrix . . . . .	8
8	Covariance matrix . . . . .	9

## 11 Copyright information of ‘PyCAMA’

Copyright © 2005 – 2023, Maarten Sneep (KNMI).

All rights reserved.

Redistribution and use in source and binary forms, with or without modification, are permitted provided that the following conditions are met:

1. Redistributions of source code must retain the above copyright notice, this list of conditions and the following disclaimer.
2. Redistributions in binary form must reproduce the above copyright notice, this list of conditions and the following disclaimer in the documentation and/or other materials provided with the distribution.
3. Neither the name of the copyright holder nor the names of its contributors may be used to endorse or promote products derived from this software without specific prior written permission.

*This software is provided by the copyright holders and contributors “as is” and any express or implied warranties, including, but not limited to, the implied warranties of merchantability and fitness for a particular purpose are disclaimed. In no event shall the copyright holder or contributors be liable for any direct, indirect, incidental, special, exemplary, or consequential damages (including, but not limited to, procurement of substitute goods or services; loss of use, data, or profits; or business interruption) however caused and on any theory of liability, whether in contract, strict liability, or tort (including negligence or otherwise) arising in any way out of the use of this software, even if advised of the possibility of such damage.*

Maarten Sneep (maarten.sneep@knmi.nl).